BNL-NCS-40911
DOE/NDC-47/U
NEANDC(US)-226/U
INDC(USA)-101/L
Informal Report
Limited Distribution

REPORTS TO

THE DOE NUCLEAR DATA COMMITTEE

MAY 1988

BNL-NCS--40911

DE88 013006

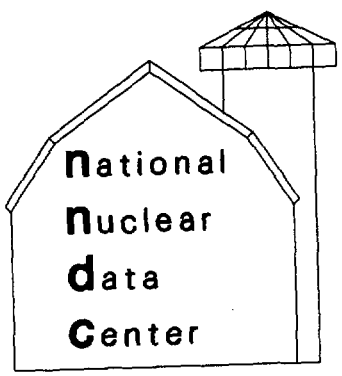

Compiled by the

NATIONAL NUCLEAR DATA CENTER

BROOKHAVEN NATIONAL LABORATORY
ASSOCIATED UNIVERSITIES, INC.

UNDER CONTRACT NO. DE-AC02-76CH00016 WITH THE
UNITED STATES DEPARTMENT OF ENERGY

Printed in the United States of America
Available from
National Technical Information Service
U.S. Department of Commerce
5285 Port Royal Road
Springfield, VA 22161

NTIS price codes:
Printed Copy: A10; Microfiche Copy: A01

PREFACE

The reports in this document were submitted to the Department of Energy, Nuclear Data Committee (DOE-NDC) in April, 1988. The reporting laboratories are those with a substantial program for the measurement of neutron and nuclear cross sections of relevance to the U.S. applied nuclear energy program.

The authors of the Status Report contributions are responsible for collecting and editing individual contributions from their laboratory and are not necessarily the sole authors of the contributions. The scientists responsible for the work described in each individual contribution are listed at the beginning of the contribution.

The material contained in these reports is to be regarded as comprised of informal statements of recent developments and preliminary data. Persons wishing to make use of these data should contact the individual experimenter for further details. The data which appear in this document should be quoted only by permission of the contributor and should be referenced as private communication, and not by this document number. Appropriate subjects are listed as follows:

1. Microscopic neutron cross sections relevant to the nuclear energy program, including shielding. Inverse reactions where pertinent are included.

2. Charged-particle cross sections, where they are relevant to (1.) above, and where relevant to developing and testing nuclear models.

3. Gamma ray production, radioactive decay, and theoretical developments in nuclear structure which are applicable to nuclear energy programs.

4. Proton and alpha-particle cross sections, at energies of up to 1 GeV, which are of interest to the space program.

These reports cannot be regarded as a complete summary of the nuclear research efforts in the U.S. A number of laboratories whose research is less programmatically oriented do not submit reports; neither do the submitted reports reflect all the work related to nuclear data in progress at the submitting laboratory.

This compilation has been produced almost completely from master copies prepared by the individual contributors listed in the Table of Contents, and reports are reproduced without change from these master copies.

The CINDA-type index which follows the Table of Contents was prepared by Norman E. Holden and Alyce Daly of the National Nuclear Data Center, Brookhaven National Laboratory, Upton, Long Island, New York.

TABLE OF CONTENTS

TABLE OF CONTENTS (cont.)

NEUTRON DATA REFERENCES

Element	Quantity	Energy (eV) Min	Energy (eV) Max	Type	Documentation Ref	Page	Date	Lab	Comments
^{1}NN	σ_{tot}		6 0+7	Theo	DOE-NDC 47	86	Apr88	LRL	Brown+ NDG
^{1}NN	$\sigma_{el}(\theta)$		6 0+7	Theo	DOE-NDC 47	86	Apr88	LRL	Brown+ NDG
^{1}H	$\sigma_{el}(\theta)$	NDG		Eval	DOE-NDC-47	129	Apr88	LAS	Carlson+ NDG. ENDF/B-6.
^{1}H	$\sigma_{el}(\theta)$	NDG		Revw	DOE-NDC-47	147	Apr88	ORL	Peelle+ NDG.
^{1}H	σ_{pol}	1 7+7		Expt	DOE-NDC-47	169	Apr88	TNL	Walter+ NDG. MONTE CARLO CORR
^{2}H	$\sigma_{el}(\theta)$	1 2+7		Theo	DOE-NDC-47	166	Apr88	TNL	Walter+ NDG. CFD EXPT.
^{2}H	σ_{pol}	1 2+7		Theo	DOE-NDC-47	166	Apr88	TNL	Walter+ NDG. CFD EXPT.
^{2}H	σ_{pol}	1 2+7		Expt	DOE-NDC-47	171	Apr88	TNL	Walter+ NDG. (N,2N) REACTION.
^{2}H	$\sigma_{n,2n}$	1 2+7		Expt	DOE-NDC-47	171	Apr88	TNL	Walter+ NDG. ANAL. POWER.
^{3}He	$\sigma_{n,p}$	NDG		Eval	DOE-NDC-47	129	Apr88	LAS	Carlson+ NDG. ENDF/B-6.
^{3}He	$\sigma_{n,p}$	1 0+0	7 5+5	Expt	DOE-NDC-47	125	Apr88	NBS	Behrens+ NDG. TB ANALYZED.
^{3}He	$\sigma_{n,p}$	NDG		Revw	DOE-NDC-47	147	Apr88	ORL	Peelle+ NDG.
^{6}Li	$\sigma_{el}(\theta)$	2 4+7		Expt	DOE-NDC-47	150	Apr88	OHO	Hansen+ NDG.
^{6}Li	σ_{pol}	5 0+6	1 7+7	Expt	DOE-NDC-47	168	Apr88	TNL	Walter+ NDG.
^{6}Li	$\sigma_{dif\ inl}$	2 4+7		Expt	DOE-NDC-47	150	Apr88	OHO	Hansen+ NDG.
^{6}Li	$\sigma_{n,p}$	1 2+8		Expt	DOE-NDC-47	38	Apr88	DAV	Wang+ NDG. CS, ANG DIS CFD CALC.
^{6}Li	$\sigma_{n,p}$	1 2+8		Expt	DOE-NDC-47	150	Apr88	INU	Pacanic+ NDG.
^{6}Li	$\sigma_{n,t}$	NDG		Eval	DOE-NDC-47	129	Apr88	NBS	Carlson+ NDG. ENDF/B-6.
^{6}Li	$\sigma_{n,t}$	NDG		Revw	DOE-NDC-47	147	Apr88	ORL	Peelle+ NDG.
^{7}Li	$\sigma_{el}(\theta)$	2 4+7		Expt	DOE-NDC-47	150	Apr88	OHO	Hansen+ NDG.
^{7}Li	$\sigma_{dif\ inl}$	2 4+7		Expt	DOE-NDC-47	150	Apr88	OHO	Hansen+ NDG.
^{7}Li	$\sigma_{n,nt}$	2 0+6	1 8+7	Theo	DOE-NDC-47	106	Apr88	LAS	Young. GRPH CFD ENDF/B-5
^{7}Be	$\sigma_{n,p}$	2 5 2	1 4+4	Expt	DOE-NDC-47	97	Apr88	LAS	Koehler+ NDG. M,G STATE CS.
^{9}Be	σ_{tot}	1 0+6	1 4+7	Expt	DOE NDC-47	1	Apr88	ANL	Smith+ NDG.
^{9}Be	σ_{tot}	+5	2 0+7	Eval	DOE-NDC-47	12	Apr88	ANL	Sugimoto+ NDG.
^{9}Be	σ_{el}	4 5+6	1 0+7	Expt	DOE-NDC-47	1	Apr88	ANL	Smith+ NDG. ANGLE INTEGRATED.
^{9}Be	$\sigma_{el}(\theta)$	4 5+6	1 0+7	Expt	DOE-NDC-47	1	Apr88	ANL	Smith+ NDG.
^{9}Be	$\sigma_{el}(\theta)$	8 0+6	1 7+7	Theo	DOE NDC 47	79	Apr88	LRL	Hansen+ NDG. CFD EXPT
^{9}Be	σ_{pol}	8 0+6	1 7+7	Theo	DOE NDC 47	79	Apr88	LRL	Hansen+ NDG. CFD EXPT
^{9}Be	$\sigma_{dif\ inl}$	4 5+6	1 0+7	Expt	DOE NDC 47	1	Apr88	ANL	Smith+ NDG. 2.43 MEV LVL EXC.
^{9}Be	$\sigma_{n,x}$	4 5+6	1 0+7	Expt	DOE NDC 47	1	Apr88	ANL	Smith+ NDG. TOTAL ELASTIC
^{9}Be	$\sigma_{n,xn}$		1 0+8	Expt	DOE NDC 47	177	Apr88	LAS	Gould+ NDG

NEUTRON DATA REFERENCES

Element	Quantity	Energy (eV) Min	Max	Type	Documentation Ref	Page	Date	Lab	Comments
^{9}Be	$\sigma_{n,2n}$	4.0+6	1.0+7	Expt	DOE-NDC-47	1	Apr88	ANL	Smith+ NDG. (NON ELASTIC) INELASTIC
^{9}Be	$\sigma_{n,2n}$	NDG		Eval	DOE-NDC-47	133	Apr88	OHO	Knox+ NDG.
^{10}B	$\sigma_{el}(\theta)$	3.0+6	1.2+7	Expt	DOE-NDC-47	157	Apr88	OHO	Sadowski+ NDG. MULTIPLE SCAT CORR
^{10}B	$\sigma_{el}(\theta)$	2.5-2	1.4+7	Theo	DOE-NDC-47	157	Apr88	OHO	Sadowski+ NDG. R-MATRIX ANAL.
^{10}B	$\sigma_{dif\,inl}$	2.5-2	1.4+7	Theo	DOE-NDC-47	157	Apr88	OHO	Sadowski+ NDG. R-MATRIX ANAL.
^{10}B	$\sigma_{dif\,inl}$	3.0+6	1.2+7	Expt	DOE-NDC-47	157	Apr88	OHO	Sadowski+ NDG. MULTIPLE SCAT CORR
^{10}B	$\sigma_{n,n'\gamma}$	1.0+5	1.0+7	Expt	DOE-NDC-47	135	Apr88	ORL	Dickens+ NDG.
^{10}B	$\sigma_{n,X\gamma}$	1.0+5	1.0+7	Expt	DOE-NDC-47	135	Apr88	ORL	Dickens+ NDG.
^{10}B	$\sigma_{n,p}$	2.5-2	1.4+7	Theo	DOE-NDC-47	157	Apr88	OHO	Sadowski+ NDG. R-MATRIX ANAL.
^{10}B	$\sigma_{n,d}$	2.5-2	1.4+7	Theo	DOE-NDC-47	157	Apr88	OHO	Sadowski+ NDG. R-MATRIX ANAL.
^{10}B	$\sigma_{n,t}$	2.5-2	1.4+7	Theo	DOE-NDC-47	157	Apr88	OHO	Sadowski+ NDG. R-MATRIX ANAL.
^{10}B	$\sigma_{n,\alpha}$	NDG		Eval	DOE-NDC-47	129	Apr88	NBS	Carlson+ NDG. ENDF/B-6.
^{10}B	$\sigma_{n,\alpha}$	2.5-2	1.4+7	Theo	DOE-NDC-47	157	Apr88	OHO	Sadowski+ NDG. R-MATRIX ANAL.
^{10}B	$\sigma_{n,\alpha}$	NDG		Revw	DOE-NDC-47	147	Apr88	ORL	Peelle+ NDG.
^{11}B	$\sigma_{n,X\gamma}$	1.0+6	2.6+8	Expt	DOE-NDC-47	103	Apr88	LAS	Nelson+ NDG.
^{11}B	$\sigma_{n,X\gamma}$	1.0+5	1.0+7	Expt	DOE-NDC-47	135	Apr88	ORL	Dickens+ NDG.
^{12}C	$\sigma_{el}(\theta)$	1.8+7	2.6+7	Expt	DOE-NDC-47	151	Apr88	OHO	Finlay+ NDG. KERMA CALC.
^{12}C	$\sigma_{el}(\theta)$	NDG		Revw	DOE-NDC-47	147	Apr88	ORL	Peelle+ NDG.
^{12}C	σ_{pol}	1.8+7		Expt	DOE-NDC-47	173	Apr88	TNL	Walter+ NDG. J.PHYS/G TBP.
^{12}C	$\sigma_{dif\,inl}$	1.8+7	2.6+7	Expt	DOE-NDC-47	151	Apr88	OHO	Finlay+ NDG. KERMA CALC.
^{12}C	$\sigma_{n,X\gamma}$	1.0+6	2.0+8	Expt	DOE-NDC-47	103	Apr88	LAS	Nelson+ NDG.
^{12}C	$\sigma_{n,p}$	5.0+7	5.0+8	Expt	DOE-NDC-47	39	Apr88	LAS	Haight+ NDG. FORWARD ANG. MEAS.
^{13}C	$\sigma_{dif\,inl}$	9.3+6	1.1+7	Expt	DOE-NDC-47	151	Apr88	OHO	Conatser+ NDG.
^{13}C	$\sigma_{n,p}$	6.5+7		Expt	DOE-NDC-47	38	Apr88	DAV	Wang+ NDG. CS, ANG DIS CFD CALC.
^{14}N	$\sigma_{el}(\theta)$	1.8+7	2.6+7	Expt	DOE-NDC-47	151	Apr88	OHO	Finlay+ NDG. KERMA CALC.
^{14}N	$\sigma_{el}(\theta)$	1.8+7	2.6+7	Expt	DOE-NDC-47	151	Apr88	OHO	Islam+ NDG. KERMA CALC.
^{14}N	$\sigma_{n,X\gamma}$	1.0+6	2.0+8	Expt	DOE-NDC-47	103	Apr88	LAS	Nelson+ NDG.
^{14}N	$\sigma_{n,X\gamma}$	1.4+7		Theo	DOE-NDC-47	71	Apr88	LRL	Resler TBL, GRPH CFD EXPT
^{15}N	$\sigma_{n,X\gamma}$	1.0+6	2.0+8	Expt	DOE-NDC-47	103	Apr88	LAS	Nelson+ NDG
^{16}O	$\sigma_{el}(\theta)$	1.8+7	2.6+7	Expt	DOE-NDC-47	151	Apr88	OHO	Finlay+ NDG. KERMA CALC
^{16}O	$\sigma_{el}(\theta)$	1.8+7	2.6+7	Expt	DOE-NDC-47	151	Apr88	OHO	Islam+ NDG KERMA CALC
^{16}O	$\sigma_{dif\,inl}$	1.8+7	2.6+7	Expt	DOE-NDC-47	151	Apr88	OHO	Finlay+ NDG KERMA CALC
^{16}O	$\sigma_{dif\,inl}$	1.8+7	2.6+7	Expt	DOE-NDC-47	151	Apr88	OHO	Islam+ NDG KERMA CALC

NEUTRON DATA REFERENCES

Element	Quantity	Energy (eV) Min	Max	Type	Documentation Ref	Page	Date	Lab	Comments
^{20}Ne	$\sigma_{n,\gamma}$	2.5+3	2.0+5	Expt	DOE-NDC-47	133	Apr88	ORL	Winters+ ASTROPHYS J
^{22}Ne	$\sigma_{n,\gamma}$	2.5+3	2.0+5	Expt	DOE-NDC-47	133	Apr88	ORL	Winters+ ASTROPHYS J
^{23}Na	$\sigma_{n,p}$	2.5.2	1.0+5	Expt	DOE-NDC-47	98	Apr88	LAS	Koehler+ GRPH. REL 6LI (N,A).
^{27}Al	σ_{pol}	5.0+6	1.7+7	Expt	DOE-NDC-47	174	Apr88	TNL	Gould+ NDG SPIN-SPIN.
^{27}Al	$\sigma_{n,\alpha}$	NDG		Revw	DOE-NDC-47	147	Apr88	ORL	Peelle+ NDG.
^{28}Si	$\sigma_{el}(\theta)$	8.0+6	4.0+7	Theo	DOE-NDC-47	167	Apr88	TNL	Walter+ NDG.
^{28}Si	σ_{pol}	8.0+6	4.0+7	Theo	DOE-NDC-47	167	Apr88	TNL	Walter+ NDG.
^{28}Si	$\sigma_{dif\ inl}$	8.0+6	4.0+7	Theo	DOE-NDC-47	167	Apr88	TNL	Walter+ NDG.
^{36}Cl	$\sigma_{n,p}$	2.5-2	1.0+5	Expt	DOE-NDC-47	98	Apr88	LAS	Koehler+ GRPH. REL 6LI (N,A).
^{40}Ca	$\sigma_{el}(\theta)$	2.0+6	8.0+6	Expt	DOE-NDC-47	53	Apr88	KTY	Hicks+ NDG.
^{40}Ca	$\sigma_{el}(\theta)$	1.8+7	2.6+7	Expt	DOE-NDC-47	151	Apr88	OHO	Finlay+ NDG. KERMA CALC.
^{40}Ca	$\sigma_{el}(\theta)$	1.8+7	2.6+7	Expt	DOE-NDC-47	151	Apr88	OHO	Islam+ NDG. KERMA CALC.
^{40}Ca	σ_{pol}	NDG		Theo	DOE-NDC-47	170	Apr88	TNL	Walter+ NDG.
^{40}Ca	$\sigma_{dif\ inl}$	1.8+7	2.6+7	Expt	DOE-NDC-47	151	Apr88	OHO	Finlay+ NDG. KERMA CALC.
^{40}Ca	$\sigma_{dif\ inl}$	1.8+7	2.6+7	Expt	DOE-NDC-47	151	Apr88	OHO	Islam+ NDG. KERMA CALC.
^{40}Ca	$\sigma_{n,\gamma}$	2.0+6	5.0+7	Expt	DOE-NDC-47	104	Apr88	LAS	Wender+ NDG. DIFF CS.
^{48}Ca	$\sigma_{el}(\theta)$	2.0+6	8.0+6	Expt	DOE-NDC-47	53	Apr88	KTY	Hicks+ NDG.
^{51}V	Evaluation	1.0-5	2.0+7	Eval	DOE-NDC-47	11	Apr88	ANL	Smith+ NDG. ENDF/B EVAL.
^{51}V	σ_{tot}		1.4+7	Expt	DOE-NDC-47	1	Apr88	ANL	Smith+ NDG.
^{51}V	$\sigma_{el}(\theta)$		1.0+7	Expt	DOE-NDC-47	1	Apr88	ANL	Smith+ NDG.
^{51}V	$\sigma_{dif\ inl}$		1.0+7	Expt	DOE-NDC-47	1	Apr88	ANL	Smith+ NDG.
^{50}Cr	Evaluation	NDG		Eval	DOE-NDC-47	148	Apr88	ORL	Larson+ NDG. ENDF/B-6.
^{52}Cr	Evaluation	NDG		Eval	DOE-NDC-47	148	Apr88	ORL	Larson+ NDG. ENDF/B-6.
^{53}Cr	Evaluation	NDG		Eval	DOE-NDC-47	148	Apr88	ORL	Larson+ NDG. ENDF/B-6.
^{53}Cr	$\sigma_{n,\gamma}$	1.0+6	2.0+7	Eval	DOE-NDC-47	144	Apr88	ORL	Shibata+ NDG.
^{53}Cr	$\sigma_{n,n'\gamma}$		1.0+7	Expt	DOE-NDC-47	135	Apr88	ORL	Dickens+ NDG.
^{53}Cr	$\sigma_{n,n'\gamma}$	1.0+6	2.0+7	Eval	DOE-NDC-47	144	Apr88	ORL	Shibata+ NDG.
^{53}Cr	$\sigma_{n,2n}$	8.1+6	2.0+7	Eval	DOE-NDC-47	144	Apr88	ORL	Shibata+ NDG.
^{53}Cr	$\sigma_{n,p}$	1.8+6	2.0+7	Eval	DOE-NDC-47	144	Apr88	ORL	Shibata+ NDG.
^{53}Cr	$\sigma_{n,np}$	1.1+7	2.0+7	Eval	DOE-NDC-47	144	Apr88	ORL	Shibata+ NDG.
^{53}Cr	$\sigma_{n,d}$	9.1+6	2.0+7	Eval	DOE-NDC-47	144	Apr88	ORL	Shibata+ NDG.
^{53}Cr	$\sigma_{n,t}$	1.0+7	2.0+7	Eval	DOE-NDC-47	144	Apr88	ORL	Shibata+ NDG.
^{53}Cr	$\sigma_{n,^3He}$	1.3+7	2.0+7	Eval	DOE-NDC-47	144	Apr88	ORL	Shibata+ NDG.

NEUTRON DATA REFERENCES

Element	Quantity	Energy (eV) Min	Max	Type	Documentation Ref	Page	Date	Lab	Comments
^{53}Cr	$\sigma_{n,na}$	9.3+6	2.0+7	Eval	DOE-NDC-47	144	Apr88	ORL	Shibata+ NDG.
^{54}Cr	Evaluation	NDG		Eval	DOE-NDC-47	148	Apr88	ORL	Larson+ NDG. ENDF/B-6.
Fe	$\sigma_{n,emis}$	1.4+7	2.6+7	Eval	DOE-NDC-47	143	Apr88	ORL	Fu. HF DOUB. DIFF. CS.
^{54}Fe	Evaluation	NDG		Eval	DOE-NDC-47	148	Apr88	ORL	Larson+ NDG. ENDF/B-6.
^{54}Fe	$\sigma_{n,p}$	8.0+6		Expt	DOE-NDC-47	153	Apr88	OHO	Saraf+ NDG. CPD HF CALC.
^{54}Fe	$\sigma_{n,a}$		1.0+7	Expt	DOE-NDC-47	6	Apr88	ANL	Smith+ NDG. DIFF. MEAS.
^{54}Fe	$\sigma_{n,a}$	8.0+6		Expt	DOE-NDC-47	153	Apr88	OHO	Saraf+ NDG. CPD HF CALC.
^{55}Fe	σ_{abs}	2.5-2		Expt	DOE-NDC-47	164	Apr88	AI	Kneff+ CS = 13.2+-2.1 B.
^{55}Fe	σ_{abs}	2.5-2		Expt	DOE-NDC-47	8	Apr88	ANL	Greenwood+ CS = 13.2+-2.1 B.
^{55}Fe	$\sigma_{n,a}$	2.5-2		Expt	DOE-NDC-47	164	Apr88	AI	Kneff+ CS = 9-18 MB.
^{55}Fe	$\sigma_{n,a}$	2.5-2		Expt	DOE-NDC-47	8	Apr88	ANL	Greenwood+ CS = 9+-4 MB.
^{56}Fe	Evaluation	NDG		Eval	DOE-NDC-47	148	Apr88	ORL	Larson+ NDG. ENDF/B-6.
^{58}Fe	$\sigma_{n,p}$	1.5+6		Expt	DOE-NDC-47	118	Apr88	MHG	Zasadny+ CS = 112.7 MB.
^{58}Fe	$\sigma_{n,p}$	8.0+6		Expt	DOE-NDC-47	153	Apr88	OHO	Saraf+ NDG. CPD HF CALC.
^{56}Fe	$\sigma_{n,a}$	8.0+6		Expt	DOE-NDC-47	153	Apr88	OHO	Saraf+ NDG. CPD HF CALC.
^{57}Fe	Evaluation	NDG		Eval	DOE-NDC-47	148	Apr88	ORL	Larson+ NDG. ENDF/B-6.
^{58}Fe	Evaluation	NDG		Eval	DOE-NDC-47	148	Apr88	ORL	Larson+ NDG. ENDF/B-6.
^{59}Co	Evaluation	NDG		Eval	DOE-NDC-47	12	Apr88	ANL	Smith+ NDG. ENDF/B EVAL.
^{59}Co	$\sigma_{el}(\theta)$	1.5+6	1.0+7	Expt	DOE-NDC-47	2	Apr88	ANL	Smith+ NDG. 18-160 DEGS.
^{59}Co	$\sigma_{dif\,inl}$	1.5+6	1.0+7	Expt	DOE-NDC-47	2	Apr88	ANL	Smith+ NDG. 18-160 DEGS.
^{59}Co	$\sigma_{dif\,inl}$	NDG		Expt	DOE-NDC-47	4	Apr88	ANL	Smith+ NDG. DOUBLE DIFF SPECTRA.
^{59}Co	$\sigma_{n,a}$	5.1+6	1.0+7	Expt	DOE-NDC-47	6	Apr88	ANL	Meadows+ NDG. DIFF. MEAS.
^{59}Co	$\sigma_{n,a}$		2.0+7	Eval	DOE-NDC-47	6	Apr88	ANL	Meadows+ NDG. MDL. CALC.
^{58}Ni	Evaluation	6.5+5	2.0+7	Eval	DOE-NDC-47	13	Apr88	ANL	Smith+ NDG. TBC.
^{58}Ni	Evaluation	NDG		Eval	DOE-NDC-47	148	Apr88	ORL	Larson+ NDG. ENDF/B-6.
^{58}Ni	σ_{tot}		1.2+7	Expt	DOE-NDC-47	3	Apr88	ANL	Smith+ NDG.
^{58}Ni	$\sigma_{el}(\theta)$	4.5+6	1.0+7	Expt	DOE-NDC-47	3	Apr88	ANL	Smith+ NDG.
^{58}Ni	$\sigma_{dif\,inl}$	4.5+6	1.0+7	Expt	DOE-NDC-47	3	Apr88	ANL	Smith+ NDG.
^{58}Ni	$\sigma_{n,d}$	8.0+6	1.1+7	Expt	DOE-NDC-47	153	Apr88	OHO	Graham+ NDG. UPPER LIMIT ONLY.
^{58}Ni	$\sigma_{a,emis}$	8.0+6	1.1+7	Expt	DOE-NDC-47	153	Apr88	OHO	Graham+ NDG.
^{58}Ni	$\sigma_{p,emis}$	8.0+6	1.1+7	Expt	DOE-NDC-47	153	Apr88	OHO	Graham+ NDG.
^{60}Ni	Evaluation	NDG		Eval	DOE-NDC-47	148	Apr88	ORL	Larson+ NDG ENDF/B-6.
^{60}Ni	$\sigma_{n,d}$	9.4+6	1.1+7	Expt	DOE-NDC-47	153	Apr88	OHO	Graham+ NDG. UPPER LIMIT ONLY

NEUTRON DATA REFERENCES

Element	Quantity	Energy (eV) Min	Max	Type	Documentation Ref	Page	Date	Lab	Comments
^{60}Ni	$\sigma_{n,emis}$	8.0+6	1.1+7	Expt	DOE-NDC-47	153	Apr88	OHO	Graham+ NDG.
^{60}Ni	$\sigma_{p,emis}$	8.0+6	1.1+7	Expt	DOE-NDC-47	153	Apr88	OHO	Graham+ NDG.
^{61}Ni	Evaluation	NDG		Eval	DOE-NDC-47	148	Apr88	ORL	Larson+ NDG. ENDF/B-6.
^{62}Ni	Evaluation	NDG		Eval	DOE-NDC-47	148	Apr88	ORL	Larson+ NDG. ENDF/B-6.
^{64}Ni	Evaluation	NDG		Eval	DOE-NDC-47	148	Apr88	ORL	Larson+ NDG. ENDF/B-6.
Cu	$\sigma_{dif\,inl}$	NDG		Expt	DOE-NDC-47	4	Apr88	ANL	Smith+ NDG. DOUBLE DIFF SPECTRA.
^{63}Cu	Evaluation	NDG		Eval	DOE-NDC-47	149	Apr88	ORL	Larson+ NDG. ENDF/B-6.
^{65}Cu	Evaluation	NDG		Eval	DOE-NDC-47	149	Apr88	ORL	Larson+ NDG. ENDF/B-6.
^{65}Cu	$\sigma_{n,2n}$	1.5+6		Expt	DOE-NDC-47	118	Apr88	MHG	Zasadny+ CS = 991 MB REL 56FE (N,P).
^{64}Zn	σ_{tot}	NDG		Theo	DOE-NDC-47	108	Apr88	LAS	Young+ NDG. HF STAT. CALC.
^{64}Zn	$\sigma_{el}(\theta)$	NDG		Theo	DOE-NDC-47	108	Apr88	LAS	Young+ NDG. HF STAT. CALC.
^{64}Zn	$\sigma_{n,p}$	1.5+6		Expt	DOE-NDC-47	118	Apr88	MHG	Zasadny+ CS = 163.2 MB REL 56FE (N,P).
^{66}Zn	σ_{tot}	NDG		Theo	DOE-NDC-47	108	Apr88	LAS	Young+ NDG. HF STAT. CALC.
^{66}Zn	$\sigma_{el}(\theta)$	NDG		Theo	DOE-NDC-47	108	Apr88	LAS	Young+ NDG. HF STAT. CALC.
^{68}Zn	σ_{tot}	NDG		Theo	DOE-NDC-47	108	Apr88	LAS	Young+ NDG. HF STAT. CALC.
^{68}Zn	$\sigma_{el}(\theta)$	NDG		Theo	DOE-NDC-47	108	Apr88	LAS	Young+ NDG. HF STAT. CALC.
^{75}As	$\sigma_{n,\gamma}$		7.0+5	Expt	DOE-NDC-47	134	Apr88	ORL	Macklin. MAXW. AVG. CS.
^{79}Br	$\sigma_{n,\gamma}$		7.0+5	Expt	DOE-NDC-47	134	Apr88	ORL	Macklin. MAXW. AVG. CS.
^{79}Br	Res.Int.Capt	NDG		Expt	DOE-NDC-47	134	Apr88	ORL	Macklin. RIG = 130+-5 B.
^{81}Br	$\sigma_{n,\gamma}$		7.0+5	Expt	DOE-NDC-47	134	Apr88	ORL	Macklin. MAXW. AVG. CS.
^{81}Br	Res.Int.Capt	NDG		Expt	DOE-NDC-47	134	Apr88	ORL	Macklin. RIG = 46.6+-1.8 B.
^{86}Kr	σ_{tot}	1.5+4	2.5+7	Expt	DOE-NDC-47	132	Apr88	ORL	Carlton+ NDG. PR/C TBP.
^{86}Kr	Res.Params	1.5+4	1.0+6	Expt	DOE-NDC-47	132	Apr88	ORL	Carlton+ NDG. PR/C TBP.
^{89}Y	$\sigma_{el}(\theta)$	8.0+6	1.7+7	Theo	DOE-NDC-47	79	Apr88	LRL	Hansen+ GRPHS. CFD EXPT.
^{89}Y	σ_{pol}	8.0+6	1.7+7	Theo	DOE-NDC-47	79	Apr88	LRL	Hansen+ GRPH. CFD EXPT.
^{89}Y	σ_{pol}	8.0+6	1.7+7	Theo	DOE-NDC-47	172	Apr88	TNL	Walter+ NDG.
^{89}Y	$\sigma_{dif\,inl}$	NDG		Expt	DOE-NDC-47	4	Apr88	ANL	Smith+ NDG. DOUBLE DIFF SPECTRA.
^{89}Y	$\sigma_{dif\,inl}$	1.1+7		Expt	DOE-NDC-47	154	Apr88	OHO	Mellema+ NDG. CFD P SCATT.
Zr	Evaluation	NDG		Eval	DOE-NDC-47	13	Apr88	ANL	Sugimoto+ NDG. TBD.
Zr	σ_{tot}		1.0+7	Expt	DOE-NDC-47	3	Apr88	ANL	Smith+ NDG.
Zr	$\sigma_{el}(\theta)$		1.0+7	Expt	DOE-NDC-47	3	Apr88	ANL	Smith+ NDG.
Zr	$\sigma_{dif\,inl}$		1.0+7	Expt	DOE-NDC-47	3	Apr88	ANL	Smith+ NDG. TBC.
^{90}Zr	$\sigma_{n,p}$	6.5+7		Expt	DOE-NDC-47	37	Apr88	DAV	Brady+ NDG. DIFF CS TO 0 DEGS

NEUTRON DATA REFERENCES

Element	Quantity	Energy (eV) Min	Max	Type	Documentation Ref	Page	Date	Lab	Comments
^{91}Zr	$\sigma_{el}(\theta)$	8.0+6		Expt	DOE-NDC-47	154	Apr88	OHO	Wang+ NDG.
^{91}Zr	$\sigma_{dif\,inl}$	8.0+6	2.4+7	Expt	DOE-NDC-47	154	Apr88	OHO	Wang+ NDG.
^{92}Zr	$\sigma_{el}(\theta)$	8.0+6		Expt	DOE-NDC-47	154	Apr88	OHO	Wang+ NDG.
^{92}Zr	$\sigma_{dif\,inl}$	8.0+6	2.4+7	Expt	DOE-NDC-47	154	Apr88	OHO	Wang+ NDG.
^{94}Zr	$\sigma_{el}(\theta)$	8.0+6	2.4+7	Expt	DOE-NDC-47	154	Apr88	OHO	Wang+ NDG.
^{94}Zr	$\sigma_{dif\,inl}$	8.0+6	2.4+7	Expt	DOE-NDC-47	154	Apr88	OHO	Wang+ NDG.
^{93}Nb	$\sigma_{el}(\theta)$	8.0+6	1.7+7	Theo	DOE-NDC-47	79	Apr88	LRL	Hansen+ NDG. CFD EXPT.
^{93}Nb	σ_{pol}	8.0+6	1.7+7	Theo	DOE-NDC-47	79	Apr88	LRL	Hansen+ GRPH. CFD EXPT.
^{93}Nb	σ_{pol}	5.0+6	1.7+7	Expt	DOE-NDC-47	174	Apr88	TNL	Gould+ GRPH. SPIN-SPIN CS.
^{93}Nb	σ_{pol}	8.0+6	1.7+7	Theo	DOE-NDC-47	172	Apr88	TNL	Walter+ NDG.
^{93}Nb	$\sigma_{dif\,inl}$	NDG		Expt	DOE-NDC-47	4	Apr88	ANL	Smith+ NDG. DOUBLE DIFF SPECTRA.
^{93}Nb	$\sigma_{dif\,inl}$	NDG		Eval	DOE-NDC-47	13	Apr88	ANL	Geraldo+ NDG. TBC.
^{93}Nb	$\sigma_{dif\,inl}$	FISS		Expt	DOE-NDC-47	43	Apr88	INL	Rogers+ 235U, 252CF SPECTRA.
^{93}Nb	$\sigma_{n,\gamma}$	1.4+7		Theo	DOE-NDC-47	73	Apr88	LRL	Reffo+ GRPH CFD EXPT.
^{93}Nb	$\sigma_{n,emis}$	1.4+7	2.6+7	Eval	DOE-NDC-47	143	Apr88	ORL	Fu. HF DOUB. DIFF. CS.
^{94}Mo	$\sigma_{n,2n}$	1.5+7		Expt	DOE-NDC-47	8	Apr88	ANL	Greenwood+ CS LT 0.81 B.
^{94}Mo	$\sigma_{n,np}$	1.5+7		Expt	DOE-NDC-47	8	Apr88	ANL	Greenwood+ (N,D) + (N,NP) + (N,PN).
^{9c}Mo	$\sigma_{n,d}$	1.5+7		Expt	DOE-NDC-47	8	Apr88	ANL	Greenwood+ (N,D) + (N,NP) + (N,PN).
In	$\sigma_{dif\,inl}$	5.0+6	8.0+6	Expt	DOE-NDC-47	4	Apr88	ANL	Smith+ NDG. DOUBLE DIFF SPECTRA.
^{116}Sn	$\sigma_{el}(\theta)$	8.0+6	1.7+7	Theo	DOE-NDC-47	79	Apr88	LRL	Hansen+ NDG. CFD EXPT.
^{116}Sn	σ_{pol}	8.0+6	1.7+7	Theo	DOE-NDC-47	79	Apr88	LRL	Hansen+ GRPH. CFD EXPT.
^{116}Sn	$\sigma_{dif\,inl}$	NDG		Theo	DOE-NDC-47	53	Apr88	KTY	Weil+ NDG. CFD STAT MDL.
^{116}Sn	$\sigma_{n,n'\gamma}$	3.1+6	4.5+6	Expt	DOE-NDC-47	61	Apr88	KTY	Weil+ NDG.
^{118}Sn	$\sigma_{dif\,inl}$	NDG		Theo	DOE-NDC-47	53	Apr88	KTY	Weil+ NDG. CFD STAT MDL.
^{120}Sn	$\sigma_{el}(\theta)$	8.0+6	1.7+7	Theo	DOE-NDC-47	79	Apr88	LRL	Hansen+ NDG. CFD EXPT.
^{120}Sn	σ_{pol}	8.0+6	1.7+7	Theo	DOE-NDC-47	79	Apr88	LRL	Hansen+ GRPH. CFD EXPT.
^{120}Sn	σ_{pol}	8.0+6	1.7+7	Theo	DOE-NDC-47	172	Apr88	TNL	Walter+ NDG.
^{120}Sn	$\sigma_{dif\,inl}$	NDG		Theo	DOE-NDC-47	53	Apr88	KTY	Weil+ NDG. CFD STAT MDL.
^{122}Sn	$\sigma_{dif\,inl}$	NDG		Theo	DOE-NDC-47	53	Apr88	KTY	Weil+ NDG. CFD STAT MDL.
^{124}Sn	$\sigma_{dif\,inl}$	NDG		Theo	DOE-NDC-47	53	Apr88	KTY	Weil+ NDG. CFD STAT MDL.
^{139}La	σ_{tot}	3.0+6	6.0+7	Theo	DOE-NDC-47	77	Apr88	LRL	Camarda+ NDG. CS (139LA-140CE)
^{139}La	$\sigma_{n,\gamma}$	1.4+7		Theo	DOE-NDC-47	73	Apr88	LRL	Reffo+ GRPH CFD EXPT.
^{140}Ce	σ_{tot}	3.0+6	6.0+7	Theo	DOE-NDC-47	77	Apr88	LRL	Camarda+ NDG.

NEUTRON DATA REFERENCES

Element	Quantity	Energy (eV) Min	Max	Type	Documentation Ref	Page	Date	Lab	Comments
^{142}Ce	σ_{tot}	3.0+6	6.0+7	Theo	DOE-NDC-47	77	Apr88	LRL	Camarda+ NDG. CS (142CE-140CE).
^{141}Pr	σ_{tot}	3.0+6	6.0+7	Theo	DOE-NDC-47	77	Apr88	LRL	Camarda+ NDG. CS (141PR-140CE).
Eu	$\sigma_{n,X\gamma}$	8.0+2	3.0+6	Expt	DOE-NDC-47	103	Apr88	LAS	Wender+ NDG.
Eu	$\sigma_{n,X\gamma}$	5.0+5	2.0+8	Expt	DOE-NDC-47	103	Apr88	LAS	Nelson+ NDG.
Gd	$\sigma_{n,X\gamma}$	8.0+2	3.0+6	Expt	DOE-NDC-47	103	Apr88	LAS	Wender+ NDG.
Gd	$\sigma_{n,X\gamma}$	5.0+5	2.0+8	Expt	DOE-NDC-47	103	Apr88	LAS	Nelson+ NDG.
^{152}Gd	$\sigma_{n,\gamma}$	5.0+3	5.0+5	Expt	DOE-NDC-47	134	Apr88	ORL	Beer+ MAXW AVG. CS.
^{154}Gd	$\sigma_{n,\gamma}$	5.0+3	5.0+5	Expt	DOE-NDC-47	134	Apr88	ORL	Beer+ MAXW AVG. CS.
^{155}Gd	$\sigma_{n,\gamma}$	5.0+3	5.0+5	Expt	DOE-NDC-47	134	Apr88	ORL	Beer+ MAXW AVG. CS.
^{157}Gd	$\sigma_{n,\gamma}$	5.0+3	5.0+5	Expt	DOE-NDC-47	134	Apr88	ORL	Beer+ MAXW AVG. CS.
^{165}Ho	$\sigma_{dif,inl}$	5.0+6	8.0+6	Expt	DOE-NDC-47	4	Apr88	ANL	Smith+ NDG. DOUBLE DIFF SPECTRA.
^{165}Ho	$\sigma_{n,X\gamma}$	8.0+2	3.0+6	Expt	DOE-NDC-47	103	Apr88	LAS	Wender+ NDG.
^{181}Ta	$\sigma_{dif,inl}$	5.0+6	8.0+6	Expt	DOE-NDC-47	4	Apr88	ANL	Smith+ NDG. DOUBLE DIFF SPECTRA.
^{181}Ta	$\sigma_{n,X\gamma}$	2.0+6	1.0+8	Expt	DOE-NDC-47	177	Apr88	LAS	Gould+ NDG.
^{189}Os	σ_{tot}	6.0+0	5.0+5	Expt	DOE-NDC-47	132	Apr88	ORL	Carlton+ NDG.
^{189}Os	Res.Params.	6.0+0	1.7+2	Expt	DOE-NDC-47	132	Apr88	ORL	Carlton+ NDG.
^{189}Os	$\langle\Gamma\gamma\rangle/D$		1.7+2	Expt	DOE-NDC-47	132	Apr88	ORL	Carlton+ S = 3.1+-0.7x(10-4). TBP.
^{192}Os	σ_{tot}	NDG		Expt	DOE-NDC-47	51	Apr88	KTY	Hicks+ NDG.
^{192}Os	$\sigma_{el}(\theta)$	NDG		Expt	DOE-NDC-47	51	Apr88	KTY	Hicks+ NDG.
^{192}Os	$\sigma_{dif,inl}$	NDG		Expt	DOE-NDC-47	51	Apr88	KTY	Hicks+ NDG.
^{194}Pt	σ_{tot}	NDG		Expt	DOE-NDC-47	51	Apr88	KTY	Hicks+ NDG.
^{194}Pt	$\sigma_{el}(\theta)$	NDG		Expt	DOE-NDC-47	51	Apr88	KTY	Hicks+ NDG.
^{194}Pt	$\sigma_{dif,inl}$	NDG		Expt	DOE-NDC-47	51	Apr88	KTY	Hicks+ NDG.
^{196}Pt	$\sigma_{n,n'\gamma}$	NDG		Expt	DOE-NDC-47	57	Apr88	KTY	Yates+ NDG.
^{197}Au	$\sigma_{n,\gamma}$	NDG		Eval	DOE-NDC-47	129	Apr88	NBS	Carlson+ NDG. ENDF/B-6.
^{197}Au	$\sigma_{n,\gamma}$	NDG		Revw	DOE-NDC-47	147	Apr88	ORL	Peelle+ NDG.
^{202}Hg	$\sigma_{n,n'\gamma}$	NDG		Expt	DOE-NDC-47	57	Apr88	KTY	Yates+ NDG.
^{204}Hg	$\sigma_{n,n'\gamma}$	NDG		Expt	DOE-NDC-47	57	Apr88	KTY	Yates+ NDG.
Pb	Evaluation	NDG		Eval	DOE-NDC-47	149	Apr88	ORL	Larson+ NDG. ENDF/B-6.
Pb	$\sigma_{n,emis}$	6.5+7		Expt	DOE-NDC-47	38	Apr88	DAV	Hjort+ NDG. DOUB. DIFF CS.
^{204}Pb	σ_{tot}	3.0+5	4.0+6	Expt	DOE-NDC-47	52	Apr88	KTY	Hanly+ NDG.
^{204}Pb	$\sigma_{el}(\theta)$	2.5+6	8.0+6	Expt	DOE-NDC-47	52	Apr88	KTY	Hanly+ NDG.
^{204}Pb	$\sigma_{dif,inl}$	2.5+6	8.0+6	Expt	DOE-NDC-47	52	Apr88	KTY	Hanly+ NDG.

NEUTRON DATA REFERENCES

Element	Quantity	Energy (eV) Min	Max	Type	Documentation Ref	Page	Date	Lab	Comments
^{204}Pb	$\sigma_{n,n'\gamma}$	NDG		Expt	DOE-NDC-47	60	Apr88	KTY	Hanly+ NDG.
^{206}Pb	σ_{tot}	3.0+5	4.0+6	Expt	DOE-NDC-47	52	Apr88	KTY	Hanly+ NDG.
^{206}Pb	$\sigma_{el}(\theta)$	2.5+6	8.0+6	Expt	DOE-NDC-47	52	Apr88	KTY	Hanly+ NDG.
^{206}Pb	$\sigma_{dif,inl}$	2.5+6	8.0+6	Expt	DOE-NDC-47	52	Apr88	KTY	Hanly+ NDG.
^{208}Pb	σ_{tot}	1.0+6	1.7+8	Eval	DOE-NDC-47	141	Apr88	ORL	Johnson+ NDG.
^{208}Pb	$\sigma_{el}(\theta)$	8.0+6	1.7+7	Theo	DOE-NDC-47	79	Apr88	LRL	Hansen+ NDG. CFD EXPT.
^{208}Pb	$\sigma_{el}(\theta)$	8.0+6		Expt	DOE-NDC-47	170	Apr88	TNL	Walter+ NDG.
^{208}Pb	σ_{pol}	8.0+6	1.7+7	Theo	DOE-NDC-47	79	Apr88	LRL	Hansen+ NDG. CFD EXPT.
^{208}Pb	σ_{pol}	6.0+6	1.0+7	Expt	DOE-NDC-47	170	Apr88	TNL	Walter+ NDG.
^{208}Pb	$\sigma_{dif,inl}$	5.0+6	1.1+7	Eval	DOE-NDC-47	159	Apr88	OHO	Cheema+ NDG. DWBA ANALYS.
^{208}Bi	$\sigma_{n,\gamma}$	1.0+3	2.0+7	Theo	DOE-NDC-47	83	Apr88	LRL	Gardner+ GRPH. M,G-STATE PROD.
^{208}Bi	Evaluation	NDG		Eval	DOE-NDC-47	12	Apr88	ANL	Smith+ NDG. TBC. ENDF EVAL.
^{209}Bi	$\sigma_{el}(\theta)$	2.0+7	2.4+7	Expt	DOE-NDC-47	155	Apr88	OHO	Das+ NDG.
^{209}Bi	$\sigma_{dif,inl}$	5.0+6	8.0+6	Expt	DOE-NDC-47	4	Apr88	ANL	Smith+ NDG. DOUBLE DIFF SPECTRA.
^{209}Bi	$\sigma_{n,emis}$	1.4+7	2.6+7	Eval	DOE-NDC-47	143	Apr88	ORL	Fu. HF DOUB. DIFF. CS.
^{232}Th	$\sigma_{el}(\theta)$	1.9+5	2.5+6	Eval	DOE-NDC-47	113	Apr88	LTI	Sheldon+ NDG. ANG DIS, EXC FCN.
^{232}Th	$\sigma_{dif,inl}$	2.2+6	3.2+6	Expt	DOE-NDC-47	112	Apr88	LTI	Beghian+ GRPH. EXC. FCN, ANG DIS.
^{232}Th	$\sigma_{n,f}$	1.0+6	4.0+8	Expt	DOE-NDC-47	102	Apr88	LAS	Lisowski+ NDG. REL 235U (NF).
^{232}Th	Frag Spectra	7.2+5	3.1+6	Theo	DOE-NDC-47	77	Apr88	LRL	Becker+ NDG. LEGENDRE EXPANSION.
^{235}U	σ_{tot}		1.0+2	Eval	DOE-NDC-47	145	Apr88	ORL	Derrien+ MULTI-LVL R-MATRIX.
^{235}U	σ_{tot}	1.0+0	1.0+4	Expt	DOE-NDC-47	138	Apr88	ORL	Harvey+ NDG.
^{235}U	$\sigma_{el}(\theta)$	1.9+5	2.5+6	Eval	DOE-NDC-47	113	Apr88	LTI	Sheldon+ NDG. ANG DIS, EXC FCN.
^{235}U	$\sigma_{n,\gamma}$		1.0+2	Eval	DOE-NDC-47	145	Apr88	ORL	Derrien+ MULTI-LVL R-MATRIX.
^{235}U	$\sigma_{n,f}$	6.0+5	7.5+8	Expt	DOE-NDC-47	155	Apr88	LAS	Rapaport+ NDG.
^{235}U	$\sigma_{n,f}$	2.5-2		Expt	DOE-NDC-47	100	Apr88	LAS	Talbert+ CS (26.1 MIN-M-STATE).
^{235}U	$\sigma_{n,f}$	1.0+6	4.0+8	Expt	DOE-NDC-47	102	Apr88	LAS	Lisowski+ NDG. RATIO MEAS.
^{235}U	$\sigma_{n,f}$	+6		Expt	DOE-NDC-47	125	Apr88	NBS	Carlson+ NDG.
^{235}U	$\sigma_{n,f}$	NDG		Eval	DOE-NDC-47	129	Apr88	NBS	Carlson+ NDG. ENDF/B-6.
^{235}U	$\sigma_{n,f}$	2.5+6		Expt	DOE-NDC-47	127	Apr88	NBS	Duvall+ NDG. TBD.
^{235}U	$\sigma_{n,f}$	2.5-2	1.0+3	Expt	DOE-NDC-47	124	Apr88	NBS	Schrack+ NDG. TBP.
^{235}U	$\sigma_{n,f}$		1.0+2	Eval	DOE-NDC-47	145	Apr88	ORL	Derrien+ MULTI-LVL R-MATRIX.
^{235}U	$\sigma_{n,f}$	NDG		Revw	DOE-NDC-47	147	Apr88	ORL	Peelle+ NDG.
^{235}U	ν_d	NDG		Expt	DOE-NDC-47	115	Apr88	LTI	Couchell+ NDG. EQUIL. SPECTRA.

NEUTRON DATA REFERENCES

Element	Quantity	Energy (eV) Min	Max	Type	Documentation Ref	Page	Date	Lab	Comments
^{238}U	σ_{tot}	5.0+4	2.0+7	Eval	DOE-NDC-47	13	Apr88	ANL	Smith+ NDG.
^{238}U	$\sigma_{el}(\theta)$	1.9+5	2.5+6	Eval	DOE-NDC-47	113	Apr88	LTI	Sheldon+ NDG. ANG DIS. EXC FCN.
^{238}U	$\sigma_{dif.inl}$	2.2+6	3.2+6	Expt	DOE-NDC-47	112	Apr88	LTI	Beghian+ NDG. AND DIS. EXC FCN.
^{238}U	$\sigma_{n,\gamma}$	NDG		Eval	DOE-NDC-47	129	Apr88	NBS	Carlson+ NDG. ENDF/B-6.
^{238}U	$\sigma_{n,\gamma}$	1.0+3	1.0+5	Expt	DOE-NDC-47	137	Apr88	ORL	Macklin+ NDG.
^{238}U	$\sigma_{n,\gamma}$	NDG		Revw	DOE-NDC-47	147	Apr88	ORL	Peelle+ NDG.
^{238}U	$\sigma_{n,f}$	1.9+6	2.6+6	Expt	DOE-NDC-47	5	Apr88	ANL	Meadows+ REL 237NP (N,F).
^{238}U	$\sigma_{n,f}$	1.0+6	4.0+8	Expt	DOE-NDC-47	102	Apr88	LAS	Lisowski+ NDG. REL 235U (NF).
^{238}U	$\sigma_{n,f}$	NDG		Eval	DOE-NDC-47	129	Apr88	NBS	Carlson+ NDG. ENDF/B-6.
^{238}U	$\sigma_{n,f}$	NDG		Revw	DOE-NDC-47	147	Apr88	ORL	Peelle+ NDG.
^{238}U	ν_d	NDG		Expt	DOE-NDC-47	115	Apr88	LTI	Couchell+ NDG. EQUIL. SPECTRA.
^{238}U	ν_d	FAST		Expt	DOE-NDC-47	115	Apr88	LTI	Couchell+ GRPHS. N. SPECTRA.
^{238}U	$\sigma_{\gamma,n}$	NDG		Expt	DOE-NDC-47	121	Apr88	MHG	Quang+ NDG.
^{237}Np	$\sigma_{n,f}$	1.0+6	4.0+8	Expt	DOE-NDC-47	102	Apr88	LAS	Lisowski+ NDG. REL 235U (NF).
^{238}Pu	$\sigma_{n,f}$	1.0-1	1.0+2	Expt	DOE-NDC-47	163	Apr88	RPI	Alam+ NDG. NSE. TBP.
^{238}Pu	Res.Int.Fiss	NDG		Expt	DOE-NDC-47	163	Apr88	RPI	Alam+ RIF = 15.9 B, NSE TBP.
^{238}Pu	Res.Params.	NDG		Expt	DOE-NDC-47	163	Apr88	RPI	Alam+ NDG. NSE TBP.
^{239}Pu	σ_{tot}		1.0+3	Eval	DOE-NDC-47	145	Apr88	ORL	Derrien+ MULTI-LVL R-MATRIX.
^{239}Pu	σ_{tot}	1.0+0	1.0+4	Expt	DOE-NDC-47	138	Apr88	ORL	Harvey+ NDG.
^{239}Pu	$\sigma_{dif.inl}$	NDG		Expt	DOE-NDC-47	112	Apr88	LTI	Beghian+ NDG. TBD.
^{239}Pu	$\sigma_{n,\gamma}$		1.0+3	Eval	DOE-NDC-47	145	Apr88	ORL	Derrien+ MULTI-LVL R-MATRIX.
^{239}Pu	$\sigma_{n,f}$	1.0+6	4.0+8	Expt	DOE-NDC-47	102	Apr88	LAS	Lisowski+ NDG. REL 235U (NF).
^{239}Pu	$\sigma_{n,f}$	NDG		Eval	DOE-NDC-47	129	Apr88	NBS	Carlson+ NDG. ENDF/B-6.
^{239}Pu	$\sigma_{n,f}$		1.0+3	Eval	DOE-NDC-47	145	Apr88	ORL	Derrien+ MULTI-LVL R-MATRIX.
^{239}Pu	$\sigma_{n,f}$	NDG		Revw	DOE-NDC-47	147	Apr88	ORL	Peelle+ NDG.
^{239}Pu	ν_d	NDG		Expt	DOE-NDC-47	115	Apr88	LTI	Couchell+ NDG. EQUIL. SPECTRA.
^{240}Pu	Evaluation	NDG		Eval	DOE-NDC-47	149	Apr88	ORL	Weston+ NDG. ENDF/B-6.
^{242}Cm	$\sigma_{n,f}$	1.0-1	1.0+2	Expt	DOE-NDC-47	163	Apr88	RPI	Alam+ NDG. NSE. TBP.
^{242}Cm	Res.Int.Fiss	NDG		Expt	DOE-NDC-47	163	Apr88	RPI	Alam+ RIF = 12.9 B, NSE TBP.
^{242}Cm	Res.Params.	NDG		Expt	DOE-NDC-47	163	Apr88	RPI	Alam+ NDG. NSE TBP.

ARGONNE NATIONAL LABORATORY

A. TOTAL AND SCATTERING CROSS-SECTION MEASUREMENTS

The following titles relate to program elements which have recently been completed or are very near completion. Other less advanced aspects of the program cover a far wider mass range, with incident neutron energies of ≤ 10.0 MeV. Among these, e.g., are included on-going studies of Ca, Ga, Ge, Fe, Cr, In and Cd. Individuals who have a special need for scattering information are invited to contact A. B. Smith to determine the possible availability of preliminary data, or even for the implementation of new measurements responsive to particular needs.

1. Neutron Total and Scattering Cross Sections of Beryllium
(A. Smith, P. Guenther and J. Whalen)

The total cross section measurements are complete from 1.0 to ≈ 14.0 MeV. The differential elastic-scattering cross sections extend from 4.5 to 10.0 MeV in steps of ≈ 0.5 MeV. These elastic-scattering results are being very carefully verified. The results indicate that the angle-integrated elastic scattering cross section is known to several percent. Thus it is possible to deduce the nonelastic cross section to a similar level of uncertainty. Concurrently, the cross section for the inelastic excitation of the 2.43 MeV level is determined to ≈ 5-10% accuracy. Combined, these results seem to imply that the (n,2n) cross section from ≈ 4.0 to 10.0 MeV is now known to within an uncertainty of ≈ 5%. The measured values will be transmitted to Ohio University for R-matrix interpretation, and they are also being used in the beryllium evaluation cited in Section F.4 of this report. This work represents a contribution to the BES task force on beryllium cross sections for fusion-energy programs [1].

1. Office of Basic Energy Sciences Program to Meet the High Priority Nuclear Data Needs of the Office of Fusion Energy-1986 Review, September 17-19, 1986, Argonne National Laboratory, eds. D.L. Smith and H.D. Knox, Report DOE/ER/02490-4, Ohio University, Athens, Ohio (1986).

2. Fast Neutron Scattering from Vanadium
(A. Smith, P. Guenther and R. Lawson)

The measurement program, cited in the 1987 DOENDC Report, has been completed. The neutron-scattering data base now extends to ≈ 10.0 MeV, with sufficient detail to define the gross fluctuating structure. The total cross section results extend to ≈ 14.0 MeV. The physical interpretation effort is nearing completion. It is clear that the parameters of the relevant optical potential are energy dependent, as generally predicted by the dispersion

relationship. Moreover, the character of the energy dependencies changes at about 16-18 MeV above the Fermi energy, making a transition from the lower-energy parameters to those commonly encountered in "global" models. The transition is probably associated with the Fermi surface anomaly. The use of the dispersion relation predicts this behavior in a physically logical way, and provides a vehicle for extrapolating the potential to bound energies. The latter extrapolation is reasonably consistent with the real-potential parameters implied by the binding energies of known particle- and hole-states. The model has proven to be very useful in the vanadium evaluation cited in Section F.1.

3. Energy Dependence of the Optical Model for Fast-Neutron Scattering from Cobalt
(A. Smith, P. Guenther and R. Lawson)

This study of fast-neutron interactions with cobalt has been completed. Differential elastic- and inelastic-scattering cross sections were measured from ≈ 1.5 to 10.0 MeV over the scattering-angle range ≈ 18 to 160 degrees, with sufficient detail to define the energy-averaged behavior. Inelastic neutron groups were observed corresponding to "levels" at 1115, 1212, 1307, 1503, 1778, 2112, 2224, 2423, 2593 and 2810 keV. The experimental results were interpreted in terms of the spherical optical-statistical and coupled-channels models. A successful description of the elastic scattering below 10.0 MeV and the total cross section in the range 0-20.0 MeV was achieved using the spherical optical model with energy dependent strengths and geometries. These dependencies are large below ≈ 7.0 MeV, but become smaller and similar to those reported for "global" potentials at higher energies. This change of parameter energy dependence occurs at ≈ 19.0 MeV above the Fermi energy. It has also been seen in Bi-209 and probably marks the onset of the Fermi surface anomaly. Inelastic scattering to the levels below ≈ 1.8 MeV displays a forward-peaked behavior. This non-statistical effect is interpreted using a weak-coupling model in which an f-7/2 proton hole is coupled to the 2+ state in Ni-60. This vibrational characteristic provides an explanation for the unusual energy dependence and relatively small radius found for the imaginary optical potential. This coupling also contributes to the large value of this potential. The real spherical optical-model potential derived from the neutron-scattering results was extrapolated to bound energies using the dispersion relation and the method of moments. The resulting real-potential strength and radius peak at ≈ -10.0 MeV, while the diffuseness is at a minimum at this energy. The extrapolated potential is ≈ 8% larger than that implied by particle-state energies, and ≈ 13% smaller than indicated by hole-state energies. The measurements and model were an essential factor in the cobalt evaluation cited in Section F.2. This work is described in a laboratory report [1], and it has been accepted for publication in Nuclear Physics.

1. A. Smith, P. Guenther, J. Whalen and R. Lawson, ANL/NDM-101 (1987).

4. Fast Neutron Total and Scattering Cross Sections of Ni-58
(A. Smith, P. Guenther, J. Whalen and R. Lawson)

As noted in the 1987 DOENDC Report, we have measured total cross sections to 12.0 MeV and differential elastic- and inelastic-scattering results from 4.5 to 10.0 MeV, in steps of ≈ 0.5 MeV. The inelastic scattering involves mainly the first 2+ level which is strongly excited via direct processes. Additional high-resolution measurements, employing 15 m flight paths, define the excitation of levels up to 6.0 MeV. These latter measurements indicate that the level density does not increase with excitation at nearly the rate predicted by commonly-used continuum statistical representations. The data base, consisting of the present experimental results and lower-energy values previously reported from this laboratory [1], is being interpreted in terms of spherical and deformed (vibrational) models. There are interesting aspects of these interpretations, e.g., the measured values and associated models for elastic-scattering from Co-59 and Ni-58 are surprisingly different. This was experimentally verified by direct measurements of the ratios of elastic-scattering cross sections for these nuclei, and it cannot be accounted for by reasonable deformation effects. Large spin-orbit force differences might be responsible, but this seems physically unacceptable.

1. C. Budtz-Joergenson et al., Z. Phys. A319, 47 (1984).

5. Fast-Neutron Scattering from Elemental Zirconium
(M. Sugimoto*, A. Smith, P. Guenther and R. Lawson)

Elastic-scattering measurements, cited in the 1987 DOENDC Report, are complete to ≈ 10.0 MeV and the interpretation is proceeding. The primary problem in the experimental analysis is the treatment of very different compound-elastic contributions from the various isotopes making up the element. These differences complicate modeling of the neutron interaction with elemental Zr. Inelastic-scattering measurements are in progress and total cross sections measurements are complete to ≥ 10.0 MeV.

* Visiting Scientist. Permanent address: JAERI, Tokai Establishment, Japan.

6. The Energy Dependence of the Optical-Model for Fast-Neutron Scattering from Bismuth
(R. Lawson, P. Guenther and A. Smith)

This work, cited in the 1987 DOENDC Report, has been published in Physical Review [1].

1. R. Lawson, P. Guenther and A. Smith, Phys. Rev. C36, 1554 (1987).

7. Double-differential Inelastic-neutron Emission Measurements and Analysis

(P. Guenther and A. Smith)

This program aims to investigate the dependence of level-density parameters on nuclear mass and excitation. It exploits the observation that both the spontaneous-fission neutron field of Cf-252 and the emission spectra of many excited nuclei exhibit a Maxwellian-like energy distribution [1]. A simple analysis of the ratio of such spectra yields the nuclear temperature, a parameter often used in computer calculations of continuum-neutron distributions, under the assumptions of the statistical model. Results on Cu, Y and Nb have been reported [2] and those for Co are now being incorporated in an evaluation of Co (see Section F.2). New measurements have been made on In, Ta, Ho and Bi over the incident neutron energy range of 5-8 MeV. A preliminary analysis of the data indicates that the ratios for In, Ho and Ta readily yield the nuclear temperature, while those for Bi require a more detailed examination. That a paucity of levels persists well up in nuclear excitation energy may be understood because of Bismuth's proximity to the doubly-magic configuration. These results will be communicated at an upcoming Coordinated Research Program meeting at IAEA headquarters in Vienna [3].

---

1. P. Guenther and A. Smith, "Angular-distribution Neutron-emission Spectra of Niobium Following Bombardment by Fast Neutrons", Proc. Intl. Conf. on Nuclear Data for Basic and Appl. Science, Santa Fe, NM, May 13-17, 1985, p. 955 (1986).
2. P. Guenther and A. Smith, Bull. Am. Phys. Soc. 31, No. 8, p. 1237 (1986).
3. Second Mtg. of the Participants of the Coordinated Research Programme on the Measurement and Analysis of Double-differential Neutron Emission Spectra in (p,n) and (α,n) Reactions, February 8-10, 1988, IAEA, Vienna.

B. FISSION CROSS-SECTION MEASUREMENTS

1. An Integral Test of Several Fission Cross Sections in the Neutron Spectrum Produced by 7-MeV Deuterons Incident on a Thick Be-Metal Target

(Y. Watanabe*, J. W. Meadows and D. L. Smith)

The analysis has been completed for data obtained from integral neutron-fission cross-section ratio measurements in the continuum neutron spectrum produced by bombardment of a thick Be-metal target with 7-MeV deuterons. The ratios obtained are: Th-232/U-235, Np-237/U-235, U-238/U-235, Np-237/U-238, Th-232/Np-237, U-236/U-235, Pu-239/U-235, U-233/U-235, U-234/U-235, U-234/U-238 and U-236/U-235. A consistent set of fission cross section ratios relative to U-235 was obtained and compared with calculated values based on the representation of the neutron spectrum derived from time-of-flight measurements and the ENDF/B-V and JENDL-2 evaluations of the

differential cross sections. It was found that the results are relatively insensitive to small changes in the representation of the neutron spectrum. The calculated and experimental values for most of the isotopes are consistent within the experimental error, but for U-234 and U-236 the calculated cross sections are high by 6-7% which suggests that a re-normalization of these cross-sections may be needed in the 1-6 MeV region. The results of this investigation have been published in Annals of Nuclear Energy [1].

---

* Exchange Associate. Permanent address: Dept. of Nuclear Engineering, Kyushu University, Japan.

1. Y. Watanabe, J.W. Meadows and D.L. Smith, Annals of Nuclear Energy 14, 563 (1987).

2. Fission Cross-section Ratios at 14.7 MeV

(J.W. Meadows)

Results from this investigation, cited in the 1987 DOENDC Report, have been documented in laboratory reports [1,2] and an article has been submitted to Annals of Nuclear Energy for publication.

---

1. J.W. Meadows, ANL/NDM-97 (1986).
2. J.W. Meadows, ANL/NDM-98 (1987).

3. A Search for Structure in the U-238 Fission Cross Section Near 2.3 MeV

(J.W. Meadows, D.L. Smith and L.P. Geraldo*)

High resolution measurements of the U-238 fission cross section between 0.5 and 4.0 MeV neutron energy by Blons et al. [1] showed considerable fine structure. Much of this structure was on an energy scale of a few keV and involved changes in the cross section of 1 to 2%. However, at about 2.3 MeV there was a "hole" where the cross section varied by over 8%. Recently, in connection with an evaluation of the U-238 fission cross section, Poenitz [2] pointed out that it would be very desirable to confirm the existence of this feature. The prior data either had too poor resolution or had data points too widely spaced to see such structure. He further pointed out that the "hole" could be observed with relatively modest energy resolution, and recommended that a set of measurements be undertaken to either confirm or deny this particular feature of Blons et al. data.

We have carried out a measurement of the U-238 fission cross section relative to Np-237 in the neutron energy region 1.9-2.55 MeV. The Np-237 fission cross section was chosen as the reference, rather than the more usual and better known U-235, because the threshold in the (n,f) reaction made a large correction for low-energy room-return neutrons unnecessary.

Measurements were made at 20-keV intervals with an energy resolution of about 35 keV and a statistical accuracy of 0.7-0.8%. No evidence of structure was observed. Rather the U-238 fission cross section appeared to increase monotonically between 1.9 and 2.2 MeV at a rate of about 15% per MeV. Between 2.25 and 2.55 MeV it decreased at about the same rate.

---

* Visiting Scientist. Permanent address: IPEN, Sao Paulo, Brazil.

1. J. Blons, C. Mazur and D. Paya, Proc. 1975 Kiev Conference 6, 24 (1975).
2. W.P. Poenitz, private communication.

C. ACTIVATION CROSS-SECTION MEASUREMENTS

1. Differential Measurements and an Evaluation of the Co-59(n,α)Mn-56 Reaction Cross Section

(J.W. Meadows, D.L. Smith and R.D. Lawson)

This work, cited in the 1987 DOENDC Report, has been completed. The activation method has been used to measure differential cross sections for the Co-59(n,α)Mn-56 reaction in the threshold region from 5.07 to 9.98 MeV. The results from this investigation, along with other recent experimental data from the literature, were employed to adjust the ENDF/B-V evaluation for this reaction by means of the generalized least-squares method, thereby producing a new evaluation which better reflects contemporary knowledge of the cross section over the energy range which has been explicitly addressed by differential experiments (5.5-18 MeV). Nuclear-model calculations were also performed in order to develop a physically-reasonable differential cross-section shape for extrapolation towards threshold so that this evaluation spans the entire energy range required for ENDF/B (threshold to 20 MeV). Attention was given in this work to covariances, in both the measurement and evaluation processes. Finally, the resulting differential evaluation was employed in calculations of fission-spectrum averaged cross sections which were then found to compare quite favorably with corresponding measured values from the literature. The results of this work have been published [1] and they are also included in a comprehensive evaluation of cobalt, as discussed in Section F.2.

---

1. J.W. Meadows, D.L. Smith and R.D. Lawson, Annals of Nuclear Energy 14, 603 (1987).

2. Differential Cross-section Measurements for the Fe-54(n,α)Cr-51 Reaction

(D.L. Smith, J.W. Meadows, L. R. Greenwood, W. Mannhart* and L.P. Geraldo**)

Differential activation cross section measurements have been performed in the neutron energy range from threshold to ≤ 10 MeV using natural Fe

samples and U-238 fission as the neutron-fluence standard. Gamma-rays emitted in the decay of Cr-51 were observed with a Ge detector calibrated using standard gamma-ray sources from the National Bureau of Standards and a Cr-51 reference standard from Physikalisch-Technische Bundesanstalt (PTB), Fed. Rep. of Germany. Final analysis of the data is awaiting receipt of some calibration results from PTB.

---

* Visiting Scientist. Permanent address: PTB, Braunschweig, Fed. Republic of Germany.
** Visiting Scientist. Permanent address: IPEN, Sao Paulo, Brazil.

3. Integral Activation Cross Section Measurements and Consistency Test for Various Representations of the Be(d,n) Thick-target Neutron Spectrum

(D.L. Smith, J.W. Meadows, P.T. Guenther and L. R. Greenwood)

Final integral activation cross section results have been obtained for thirteen different reactions of interest for fission- and fusion-energy applications. These results have been combined with several representations of the Be(d,n) spectrum produced by 7-MeV incident deuterons using the least-squares adjustment procedure embodied in the code STAYS'L [1]. It has been found that reasonably good C/E consistency can be obtained with very minor adjustments to either the cross sections or the neutron spectrum representation if a neutron spectrum representation based on time-of-flight measurements with a fission chamber are employed as the a priori for the adjustment procedure. In all instances the C/E values differed from unity by no more than 10%. Preliminary results from this investigation were reported at the 6th ASTM/EURATOM Symposium on Reactor Dosimetry [2]. A journal article describing this work will be prepared following completion of a detailed assessment of uncertainties for the measured integral activation cross sections.

---

1. F.G. Perey, ORNL/TM-6062 (1977).
2. D.L. Smith, J.W. Meadows, P.T. Guenther and L.R. Greenwood, "Development of the Be(d,n) Neutron Source for Cross-Section Investigations in the Few MeV Energy Range", Proc. 6th ASTM/EURATOM Symposium on Reactor Dosimetry, Jackson Hole, Wyoming, May 31-June 5, 1987.

4. Neutron-activation Cross-section Measurements at 14.7 MeV

(J.W. Meadows, D.L. Smith, M.M. Bretscher and S.A. Cox)

This work, cited in the 1987 DOENDC Report, has been published in Annals of Nuclear Energy [1].

---

1. J.W. Meadows, D.L. Smith, M.M. Bretscher and S.A. Cox, Annals of Nuclear Energy 14, 489 (1987).

5. The Production of Nb-91, Mo-93 and Nb-93m by 14.7-MeV Neutrons and the Half Life of Nb-91
(L.R. Greenwood and D.L. Bowers)

Previously we have reported cross section measurements near 14.7 MeV for the production of Nb-94 (20300 y) from natural and enriched Mo-94 targets [1]. These samples were irradiated at the Rotating Target Neutron Source II at Lawrence Livermore National Laboratory, and the Nb-94 activity was determined by Ge gamma spectroscopy. Recently we have measured the X-ray activities of Nb-91 (680 y), Mo-93 (3500 y) and Nb-93m (16.13 y) from the same samples using a thin Ge detector and a Nb-93m standard from the U.S. National Bureau of Standards (SRM 4267). The cross section for the production of Nb-91 at 14.7 ± 0.5 MeV was found to be 602 ± 119 millibarns. the largest part of the uncertainty in this measurement comes from the half life, which is only known to 19%. Our result represents the total production of Nb-91 from Mo-94 and includes the (n,2n) reactions to both the ground state and isomeric state in both Mo-91 and Nb-91, as well as the (n,d+np+pn) reactions. If we compare our result to previous data for these reactions, we find that our cross section is about twice what would be expected. Ours is the only direct measurement of Nb-91; previous data measured only Mo-91 and we have estimated the contribution from the (n,d+np+pn) channels using the THRESH2 computer code. The most likely explanation for this difference is that the half life of Nb-91 is closer to 350 years rather than the value of 680 ± 130 years reported previously.

We were also able to measure the combined activities of Mo-93 and Nb-93m, both of which have the same X-rays. This places upper limits on the cross sections of 810 mb for Mo-94(n,2n)Mo-93 and 26 mb for Mo-94(n,d+np+pn)Nb-93m. We are now attempting to chemically separate the Nb and Mo which would determine cross sections for each nuclide. These results will be published shortly [2]. These measurements are needed in order to predict the production of long-lived radioisotopes in fusion reactor materials for maintenance and waste disposal applications.

1. L.R. Greenwood, D.G. Doran and H.L. Heinisch, Phys. Rev. C34, 76 (1987).
2. L.R. Greenwood and D.L. Bowers, J. of Nuclear Materials.

6. Enhanced Helium Production from Iron
(L.R. Greenwood and D.G. Graczyk)

Analyses of iron samples irradiated up to 10**27 n/m**2 in the High Flux Isotopes Reactor (HIFR) at Oak Ridge National Laboratory found more helium than was expected from fast neutron reactions. The helium measurements by D.W. Kneff (Rockwell International) showed an excess which increased with the neutron fluence. This excess can be explained in two ways, either by fast reactions with transmuted iron isotopes or by a thermal neutron reaction with Fe-55 (2.7 y). Mass spectrometric measurements of the transmuted iron isotopes in each sample were coupled with THRESH2

predictions to estimate the proper fast-neutron helium production. These calculations only explain about half of the excess helium which was observed. Due to the large uncertainty in the isotopic (n,α) cross sections from THRESH2, we can only place limits on the cross sections for each process. If the fast reactions proceed in accordance with the THRESH2 calculations, then the thermal helium cross section for Fe-55 is 9 ± 4 millibarns. The mass spectrometric data establishes that the thermal, total absorption cross section for Fe-55 is 13.2 ± 2.1 barns, a value which is much lower than the previous estimate of 170 barns. This helium effect is of interest since it can be used to enhance helium production for ferritic materials in order to simulate damage in fusion reactor materials. Isotopic tailoring could enhance the helium production at least a factor of 6 for a one-year irradiation in HFIR. If there is a thermal helium reaction for Fe-55, then we could achieve fusion-like ratios of helium-to-dpa damage by doping samples with Fe-55 prior to irradition. This work will be published shortly [1]. Further work is being planned to irradiate separated isotopes of iron in order to determine fast helium cross sections for each isotope and to establish whether or not there is a thermal helium cross section for Fe-55.

1. L.R. Greenwood, D.G. Graczyk and D.W. Kneff, J. of Nuclear Materials.

D. NEUTRON SPECTRUM MEASUREMENTS

1. Ratio of the Prompt-Fission-Neutron Spectrum of Pu-239 to that of U-235

(M. Sugimoto*, A. Smith and P. Guenther)

This work, cited in the 1987 DOENDC Report, has been published in Nuclear Science and Engineering [1].

* Visiting Scientist. Permanent address: JAERI, Tokai Establishment, Japan.

1. M. Sugimoto, A. Smith and P. Guenther, Nucl. Sci. and Engineering 97, 235 (1987).

2. Spectrum of Neutrons Emitted from a Thick Beryllium Target Bombarded with 7 MeV Deuterons

(A. Smith, P. Guenther and B. Micklich*)

Spectra of neutrons emitted from a thick beryllium target bombarded with 7 MeV deuterons were measured at 25 reaction angles distributed between 0 and 159 degrees, and over the neutron-energy range ≤ 0.8 to > 11.0 MeV. These spectra were determined relative to the standard Cf-252 prompt fission-neutron spectrum using organic scintillation detectors and fast time-of-flight techniques. The results are available as numerical tables of

angle-energy differential distributions, and as numerical group cross sections suitable for establishing a reference field for applied studies. These results are particularly suited for mocking up neutron distributions in a fusion-blanket. This work is described in a laboratory report [1].

---

* Dept. of Nuclear Engineering, Univ. of Illinois, Urbana, Illinois.

1. A. Smith, P. Guenther and B. Micklich, ANL/NDM-103 (1988).

3. Investigation of the Low-energy Portion of the Neutron Spectrum from Bombardment of Thick Be-metal Targets with Deuterons

(J.W. Meadows, D.L. Smith and L.P. Geraldo*)

We have undertaken a comprehensive program of measuring the thick-target Be-9(d,n) neutron spectrum over a wide range of deuteron energies (≤ 7 MeV), neutron energies (≥ 10 keV to ≤ 12 MeV) and angles (zero to ≤ 160 degrees), e.g., see Section D.2 of this report and an earlier laboratory report [1]. Here we describe time-of-flight measurements conducted in 1987 with a fission chamber containing uranium enriched in U-235. This work incorporates the high-intensity cave facility recently installed in our laboratory [2]. So far, data have been acquired at a flight path of about 2.6 m at zero degrees for several deuteron energies in the range 4-7 MeV in order to carefully determine the nature of the low-energy portion of the neutron spectrum. Attention has been given to insuring the fidelity of the pulsed deuteron beams employed (e.g., elimination of beam sweep-retrace components) and to limiting the effects of scattered neutrons (i.e., neutrons which do not come directly from the target). Procedures for processing these data are under development, and additional data will be acquired in this experimental arrangement during 1988. Qualitative results obtained to date seem to indicate that there are relatively few neutrons in the primary spectrum at energies below 200 keV, a situation which bodes well for the use of these spectra for the integral testing of fast-neutron activation cross sections (e.g., see Section C.3 of this report).

---

* Visiting Scientist. Permanent address: IPEN, Sao Paulo, Brazil.

1. D.L. Smith, J.W. Meadows and P.T. Guenther, ANL/NDM-90 (1985).
2. D.L. Smith and J.W. Meadows, ANL/NDM-95 (1986).

E. INTEGRAL DATA-TESTING MEASUREMENTS

1. Integral Beryllium Studies

(A. Smith and B. Micklich*)

The neutron leakage spectrum from a beryllium sphere placed about the Be(d,n) source was precisely measured at ten reaction angles distributed between 0 and 158 degrees. The sphere was 8 inches in diameter, with a 2.5 inch diameter central cavity into which the source was placed. The mass of

the sphere was 7.87 kg. Spectra were measured with and without the sphere about the source, over the neutron energy range ≈ 0.8 to 11.0 MeV. The resulting transmissions clearly display the gross structure of the beryllium cross section, and they are sensitive to multiplication and scattering effects. Interpretation of the experimental results is proceeding mainly through use of the monte-carlo code MCNP and the ENDF/B-V data base. Preliminary calculational results are currently being refined using the improved source spectrum described in Section D.2 of this report. The calculational-experimental comparisons (C/E) will provide a measure of the adequacy of the existing ENDF/B beryllium data representation. Alternative beryllium data sets and calculational methods will also be used in the interpretation of the data, particularly ENDL and the TART monte-carlo code. These comparisons, together with the microscopic beryllium work cited in Section A.1 of this report, should result in a better understanding of the use of beryllium multipliers in fusion-energy systems.

---

* Dept. of Nuclear Engineering, Univ. of Illinois, Urbana, Illinois.

2. Integral Niobium Studies

(A. Smith, P. Guenther and B. Micklich*)

The planned measurements, cited in the 1987 DOENDC Report, were undertaken in 1987. While these were of a preliminary nature, they demonstrated the practicality of such measurements. This experiment consisted of observing the neutron spectra transmitted through a ≈ 25-cm diameter spherical shell of niobium from a Be(d,n) neutron source placed at its center. Monte-carlo interpretation of the results should give guidance as to the adequacy of existing evaluated microscopic neutron-data files. More quantitative measurements are planned when the apparatus for precisely aligning and supporting the very heavy niobium sphere is available.

---

* Dept. of Nuclear Engineering, Univ. of Illinois, Urbana, Illinois.

F. NUCLEAR-DATA EVALUATION ACTIVITIES

This program is generally formulated as a unified measurement, interpretation, evaluation and integral-test effort. Evaluations currently in progress and nearing completion are described below.

1. Vanadium

(A. Smith, D. Smith, J. Meadows, P. Guenther, T. Djemil* and R. Howerton**)

A comprehensive evaluated neutronic data file extending from 10**-5 eV to 20 MeV is nearing completion. The only remaining components to be

finished are: File-6 (energy-angle continuum-inelastic neutron spectra), File-33 (uncertainty specifications), and photon production. There are some significant changes from the ENDF/B-V file for this element. Associated documentation is currently available in draft form.

---

* Dept. of Nuclear Engineering, Univ. of Illinois, Urbana, Illinois.
** Lawrence Livermore National Laboratory, Livermore, California.

2. Cobalt
(A. Smith, D. Smith, P. Guenther, M. Sugimoto*, R. Lawson, J. Meadows and R. Howerton**)

A comprehensive evaluated neutronic data file for cobalt is nearing completion. Evaluation of all the cross sections and most of the angular distributions and emission spectra is finished above 0.1 MeV. Uncertainty specifications (File-33) for the prominent processes are completed. The resonance representation below 0.1 MeV and the File-6 representation of the continuum-inelastic spectra are in progress. Photon production remains to be completed. There are major changes from ENDF/B-V. Documentation for this work is available in draft form.

---

* Visiting Scientist. Permanent address: JAERI, Tokai Establishment, Japan
** Lawrence Livermore National Laboratory, Livermore, California.

3. Bismuth
(A. Smith, D. Smith, R. Lawson, P. Guenther, M. Sugimoto*, and R. Howerton**)

A comprehensive evaluated neutronic file for bismuth is approaching completion. Remaining to be done are: the resonance region, uncertainty specifications, File-6 for continuum-inelastic scattering, and photon production. The results are an extension of ENDF/B-V, with no large changes. Draft documentation is available for completed sections.

---

* Visiting Scientist. Permanent address: JAERI, Tokai Establishment, Japan
** Lawrence Livermore National Laboratory, Livermore, California.

4. Total Cross Section of Beryllium
(M. Sugimoto* and A. Smith)

An evaluation of the total cross section for Be has been completed from several hundred keV to 20 MeV, with detailed attention to uncertainties. It is planned to extend this effort to include other aspects of neutron

interaction with beryllium.

* Visiting Scientist. Permanent address: JAERI, Tokai Establishment, Japan

5. Elemental Zirconium
(M. Sugimoto* and A. Smith)

Work has commenced on a comprehensive neutronic evaluation for this element. The data base is being assembled from the files of the National Nuclear Data Center and the contemporary ANL measurement program.

* Visiting Scientist. Permanent address: JAERI, Tokai Establishment, Japan

6. Nickel-58
(A. Smith)

A partial evaluation, extending only from the upper limit of the resonance region (≈ 650 keV) to 20 MeV, is in progress. This work makes use of experimental and theoretical results obtained from other aspects of the ANL program.

7. Nb-93(n,n')Nb-93m
(L.P. Geraldo* and D.L. Smith)

The revision of an earlier evaluation from this group [1] is being undertaken due to the availability of extensive new data for this important dosimetry reaction. The data base has been collected and examined and the computer code UNFOLD [2], which will be used to perform this evaluation in accordance with the method of least squares, has been converted for operation on an IBM PC and compatibles. It is anticipated that this evaluation may very well incorporate certain clean integral results (e.g., those measured in the Cf-252 spontaneous-fission neutron spectrum or in very well characterized fast-reactor spectra) as well as differential data. Nuclear model calculations will also be employed to extend the evaluation toward threshold in a region where differential data are non-existent.

* Visiting Scientist. Permanent address: IPEN, Sao Paulo, Brazil.

1. A. Smith, D. Smith and R. Howerton, ANL/NDM-88 (1985).

8. Uranium-238
(A. Smith, M. Sugimoto* and R. Lawson)

Work has started on this file. It will extend in neutron energy from the inelastic-scattering threshold (≈ 50 keV) to 20 MeV. Work on the total

cross section is finished, including a detailed specification of uncertainties. Documentation on the work completed to date is available in draft form.

---

* Visiting Scientist. Permanent address: JAERI, Tokai Establishment, Japan.

9. Adjustment of Evaluated Fission Cross Sections by Integral Data
(Y. Kanda*, Y. Uenohara*, D.L. Smith and J.W. Meadows)

Fission cross sections evaluated from differential experiments are adjusted by using integral data measured in the continuum spectrum produced by bombardment of a thick Be-metal target with deuterons. Since fission cross sections are among the most important quantities in evaluated files they are expected to be more accurately known than other reaction processes, with the possible exception of total cross sections. Simultaneous evaluations based entirely on differential data have been previously performed to meet this requirement [1,2]. However, good quality integral experiments are intrinsically valuable for cross section evaluation purposes because they provide a determination of mean cross sections which are distinct from results deduced from the differential experiments. The method employed in the present work permits a useful adjustment of the evaluated data files by means of such integral data in order to achieve consistency. This approach has not been widely employed previously because of a scarcity of appropriate data and computer memory limitations. In the present work, several specific fission cross sections compiled in the evaluated data files have been adjusted using available integral ratio data [3] in order to examine their mutual consistency. Evaluated results from prior work [2] have been used for this purpose. It is found that the adjustment procedure produces only very slight changes in the evaluated differential cross sections, thereby indicating that the integral data are quite consistent with the prior evaluated differential results.

---

* Dept. of Energy Conversion Engineering, Kyushu University, Japan.

1. A.D. Carlson, W.P. Poenitz, G.M. Hale and R.W. Peele, Radiat. Eff. 96, 87 (1986).
2. Y. Kanda, Y. Uenohara, T. Murata, M. Kawai, H. Matsunobu, T. Nakagawa, Y. Kikuchi and Y. Nakajima, Radiat. Eff. 96, 225 (1986).
3. Y. Watanabe, J.W. Meadows and D.L. Smith, Annals of Nuclear Energy 14, 563 (1987).

G. NUCLEAR THEORY AND MODEL CODE DEVELOPMENT

1. Model Codes
(R.D. Lawson)

We continue to modify and make additions to our nuclear-model

calculational capabilities. Spherical optical-statistical-model calculations are made using the code ABAREX, and similar work on deformed nuclei can be made using J. Raynal's code ECIS. Also of particular importance in our evaluations is a Weisskopf-Ewing code, CADE, written by D. Wilmore of Harwell (England). This code has been used in conjunction with the Lawrence Livermore National Laboratory code ALICE by M. Blann to estimate various reaction cross sections. Recently we obtained a version of the Los Alamos code GNASH which runs on a Cray computer. Once the operating system on the new ANL Cray system is completely debugged, we intend to implement this code as well.

2. High-spin Particle-hole States in Light- and Medium-Weight Nuclei
(R.D. Lawson)

Over the past few years there has been a great deal of interest in the properties of negative-parity particle-hole states in nuclei. In particular, states in which a single particle is excited from the highest spin state of the valence shell (denoted by j) to the largest spin available in the next shell (defined to be j') have been studied in even-even nuclei for the stretched-spin case (i.e., where the angular momentum of the resultant state is I=j+j'). Shell model calculations concerning the structure of these states have been made and compared with the results of (p,p') and (e,e') experiments. Recent work of this nature on Mg-26 and Cr-52 has been submitted for publication in Physical Review.

H. ANALYTICAL METHODS DEVELOPMENT

Considerable progress has been made during this reporting period in implementing new or upgraded methods used in the analysis of data. In several instances this work is associated with the gradual conversion of our existing computational activities from older computer systems to IBM or compatible PC's, a Micro-Vax II/GPX Workstation and upgraded mainframe systems at the ANL Computing Facility.

1. Upgrade of Monte-carlo Codes used for Multiple-event Correction of Neutron Scattering Data
(A.B. Smith)

Efficient and accurate analysis of the large volume of neutron scattering data generated in this laboratory with the ten-channel spectrometer is an essential feature of our neutron scattering program. Computer codes have been employed for many years in this laboratory to correct the raw data for multiple events. A revised package of these with several improved features has been prepared using an essentially computer-independent format involving a simple version of FORTRAN (generally consistent with FORTRAN II) which has been found to be very appropriate for

this purpose. This package has been found to run successfully on a series of older computers (e.g., the SEL 840MP, CDC-1784 and DEC PDP-11) and on newer systems (e.g., the DEC Micro-Vax II/GPX and IBM-3033). These codes, including detailed documentation, are available upon request.

2. Neutron-scattering Data Analysis Code (SCATTER)
(P.T. Guenther)

A new data handling and analysis code has been developed for IBM or compatible PC's which accommodates the unique data processing requirements of the neutron scattering program centered on the ten-channel spectrometer at this laboratory. The advent of fast, powerful personal computers has made possible the integration of numerous fragmented data processing steps with the attendant advantages of i) faster processing times, ii) less intermediate storage on transfer media (e.g., magnetic tapes), iii) convenient and constant access to the computer and iv) systematic and file-oriented handling and storage of data. This code has had its initial use in the analysis of the double-differential neutron emission data mentioned in Section A.7 of this report. The processing effort was reduced by an order of magnitude or more relative to earlier experience, while demands on the peripheral equipment was significantly reduced. It is also hoped that this processing code will facilitate the use of our computing capabilities by visiting investigators.

3. Implementation of the Data Evaluation Code GMA on a PC
(M. Sugimoto*)

The least-squares evaluation program GMA by W.P. Poenitz [1] has been implemented for operation on IBM or compatible PC's. This code has been written in Turbo Pascal, and it makes extensive use of commercial graphics routines available for operation within the framework of this language. The code has been used extensively in the evaluation program described earlier in this report. It is well documented and comes with a tutorial package.

---

* Visiting Scientist. Permanent address: JAERI, Tokai Establishment, Japan.

1. W.P. Poenitz, private communication.

4. Conversion of Activation Data Processing Routines to a PC
(L.P. Geraldo* and D.L. Smith)

Work is in progress to convert an existing package of activation data processing codes, including routines used in the analysis of covariance information, from an older computer system to IBM or compatible PC's. Several codes have been converted and tested with good results. Work on this project will be continued in 1988, and relevant data bases maintained in

formats applicable to an older computer system will be converted to storage media compatible with the PC's.

* Visiting Scientist. Permanent address: IPEN, Sao Paulo, Brazil.

5. Generation of Covariances for Experimental Data Sets
(D.L. Smith)

This work, cited in the 1987 DOENDC Report, has been published in Nuclear Instruments and Methods in Physics Research [1].

1. D.L. Smith, Nucl. Instr. and Meth. in Physics Research A257, 365 (1987).

6. Covariance Matrices for Collapsed Data Sets
(D.L. Smith)

This work, cited in the 1987 DOENDC Report, has been published in Nuclear Instruments and Methods in Physics Research [1].

1. D.L. Smith, Nucl. Instr. and Meth. in Physics Research A257, 361 (1987).

7. Probability Theory in Nuclear-Data Research
(D.L. Smith)

This monograph effort was continued at a modest level during the reporting period, with the result that several chapters in the second volume of this series were completed. Production of the first volume, assigned the Argonne report series number ANL/NDM-92, has been unavoidably delayed by the the need to transcribe the finished text from an older (non-compatible) wordprocessing system to our contemporary PC system. It is expected that this long overdue document will be available for distribution to the nuclear data community in 1988.

8. An Investigation of the Effects of Long-ranged Correlations in the Covariance Matrices of Nuclear Data
(D.L. Smith)

Attention has been called to the considerable sensitivity of uncertainty calculations to the magnitude of the long-range correlations which appear in covariance matrices. If such correlations do exist, they must be included in order to properly assess the impact of the uncertainties in the data. If, however, certain assumed long-range correlations are unrealistic, then analyses involving such correlation information are almost certain to produce misleading results. This issue has been explored in

general terms, and its importance illustrated by the consideration of examples based in part on recent work in this laboratory. Some practical suggestions have been generated for dealing with the matter of correlations in instances where the available information is incomplete. This work is described in a laboratory report [1].

1. D.L. Smith, ANL/NDM-99 (1987).

9. Investigation of the Influence of the Neutron Spectrum in Determinations of Integral Neutron Cross-section Ratios
(D.L. Smith)

Ratio measurements are routinely employed in studies of neutron interaction processes in order to generate new differential cross-section data or to test existing differential cross-section information through examination of the corresponding response in integral neutron spectra. Interpretation of such data requires that careful attention be given to details of the neutron spectra involved in these measurements. Two specific tasks are undertaken in the present investigation: i) Using perturbation theory, a formula is derived which permits one to relate the ratio measured in a realistic quasi-monoenergetic spectrum to the desired pure monoenergetic ratio. This expression involves only the lowest-order moments in the neutron-energy distribution and corresponding parameters which serve to characterize the energy dependence of the differential cross sections, quantities which can generally be estimated with reasonable precision from the uncorrected data or from auxiliary information. ii) Using covariance methods, a general formalism is developed for calculating the uncertainty of a measured integral cross-section ratio which involves an arbitrary neutron spectrum. This formalism is employed to further examine the conditions which influence the sensitivity of such measured ratios to details of the neutron spectra and to their uncertainties. Several numerical examples are considered in order to illustrate these principles, and some general conclusions are drawn concerning the development and testing of neutron cross-section data by means of ratio experiments. This work is described in a laboratory report [1].

1. D.L. Smith, ANL/NDM-102 (1987).

10. Investigation of the Nature of Positive Definiteness for Covariance Matrices
(L.P. Geraldo* and D.L. Smith)

Some basic mathematical features of covariance matrices have been reviewed, particularly as they relate to the property of positive definiteness, and the physical implications of positive definiteness have

been examined. Consideration has been given to the origins of non-positive definite matrices, to procedures which encourage the generation of positive definite matrices and to the testing of covariance matrices for positive definiteness. Attention has been paid to certain problems associated with the construction of covariance matrices using information which is obtained from evaluated data files recorded in the ENDF format. Examples pertaining to key points for each of the topic areas covered have been studied. A laboratory report on this work is in preparation.

---

* Visiting Scientist. Permanent address: IPEN, Sao Paulo, Brazil.

I. INSTRUMENTATION DEVELOPMENT

1. Harmonic Buncher

(A. Smith and J. Meadows)

An harmonic bunching system has been designed and constructed for use at the Fast Neutron Generator. The objective is a 3- to 4-fold increase in peak-pulse intensity while retaining a burst duration of ≈ 1.0 nsec. This system is ready for installation at the accelerator.

2. Upgrade of Digital Computer Systems

(J. Whalen, J. Meadows, A. Smith, R. Whitman, P. Guenther, D. Smith, M. Sugimoto* and L. Geraldo**)

A group-wide effort is well underway at the Fast Neutron Generator Laboratory to upgrade the in-house digital computer systems available to meet the needs of this facility for on-line data acquisition, data processing, database management, communications and word processing. Several IBM and compatible PC's in the XT or AT class have been acquired and implemented and more will be added as needed. These computers provide word processing, database management, communications and modest graphics capabilities, and they are also being heavily used for various data analysis and computational tasks (e.g., see Sections H.2, H.3 and H.4 of this report). A DEC Micro-Vax II/GPX workstation has just been delivered. This system, currently configured for two time-sharing users (though it can be expanded), will be used primarily for heavy-duty laboratory computations, especially monte-carlo simulations, the manipulation of large data bases, e.g., such as ENDF/B files and experimental data libraries obtainable from the CSISRS files at Brookhaven National Laboratory, for external communication and for sophisticated graphics applications. Currently, most on-line data acquisition tasks are being relegated to available DEC PDP-11 systems, but other options, e.g., the use of IBM or compatible PC's (particularly for multi-channel analyzer emulation) and the Micro-Vax system, are being explored. Work is also in progress on the development of

methods to link these various systems into an integrated internal network, and to acquire the hardware and establish the procedures which are required for convenient external communications.

---

* Visiting Scientist. Permanent address: JAERI, Tokai Establishment, Japan.
** Visiting Scientist. Permanent address: IPEN, Sao Paulo, Brazil.

1. BROOKHAVEN NATIONAL LABORATORY

The reactor-based neutron-nuclear physics research at BNL is composed of three categories: the study of nuclear structure with the (n,γ) reaction, the (n,γ) reaction mechanism and its application to pure and applied physics, and the spectroscopy of neutron-rich, fission product nuclides. These programs use the H-1 and H-2 beam ports of the HFBR. The tailored beam facility produces beams of thermal, 2- and 24-keV neutrons. A monochromator is used for resonance neutron studies. The TRISTAN on-line mass separator is used with a U-235 target to produce fission product nuclei. These facilities are operated in collaboration with a wide variety of collaborators from national laboratories and universities. The following sections describe the recent (n,γ) and TRISTAN studies of relevance to this report.

A. p-n INTERACTION AND COLLECTIVITY IN NUCLEI

This general topic concerns a broad variety of interrelated subjects, including nuclear phase transitions, the development of collectivity, the evolution of subshell structure, the behavior of intruder states, and the structure of the valence space. These areas have long been of interest to TRISTAN because of the access it provides to the phase transitional regions around A=100 and A=150, and to near semi-magic nuclei such as cadmium where intruder states are systematically observed, and because of the g-factor measurement capabilities which have been developed into a tool for rather directly counting effective numbers of valence nucleons.

In the last couple of years it has proved possible to interpret nuclear g-factors, of 2^+_1 states, in terms of the number of valence protons or neutrons. The idea is based on the Interacting Boson Approximation (IBA) but is nearly parameter-free in that model and therefore is not subject to the normal uncertainties in parameterizing the Hamiltonian. The relevant equation is

$$g(2^+_1) = g_\pi N_\pi + g_\nu N_\nu .$$

Here, g_π and g_ν are boson g-factors: they can be determined by global fits to extended sequences of nuclei. Then, given either N_π or N_ν, the other quantity can be extracted from the known $g(2^+_1)$ factor. An even better approach, developed in the last year, is to utilize a second equation, for $B(E2:2^+_1 \rightarrow 0^+_1)$ values, to provide two equations in the two unknowns, N_π and N_ν. Unfortunately, while the g-factor expression is very general and does not depend on details of the nuclear structure involved, analytic expressions for the B(E2) values have only been known for the three symmetries of the IBA. Therefore, to pursue this effort it has been necessary to develop an approximate analytic expression for the B(E2) values that has rather broad applicability. This has been done, in

collaboration with A. Wolf of Israel, who spent a sabbatical year at TRISTAN. As a result, g_π and g_ν values are now known for essentially all nonclosed shell nuclei from A=80-200. The latter exhibit a systematic variation with mass which is still not completely understood theoretically and presents a challenge to microscopic models of the valence space. In particular, an anomaly in g_π and g_ν has been discovered in the Er and Yb regions which may be related to a saturation of collectivity in this region (see below) and to properties of the newly-discovered isovector collective mode. As for the N_π and N_ν values, it has been possible to map out the proton and neutron valence nucleon numbers in great detail in the entire rare earth region. Two results are of considerable importance. In the A=150 transitional region, the N_ν values were found to behave normally, that is, the empirically-extracted values are the same as those one would obtain simply by counting from an N=82-126 shell. The N_π values, on the other hand, exhibit a sharp discontinuity, when plotted against neutron number, at N=90. This reflects the, now well known, breakdown of the Z=64 subshell gap as neutrons are added in the $1h_{9/2}$ orbit: the strong attractive p-n interaction between neutrons in this orbit and protons in the $1h_{11/2}$ orbit produces a lowering of the single particle energy of the latter which obliterates the Z=64 gap and changes, rather suddenly, the effective counting of valence protons. Thus these results provide a rationale and justification for the sudden onset of deformation near A=150. In the Er and Yb region, both N_π and N_ν, but especially the latter, cease increasing as valence nucleons are added toward midshell: this is in striking contrast with the expected behavior but in fact is consistent with a new interpretation of the systematic variation of B(E2) values in the rare earth and actinide nuclei that we have proposed this year.

This interpretation begins by noting the heretofore unrecognized fact that $B(E2:2^+_1 \rightarrow 0^+_1)$ values in deformed nuclei do <u>not</u> increase as the square of the valence nucleon number as nearly all models based on the valence space require. Rather, they saturate to nearly constant values as midshell is approached. This observation poses a serious difficulty for such models, in contrast to geometrical models where $B(E2) \propto \beta^2$ and therefore saturates as equilibrium deformations saturate. A solution to this potential difficulty stems naturally from a more detailed consideration of the p-n interaction. In the last couple of years, the so-called N_pN_n scheme has been proposed and has found remarkable success in systematizing the behavior of extended sequences of nuclei, especially in phase transitional regions. The quantity N_pN_n, calculated using the valence nucleon numbers, is intended to be a crude first-order measurement of the integrated p-n interaction strength. While nuclear observables behave smoothly against N_pN_n, they are not, in general, linear in this variable. Perhaps the reason is that the quantity N_pN_n neglects the orbit dependence of the p-n interaction. Specifically, near the beginnings of major shells valence neutrons and protons both enter equatorial, downsloping (in a Nilsson diagram) orbits with high mutual overlap. However, as more and more valence nucleons are added, the Pauli Principle mandates that they enter orbits oriented at successively greater angles to the equatorial plane.

Neutrons in such orbits will then, for example, have reduced overlap with equatorial proton orbits and vice versa. Therefore, while at the beginning of a shell, the p-n interaction strength will indeed scale linearly as N_pN_n, toward midshell it would be expected to level off and saturate. We have carried out detailed calculations during this period, using the Nilsson model and a BCS formalism to explicitly calculate the integrated quadrupole p-n interaction strength and have verified that this simple picture is indeed correct. If the p-n interaction strengths thus calculated are equated with effective N_pN_n values, denoted $(N_pN_n)^{eff}$, then one can use this technique to extract effective N_p and N_n values. When this is done, and B(E2) values are recalculated, the latter quite accurately reproduce the empirical saturation in B(E2) values noted above. Also, the extracted N_p and N_n values are consistent with those obtained empirically from the $g(2^+_1)$ factors.

Many of these ideas have developed as consequences of interpreting-factors measured at TRISTAN in the last few years. In particular, during this time period, difficult measurements of the $g(2^+_1)$ factors of ^{142}Ba were carried out. Earlier a similar measurement had been done but with much lower statistics. The point in the present case was that, since the above kinds of analyses relied heavily on the basic structure of the IBA g-factor expression, it seemed imperative to test its applicability in a region where the IBA predictions differed from other models and where there were no specific subshell effects that could obscure the issue. The hydrodynamical estimate, Z/A, and the modification to this by Greiner to incorporate different proton and neutron deformations, both give similar predictions for $g(2^+_1)$ for the Ba isotopes. In contrast, the IBA predicts strongly increasing g-factors as the closed shell at ^{138}Ba is approached. The differences only become substantial in ^{142}Ba but require a highly sensitive measurement to distinguish the two models. The resulting data were accumulated over more than one reactor cycle during FY 1987 and indeed confirmed the IBA predictions rather precisely.

The success of our efforts to interpret the structure of the valence space in terms of g-factors in the A=150 and rare earth regions has led to an attempt to extend this technique to the A=100 region with a measurement of the $g(2^+_1)$ factor for ^{98}Sr. The measurement, which is the first g-factor for this nucleus, has been completed. The results are analyzed, and an interpretation is in progress. It appears that the $g(2^+_1)$ factor is greater than expected from the IBA: an explanation of this fact should shed additional light on the structure of the A=100 transition region.

Another topic studied during this time period along the same lines is the proposal of the P-factor as an improved N_pN_n scheme. P is defined as $P=N_pN_n/(N_p+N_n)$ and can be looked on in any of several ways: as a normalized N_pN_n factor, as representing the ratio of the integrated strength of the p-n interaction and the pairing interaction, or, more intuitively, as simply the average number of p-n interactions of each valence particle. When the data for nuclear transition regions are plotted against P, it is found that a given region exhibits a similar dependence as

in the N_pN_n scheme but that plots for different regions are much more coalesced in a P-factor plot than against N_pN_n. It seems that all transition regions in heavy nuclei take place around P values from P=4-5. Whereas the N_pN_n scheme provided a relative measure of collectivity, the P-factor plots provide an absolute parameterization. Moreover, the specific values of P where transition regions take place, namely 4-5, are of interest in themselves. Since typical p-n interaction strengths are on the order of 200 keV, whereas the like nucleon pairing interaction is approximately 1 MeV, the P_{crit} values of 4-5 correspond to just that point in the valence space where the integrated p-n strength will begin to dominate the integrated pairing strength.

One of the easiest measurements that can be carried out at TRISTAN is that of nuclear masses, generally via Q_β values. The measurement of a number of these this year and in previous years has stimulated an interest in the systematics of nuclear masses. As a result one effort has been to study the systematics of these against P. The result has been the discovery that plots of semi-empirical microscopic masses (empirical masses minus spherical macroscopic masses) against P fall on nearly straight lines. While this is not at all yet understood theoretically, it provides a possible new tool for the prediction of atomic masses. Such a program is under investigation and tests are currently being planned.

A final effort in understanding the effects of the p-n interaction and of nuclear transition regions has been the development of a number of level schemes in the A=100 region, for both odd and even mass nuclei. These include empirical studies at TRISTAN within the last year of ^{96}Y, ^{98}Mo, ^{96}Zr, ^{98}Y, ^{101}Nb, and ^{102}Zr. Some of these studies relate more to shell structure and β-decay theory and will be discussed below. However, the studies around A=101 have revealed possible evidence for pairing-free rotational motion, that is, rotational motion in which the inertial parameter equals the rigid body value. The issue is not completely clear, as yet, and may be instead an effect of Coriolis mixing. However, the possibility is intriguing and may relate to the particularly strong p-n interactions among overlapping orbits in this mass region.

B. NUCLEAR SYMMETRIES

This has been a topic of study for many years now in this program and continuing work was carried out during this year. Since the concepts are more familiar than that of the newly-evolving understanding of the p-n interaction, the discussion here can be briefer.

The IBA predicts three basic nuclear symmetries, that is, rotational (SU(3)), vibrational (U(5)), and axially asymmetric rotors (γ soft) or O(6). It has now turned out that the first known examples of all three of these symmetries have been discovered in this program: specifically the first O(6) nucleus, ^{196}Pt, was discovered in a detailed (n,γ) study a number of years ago, the only good examples of SU(3) in the Yb and Hf

nuclei near neutron number N=104 (note that while deformed nuclei are certainly rotational in character, most do not satisfy the specific requirements of SU(3) symmetry) were found in 1986 via a study of ^{178}Hf and an interpretation of neighboring nuclei, and, finally, the first good example of near harmonic vibrational motion was discovered in a TRISTAN experiment on ^{118}Cd. Furthermore, the best examples to date of evidence for nuclear supersymmetry have been found in (n,γ) studies here of ^{195,197}Pt and the first study of an odd-odd symmetry, in ^{198}Au, were also carried out in an ARC study here (with the result that little evidence for this proposed extension of the supersymmetry concept was found). In the current time period further studies of symmetries were carried out primarily in the Te isotopes, specifically ^{124,126}Te in which ARC studies at 2 and 24 kilovolts were done to test a recent proposal by Hamilton et al. that these nuclei also exhibit O(6) symmetry. The results, currently still under analysis, tentatively indicate that there is, in fact, virtually no solid evidence for O(6) character in these nuclei and that, rather, they more likely resemble vibrational nuclei with low lying intruder states.

The study of intruder states in Cd a few years ago which set out to test the prediction that these states should rise in energy away from midshell, because of decreased p-n interaction in their configurations, not only revealed the essential correctness of this idea but also disclosed that the higher intruder energy in ^{118}Cd left behind a virtually unperturbed near harmonic vibrational spectrum among the "normal" levels. As noted above, this was the first example of a good near harmonic vibrator and has spurred further studies to find additional examples. With the new capabilities of TRISTAN, stemming from improved ion sources, we have begun looking at ^{120,122}Cd with an order-of-magnitude more intensity than heretofore available and are planning to extend the search for vibrational structure, and its evolution, to still further neutron rich nuclei. Moreover, and of particular importance (see below) the new timing capabilities being developed will enable much more sensitive tests of symmetry structure by permitting the measurement of absolute transition rates, in particular B(E2) values.

Finally, an experiment being carried out in collaboration with the ILL in Grenoble to measure the lifetime of the 0^+_3 state in ^{196}Pt will provide the most critical test yet of O(6) character in that nucleus. This state has O(6) quantum numbers, $\sigma=\sigma_{max}-2=N-2$. Its decay to the first 2^+ state should be highly forbidden in this symmetry while, in U(5), this decay route is an allowed collective transition. Thus far, it has proved impossible in Coulomb excitation studies, to successfully reach this state and measure its B(E2) value. However, by using the double flat crystal spectrometers of GAMS 4 in Grenoble it is possible to measure the Doppler broadening of the decay line following recoil after emission of a primary γ ray in ^{196}Pt. Note that the recoil energy is $\leq$ 1 keV and therefore the measurement requires extremely high resolution. The data will be taken and the results analyzed during FY 1988.

C. NUCLEI NEAR NEW MAGIC REGIONS

As noted earlier, the ability of TRISTAN to access nuclei near new magic numbers provides an important test of shell model predictions. Thus far, unfortunately, while a number of empirical studies have been carried out, especially in the A≈80 region, the theoretical apparatus and codes have not been available nor has our own expertise developed sufficiently to enable much practical interpretation. This situation has now considerable changed with the installation of the Wildenthal shell model code. It is expected, then, that in the next year or two, we will be able to exploit the measurements at TRISTAN to provide interesting tests of the shell structure in these regions. Some results are already in hand. The two principal prongs of this effort thus far have centered on the study of the subshell structure near ^{96}Zr, which is linked to the coexistence of nearly doubly magic normal states and more collective intruder states, and the discovery of some $0^- \rightarrow 0^+$ β-decay transitions which are among the fastest first forbidden log ft values known to exist. The first topic involves an attempt to delineate empirically and understand theoretically the nature of the intruder states in ^{96,98}Zr and neighboring nuclei. Competing interpretations of these states involve both α-particle and two-proton excitations: the data themselves are conflicting and, thus far, have not been shown to lead to interpretations free of inconsistencies. With this in mind, extensive studies of these nuclei have been carried out at TRISTAN in collaboration with Kentucky, Lawrence Livermore National Laboratory (LLNL), Budapest, and Julich. The result is a marked extension of the empirical knowledge in these nuclei, along with a characterization of a number of levels in these nuclei as belonging to the intruder families. Moreover, a TRISTAN study of the absolute normalization of γ and β intensities in this region has shown that previous estimates for ^{98}Zr were off by a factor of four. Since the normal states should predominantly involve proton $p_{1/2}$ excitations, while the intruder levels must involve $g_{9/2}$ excitations, β decay from the Y parent should be forbidden to the latter. The relative decay branches therefore provide a measure of the mixing of the normal and intruder configurations and the factor of four alteration in the empirical branching ratio entails a radical revision, now, in our understanding of the mixing of these configurations. Since such mixing is predominantly two-state in character these results allow an extraction of the mixing matrix elements and therefore a test of microscopic models of the intruder mechanism.

The TRISTAN study of ^{96}Y decay, and the assignment of the Y parent as $J^\pi=0^-$, has led to the possibility of studying a fast first-forbidden $0^- \rightarrow 0^+$ β decay in a nearly double-magic nucleus (^{96}Zr). The result, a log ft of 5.6, is, as mentioned above, one of the fastest known. Since the wave functions of the normal states in ^{96}Zr, which has a closed proton shell at Z=40 and a nearly-magic neutron number of N=56 ($d_{5/2}$ subshell) are rather well known, a comparison of the empirically-measured absolute log ft value with one calculated in the shell model allows a sensitive test of the presence of meson exchange effects in β decay. The Zr example is comparable in quality, in fact, to those in much lighter nuclei, such as

^{16}O, and is one of the only tests available in heavy nuclei. The data and calculations have been carried out, the results are being analyzed, and preliminary conclusions indicate positive evidence for meson exchange effects of the same order as found in light nuclei.

D. NUCLEI NEAR THE r-PROCESS PATH

As noted in the introductory comments, the calculation of r-process nucleosynthesis is beset with currently insurmountable difficulties because these calculations require input of both stellar and nuclear parameters and the latter are more or less completely unknown for the neutron rich nuclei through which the r-process path flows. Therefore the empirical characterization of any of these nuclei, and in particular those where the r-process path passes through closed shells, is extremely critical in restricting the possible stellar scenarios. The three most critical nuclei are ^{80}Zn, ^{130}Cd, and ^{195}Tm. The last, of course, cannot be obtained at TRISTAN but the first two can be. The ^{80}Zn study was first reported a couple of years ago and the full level scheme was published in the last year. An attempt to study the ^{130}Cd region has so far not been successful due to the combination of low yields and conflicting lifetimes from nearby nuclei in the 130 mass chain. Nevertheless, it is hoped that, with improved ion sources, such a study will be feasible in the near future. The r-process exhibits smaller mass peaks in the A=100 and A=160 mass regions as well. Therefore, studies of nuclei in these regions, such as those described above, are also useful input to understanding the r-process.

One of the principal advantages of the new mode of operation at TRISTAN in which a collaborative team from BNL, Ames Laboratory, and Clark University participate in a coherent, coordinated physics research program, is that many experiments are now feasible which were not heretofore possible. Frequently this involves simply the length of time that can be devoted to a given measurement. Some of the critical studies in the past year, such as g-factor measurements in ^{142}Ba and ^{98}Sr, as well as the ^{80}Zn study and the timing measurements (see below) have exploited precisely this fact. As a result, however, the number of experiments carried out is numerically less. The priorities during the last year have been such that no further effort was made on the astrophysics-related theme of TRISTAN research. This is only a temporary hiatus and such research will be continued during the rest of FY 1988 and in subsequent years.

E. NUCLEAR LIFETIMES BY FAST ELECTRONIC TIMING METHODS

Although great progress has been made in understanding neutron rich nuclei far off stability in the last decade, much of the interpretation has, perforce, relied on level spin parity assignments, level energies, branching ratios, mixing ratios, and β-decay rates. A critical missing ingredient has been the ability to measure absolute transition rates, in particular B(E2) values. Such a problem is not present for neutron

deficient nuclei for which the recoil following their production in heavy ion reactions allows the use of various Doppler techniques. In contrast, on the neutron rich side, lifetimes are generally only accessible via electronic timing and have, therefore, generally been limited to the nanosecond (ns) range. A number of years ago efforts at fast timing measurements were carried out using fast plastic detectors but technological limitations in detector quality and timing characteristics precluded much success. However, recently, the advent of fast BaF_2 detectors and thin β detectors have provided the possibility for a rejuvenation of this technique. The basic idea is twofold corresponding to the two radiations (β followed by γ) involved. By using thin β detectors approximately equal energies are deposited regardless of the emitted β-ray energy itself. This gives very uniform β timing signals. Secondly, the BaF_2 detector provides extremely fast timing on the γ rays. The combination leads to the possibility of picosecond (ps) range timing capabilities. In the TRISTAN experimental setup, a third detector, of intrinsic Ge type, is used to form a triple coincidence that further simplifies the interpretation of complex decay routes. With this approach, it is rather easily possible to measure nuclear level lifetimes in the 50 ps to 1 ns range. To extend the capabilities to below approximately 30 ps, requires great care, precise geometrical alignment (since at this level of accuracy one must take account of variations of electron flight paths in the photomultiplier base), and extensive calibrations with known lifetimes. In the last year and a half TRISTAN has pioneered the development of such fast timing techniques and has succeeded to an extent far beyond even our own expectations. Originally we were anticipating the measurement of lifetimes in the 30-100 ps range but it now appears that measurements down to as low as full ps are possible and lifetimes in the 10-20 ps range seem to be rather easily obtained. This program has entailed a substantial amount of development work, modification and improvement of the techniques, and test measurements. The facility will be described briefly below. First, however, it is worthwhile to emphasize the importance of it and what the capabilities are in terms of nuclear structure, as we anticipate that such timing measurements will form a key element in future TRISTAN studies.

The number of possible measurements that are of nuclear structure importance is considerable. We will only mention a few. Clearly, the study of nuclear phase transitions, such as that near A=100 and A=150, would benefit greatly from the measurement of absolute B(E2) values for the decay of the 2^+_1 state, as well as of vibrational states such as the lowest intrinsic 0^+ states and the 2^+_2 level. These levels evolve from j^n shell model configurations near magic nuclei, to generalized $j_1{}^{n_1}$, $j_2{}^{n_2}$ configurations slightly further on, to vibrational excitations, and finally, via a transition region, to the ground state rotational band and the lowest vibrational excitations (β and γ vibrations) of deformed nuclei. The possibility of mapping this behavior throughout a transition region is an exciting one that is now offered by these timing techniques. Secondly, while there are, we think, secure theoretical foundations for the understanding of intruder states in vibrational nuclei near closed shells (e.g., the Cd and Sn nuclei), this entire field has been beset in the past

by rather large amounts of qualitative or hand-waving conclusions and interpretations. Partly this is based on precisely the lack of absolute B(E2) values connecting the various levels and the reliance on branching ratios. For example, the interpretation of the 0^+_2 level in the Cd isotopes as the normal two-phonon vibration and the 0^+_3 level as the intruder state is based primarily on branching ratios to the 2^+_1 level and on energy systematics. A definitive interpretation can only be forthcoming after absolute B(E2) values are measured. Combined with the ability of TRISTAN to access a range of Cd isotopes from ^{116}Cd to, possibly ^{124}Cd, the possibility of measuring absolute B(E2) values for these nuclei offers, for the first time, the possibility to investigate deeply the evolution of intruder and vibrational structures and their mixings throughout an extensive series of nuclei. Thirdly, of course, similar arguments apply to intruder states in transitional regions such as near ^{98}Zr and to intruder states that occur in coexistence with normal levels which are magic in character (^{96}Zr). Another area where timing measurements might possibly be of use is in the study of negative parity states (the decay of 3^- and 1^- levels), in particular in the Ba region where competing models depict such excitations alternately as octupole vibrations, α-particle clusters, or f-p boson effects. Fourthly, absolute B(E2) values for nuclei along the r-process path can be of use in removing ambiguities in the nuclear partition function which enters into the Saha equation for the r-process.

It should be clear from the above descriptions of the physics possibilities of the new timing measurements and of the apparatus being developed, that this new technique offers a major area for productive TRISTAN research for the foreseeable future. We anticipate that it will become a major component of the program in FY 1988, FY 1989, and FY 1990 (see sections below), along with a continuation of the active g-factor measurement aspect of the program, which we now expect will also extend to odd-mass nuclei. Currently, the TRISTAN fast timing capabilities are state-of-the-art or beyond: they involve both in-house expertise and the essential collaboration of M. Moszynski who is a world-renowned expert in photomultiplier timing technology. Our collaboration with Moszynski has proved fruitful over the last year and we anticipate return visits in the spring of 1988 and in subsequent years. We do not yet know how far the technique can be pushed although it seems clear that 10 ps is obtainable and lower lifetimes may also be accessible. Finally, it might be worth noting that the exploitation of this technique would be increased even further if it were combined with the upgrade of the TRISTAN facility attained by moving the ion source closer to the reactor.

The timing technique developed at TRISTAN is based on a triple coincidence between the β's that feed a level and two subsequent γ-ray deexcitations. The time between the β particle (detected by a fast plastic scintillator) and the deexciting γ recorded in a fast BaF_2 crystal is determined by a Time to Amplitude Converter (TAC). The other coincident γ transition (recorded by a high resolution Ge-detector) acts as a selector for the desired decay branch. A judicious choice of the selecting transition results in an enormous decrease in the complexity of the coincident γ

spectrum recorded in the fast BaF_2 scintillator. Typically, the spectrum is reduced to one dominating transition. Although this feature of selectivity by triple coincidence has been used in timing measurements before, it has been applied only to decays with a low Q_β, where the timing response of the detectors depends very sensitively to the energies of both β and γ transitions, making this technique applicable to only a few specific levels in a few nuclei.

The TRISTAN technique maintains the high selectivity of triple coincidences with a Ge-detector, but avoids the β energy sensitivity problems by utilizing a thin plastic Δ-E detector which has a uniform β response. Due to the thinness of the detector, the β's lose only a portion of their energy ($\approx$500 keV) giving signals that are essentially independent of their initial energy. The uniformity of the β signal is further ensured by electronically selecting a narrow energy range. Thus, this technique ensures a uniform detector response for β transitions with endpoint energies above 1.5 MeV. It is important to note that this response is the same for all members of a decay chain, and for other mass chains. Thus, there will normally exist ample opportunity for calibrations and cross tests using known lifetimes in the nuclide being studied and its neighbors. This is especially important since the timing response of the BaF_2 detector is strongly energy dependent.

BaF_2 is the newest discovery in fast scintillating crystals. It is relatively easy to handle and machine, and has high efficiency for detecting γ radiation especially by the photoelectric effect. BaF_2 crystals have two light components, a fast component giving timing comparable to that of fast plastics, and a slower component giving energy resolution comparable to that of NaI(Tl) scintillators. After initial tests, a collaboration with M. Moszynski from the Institute for Nuclear Studies, Warsaw, Poland, was begun. Using his expertise, the best timing resolution available anywhere was obtained. A resolution of 65 ps for the β detector and 75 ps for the BaF_2 crystal (at ^{60}Co energies or equivalent) were obtained. This resolution made it possible to use the setup on-line and measure half-lives of a number of levels (accessible in β decay of fission products) that have been previously measured by Coulomb excitation or equivalent methods. The time resolution allowed centroid shift measurements to be made with high accuracy excitement. The energy response was measured using a long-lived source as a reference for a prompt response. The resulting precision of the centroid shift is limited by the statistics of the measurement and calibration data and is of the order of 1-2 ps for the strongest lines. However, due to systematic errors and other phenomena that are not fully understood, the practical limit, at this time, is as about 10 ps. Further investigations during FY 1988 will reduce this limit. Already there are indications that 5 ps lifetimes can be measured. The timing system is also capable of measurement of the half-lives as short as 40 ps by means of a slope method which involves simply the measurement of the exponential slope of the delayed part of the TAC spectrum and yields, directly, the level half-life.

Currently the timing apparatus is being used to measure lifetimes in a series of neutron-rich Cd nuclei. Special emphasis is being placed on the measurement of a number of levels in ^{118}Cd. This nucleus is of particular interest, since it represents the first known case of an ideal vibrator. Analysis of the data is in progress, and will be completed in FY 1988. Full and detailed analysis of these first results will provide valuable insights to the limitations and problems associated with this triple coincidence technique.

In further collaboration with M. Moszynski, effects which contribute to systematic errors will be investigated so that additional improvements to the technique can be devised.

F. National Nuclear Data Center

1. Cross Section Evaluation Working Group (CSEWG)

CSEWG completed its 21st year of activity with its annual meeting on May 12-14, 1987. Emphasis in the past few years has been on completion of a simultaneous, self-consistent fit to the "neutron standard" cross sections. The fit has included both the 2200 meter per second data for the important fissile nuclides, the six standard cross sections and cross sections for several reactions closely linked to the standard cross sections via ratio measurements such as 239-Pu(n,f) and 238-U(n, γ).

The standards evaluation is complete. The data are available from NNDC as tables of E, σ(E), $\Delta\sigma$(E) or as ENDF-6 format sections of σ(E). The uncertainties are still preliminary and the covariance matrices are not yet available. A subcommittee of JEF, the European counterpart of CSEWG, has reviewed the CSEWG standards effort and concluded that it represented a high quality effort involving a careful review of the existing data base and best state of the art analysis methods. They concluded that the results were the best that could be obtained with present technology.

Work continues on the evaluations which will be contained in ENDF/B-VI. A 240-Pu evaluation by L. Weston, ORNL, has been submitted to Brookhaven. We expect to receive the remaining evaluations within the next 9 months. Review of the evaluations, both microscopic and integral, should be completed so as to release ENDF/B-VI in about one year. Unfortunately, little work will be done in the fission product area due to lack of funding.

Major new formats for the resolved resonance region were adopted. The Reich-Moore format was restored to its ENDF-5 format and approved for use for any nuclide where inelastic competition is negligible. A new generalized R-matrix format was also approved. More than two resonance regions (i.e., multiple resolved resonance regions) have been adopted for handling the new U-235 evaluation.

2. Nuclear Data Sheets

The NNDC has been producing the Nuclear Data Sheets at the rate of about an issue a month. Of these, nine issues a year are devoted to nuclear structure evaluation and the remaining three to the publication of Recent References.

The Center evaluated A=68, 71, 139, 144, 152 and 163 and submitted them for publication; A=69, 147 and 148 are being evaluated.

The U.S. is part of an international network of evaluators contributing recommended values of nuclear structure information to the Evaluated Nuclear Structure Data File (ENSDF). Publication of the Nuclear Data Sheets proceeds directly from this computerized file. In addition to the U.S., evaluations have been received or are anticipated from the Federal Republic of Germany, U.S.S.R., France, Japan, Belgium, Kuwait, Sweden, the People's Republic of China and Canada. India has joined the network and has started evaluation of mass-chains.

A new concise format for the published A-chains in the Nuclear Data Sheets has been approved by the international network and adopted. This format reduces the size of the publication without omitting essential information and improves its readability.

3. Online Services

For approximately 30 months, the NNDC has offered online access to several of its nuclear data bases. This service is available on the NNDC's VAX-11/780 computer via HEPNET (PHYSNET) or over telephone lines. In the past year, access to ENDF has been added to existing access to NSR, CINDA ENSDF and the numerical nuclear data base, NUDAT. We have recently provided NEWS, file transfer and electronic mail facilities and we intend to add access to the experimental nuclear reaction data base, CSISRS. During the past year, the service has been used by more than 30 researchers. Approximately 4500 retrievals have been done in that period with about 260 hours of connect time used. More than one-half of the accesses have been to the NSR data base. Last spring, the NNDC produced online systems and data bases for NSR, ENSDF, and NUDAT which have been installed on the Nuclear Energy Agency Data Bank VAX computer and will be available to researchers in their service area.

4. Neutron Data Atlas

Considerable effort has been devoted to production of the next edition of the neutron data atlas (formerly BNL-325). A thorough review of the existing neutron cross section data base for both completeness and accuracy was done. As a result of the review, the quality of both CINDA and CSISRS have been significantly improved. Photo-ready copy for all pages of the book have been completed. Publication was delayed because of contractual

differences between BNL and the publisher. We expect to have the publication available in May from Academic Press. Preliminary prices are $60 for hard bound and $30 for soft bound editions.

5. Charged Particle Reaction Data

Before the Nuclear Data Project at ORNL was reorganized in the late 1970's, it included a small charged particle reaction data compilation activity. This activity was transferred to the NNDC along with the responsibility for publishing the NUCLEAR DATA SHEETS. For several years after the transfer, as part of an international charged particle data compilation effort, we were able to continue to produce a bibliography of charged particle cross sections and thick target yields. Funding cuts forced us to discontinue that activity, but we were able to continue the publication of the bibliography with a reduced effort by deriving the publication from the NSR data base. In the past year, NNDC held the second meeting of the Medium Energy Nuclear Data Working Group, which includes among its activities a benchmark comparison of high energy nuclear model codes.

Several new compilations of high energy charged particle data have been added to the experimental data file, CSISRS, with the help of a visiting scientist from the People's Republic of China.

High energy neutron and proton induced libraries for Fe-56 have been prepared in the ENDF-6 formats.

COLORADO SCHOOL OF MINES

The research program at the Colorado School of Mines is centered on two main areas: measurements of charged particle induced nuclear reaction cross sections at very low energies and the application of these cross section measurements to the diagnostics of controlled fusion reactors. This report discusses our measurements. The breadth of reactions which we are able to study has been greatly improved by the recent acquisition of a new low energy, high current General Ionex model 1545 180 keV charged particle accelerator. This accelerator is in its initial stages of operation and preliminary results are reported.

A. MEASUREMENTS

1. Fusion gamma ray measurements (F.E. Cecil, F.J. Wilkinson III and D.M. Cole)

We have recently completed a multi-year project directed toward the measurements of the gamma ray to charged particle branching ratios of the d-d, d-t and d-3He reactions at low energies. The results of these measurements have been published[1-3] and are summarized in the Fig. A-1.

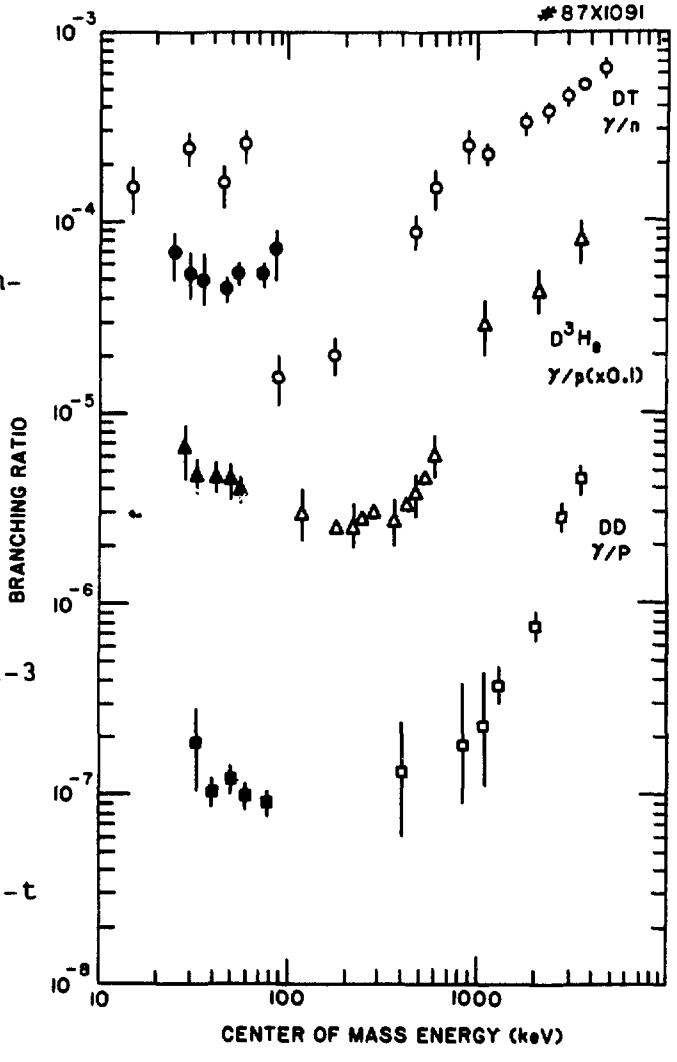

Fig. A-1. Gamma ray to charged particle ratios of the d-d, d-t and d-3He reactions. Present measurements are solid symbols.

1. F.E. Cecil and F.J. Wilkinson, Phys. Rev. Letts 53 (1984) 767.
2. F.J. Wilkinson and F.E. Cecil, Phys. Rev. C 31 (1985) 2032.
3. F.E. Cecil et al. Phys. Rev. C 32 (1985) 690.

2. Low energy capture cross sections. (F.E. Cecil and J.C. Scorby)

We have undertaken a new series of capture cross section measurements. These include the d-p, d-^{4}He, p-^{7}Li and p-^{11}B reactions atlow energies. The d-p capture reaction has been studied by bombarding a thick deuterated polyethelene target with a proton beam. The thick target yield of the 5.5 MeV gamma ray from this reaction has been measured between lab energies of 10 and 175 keV and is shown in Fig. A-2.

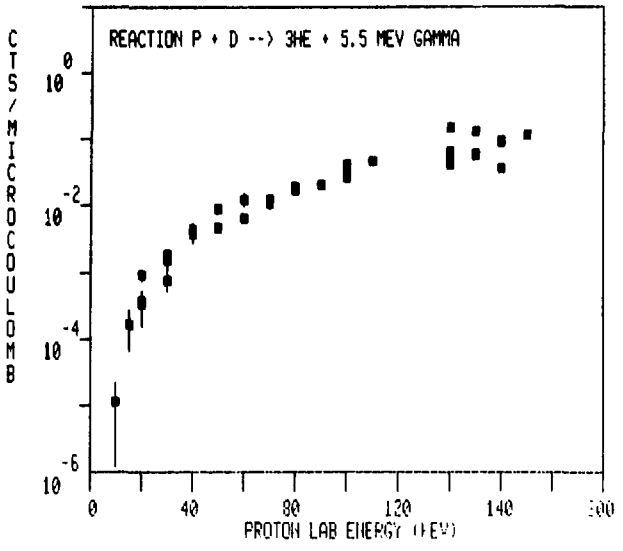

Fig. A-2. Yield of capture gamma ray from d-p reaction.

3. Secondary ion reaction spectroscopy (SIRS) (F.E. Cecil and J.A. McNeil)

We have measured the yield of the 3 MeV proton from the low energy d-d reaction during the bombardment of a deuterated-polyethelene target with protons and alpha particles. These yields are shown in Fig. A-3. These reactions presumably result from knocked-on target deuterons interacting with other target deuterons. The observation of these reaction products, which we call

Secondary Ion Reaction Spectroscopy (SIRS), may afford the opportunity for the measurement of total ion-deuteron total nuclear scattering cross sections at very low energies.

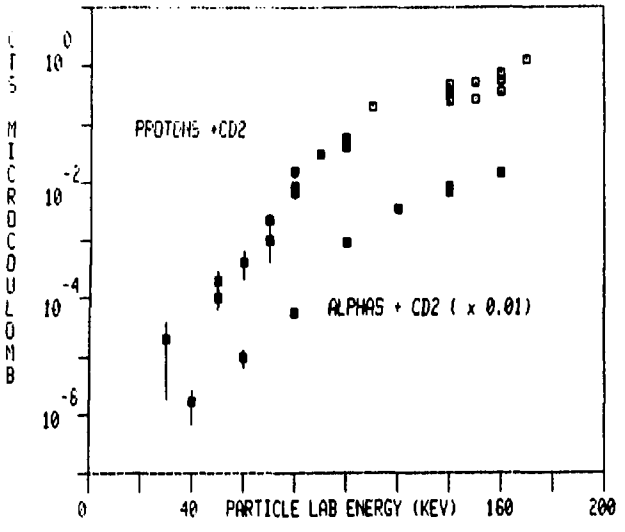

Fig. A-3 Yield of 3 MeV protons during the bombardment of CD2 target with protons (open squares) and alpha particles (solid squares).

CROCKER NUCLEAR LABORATORY AND DEPARTMENT OF PHYSICS
UNIVERSITY OF CALIFORNIA, DAVIS

A. MEASUREMENTS

1. Excitation of Isovector Monopole and Quadrupole Giant Resonances in ^{90}Zr(n,p) at 65 MeV.[#] [§] (T.D. Ford,[*] J.L. Romero, F.P Brady, C.M. Castaneda, J.R. Drummond, B. McEachern,[†] D.S. Sorenson, Zin Aung;[*] N.S.P. King;[‡] Amir Klein and W.G. Love[♡])

The ^{90}Zr(n,p)^{90}Y reaction at 65 MeV has been studied over a wide range of angles down to 0°. The data confirm the isovector monopole giant resonance recently observed in ($\pi^{\pm}$,π^0) data. In addition, the data together with an RPA-DWA analysis provide evidence for the $T+1$ isospin component of the isovector quadrupole giant resonance and for a new giant resonance, the spin monopole, both centered near $Q_{np} = -21$ MeV.

2. Gamow Teller and Spin-Dipole Strength in ^{90}Zr(n,p) at 65 MeV.[§] (F.P. Brady, T.D. Ford,[*] J.L. Romero, C.M. Castaneda, J.R. Drummond, E. Hjort, B. McEachern,[†] D.S. Sorenson, and Zin Aung;[*] N.S.P. King;[‡] Amir Klein and W.G. Love[♡])

^{90}Zr(n,p) differential cross sections at 65 MeV have been measured over a range of angles down to 0°. At low excitations the main strength appears to be in three concentrations of spin-dipole strength. Within certain limits Gamow Teller (GT) strength is not evident in the spectra. Together with the existing ^{90}Zr(p,n) data (as interpreted via theoretical calculations) the (n,p) results indicate that the Ikeda (GT) sum rule is satisfied to within $\lesssim$ 10% and that the mixing of Δ-hole excitations is of limited importance.

Published in *Physics Letters* B195, 311 (1987).
§ Work supported by the National Science Foundation grants PHY81-21003 and 84-19380 (UCD) and 85-42806 (UG).
* Present address: Institut für Kernphysik, KFK, D-7500, Karlsruhe, Fed. Rep. Germany.
† Associated Western Universities Fellow.
* Fulbright Scholar from University of Rangoon, Burma.
‡ Los Alamos National Laboratory, Los Alamos, NM 87545.
♡ Department of Physics and Astronomy, University of Georgia, Athens, GA 30602.

3. Pb (n,n'x) at 65 MeV and the Isospin Structure of the Giant Quadrupole Resonance.[†] (E.L. Hjort, F.P. Brady, J.L. Romero, J.R. Drummond, M.A. Hamilton and B. McEachern; R.D. Smith,[*] V.R. Brown, F. Petrovich[‡] and V.A. Madsen[*])

The first Pb (n,n'x) double differential cross sections have been measured for 65 MeV incident neutrons. These are compared to earlier (p,p'x) data. The isovector sensitivity of these nucleon probes is used to determine $M_n/M_p \lesssim N/Z = 1.54$ for the giant quadrupole resonance (GQR). This result is in agreement with several microscopic RPA calculations and in disagreement with a π^-/π^+ study which gives $M_n/M_p = 3.8 \pm 1.2$. The GQR M_p extracted from a recent ^{208}Pb (e,e'n) coincidence experiment is also in agreement with the RPA calculations and inconsistent with the pion work.

4. (n,p) Reaction Studies at Intermediate Energies.[§] (K. Wang, D. Pocanic, C.J. Martoff, and S.S. Hanna;[‡] F.P. Brady, J.L. Romero, C.M. Castaneda, J.R. Drummond, and B.C. McEachern; R.C. Byrd, C.C. Foster, and D.L. Friesel;[◇] J. Rapaport, and D. Wang[♡])

The (n,p) reaction has been studied at 120 MeV on the ^{6}Li nucleus and at 65 MeV on the ^{13}C nucleus. Cross sections and angular distributions were obtained; the results are compared with a DWBA calculation and with other experiments with different probes. The main interest in the experiments is to study isovector spin excitations and other multipole transitions. From the experimental value of the zero degree cross section, the spin-isospin part of the integral of the N-N effective interaction can be extracted by using the experimental GT transition strength and the formula for the $O°$ cross section from DWBA theory.

---

† Work supported by the National Science Foundation Grant 84-19380.

* Present address: MS B 243, T2 Group, LANL, Los Alamos, NM 87545.

‡ Permanent address: Physics Department, FSU, Tallahassee, FL 32306.

* Permanent address: OSU, Corvallis, OR 97330.

§ Presented at the "International Symposium on Medium Energy Physics", June 23-27, 1987, Beijing, China.

‡ Department of Physics, Stanford University, Stanford, CA 94305.

◇ Indiana University Cyclotron Facility, Bloomington, IN 47405.

♡ Department of Physics, Ohio University, Athens, OH 45701.

5. Excitation Function for the $^{12}C(n,p)^{12}B$ Reaction at $\theta_L = 17°$ for Incident Neutrons Between 30-150 MeV.[§] [*] (J. Rapaport;[†] J.L. Ullmann, R.C. Haight and S.A. Wender;[*] F.P. Brady, J. Drummond, E. Hjort, J.L. Romero and D. Sorenson)

The recently commissioned LANL high energy white neutron source was used to measure proton emission spectra at $\theta_L = 17°$ from an active CH target for $30 < E_n < 150$ MeV incident neutron energies. The excitation function for the $\theta_L = 17°$ differential cross section peaks at around 85 MeV incident neutron energy. Part of this cross section is interpreted as exciting the maximum of the dipole strength in ^{12}B. Details of this new facility will be presented.

6. Capabilities and Plans for Preequilibrium Nuclear Reaction Measurements at Target-4 at LAMPF.[§◇] (R.C. Haight, J.L. Ullmann, P.W. Lisowski, S.A. Wender, R.O. Nelson, S. Seestrom-Morris, and N.S.P. King;[‡] J. Rapaport and P. Zecker;[♡] F.P. Brady, J.L. Romero, E.J. Hjort, D.S. Sorenson and J.R. Drummond; C.R. Howell and W. Tornow.[♭])

The Target-4 neutron source at the Los Alamos Meson Physics Facility (LAMPF) has recently been commissioned and used as "white" source of fast neutrons from 1 to 500 MeV. A 90-meter flight path at a neutron production angle of 15 degrees has been characterized for neutron flux and spectral shape. The flux and shape agree well with calculated values showing that this is indeed an intense and useful white neutron source. Initial measurements of the $^{12}C(n,p)$ reaction at forward angles have been made in the energy range 50 to 500 MeV. The results point the way to improve detector schemes and to a program of (n,p) cross section measurements in the energy range where preequilibrium processes dominate much of the charged-particle emission spectra.

---

§ Supported in part by DOE and NSF grants.

* Abstract Submitted for the Baltimore, MD Meeting of the American Physical Society, April 18–21, 1988.

† Ohio University.

* Los Alamos National Laboratory.

◇ Presented at Specialists' Meeting on Preequilibrium Nuclear Reactions, Semmering, Austria, February 10–12, 1988.

‡ Los Alamos National Laboratory, Physics Division, Los Alamos, NM 87545.

♡ Ohio University, Physics Department, Athens, OH 45701.

♭ Duke University, Physics Department, Durham, NC 27706.

A. EXPERIMENTAL STUDIES

1. Systematic Study of the Half-Lives of Short-Lived Neutron-Rich Rare Earth Isotopes Produced in ^{252}Cf Fission (R. C. Greenwood, R. A. Anderl, J. D. Cole, M. A. Lee, H. Willmes*)

In a continuation of our earlier effort to identify new neutron-rich isotopes produced in spontaneous fission of ^{252}Cf using fast radiochemical separation techniques,[1-3] we have recently reported on the identification of six new neutron-rich rare-earth isotopes using the INEL ISOL facility.[4] Subsequently, we have extended that effort to include another new isotope, ^{164}Gd, refined the half-life values of ^{153}Pr and ^{157}Pm based on new measurements, and made other measurements to confirm, and improve the half-life values for, a number of other neutron-rich rare-earth nuclides. These results are summarized in Table A-1.

In view of the importance of gross nuclear properties, such as half-lives, of neutron rich nuclei off the line of β^- stability to astrophysical calculations involving the rapid neutron-capture process (r-process), it is instructive to compare the measured half-life values in Table A-1 to the predictions of existing models. At the present time, there exist two sets of half-life predictions, one by Takahashi et al.[5] based on the gross theory of beta decay and another by Klapdor et al.[6] based on a microscopic model employing a description of the distribution of beta strength. Such a comparison for each of the measured isotopes is shown in Table A-1. The results of this comparison follow the general trend noted by Kratz[7,8] and confirmed in our earlier study[4], namely that the model of Takahashi et al.[5] for nuclei far from stability systematically overestimates and the model of Klapdor et al.[6] generally underestimates the measured half-lives. Specifically, for the neutron-rich isotopes of Pr through Gd for which we have obtained half-life values, we conclude (1) that as one goes further away from the line of beta stability, the ratios R computed using the model of Takahashi et al.[5] tend towards values which are <0.4, and (2) that the values of

---

* University of Idaho

1 R. C. Greenwood et al., Radiochimica Acta 30, 57 (1982).
2 J. D. Baker et al., J. Inorg. Nucl. Chem. 42, 1547 (1980).
3 R. J. Gehrke et al., Radiochimica Acta 31, 1 (1982).
4 R. C. Greenwood et al., Phys. Rev. C 35, 1965 (1987).
5 K. Takahashi et al., At. Data Nucl. Data Tables 12, 101 (1973).
6 H. V. Klapdor et al., At. Data Nucl. Data Tables 31, 81 (1984).
7 K. -L. Kratz, Z. Phys. A 312, 236 (1983).
8 K. -L. Kratz, Nucl. Phys. A417, 447 (1984).

TABLE A-1. Half-life values (in sec.) measured for the new neutron rich rare-earth isotopes and their comparison with the results of two theoretical predictions.

Isotope	Experimental		Theoretical		R = (obs./pred.)	
	Present work	Other work	Takahashi et al.	Klapdor et al.	Takahashi et al.	Klapdor et al.
^{151}Pr	18.90±0.07	4.0±0.7 (Ref.1) 22.4±1.5 (Ref.2) 14 (Ref.3)	34		0.56	
^{152}Pr	3.7±0.2	3.24±0.19(Ref.4) 3.8±0.2 (Ref.5)	13	3.93	0.28	0.94
^{153}Pr	4.28±0.11		13	2.81	0.33	1.52
^{153}Nd	28.9±0.4	32±4 (Ref.2)	58		0.50	
^{154}Nd	25.9±0.2	26±2 (Ref.6)	77		0.34	
^{155}Nd	8.9±0.2		18	15.3	0.49	0.58
^{156}Nd	5.47±0.11		21	8.36	0.26	0.65
^{153}Pm	315±1	330±12 (Ref.7) 318±18 (Ref.8)	229		1.38	
^{155}Pm	41.5±0.2	48± 4 (Ref.9)	74	21.2	0.56	1.96
^{156}Pm	26.70±0.10	28.2±1.1 (Ref.10)	25	8.39	1.07	3.18
^{157}Pm	10.50±0.12		25	4.68	0.42	2.24
^{158}Pm	4.8±0.5		10	2.31	0.48	2.08
^{157}Sm	483±2	480±30 (Ref.11) 480±60 (Ref.12) 402±24 (Ref.10)	110		5.3	
^{158}Sm	318±2	331±5 (Ref.13) 312±12 (Ref.10)	390		0.82	
^{159}Sm	11.37±0.15	15±2 (Ref.10)	37	10.1	0.31	1.13
^{160}Sm	9.6±0.3	8.7±1.4 (Ref.10)	74	6.06	0.13	1.58
^{161}Eu	24±4	27±3 (Ref.10)	64	24.8	0.38	0.97
^{162}Eu	10.6±1.0		20	9.35	0.53	1.13
^{163}Gd		68±3 (Ref.14)	110	66.3	0.62	1.03
^{164}Gd	45±3		229	31.8	0.20	1.42

1. J. B. Wilhelmy et al., UCRL-19530, 178 (1970).
2. J. A. Pinston et al., Atomic Masses and Fundamental Constants 6, ed. J. A. Nolan, W. Benenson (Plenum, New York, 1980),
3. H. Mach et al., Bull. Am. Phys. Soc. 32, 1018 (1987).
4. J. C. Hill et al., Phys. Rev. C 27, 2857 (1983).
5. M. Brugger et al., Nucl. Instrum. Methods A234, 218 (1985).
6. T. Karlewski et al., Z. Phys. A322, 177 (1985).
7. K. Kotajima, Nucl. Phys. 39, 89 (1962).
8. R. K. Smither et al., Phys. Rev. 187, 1632 (1969).
9. R. C. Greenwood et al., Radiochimica Acta 30, 57 (1982).
10. H. Mach et al., Phys. Rev. Lett. 56, 1547 (1986).
11. N. Kaffrell, Phys. Rev. C 8, 414 (1973).
12. J. M. D'Auria et al., Can. J. Phys. 51, 686 (1973).
13. J. D. Baker et al., J. Inorg. Nucl. Chem. 42, 1547 (1980).
14. R. J. Gehrke et al., Radiochimica Acta 31, 1 (1982)

R computed using the model of Klapdor et al.[1] are systematically too low for the Nd and too high for the Pm isotopes, respectively. Furthermore, the sawtooth pattern in R values proposed in Ref. 2 using the predictions of Klapdor et al.[1], with turning points at Z = 59 and 65, is not supported by the present data. Rather, we note that it is the abnormally large values of R for the Pm data alone which might lead one to suggest such a sawtooth pattern.

2. Beta Strength Functions for Fission-Product Isotopes (R. C. Greenwood, M. A. Lee, R. G. Helmer, C. W. Reich)

A new thrust of our nuclear data measurement activity during the past year has been the development of a total absorption gamma-ray spectrometer system coupled to the INEL ISOL facility for measurement of beta strength-function distributions of short-lived fission-product nuclides. The gamma-ray spectrometer being used in this system consists of a large NaI(Tl) scintillator, which has dimensions 25.4-cm diameter x 30.5-cm length with a 5.1-cm diameter x 20.3-cm long axial well. Tests conducted to date with this scintillator have shown that it has excellent resolution, with full-width half-maximum values of <8% at 661-keV and ~3.5% at 6.8-MeV gamma-ray energies. The NaI(Tl) detector has been installed in a shielded cave at the INEL ISOL facility and a new ion-collection station and tape transport line has been developed to allow for rapid movement of the mass-separated fission isotope samples into the well of the scintillator. Studies of the background radiation spectrum measured with this scintillation detector have shown that, in the energy region above 3 MeV, it results primarily from neutron capture in I, presumably because of the close proximity of the ^{252}Cf shielded cave. Consequently, the NaI(Tl) shielding arrangement is currently being modified to install sufficient borated-polyethylene absorber to reduce the neutron-induced background counts to an acceptable level.

The use of total gamma-ray absorption spectrometry to obtain beta strength-function distributions is not straightforward, in that a number of sometimes contradictory experimental requirements must be met. These requirements can be summarized as (1) close to total gamma-ray absorption in 4π geometry, (2) no detection of the betas in the NaI(Tl) scintillator, (3) no gamma-ray absorption external to the NaI(Tl) scintillator (which is in clear contradiction with (2)), and (4) total-absorption-peak efficiencies which are independent of the decay paths from the beta-fed excited states. Studies are currently underway to develop a final arrangement for the spectrometer system which best meets these criteria. The most promising such arrangement appears at this time to involve a beta-gamma coincidence requirement, with the beta detector in less than 2π geometry, with a small amount of beta-absorbing material between the source and the scintillator.

---

[1] H. V. Klapdor et al., At. Data Nucl. Data Tables 31, 81 (1984).
[2] H. Mach et al., Phys. Rev. Lett. 56, 1547 (1986).

In parallel with this activity to develop a total absorption gamma-ray spectrometer system for beta strength-function distributions has been an activity to implement a suitable computer code to unfold the expected complex gamma-ray spectral distributions. Rather than writing a new code we have obtained the code UNFOLD from Dr. Radford at Chalk River National Laboratory and are in the process of adapting it to our application. In this code one starts with a set of measured (or computed) spectra for monoenergetic photons, processes them to remove full-energy and escape peaks, and interpolates between them to obtain response functions at intermediate photon energies. Using these sets of response functions, a successive stripping procedure from the highest measured energy is used to obtain a photon energy distribution from a measured spectral distribution. Because of expected weak beta-decay feeding to excited states close to the beta-decay energy, such a stripping procedure, rather than a matrix unfolding technique, would appear to represent the preferred method of spectral analysis. To date, test problems have been successfully run with this code using our MicroVAX-based analysis system.

3. Niobium Irradiations in Standardized Neutron Fields (JW Rogers, J. D. Baker, R. J. Gehrke)

The niobium materials irradiated in ^{252}Cf spontaneous fission neutron and ^{235}U fission neutron fields were prepared for measuring the ^{93m}Nb radioactivity produced by the $^{93}Nb(n,n')^{93m}Nb$ reaction.

Uniform sources were prepared by depositing the Nb solution onto paper filters. Similar amounts of solution was added to each filter paper. A teflon washer snugly protected the circumferential edge of the filter. This prevented wicking of the Nb mass and formation of a non-uniform source. The uniformity was determined by collimated scanning and autoradiography techniques. A special set of sources was prepared to measure the attenuation by the niobium in these sources and the results were in excellent agreement with the mass attenuation and energy absorption coefficients. The ^{93m}Nb radioactivities of the irradiated materials were measured using x-ray spectrometry. The reaction rates were computed and combined with the neutron fluences of the irradiations to determine fission-spectrum averaged cross sections. The results are as follows:

Spectrum	Cross Section (mb)	
	This Work	NBS[1]
^{252}Cf	150.6 ± 3.9	149. ± 10.
^{235}U	146.4 ± 3.8	164. ± 15.

[1] J. A. Grundl and C. M. Eisenhauer, "Compendium of Benchmark Neutron Fields for Reactor Dosimetry", National Bureau of Standards Publication NBSIR 85-3151 (January, 1986), pages 35 and 66.

These measurements provide what are believed to be the most accurate determinations of these cross sections that have thus far been reported.

These results have been reported at the 6th ASTM-EURATOM Symposium on Reactor Dosimetry, held in Jackson, WY in June, 1987 and will appear in the Proceedings of this symposium.

4. Intrinsic Reflection Asymmetry in ^{225}Ra: Additional Information from a Study of the α-Decay Scheme of ^{229}Th (R. G. Helmer, M. A. Lee, C. W. Reich, I. Ahmad*)

The knowledge of the decay scheme of ^{229}Th is important for both nuclear data needs (^{229}Th and its daughters are among those nuclides included in the ENDF/B Actinide File) and low-energy nuclear-structure physics (where the daugher nuclide, ^{225}Ra, is important for current ideas regarding octupole shape-related effects). Our comprehensive study of the ^{229}Th decay scheme has now been published.[1] The following is the abstract of this paper:

The level structure of ^{225}Ra has been studied by measuring the radiations associated with the α-decay of ^{229}Th. These measurements include α- and γ-singles spectra, and $\alpha\gamma$-, αe^- -, and $\gamma\gamma$-coincidence measurements. The α-spectra were measured with a high-resolution magnetic spectrometer and Si surface-barrier detectors, the γ-ray spectra with Ge and Ge(Li) semiconductor detectors and the electron spectra with a Si(Li) detector. Chemically purified and isotope separated sources were used for various experiments. These data provide the energies and intensities for 20 α-branches and for ~87 γ-rays. From this information and previous e^- spectrograph measurements, ~81 γ-rays are placed in a level scheme involving 22 excited states below 400 keV. Twenty of these excited states (excluding only tentative levels at 203 and 248 keV) can be assigned as members of four bands having $K^\pi=1/2^+$ (ground state), $1/2^-$ (55.1 keV), $3/2^+$ (149.9 keV) and $5/2^+$ (236.7 keV). It is found necessary to include an additional alternating term (B_1) in the rotational energy formula to adequately fit the energy spacings within the K=1/2 bands. This approach yields decoupling parameters of opposite sign for these two bands whose absolute values are closer to each other than previously deduced, which has relevance to their interpretation as being a parity doublet. We propose a band structure for the $3/2^+$ band at 149.9 keV that is significantly different from earlier proposals. Under this proposal, the energy-level spacings depart substantially from a simple I(I+1) pattern. No conclusive evidence has been found for the presence of a $K^\pi=5/2^-$ band which could be the parity-doublet partner of the well established

*Argonne National Laboratory

[1] R. G. Helmer, M. A. Lee, C. W. Reich and I. Ahmad, Nucl. Phys. A474, 77 (1987).

"favored" $5/2^+$ band at 236.7 keV. According to the predictions of models which include stable octupole deformed nuclear shapes, the members of such a $5/2^-$ band will be fed by α-transitions having relatively small hindrance factors; and they should, consequently, have been observed. Although the existence of reflection-asymmetric shapes in ^{225}Ra is an open question at present, the bulk of the available evidence on this nuclide can be accounted for, at least qualitatively, by the hypothesis that it possesses a static octupole-deformed shape. However, the nonobservation of the expected $K^\pi=5/2^-$ band and the large difference in the α-hindrance factors of the spin-7/2 members of the $K^\pi=1/2^+$ and $1/2^-$ bands represent potential problems for this interpretation which need to be studied further.

B. NUCLEAR DATA EVALUATION

1. Mass-Chain Evaluation for the Nuclear Data Sheets (M. A. Lee, R. G. Helmer, C. W. Reich)

As part of our involvement in the work of the International Nuclear Structure and Decay Data Evaluation Network, which carries out the evaluation of basic nuclear-physics data for publication in the Nuclear Data Sheets, we have the evaluation responsibility for the ten mass chains in the region $153 \leq A \leq 162$. The plan for the evaluation of these mass chains has been to undertake those most out of date first.

The status of the evaluation work for our region of responsibility can be summarized as follows:

A-Chain	Status (according to currency)
153	evaluation underway; last published 1982
161	evaluation underway; last published 1984
157	submitted for publication (1987)
158	submitted for publication (1987)
159	NDS 53 (1988)
154	NDS 52 (1987)
155	NDS 50 (1987)
156	NDS 49 (1986)
160	NDS 46 (1985)
162	NDS 44 (1985)

As is evident from this listing, with the completion of A=153, our mass chains will satisfy one of the desired objectives of the international evaluation network, namely currency < 5 years.

The mass -chain evaluation effort at INEL is affected favorably by our use of IBM-AT PC's to construct and edit the various individual data sets and by the fact that we are beginning to recycle our previous evaluations.

2. Evaluation of Decay Data for ENDF/B-VI (C. W. Reich, R. G. Helmer, M. H. Putnam)

Within the framework of the Cross Sections Evaluation Working Group, we have the responsibility for the evaluated experimental decay data in ENDF/B. At present, we are involved in preparing the evaluated decay-data sets for Version VI of ENDF/B. This involves upgrading the existing data, as well as expanding the number of nuclides for which such information will be available. Three general categories of nuclides are involved, namely, those in the Actinide File (~100 nuclides), the Activation File (~150 nuclides) and the Fission-Product File (~750 nuclides). To avoid proliferation of data evaluations containing only slightly different "adopted" values for various quantities, we are using the Evaluated Nuclear Structure Data File (ENSDF) as the starting point for this effort, supplementing and updating it as felt necessary. The first of the "Files" to be treated is the Activation File; and our work on it is presently nearing completion.

3. IAEA Coordinated Research Program on Decay Data for Ge Detector Efficiency Calibration (R. G. Helmer)

A Coordinated Research Program (CRP) was convened in June, 1987, at Rome by the International Atomic Energy Agency (IAEA) to discuss the quality of the decay data for the nuclides commonly used for the efficiency calibration of Ge detectors for gamma- and x-ray spectrometry. The participants in the meeting were from nine laboratories in seven countries, including R. G. Helmer from the INEL.

The goal of this group will be to get subsequent evaluators to use the values it recommends and, thereby, generate one internationally adopted set of values. The quantities to be evaluated are the nuclide half-life and the emission probabilities of the gamma and x-rays that can be used for Ge detector efficiency calibrations. It is also the purpose of the group to identify cases for which new measurements are needed, that is, where the data are poor or discrepant.

At an advisory group meeting in 1985 a list of 32 nuclides, given in Table B-1, was agreed on. Evaluations of the data for these nuclides were carried out for this CRP meeting At INEL, we have the responsiility for the evaluations for ^{94}Nb, ^{95}Nb, ^{152}Eu, and ^{203}Hg.

TABLE B-1. Nuclides to be Considered in the IAEA Review of Decay Data

^{22}Na	^{75}Se	^{137}Cs
^{24}Na	^{85}Sr	^{139}Ce
^{46}Sc	^{88}Y	^{152}Eu
^{51}Cr	^{93m}Nb	^{154}Eu
^{54}Mn	^{94}Nb	^{155}Eu
^{55}Fe	^{95}Nb	^{198}Au
^{56}Co	^{109}Cd	^{203}Hg
^{57}Co	^{111}In	^{228}Th(with
^{58}Co	^{125}I	daughters)
^{60}Co	^{133}Ba	^{241}Am
^{65}Zn	^{134}Cs	^{243}Am

4. Participation in One of the Working Groups of the ICRM (R. G. Helmer)

R. G. Helmer of INEL is Coordinator of the Gamma-and Beta-Ray Spectrometry Working Group of the International Committee for Radionuclide Metrology (ICRM), which represents metrology groups in 23 countries. In response to technical interest and leadership availability, three actions have developed. These are: the measurement of the emission probabilities of the gamma rays from ^{75}Se decay, to be led by R. Jedlovszky of the National Office of Measures in Hungary; a study of detection limits, to be led by J. E. Cline of Science Applications International, U.S.A., and one on peak-area fluctuations, to be led by F. E. Schima of the National Bureau of Standards, U.S.A.

DECAY STUDIES OF FISSION PRODUCTS WITH THE TRISTAN SEPARATOR

The TRISTAN on-line mass separator facility at the High Flux Beam Reactor at Brookhaven National Laboratory is used to study the decays of mass-separated neutron-rich nuclides produced in thermal neutron fission of ^{235}U. A number of different elements can be ionized and separated using a variety of ion sources. Measurements made at TRISTAN are discussed below. Members of the Ames Laboratory group (John C. Hill, F. K. Wohn, and J. A. Winger) have collaborated with other users from BNL (R. F. Casten, R. L. Gill, and H. Mach), A. Wolf and Z. Berant (Nuclear Research Centre, Beer Sheva, Israel) D. S. Brenner (Clark U.) and R. F. Petry (U. of Oklahoma). Experiments involved decay scheme studies via γ-ray spectroscopy, $\gamma\gamma$ angular correlations, $\beta\gamma$ coincidences and perturbed angular correlations.

1. Decay of ^{74}Cu to Levels in Even-Even ^{74}Zn (Hill et al.)

The plasma ion source at TRISTAN has been used to produce useful quantities of the neutron-rich Cu fission products. Preliminary experiments gave a half-life of 1.8s for Cu. γ singles and $\gamma\gamma$ coincidence measurements revealed a strong γ ray at 606 keV and weaker γ rays at 812, 1065, 1168, and 1671 keV. Using the coincidence information a preliminary level scheme for ^{74}Zn was constructed with levels at 606, 1418, 1671, and 2839 keV. Up until this work, no information was available on excited states in Zn isotopes heavier than ^{72}Zn. Systematics of the 2^+ states in Zn isotopes indicate an energy minimum at A = 74 which may reflect a neutron subshell closure at N = 38. More detailed γ measurements and a Q_β experiment are planned in the near future and a search for the interesting 0_2^+ state will be made.

2. Decay of the "Waiting Point" Nucleus ^{80}Zn (Winger et al.)

The decay of the "waiting point" nucleus ^{80}Zn is of great interest since it corresponds to one of three places where the r-process in nucleosynthesis hesitates as it crosses a magic neutron line (in this case N = 50). Preliminary results from this study have been reported earlier. A total of 26 γ rays were placed in a level scheme with 13 excited states up to 2655 keV. This material has been published in Phys. Rev. C.[1]

3. Test of the Singly Magic Character of the N = 50 Isotone ^{83}As (Winger et al.)

The study of the decay of ^{83}Ge (1.85s) to the N = 50 isotone ^{83}As has been completed and submitted to Phys. Rev. C for publication. Based on

---

[1]Winger, Hill, Wohn, Moreh, Gill, Casten, Warner, Piotrowski, and Mach, Phys. Rev. C 36, 758 (1987).

γ singles and $\gamma\gamma$ coincidence measurements a total of 51 γ rays were placed in a level scheme for ^{83}As with 27 levels up to 4.84 MeV. About half of the β intensity to excited states in ^{83}As populates a group of levels above 3.5 MeV which can be interpreted as primarily core polarization neutron particle-hole states. The density of levels up to 2.0 MeV is reasonably well reproduced by shell-model calculations assuming ^{78}Ni to be a closed doubly magic core.

4. The Structure of Odd-Odd ^{100}Y from Decay of ^{100}Sr (Wohn et al.)

The decay of ^{100}Sr (193ms) to levels in ^{100}Y was studied using a high temperature thermal ion source that is particularly advantageous for studying the deformed A $\simeq$ 100 region, since it is a good source of the alkaline earth elements. This study is now complete and has been published in Phys. Rev. C.[2] In that paper a discussion of the two-quasiparticle nature of some of the levels is given.

5. Single-Proton Nilsson Structure of the Z = 39 Nucleus ^{101}Y (Wohn et al.)

The TRISTAN high temperature thermal ion source has been used to study the A = 101 decay chain. These studies are of great interest in elucidating the Nilsson single-particle structure of the highly deformed nuclei in the A $\simeq$ 100 region. The first of these studies to be completed was the decay of ^{101}Sr (121 ms) to levels in the Z = 39 nucleus ^{101}Y. A total of 96 γ rays were placed in a decay scheme with 34 levels. The first 14 levels in ^{101}Y (below 1.1 MeV) are identified as members of four rotational bands associated with the Nilsson orbitals (with bandhead energies in keV) 5/2[422](0),3/2[301](510),5/2[303](666), and 1/2[301](890). These assignments are confirmed by simple particle-rotor calculations consisting of single quasiparticles coupled to an axially symmetric core. This material has been submitted for publication to Phys. Rev. C.

6. Single-Proton Nilsson Structure of the Z = 41 Nucleus ^{101}Nb (Wohn et al.)

Sources of ^{101}Zr were prepared at TRISTAN in order to study the structure of single quasiproton Nilsson states and their accompanying bands. A preliminary half-life for ^{101}Zr of 2.28s was determined. A preliminary decay scheme has been constructed on the basis of γ singles and $\gamma\gamma$ coincidence information. Data analysis is still in progress but over 50 γ rays have been associated with ^{101}Zr decay and three Nilsson bands have been identified in the odd proton nucleus ^{101}Nb.

---

[2]Wohn, Hill, Winger, Petry, Goulden, Gill, Piotrowski, and Mach, Phys. C. 36, 1118 (1987).

7. Single-Neutron Nilsson Structure of ^{101}Zr and ^{101}Mo (Wohn et al.)

Using the TRISTAN high temperature thermal ion source we have studied the decays of ^{101}Y whose half-life was measured to be 0.457s and ^{101}Nb whose half-life was measured to be 6.57s to levels in the odd neutron nuclei ^{101}Zr and ^{101}Mo respectively. In each case γ singles and $\gamma\gamma$ coincidence studies were carried out. In ^{101}Nb decay all of the γ rays seen by previous observers were identified and the total number of γ rays from ^{101}Nb decay has about doubled. Analysis of the ^{101}Nb decay data is in progress and a complete decay scheme has yet to be constructed. Analysis also continues on the decay of ^{101}Y to levels in ^{101}Zr. Over 80 γ rays have been attributed to ^{101}Y decay and a preliminary level scheme has been constructed with 30 levels up to 2023 keV. Four single quasineutron Nilsson bands have been identified.

8. Decay of the Low-Spin Isomer of ^{102}Y (Hill et al.)

The TRISTAN high temperature thermal ion source has been used to prepare more intense sources of the low-spin isomer of ^{102}Y which decays to levels in ^{102}Zr. Since very little primary Y is produced by our ion source we expect that most of the ^{102}Y activity results from the decay of ^{102}Sr($J^{\pi} = 0^{+}$) thus populating the low-spin ^{102}Y isomer. A prime motivation in this study is to search for excited 0^{+} states in ^{102}Zr in order to determine if the shape coexistence observed in ^{100}Zr disappears resulting in a fully deformed structure in ^{102}Zr. We have studied ^{102}Y by γ singles and $\gamma\gamma$ coincidence measurements, and data analysis is still in progress. A preliminary half-life of 0.4s was determined. The γ spectrum is sparse with only 6 γ rays identified so far in contrast to ^{102}Sr which has a rather rich γ ray spectrum probably indicating that a significant portion of the β intensity goes through the ^{102}Zr ground state.

UNIVERSITY OF KENTUCKY

That part of the research program in experimental low energy nuclear physics at the University of Kentucky which is carried out in the Van de Graaff Laboratory consists of four main efforts; neutron scattering, nuclear structure studies, capture reaction studies, and work on the details of the optical potential. Individual experiments often have at least a partial motivation of trying to answer a question of astrophysical interest. Other experimental work in nuclear physics in the areas of intermediate energy and of radioactive decay are carried out at other sites and was not included in this report.

A. NEUTRON SCATTERING

1. Collective, Shape-Transitional Nuclei (S.E. Hicks, J. Hanly, G.R. Shen, and M.T. McEllistrem)

a. Nuclear Dynamics from Coupled Elastic and Inelastic Scattering

The measurements of differential scattering cross sections and of total cross sections in the Os and Pt isotopes have been completed, and all data corrections to obtain cross sections have been made. The interpretations in terms of nuclear structure have also been largely, although not entirely, completed. We have learned that the Os and Pt nuclei with A $\geq$ 190 are all γ-soft nuclei rather than γ-rigid. Results for ^{194}Pt have been published to date in two papers.[1,2] These results give the surprising result that neutron induced collective excitations are much stronger than those revealed in Coulomb excitation. Furthermore, the description of the structure required to represent the neutron scattering cross sections sees a somewhat different set of E2 matrix elements than that found in Coulomb excitation. Relative excitations of levels are subtly different in neutron scattering than in electromagnetic excitation. Neutron scattering and Coulomb excitation both show that the excitation dynamics are those of a γ-soft nucleus, even though the excitations are different with the two classes of experiments.

These results for ^{194}Pt are made more interesting by finding that very different conclusions are provided by our interpretations for ^{192}Os. These interpretations, completed but not yet submitted for publication, show once again, also in accord with the Coulomb excitation results, that a γ-soft picture of the structure of this nucleus is alone consistent with the scattering cross sections, both elastic and inelastic. Several different γ-soft models are shown to give slightly different results, all in rather good agreement with our cross sections, except for minor differences. Surprisingly, however, if we simply take the set of E2 matrix elements connecting scattering

---

[1] Mirzaa, Delaroche, Weil, Hanly and McEllistrem, Phys. Rev. C32, 1488 (1985).

[2] Hicks, Delaroche, Mirzaa, Hanly and McEllistrem, Phys. Rev. C36, 73 (1987).

channels from the Coulomb excitation experiments, without appeal to any model, we get the very best description possible of our neutron scattering data. This is in sharp contrast to our results for ^{194}Pt. These results are being prepared for publication.

These contrasting results for the two shape transitional nuclei are in accord with the long held prejudice here that when the nucleus becomes well deformed, the valence neutron and proton fluids of the target nucleus are strongly coupled to each other, so all hadron scattering sees the same collective excitations. Conversely when collective nuclei are not stably deformed, when they have no stable shapes, then the neutron and proton fluids behave separately, leading to differences in scattering by different hadrons. The first excited state quadrupole moment of ^{194}Pt is essentially zero, while that of ^{192}Os is quite large, about 2/3 of the geometric rotational value. This is in accord with the suggestion that ^{192}Os is deformed, whereas ^{194}Pt is not; thus all hadrons see the same excitations in the Os nucleus, but not in ^{194}Pt.

b. Dispersion Corrections to Mean Fields

Our analyses, first of neutron scattering by ^{194}Pt and then separately by the other shape transitional nuclei, called for potentials or mean scattering fields whose strengths saturated below about 5 MeV. This "strange" saturation was systematic and unclear to us. Just at this time Mahaux and Ngo, and later Mahaux and Sartor and C. H. Johnson were demonstrating that dispersion relations, analogous to the well known Kramers-Kronig disperson relations in optics, were connecting the real and imaginary (absorptive) parts of the scattering field, just as optical dispersion connects the real and imaginary parts of the index of refraction.

Careful application of these dispersion relations, just completed, not only explains the saturation of potential strength, but also allows us to show a clear relation between the scattering potentials and the potentials needed to bind single particle levels in the compound nuclei. What had seemed to be a serious problem turns out to be an essential clue to extending a consistent description of the neutron plus target system to both negative and positive neutron energies. This is the first time that these dispersion relations are demonstrated for coupled-channels models with collective nuclei. They had only been well developed for closed-shell, spherical nuclei. A manuscript describing these results has been accepted for publication.[3]

2. Spherical Nuclei

a. Pb Isotope Scattering Study. (J. Hanly, S.E. Hicks, S.F. Hicks, G.R. Shen, J.L. Weil, and M.T. McEllistrem)

Measurements of differential scattering cross sections at 2.5, 4.6, and 8.0 MeV have been completed and reduced to cross sections, with all

---

[3] S.E. Hicks and M.T. McEllistrem, Phys. Rev. C37 (in press).

sample-size dependent and other corrections made. These measurements and data analyses have been completed for two isotopes, ^{204}Pb and ^{206}Pb. The total cross sections from 0.3 MeV to 4.0 MeV incident neutron energy were also measured. The separated isotope samples used had moderate enrichments, only 71.4% for ^{204}Pb and 88% ^{206}Pb for a radiolead sample. Thus very careful isotopic corrections had to be worked out using our data for the two indicated isotopes and data from the National Nuclear Data Center for ^{208}Pb and ^{207}Pb. These were particularly critical corrections for the total cross sections, since they are very sensitive to weak collective effects in scattering. We wished to ascertain with confidence these small collective amplitudes. The corrections were also very important for the differential elastic scattering cross sections, which are subtly different for the different Pb isotopes.

An important correction for the total cross sections is that for resonance self-shielding, an effect which results from the fact that the effective sample thickness changes on and off very strong resonances at low incident neutron energies. To make this correction, a special code, SESHRX, had been developed by Profs. Weil and Ron Winters of Denison University. This code had to be further developed and tested by John Hanly to assure its use with confidence for the rather large corrections encountered with the Pb isotopes.

The total cross sections and the elastic and inelastic scattering cross sections at 2.5 MeV have been interpreted in terms of simple structure models to test the strength of the weak collective excitation amplitudes found in ^{204,206}Pb. The surprising result is that the collective amplitudes for neutron scattering are a full 50% larger than those found in Coulomb excitation experiments. This impressive result is tentative, waiting upon the completion of the analyses of the 4.6 MeV and 8 MeV measurements within the same framework as the total cross sections and the 2.5 MeV measurements.

b. Scattering Study of Five Even-A Sn Isotopes (J. L. Weil and Z. Gacsi)

Work during the last year on the analysis and interpretation of neutron scattering for the five even-A isotopes with A = 116 to 124 has provided further details about the description of neutron scattering cross sections. Earlier work had shown that the combined width fluctuation and channel-channel correlation corrections were both necessary and contributed to highly successful descriptions of inelastic scattering cross sections. New work shows that it is also important to make the scattering potential in each scattering channel explicitly dependent on the neutron energy in that channel. Further detailed examination of the residual differences between measured inelastic scattering cross sections and those calculated with the statistical model shows that the 10 to 20% residual differences exhibit a systematic, level-spin dependent behavior.

c. Ca Isotopes Scattering Study (S.E. Hicks, S.F. Hicks, G.R. Shen, and M.T. McEllistrem)

All data taking is now complete for the ^{40}Ca and ^{48}Ca differential scattering cross section measurements, and all measurements have

been reduced to corrected cross sections. To complete the corrections for multiple neutron scattering in the sample, the forced collision Monte-Carlo code MULCAT had to be developed to take multi-element samples, and also adapted to work for samples in the form of a rectangular parallelepiped. These developments were completed by Sally Fisher Hicks, and the new form of the Monte-Carlo code is called "MULSQUARE".

The level density in the compound system ^{41}Ca is high enough that with the experimental energy spread of about 40 keV an appropriate energy-averaged cross section set was obtained. The measured cross sections are thus well represented with an energy-dependent, complex potential well and a coupled-channels model with coupling to the 3^- and 2^+ levels at excitation energies of 3.73 and 3.92 MeV, respectively, in ^{40}Ca. The data are also consistent with older data from this and other laboratories, wherever the different data sets overlap.

The ^{40}Ca + n data were taken for three reasons: 1) To test the older data sets for incident neutron energies from 2 to 8 MeV energy. These tests were eminently successful; the agreement with older Kentucky measurements for elastic scattering, for example, was excellent. 2) To provide a test of the adequacy of the redesigned multiple scattering code for rectangular samples, with highly asymmetric shapes. This could be done because it was possible to prepare samples both in the standard cylindrical form and in the form of square cross section plates whose thickness was only 1/4 that of the other dimensions. The results of these tests indicates that for angles between 40° and 70° residual differences of 5 to 10% exist between results for the well tested cylindrical sample form of the multiple scattering corrections and the results with the newer square, plate-shaped samples. The plate-shaped samples, and multi-element capabilities, were necessary because the highly enriched ^{48}Ca sample was available only as $CaCO_3$ in that shape. The residual correction differences at the indicated angles occurred because the O and Ca cross sections resonate strongly, and corrections are especially difficult for those angles which correspond to the detector seeing the samples along the plane of the plates. 3) The third reason for working with ^{40}Ca was to provide a base for comparison with the new results being obtained for scattering by ^{48}Ca, which is also doubly magic.

The study of neutron scattering by ^{48}Ca was of course the primary goal, and already several exciting results have come from this study. First, the $d_{5/2}$ scattering amplitude is much enhanced in ^{48}Ca scattering, as compared to that for ^{40}Ca. This is because the ^{48}Ca size is correct to bring the $d_{5/2}$ size resonance into the incident neutron energy interval near 2 to 4 MeV. The strong enhancement of the d-wave scattering is evident in a comparison of the elastic scattering differential cross sections, where the large d-wave amplitude for ^{48}Ca is evident in almost every elastic scattering angular distribution measured between 2 and 6 MeV; that same amplitude is not enhanced for scattering by ^{40}Ca. Only when the incident energy is near 8 MeV does the characteristic difference of the enhanced d-wave scattering almost disappear; scattering for the two nuclei then becomes quite similar.

Second, and related to this, there are quite strong core-coupled resonances in

the ^{48}Ca scattering, either entirely $d_{5/2}$ resonances or at least dominated by those of that partial wave. The presence of these resonances in the energy interval from 0.9 to 3 MeV incident was well known from the phase shift analysis of the total cross sections measured at ORELA, the analysis being done by C. H. Johnson of ORNL and R. Carleton of Middle Tennessee University. We find that our differential cross section measurements, both on and off d-wave resonances, are generally well characterized by the phase shifts provided from the total cross section analysis of Carleton and Johnson. The rapid variation of the angular distributions on and off resonance is well represented. Of course, the differential cross sections are not well fit; modifications of the phases will be needed to provide a good description to both the differential scattering measurements as well as the total cross sections. The differential cross sections will be especially helpful in providing the nonresonant, potential scattering phases.

A very satisfying set of results arose from the analysis of the 8 MeV incident energy differential cross section set. These elastic and inelastic scattering cross sections, together with the total cross sections near that energy, could only be fit with a model which carefully included coupling to several core excited states in the scattering analysis, including 3^-, 2^+ and other states. Total cross sections, elastic scattering differential cross sections, and inelastic scattering differential cross sections combined fix the strengths of the scattering potentials as well as the coupling strengths for the different core-excited states. The fixing of these parameters to describe the 8 MeV data set, together with following the potential to lower energy to maintain a good description of the general energy dependence of the total cross sections, produces a "shell-model-in-the-continuum" which then automatically generates $d_{5/2}$ resonances, or "hallway" resonances in the language of intermediate structure. These hallway resonances occur at energies close to those measured and with relative widths similar to those of the resonances observed in the total cross sections. In other words these resonances from 1 to 3 MeV incident energies are just what one needs to be consistent with the 8 MeV scattering cross sections. Much physics information about the A = 49 system is contained in the details of this description; that will be the subject of later reports.

d. Reorientation Cross Sections and Potentials

Several examples exist of differential cross section sets for even-A nuclei and their odd-A neighbors. For those odd-A nuclei with large ground state spins, $J \geq 3/2$, the diffraction minima are much shallower than those for the even-A neighbors. This is particularly the case for nuclei known to be deformed, like the stable uranium nuclei. Satchler had shown several years ago, in a weak-coupling model, that ground-state reorientation of a deformed nucleus in scattering could lead to some filling-in of the minima.

Christian Lagrange had tested that possible explanation at the suggestion of one of us (MTM) and found that the degree of reorientation so achieved was quite inadequate to explain the observed differences between the minima for odd-A and even-A neighbors. We have reexamined this problem by including

reorientation resulting from inelastic excitation of collective levels. The reorientation resulting from inelastic scattering is far greater than that of the ground-state alone; while ground-state reorientation amplitudes provide small effects, the principal effects come from inelastic excitations. These completely account for odd-A, even-A neighbor differences in scattering. These findings have been published.[4]

3. Projected Work In Neutron Scattering

a. Collective Nuclei

The analysis and interpretation of scattering from the Os and Pt nuclei at three incident neutron energies will be completed during the next year. Three papers dealing with these matters are in various stages of preparation at the present; they should be submitted for publication within the next few months. The scattering from non-deformed ^{196}Pt will show strong differences in collective excitations from those revealed with electromagnetic excitation, and, in contrast, the scattering from the deformed Os nuclei will show essentially the same collective excitations as do Coulomb excitation experiments.

A new study will be begun including semi-magic ^{142}Nd and ^{144}Sm. This study will probe for higher energy collective excitations, more similar to those of the Ca isotopes, than those of the deformed Sm and Os isotopes. From these higher energy excitations one might expect to see the development of collectivity associated with closeness or remoteness to the proton magic number 64. It is somewhat accepted now that $Z = 64$ provides a good energy gap if the neutron number $N < 90$. Thus in these neutron-magic nuclei we should be able to see different collective character for those excitations involving proton particle-hole amplitudes. These highly enriched scattering samples are also sought here to look for two-phonon E3 excitations. Such excitations should be excitable directly with E2 amplitudes, and may be much more evident in the neutron scattering spectra than in γ-ray decay studies proposed elsewhere in this proposal.

Finally, the now established dispersion-corrected scattering potentials can be studied in nuclei near the region of strong collective excitations but for nuclei which are themselves spherical.

b. ^{48}Ca Study

The resonance and non-resonance interpretations of neutron scattering from ^{48}Ca will be completed for neutron energies from 2 MeV to 8 MeV, and the strength of coupling will be related to the escape widths of intermediate resonances caused by the coupling. We expect to be able to discern the nucleon configurations and core excitations which are coherently combined in at least a few of the strong core-coupled resonances; this will give insight into collective excitations for nuclei near A = 48.

---

[4] S.E. Hicks and M.T. McEllistrem, Nucl. Phys. A468, 372 (1987).

c. Pb Isotope Study

Analyses of the weak collective effects in neutron scattering from the Pb nuclei with A = 204 and 206 should be completed during the next two years. These analyses will be based on differential cross sections measured at three incident neutron energies of 2.5, 4.6, and 8 MeV as well as the total cross sections measured over the neutron energy interval from 0.3 MeV to 4 MeV. This extensive set of carefully measured cross sections should enable us to separate confidently the weak collective effects of the two nuclei, and study their relationship to each other.

B. NUCLEAR STRUCTURE STUDIES

1. Collective Effects In Shape Transitional and Spherical Nuclei.

In our spectroscopic measurements, we employ the $(n,n'\gamma)$ or INS reaction with detection of the emitted γ rays to characterize the states excited by inelastic scattering. Our interests for many years have been in the transitional region just below the lead nuclei. We are continuing work in this region, but have also enlarged our effort to include selected, more spherical nuclei.

a. Transitional Nuclei (S.W. Yates, G. Molnar, E.W. Kleppinger and R.A. Gatenby)

The platinum nuclei have proven quite difficult to interpret in terms of traditional descriptions. The application of boson calculational techniques seemed to have provided a unified and consistent description of nuclei throughout this region; however, recent measurements have even called into question the validity of the O(6) description of ^{196}Pt. To address these and other questions, we have studied this nuclide by the $(n,n'\gamma)$ reaction, with particular attention being paid to the role of M1 transitions which would be implied by IBA-2 models with sharp differences between neutron and proton excitations. We do not observe large M1 contributions in the decays of any of the low-lying excitations of ^{196}Pt, nor can we identify obvious candidates at higher energies for mixed-symmetry states.

As a logical extension of our studies of lighter Os, Pt, and Hg nuclei, we have recently studied the heaviest stable Hg nuclei, ^{202}Hg and ^{204}Hg, with the $(n,n'\gamma)$ reaction. Much new information about little-studied ^{204}Hg has emerged; however, the theoretical characterization of even the lowest states in this nucleus remains unclear. We hope these new experimental results will inspire work on the required large basis shell model calculations which heretofore have not been performed.

A detailed manuscript describing our studies of ^{191}Ir and ^{193}Ir to test the applicability of the interacting boson-fermion approximation (IBFA) and the various supersymmetry schemes is nearing completion. With encouragement from collaborators at LLNL who wish to obtain a more thorough understanding of the higher-lying states of these nuclides, these studies are continuing.

To complement our studies of the platinum O(6) region, we have recently begun experiments in the new region of O(6) symmetry in the Xe-Ba nuclei. We have completed a study of ^{134}Ba, the lightest stable barium nucleus for which sufficiently large scattering samples can be obtained. We have identified an additional ten new excited states below 3 MeV, and it is possible to characterize most of them.

Considerable interest has emerged following the recent discovery of collective magnetic dipole excitations in deformed nuclei. Several candidates for states which are not totally symmetric with respect to the neutron and proton degrees of freedom, so-called mixed-symmetry states, have also been suggested in spherical nuclei. On the basis of our INS spectroscopic measurements on ^{134}Ba, we have identified good candidates for mixed-symmetry states in an O(6) nucleus. A Rapid Communication describing our search for mixed-symmetry states should soon appear in The Physical Review C.[5] Briefly, we discount a previous proposal for mixed-symmetric 1^+ states in this O(6) nucleus and suggest, instead, that the 2029-keV and 2088-keV levels share the properties of the lowest mixed-symmetry 2^+ state of the neutron-proton interacting boson model (IBM-2).

For reasons similar to those for studying the odd-mass Ir nuclei, we, in collaboration with Dr. E. W. Kleppinger and her students from Berea College, have initiated a study of ^{135}Ba. We view this nucleus as perhaps the best opportunity to observe supersymmetry in this region.

b. Spherical Nuclei Near A = 100 (G. Molnar, S.W. Yates, R.A. Gatenby, T. Belgya and B. Fazekas)

Our collaborative studies of coexistence phenomena at double subshell closures of nuclei with Dr. Gabor Molnar of the Institute of Isotopes of Budapest, Hungary have progressed well. With the exception of some preliminary studies which were performed in Budapest before this collaboration was formally initiated, the experimental work has been concentrated at U.S. facilities. This emphasis was necessitated by the upgrading (and temporary shutdown) of the Budapest reactor and, since we had known of this upgrade for some time, was consistent with our plans.

Because of its unique character as one of the few doubly closed subshell nuclei which are available for study, our research has focussed on ^{96}Zr. Our experimental evidence from (n,n'γ) studies for a coexisting four-particle, four-hole band in this nucleus was published as a Rapid Communication,[6] and we have also examined the possibility of alpha clustering in this nucleus. A larger manuscript describing the wealth of new spectroscopic information we have obtained about ^{96}Zr is nearing completion.

Our INS studies have been complemented nicely by parallel studies by Dr. Meyer

---

[5] G. Molnar, R.A. Gatenby and S.W. Yates, Phys. Rev. C37 (in press).

[6] G. Molnar, S.W. Yates. and R.A. Meyer, Phys. Rev. C33, 1848 (1986).

and his group at LLNL with the (t,pγ) and (t,pe⁻) reactions. We have also examined the decay of the low-spin isomer of ^{96}Y into ^{96}Zr at the TRISTAN isotope separator at BNL. The latter study was extremely successful in helping us assess the collectivity of the low-lying 0+ states of ^{96}Zr. A paper describing our findings has appeared in the Physical Review C.[7]

In collaboration with coworkers at the Cyclotron Institute of the Department of Physics of University of Jyvaskyla (JYFL), Finland, we attempted lifetime measurements in ^{96}Zr by the (p,p'γ) and (p,p'e⁻) reactions using electronic timing methods. Our initial impressions were encouraging, but recent communications with the Jyvaskyla group lead us to question whether limits lower than 100 ps on any of the lifetimes can be gleaned. On the other hand, these measurements have provided new information about the level structure of this important nucleus.

Because of the failure of the experiments at JYFL to provide lifetime information about states in ^{96}Zr and the sparse knowledge of γ-ray transition rates in this nucleus, we have measured the Doppler shifts of γ rays emitted following INS and have been able to determine lifetimes of many levels. Elenkov and coworkers have demonstrated that the DSAM method following INS of reactor fast neutrons can provide lifetimes for levels in light nuclei despite the low recoil velocities involved. In medium-mass nuclei, the recoil velocities are even smaller; nonetheless, it is still possible to observe Doppler shifts of γ rays, and comparisons of measurements made in this laboratory of lifetimes in ^{56}Fe with known lifetimes indicate that the methods of evaluation are reliable. E2 transition rates of 20 to 40 W.u. confirm the presence of collective structure associated with the 1582-keV 0^+ state, which we have determined to have greater deformation than the ^{96}Zr ground state. Moreover, fast E1 transitions are observed to populate the 1897-keV 3^- octupole excitation from states in the region where a two-phonon octupole quartet of states has recently been suggested.

While at the TRISTAN facility we also obtained data on the decay of ^{98}Y to complement our data on the similar decay of lowspin ^{96}Y. The analysis of these data is progressing well, but it is a more complicated decay than that into the doubly closed subshell nucleus ^{96}Zr and will require extensive data evaluation.

We will soon initiate a study of ^{90}Zr (closed neutron shell and closed proton subshell) by the INS reaction at the University of Kentucky to evaluate the magnitude of the subshell closure. Since this is a well-studied nucleus and has a lower level density, we anticipate that this study will not be as time-consuming as those for the heavier Zr nuclei.

c. Projected Studies

Many unsuccessful searches for two-phonon octupole states (a

---

[7] Mach, Molnar, Yates, Gill, Aprahamian, and Meyer, Phys. Rev. C37, 254 (1988).

quartet of states at roughly twice the one-phonon energy that decay via enhanced E1 or E3 transitions) have been conducted in ^{208}Pb, and we have recently reported our search for these excitations in ^{146}Gd,[8] the only known even-even nucleus besides ^{208}Pb to exhibit a 3$^-$ first excited state. On the other hand, the two-phonon nature of high-spin yrast states in ^{147}Gd and ^{148}Gd is evinced by a cascade of two E3 transitions in each case. Why were these states not observed in the "core" nucleus ^{146}Gd? One is forced to believe that the reason they have been missed is that we do not have probes which will populate these states. The INS reaction is known to provide a statistical population of low-spin states and would seem ideal for exciting at least the three lowest members of the two-phonon octupole multiplet. Unfortunately, ^{146}Gd is unstable and thus not amenable to study by INS methods. ^{144}Sm is stable, however, and the low energy of the one-phonon state suggests that exciting and observing the two-phonon states is practical. We propose to make careful searches for two-phonon octupole states in this nucleus and ^{142}Nd, another N = 82 isotone, with the INS reaction. Other probes, such as the (p,p') reaction at JYFL, will be brought to bear on this problem when candidates for two-phonon excitations have been identified and further characterization is demanded.

Our studies of the doubly closed subshell nucleus ^{96}Zr have been extensive, and, as we have learned more about the myriad of excitational modes possible in this nucleus, questions which can be addressed in neighboring nuclei have arisen. For some time, we had planned complementary studies of the lifetimes of states in ^{88}Sr and ^{90}Zr, nuclei with a singly closed subshell and the closed N = 50 shell. Indeed, we now feel that complete INS studies of these nuclei are necessary to understand the behavior of the particle-hole and collective excitations in this region.

In addition to the usual excitation function and angular distribution measurements, we plan to pursue Doppler-shift lifetime measurements which proved so informative in ^{96}Zr. If information from other probes is deemed necessary, those measurements will be pursued at other laboratories.

2. Low-Lying Excitations of Spherical Nuclei

a. ^{204}Pb(n,n'γ) Studies (J. Hanly, S.E. Hicks, S.W. Yates, and M.T. McEllistrem)

The strong collective phenomena observed near A = 190 to 196 must evolve from configurations arising below neutron number N = 126. Elucidating the evolution of the weak Pb collective phenomena and their connection to hole and particle configurations depends on a good description of levels and decays in nuclei near ^{208}Pb.

Liotta and Pomar had shown, six years ago, that the few known low-lying levels of ^{204}Pb could be well described as based on the pair excitations of ^{206}Pb.

---

[8] Yates, Mann, Henry, Decman, Meyer, Estep, Julin, Passoja, Kantele, and Trzahka, Phys. Rev. C36, 2143 (1987).

Indeed, they showed a very strong overlap between single ^{206}Pb excitations and individual levels of ^{204}Pb. Thus we would expect the collective excitation amplitudes of ^{204}Pb, which are about 50% larger than those of ^{206}Pb, to be simply related to the amplitudes of the latter.

The knowledge of levels and decays of ^{204}Pb was rather sparse; for example, nothing was discussed in any of the early shell model calculations about unnatural parity levels. Thus as part of his dissertation on collective effects in the Pb isotopes, John Hanly completed a thorough study of levels and their γ-ray decays in ^{204}Pb. A paper describing that work has been submitted for publication.[9] He found that the hypothesis adopted by Liotta and Pomar, first advanced by Ko and McGrory and later developed by McGrory, that the levels of ^{204}Pb were well represented as two-boson excitations where the base bosons were ^{206}Pb levels, was supportable only for levels with excitation energies below 2 MeV. He also found a new 2^+ level, only 0.1 keV away from a previously reported 0^+ level.

b. Structure Studies of the Sn Isotopes (J.L. Weil and Z. Gácsi)

The decay scheme for ^{116}Sn based on our $(n,n'\gamma)$ results and the (n,γ) results of S. Raman of ORNL is almost in final form. A number of significant advances in the decay scheme have been made during the past year based on the work described below. That part of the decay scheme involving the $(n,n'\gamma)$ results contains approximately 100 levels. Based on our angular distribution and cross section results plus other evidence in some cases, the spin and parity of 51 of these levels has been uniquely assigned and spins have been limited to 2-3 possibilities for most other levels.

Based on the analysis of the excitation functions, we have calculated the level-excitation cross sections at neutron energies of 3.05, 3.75 and 4.50 MeV where γ-ray angular distributions were also measured. These cross sections are expected to depend on neutron bombarding energy, excitation energy and J^π of the level. The statistical model for nuclear reactions enables predictions of these cross sections. We have calculated statistical model cross sections including the level-width fluctuation and channel-channel correlation corrections using the approximation of Tepel, Hofmann, and Hermann. A comparison of our experimental level-excitation cross sections for levels with a uniquely determined J^π to the calculations shows generally good agreement except for the lowest lying levels of a given J^π where the experimental values are almost invariably much higher than the calculated ones. This seems to be true for all spins from J = 0 to 6.

Part of this discrepancy for the lowest level of given J^π, which is most severe at the lowest excitation energies, is due to direct reactions which are known to occur and whose effects are not included in the comparisons. Excluding this lowest level for each J^π the systematic behavior of $\Delta\sigma = \sigma_{exp} - \sigma_{calc}$ means that another tool exists to use in construction of a decay scheme

---

[9] Hanly, Hicks, McEllistrem and Yates, Phys. Rev. C (submitted).

and in determining spin-parity assignments. We are also using the shape of the near threshold part of the γ-ray excitation functions as an aid in determining level spins. Our detailed analyses of over 100 cross sections allows us to use them with confidence to limit possible spin assignments.

Analysis of Doppler-shifted γ rays to obtain level life-times has been held up because of a problem involving the measurement of ^{90}Zr life-times. Our measurements made with $^{90}ZrO_2$ as a scattering sample give life-times which disagree with those found in the literature by factors of three or more. This is in contradiction to a previous good agreement of life-times for ^{56}Fe measured by us with $(n,n'\gamma)$ as compared to published $(p,p'\gamma)$ results. The source of the disagreement, undoubtedly associated with the composite sample, is being sought.

c. Projected New Work

Few experiments can expose two separate levels of different spin which are presumed to be within 0.1 keV of each other. One way to search for 0^+ levels is to scatter neutrons to them at low incident neutron energies. The differential cross sections for such levels rise steeply at forward angles and back angles. We propose to carry out such a scattering experiment, using the $^7Li(p,n)^7Be$ reaction as a source of neutrons to get the small energy spread necessary for the experiment. Preliminary tests to obtain 15 keV energy spread with adequate counting rates for inelastic scattering look feasible, but very difficult. If this experiment works, we should know if there is actually a 0^+ level very near the newly discovered 2^+ level.

The γ-ray spectra of the $^{116}Sn(n,n'\gamma)$ and $^{120}Sn(n,n'\gamma)$ experiments show Doppler shifts for approximately a dozen γ rays for each nucleus. These energy shifts will be analyzed to determine level life-times for these two nuclei, and then the ^{116}Sn study will be written up for publication. Some further analysis, including a better energy calibration, remains to be done on the $^{124}Sn(n,n'\gamma)$ experiment. This will be finished up so that this study also can be written for publication. As soon as the ^{90}Zr life-time discrepancy can be cleared up, the last major obstacle to the publication of the $^{56}Fe(n,n'\gamma)$ study will have been removed. That study reports several new γ rays and levels, and newly determined life-times for several levels. A publication is already largely prepared.

C. RADIATIVE CAPTURE - CAPTURE OF ^4HE BY ^{12}C (M.A. Kovash, J.H. Trice, M. Wang, J.L. Weil; T.R. Donoghue and A. Abduljalil, Ohio State University)

Several recent publications have pointed out the sensitivity to the rate of helium burning by carbon in determining the abundance ratio of carbon to oxygen in main sequence red giant stars. At temperatures near $2x10^8$, the $^{12}C(^4He,\gamma)^{16}O$ reaction competes with the 'triple-alpha' process to consume the helium generated in the hydrogen burning phase. The abundances of all heavier elements produced during the higher temperature burning stages subsequent to helium consumption are determined by the ratio of residual carbon to oxygen. In addition, the mass of the remnant core following a supernova explosion depends upon the rate of heavy element production, and therefore sensitively

on the carbon and oxygen content of the prenova star. The astrophysically interesting rate for the capture reaction $^{12}C(^4He,\gamma)^{16}O$ is determined by the cross section near 300 keV in the center of mass --far below the coulomb barrier for this reaction. At this energy the astrophysical S-factor is largely determined by the interference between a pair of 1^-states; the narrow sub-threshold state at 7.12 MeV, and the broad unbound level at 9.6 MeV. Earlier measurements made at Caltech and Munster in the energy region of 0.94 to 3.38 MeV show disagreements of up to 50% in the cross sections and a disagreement of a factor of 3 to 5 in the extrapolated S-factor at 300 keV.

We have begun a series of measurements of this reaction cross section at the University of Kentucky to determine the relative E2/E1 cross sections and phase for ground state capture at CM energies extending from 1.5 MeV to 3.5 MeV through complete measurements of the γ-ray angular distributions. We will also determine the absolute magnitude of the cross section in this energy range through careful redundant calibrations of the target thickness and γ-ray detector efficiency.

It has been made abundantly clear from recent work that only by isolating and carefully testing the energy dependence of each component multipole can an accurate extrapolation be made to the region of 0.3 MeV. For this reason we are extending our measurements to energies well above the 9.6 MeV resonance where the E2 yield is expected to dominate the cross section. Furthermore, the cross section must be determined accurately to yield a reliable value of the extrapolated S-factor.

Consequently, we have chosen an experimental technique which is different from that employed in the previous measurements, and which is quite different from the measurements currently underway at Caltech using the recoil detection technique. (In this latest Caltech experiment only the angle-integrated reaction yield is measured and used to determine the cross section. This method is therefore fundamentally incapable of isolating and testing the important --and perhaps dominant --contribution made by quadrupole radiation.)

Gamma rays are detected in a 12" diameter x 10" NaI crystal incorporating an active self-shielded design which was developed at the University of Kentucky. The detector is segmented into a central core element of 8" diameter x 10" length, which is surrounded by a 6-segment annulus also made of NaI. Each segment is instrumented with an ADC and a TDC, allowing us to reconstruct the total energy of each gamma-ray event and to actively reject cosmic rays and other backgrounds. This discrimination is based upon the distinctive signatures these events display in the annulus. As a result, time-independent backgrounds are very strongly suppressed, allowing us to observe the weak gamma-ray transitions of interest. Also, through the use of the beam-pulsing capabilities of the UK Van de Graaff, we have a very effective tool to use in discriminating against fast neutrons from the target.

Neutron production from the ^{13}C contamination in the target has been reduced in several ways. First, we have constructed a 'clean' beam line by replacing a diffusion pump with two turbo-molecular pumps and copper-gasketed flanges. A new target chamber has been built which contains two large liquid

nitrogen-cooled internal baffles extending very close to the target. Second, we have chosen to use enriched (99.95%) ^{12}C targets evaporated onto W and Ta backings. A pulsed beam and time-of-flight methods eliminate much of the neutron background. We are also developing the use of pulse-shape discrimination to further reduce this background.

Data collection runs were made during the spring and summer of 1987 at beam energies of 3.595, 3.21, 2.95 and 2.66 MeV, corresponding to CM energies of 2.69, 2.40, 2.21 and 2.00 MeV. Angular distributions were measured at a minimum of 6 angles, typically over the range from 20 to 135 degrees. A strong interference between E1 and E2 radiations is evident at 2.66 MeV, where the angular distribution shows a large departure from the familiar dipole pattern. At this 2.00 MeV CM energy our extracted ratio of cross sections $\sigma(E2)/\sigma(E1) = 0.20 \pm 0.05$. Further measurements are under way.

D. OPTICAL POTENTIAL STUDIES (C.E. Laird,[+] D.S. Sousa,[+] G. Calkin, [+] R. Engelhardt, [+] and F. Gabbard)

This project is part of a broad study of the total proton reaction strength in the mass 40 to 90 range. The study is devoted to ascertaining the validity and/or extent of the anomalous absorptive potential reported by Kailas, et al. [Phys. Rev. C 20, 1272 (1979)]. The total proton strength is obtained by measuring the cross sections for proton elastic scattering, for (p,n) reactions, and for production of gamma-radiation by inelastic scattering and radiative capture. Over the past year we have measured gamma radiation from ^{67}Zn, $^{58,60}Ni$, and ^{45}Sc, elastic proton yields from $^{58,60}Ni$, and ^{45}Sc, elastic proton yields from $^{58,60}Ni$, and ^{45}Sc, ^{48}Ti, and ^{55}Mn, and (p,n) yields from proton induced reacton on ^{45}Sc and ^{48}Ti for proton energies from below 2 MeV to over 6 MeV. Optical model analyses of this data will aid in resolving the question of an anomalous absorptive potential.

[+] Eastern Kentucky University, Richmond, KY.

LAWRENCE BERKELEY LABORATORY

A. NUCLEAR DATA EVALUATION

1. Mass–Chain Evaluation. (E. Browne, R.B. Firestone, V.S. Shirley, and B. Singh)

The LBL Isotopes Project is responsible for evaluating mass chains with $167 \leq A \leq 194$ and for converting $33 \leq A \leq 44$ to ENSDF format. Responsibility for the following mass chains has been temporarily reassigned: A=170,171 to China, A=175,176 to India, and A=177 to Japan. A summary of the current evaluation status of LBL mass chains is given in the table below:

Table A-1. Status of LBL Mass-Chain Assignments

Mass Chain	Publication Year	Status
33–44	1978	Sent 7-87 (LBL)[a]
167	1976	(4-88) (LBL)
168	1980	In press (LBL)
169	1982	Published (LBL)
170	1987	Published (China)
171	1984	Published (LBL)
172	1987	Published (China)
173	1975	submitted 10-15-87 (LBL)
174	1984	Published (LBL)
175	1976	(India)
176	1976	(India)
177	1975	(Japan)
178	1974	Submitted 5-87 (LBL)
179	1976	Submitted 9-87 (LBL)
180	1987	Published (LBL)
181	1984	Published (LBL)
182	1975	Submitted 5-87 (LBL)
183	1987	Published (LBL)
184	1977	(3-88) (LBL)
185	1981	Published (LBL)
186	1974	Submitted 9-87 (LBL)
187	1982	Published (LBL)
188	1981	Published (LBL, Kuwait)
189	1981	Published (LBL)
190	1982	Published (LBL)
191	1980	Published; (4-88 for 2^{nd} cycle) (LBL)
192	1983	Published (LBL)
193	1981	Published (LBL)
194	1977	Submitted 10-20-87 (LBL)

[a]Radioactivity data.

Seven mass-chain evaluations were submitted by LBL between 1/1/87 and 12/31/87, and two evaluations were published. Radioactivity data for $33 \leq A \leq 44$, evaluated at LBL in 1986, and recently

adapted for ENSDF were reviewed by Endt and Van der Leun and sent to BNL for inclusion in the ENSDF file. These data are to be combined with "Adopted Levels, Gammas", adapted into ENSDF format from Endt and Van der Leun's 1978 evaluation of A=21-44. The French evaluation group is collaborating with LBL on the conversion process, and has already sent ENSDF files for A=33-38 to LBL and BNL. The Isotopes Project is currently evaluating mass chains for A=167, 184, and A=191, and expects to submit them in the Spring of 1988. The group recently added Balraj Singh, formerly with the Kuwait evaluation group, but now dividing his time between the LBL and the McMaster evaluation groups.

2. Major Horizontal Evaluations.

a. Table of Radioactive Isotopes (E. Browne, R.B. Firestone, and V.S. Shirley)

John Wiley & Sons, Inc. 1986, ISBN Number: 0-471-84909-X. This book, tailored to the needs of applied users in industry, biology, medicine, and other fields, but also serving as an indispensable reference for nuclear physicists and chemists, contains 1056 pages and sells for $59.95. Sales through August, 1986 were 1508 volumes.

b. Table of Isotopes, 7th Edition (C.M. Lederer and V.S. Shirley, editors, E. Browne, J.M. Dairiki, and R.E. Doebler principal authors)

John Wiley & Sons, Inc., 1978, ISBN Number: 0-471-04179-3. This 1630-page book, which contains nuclear structure data not presented in the *Table of Radioactive Isotopes*, is an excellent complement to the latter. The *Table of Isotopes* was reprinted in 1986 and currently sells for $48.50. 9587 volumes were sold through August 1986, and sales for the past year were 575 volumes. These books can be obtained through book stores or directly from the publisher. The addresses of the U.S. distribution centers for John Wiley & Sons, Inc. are given below.

JOHN WILEY & SONS, INC.
Eastern Distribution Center
1 Wiley Drive
Somerset, New Jersey 08873
(201) 469-4400
Telex: 833434
Cable: JONWILE SMOT

JOHN WILEY & SONS, INC.
Western Distribution Center
1530 South Redwood Road
Salt Lake City, Utah 84104
(801) 972-5828
Telex: 388308

3. Evaluation Methodology (E. Browne and R.B. Firestone)

The Isotopes Project has a continuing interest in developing methods for evaluating nuclear data in order to improve efficiency and the quality of the evaluations. The group's contributions to the mass-chain evaluation effort are described below:

a. Methods and Procedures for Analyzing Nuclear Data.

One important goal of the nuclear-data evaluation effort is to maximize the amount of information that can be extracted from the data. This requires the use of well-thought out and rigorous procedures, which often include statistical analyses of data. The Isotopes Project continues to do research in this

field, making its results available for publication by BNL in the *ENSDF Procedures Manual*, and for further distribution to the members of the Nuclear Data Network. The following papers are published in the *ENSDF Procedures Manual*:

i. E0 Transition Probabilities (R.B. Firestone)

ii. Calculated Uncertainties of Absolute γ-rays Intensities and Decay Branching Ratios (E. Browne)

The propagation of experimental uncertainties into particle emission probabilities derived from decay schemes is important for calculating average radiation energies per disintegration. This topic is being studied at LBL, and the results will become available for publication in the *ENSDF Procedures Manual*.

b. Computer Codes

The Isotopes Project develops computer codes for implementing new or revised methods and procedures, and maintains a library of codes for evaluating nuclear data for ENSDF. These codes are available in the *Berkeley ENSDF Evaluation Program Library* (BEEP). Codes SPINOZA and GABS are now being distributed by BNL to members of the Nuclear Data Network. The code GAMUT was sent to BNL recently, but documentation is still pending.

c. Electronic File–Transfer to BNL.

The Isotopes Project routinely sends mass-chain evaluations to BNL electronically via the computer network HEPnet. Both the pre- and post-review editing of the mass-chain files are done at LBL, and the corrected files are transferred to BNL. This procedure, which the group proposed in 1985,[1] eliminates almost entirely the need for editing at BNL, and results in a significant time saving for the publication process.

4. Remote Access to Databases and Computer Code Packages.

Computer guest accounts are available for use of the LBL-VAX/8650 computer cluster, which provides access to the LBL/ENSDF and BNL databases and to the LBL Physics Program Library (PPL). The latter is a subset of interactive programs from BEEP. There is no charge for this service, and those interested in using it may contact:

E. Browne or R.B. Firestone
Lawrence Berkeley Laboratory
Isotopes Project
Bldg. 50A, Room 6102
Berkeley, California 94720
Telephone: (415) 486-6152

[1] *Proposal for improving transit time in mass-chain processing with electronic computer file transfer*, Edgardo Browne and Richard B. Firestone, memorandum presented at the US Nuclear Data Network (USNDN) Meeting, Idaho Falls, November 1985.

17 guest accounts have been issued to remote users so far, and about 100 logins on these accounts were recorded during the period 11-86 to 10-87. The Isotopes Project also processes requests for data from remote users, and performed 5 database searches during the same period. Data were transmitted by both magnetic tape and via BITNET (EARNET in Europe).

B. ASTROPHYSICS

1. Measurements of Cross Sections Relevant to γ-ray Line Astronomy (K.T. Lesko, E.B. Norman, R.-M. Larimer, S. Kuhn, D.M. Meekhof, S.G. Krane, and H.G. Bussell)

Gamma-ray production cross sections have been measured for the γ-ray lines which are most strongly excited in the proton bombardments of C, N, O, Mg, Al, Si, and Fe targets of natural isotopic composition. High resolution germanium detectors were used to collect γ-ray spectra at proton bombarding energies of 8.9, 20, 30, 33, 40 and 50 MeV.

C. EXPERIMENTS WITH OASIS

1. New β-delayed Proton Emitters in the Lanthanide Region (J. Gilat, J.M. Nitschke, P.A. Wilmarth, K. Vierinen and R.B. Firestone)

The positron, electron capture and β-delayed proton decays of ^{124}Pr, ^{124,125}Ce, $^{134-136,140-142}$Eu, $^{134-136}$Sm, $^{134-136}$Pm, ^{144}Ho, ^{141,142,144}Dy, and $^{140-142,144}$Tb, were studied at the Berkeley SuperHILAC with the OASIS on-line mass separator facility. Half-lives, delayed proton branching ratios, and γ-ray energies are summarized in Table C-1.

2. Neutron−Rich Nuclei Produced by Deep Inelastic Processes (R. Chasteler, R.B. Firestone, J.M. Nitschke, K.S. Vierinen, and P.A. Wilmarth)

Recent experiments with OASIS have produced the new neutron-rich isotopes ^{171}Ho and ^{174}Er. These isotopes were produced by means of a Deep Inelastic Collision (DIC) process with a 8.5 MeV/A ^{176}Yb beam on a natural W target. Both new isotopes were identified on the basis of x-ray in coincidence with beta particles. ^{171}Ho was observed to decay with a half-life of 49 ± 5 s. Two γ rays of 199- and 280-keV were observed in coincidence with Er K x-rays. ^{174}Er was found to decay with a 202 ± 2 s half-life. 12 γ-rays were found in coincidence with Tm x-rays. A preliminary decay scheme is shown in Figure C-1.

Table C-1. Decay Summary of A = 140,141,142 Isotopes Produced with OASIS			
Isotope Z,A	Half-life This work	Literature	Radiations
^{124}Pr	1.2±0.2 s	-	βp, γ-ray 142 (with βp)
^{124}Ce	~ 6 s	6±4 s	γ-rays 120,253,544,560
^{124}La	30±2 s	29±3 s	γ-rays 230,421,576,694,1033,1262
^{125}Ce	10±1 s	11±4 s	βp, γ-rays 194,325,370,379 (70 more)
^{125}La	70±3 s	76±6 s	γ-rays 44,67,99,134,169,217,233,384, (25 more)
^{134}Eu	0.5±0.2 s	-	βp
^{134}Sm	10±2 s	12±3 s	γ-rays 110,119,162,219,229,299,380, (12 more)
^{134}Pm	~24 s	24±2 s	21 γ-rays
^{135}Eu	1.5±0.2 s	-	γ-ray 121
^{135}Sm	10±1 s	10±2 s	γ-rays 50,77,105,127,190,237,286,363,428,(13 more)
^{135}Pm	~50 s	49±7 s	40 γ-rays
^{136g}Eu	~ 5 s	-	βp,γ-rays 255,458,713
^{136m}Eu	3.2±0.5 s	-	βp, γ-rays 255,432,535,576 (20 more)
^{140}Tb	2.4±0.4 s	-	βp(7±2×10^{-5}%), γ-rays 328,628
^{140}Gd	15.8±0.4 s	-	γ-rays 175,192,379,722,750 (33 more)
^{140g}Eu	1.51±0.02 s	1.3±0.2 s	γ-rays 460,531,1068 (15 more)
^{140m}Eu	125±2 ms	-	γ-rays 175,185
^{141}Dy	0.9±0.2 s	-	βp, γ-rays 53,140,190
^{141}Tb	3.5±0.2 s	-	γ-rays 113,136,198,258,293 (30 more)
^{141g}Gd	~20 s	-	βp?, γ-rays 120,216,336
^{141m}Gd	24.5±0.9 s	22±3 s	βp?, γ-rays 60,113,119,145,198,224,258,351,361,521, (20 more)
^{141g}Eu	40±5 s	40.0±0.7 s	γ-rays 369,383,385,394,396 (20 more)
^{141m}Eu	2.7±0.3 s	3.3±0.3 s	γ-rays 96,519,804,1595
^{142}Dy	2.3±0.3 s	-	βp(~8×10^{-5}%), γ-ray 182
^{142g}Tb	597±17 ms	-	βp(~3×10^{-7}%), γ-rays 389,465,515,853
^{142m}Tb	303±7 ms	-	γ-rays 30,67,182,212
^{142}Gd	70.2±0.6 s	90±18 s	γ-rays 179,280,284,526,620 (37 more)
^{142g}Eu	2.4±0.2 s	2.4 s	γ-rays 768,890,1288,1405,1658,2056
^{142m}Eu	~70 s	73 s	γ-rays 556,768,1024
^{144}Ho	0.7±0.1 s	-	βp
^{144}Dy	9.1±0.5 s	-	βp(6±1×10^{-5}%), γ-rays 196,299 (8 more)
^{144g}Tb	-	~1.5 s	γ-rays 743,1134,1144,1877
^{144m}Tb	4.1±0.1 s	4.5±0.5 s	γ-rays 743, (15 more)

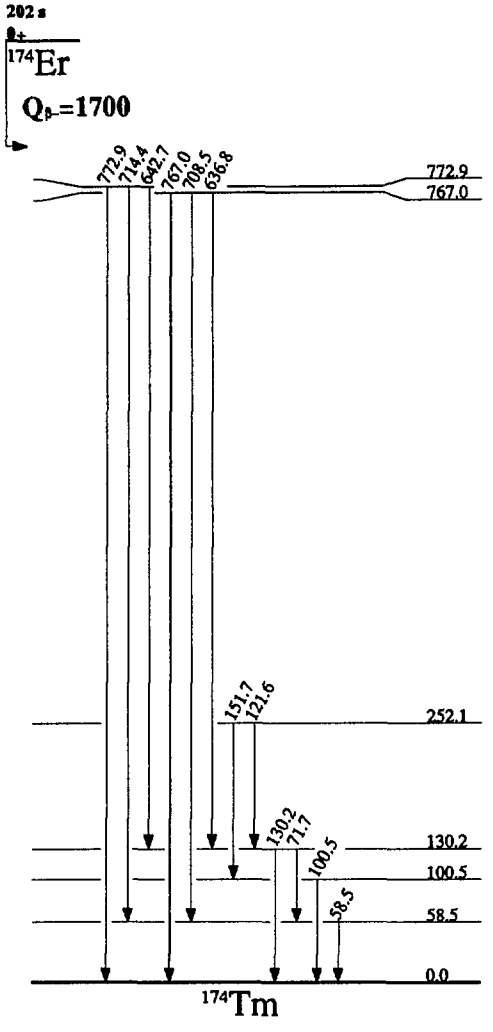
202 s
β+
174Er
Qβ=1700
772.9
714.4
642.7
767.0
708.5
636.8
772.9
767.0
151.7
121.6
252.1
130.2
71.7
100.5
58.5
130.2
100.5
58.5
0.0
174Tm

Figure C-1.

LAWRENCE LIVERMORE NATIONAL LABORATORY

A. NUCLEAR DATA APPLICATIONS - CALCULATIONS

1. Shell Model/R-Matrix Calculation of $^{14}N(n,x\gamma)$ Production for E_n = 14 MeV

(D. A. Resler)

The technique of combining the nuclear shell model with the R-matrix formalism for the calculation of double differential cross sections has been very successful at Ohio University for reactions involving the compound systems ^{7}Li and ^{8}Li.[1] We have extended this technique to both heavier nuclei and higher incident energies to calculate the $^{14}N(n,x\gamma)$ production for E_n = 14 MeV. The results of this calculation are compared with experimental data[2] measured at Oak Ridge National Laboratory in Fig. 1. When a 14-MeV neutron interacts with ^{14}N, the only significant γ-producing reactions are those which lead to the population of excited states of residual nuclei which are bound to particle emission. Of the 27 possible reactions, listed in Table 1, experimental data exists for only three of the (n,α') channels.

We have performed nuclear shell model calculations in a full $(1+2)\hbar\omega$ space for ^{14}C, ^{14}N, and ^{15}N. These represent the largest shell model calculations ever attempted for these nuclei. Using these results, spectroscopic amplitudes were calculated for the (n,n') and (n,p') reactions listed in Table 1. The shell model spectroscopic amplitudes and excitation energies were then transformed to R-matrix reduced-width amplitudes and level energies. The resulting R-matrix calculation (also the largest ever with 42 angular momentum channels) was used to calculate the double-differential cross sections for the (n,n') and (n,p') reactions listed in Table 1. Combining the calculated "initial-population" cross sections, the few experimental cross sections, and the relatively well-known branching ratios, a spectrum for the $^{14}N(n,x\gamma)$ production was calculated. Estimates were then made as to what the remaining initial-population cross sections should be based on the ORNL data. In the next few months, we will be adding the more complicated multinucleon transfer reactions (n,d'), (n,t'), and (n,α') to the shell model code so that the entire spectrum can be calculated from a fundamental nucleon-nucleon interaction.

---

[1] H. D. Knox, D. A. Resler, and R. O. Lane, Nucl. Phys. **A466** 245 (1987).
[2] J. K. Dickens, T. A. Love, and G. L. Morgan, Oak Ridge Report ORNL-4864 (1973).

Table 1: Principle reactions in the 14-MeV (n,xγ) production from ^{14}N. Initial population cross sections are listed for the curve shown in Figure 1.

Reaction	Excitation Energy (MeV)	Integrated Cross Section (mb)	Source
$^{14}N(n,n')^{14}N^*$	(2.31)	7.0	1
	3.95	19.1	1
	4.92	7.2	1
	5.11	16.6	1
	5.69	11.2	1
	5.83	25.9	1
	6.20	14.0	1
	6.45	3.1	1
	7.03	9.4	1
$^{14}N(n,p')^{14}C^*$	(6.09)	6.8	1
	6.59	1.8	1
	6.73	15.2	1
	6.90	3.8	1
	7.01	2.8	1
	7.34	11.8	1
$^{14}N(n,d')^{13}C^*$	(3.09)	5.0	2
	3.68	15.0	2
	3.85	5.0	2
$^{14}N(n,t')^{12}C^*$	(4.44)	30.0	2
$^{14}N(n,\alpha')^{11}B^*$	(2.12)	8.8	3
	4.44	14.1	3
	5.02	13.4	3
	6.74	15.0	2
	6.79	15.0	2
	7.29	15.0	2
	7.98	14.0	2
	8.56	2.0	2

1 Calculated from shell model/R-matrix

2 Extracted from ORNL (n,xγ) data

3 Measured data

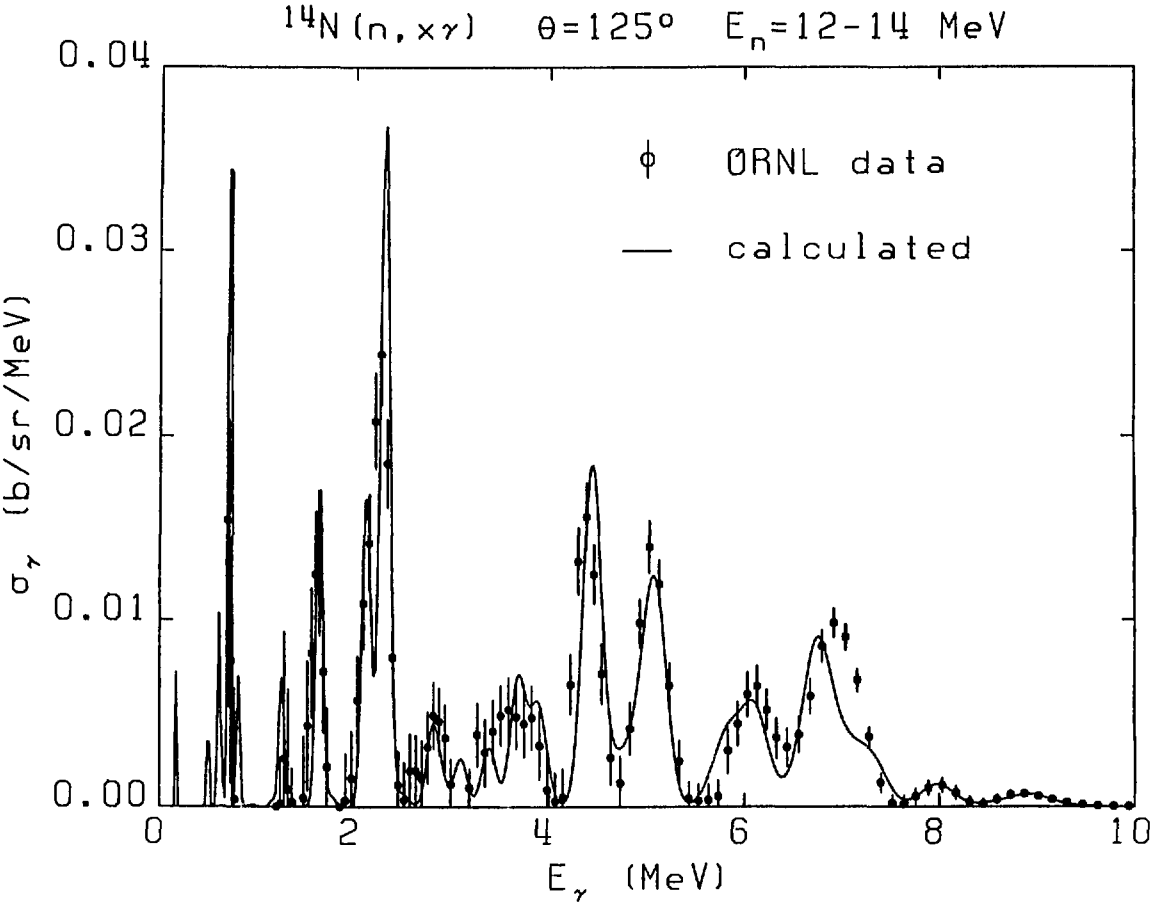

Fig. 1.

2. Precompound Gamma-ray Model
(G. Reffo*, M. Blann, and B. A. Remington)

We have used a Lorentz line-shape fit to experimental giant-dipole capture cross sections to calculate a rate of gamma-decay versus gamma-energy. We interpret this as being due to a one-body transition accompanied by gamma-radiation. This may then be used in the hybrid precompound decay model to calculate high-energy gamma-ray emission. In Fig. 1 we show results of this model programmed into the code ALICE for ^{93}Nb and ^{139}La(n,α) reactions induced by 14-MeV neutrons. The agreement with data is excellent. This model has also been tested by comparisons with γ-ray spectra from α and ^{3}He bombardment on a variety of targets from A ≃ 60 to A ≃ 150 giving compound nucleus excitation energies of 28 to 35 MeV. As is shown in Fig. 2, satisfactory agreement is obtained with experimental results.

* ENEA, Bologna, Italy

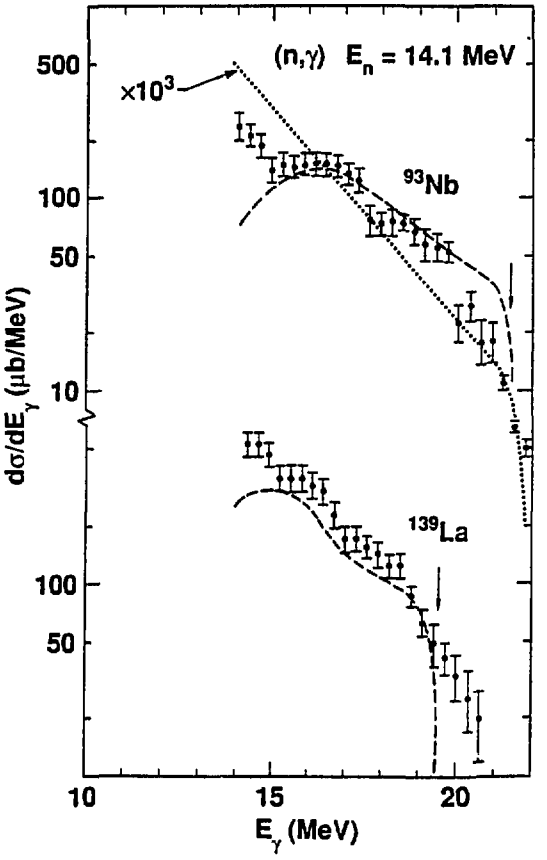
(n,γ) E_n = 14.1 MeV
×10³
^{93}Nb
^{139}La
500
100
50
10
100
50
10
15
20
dσ/dE$_\gamma$ (μb/MeV)
E$_\gamma$ (MeV)

Fig. 1.

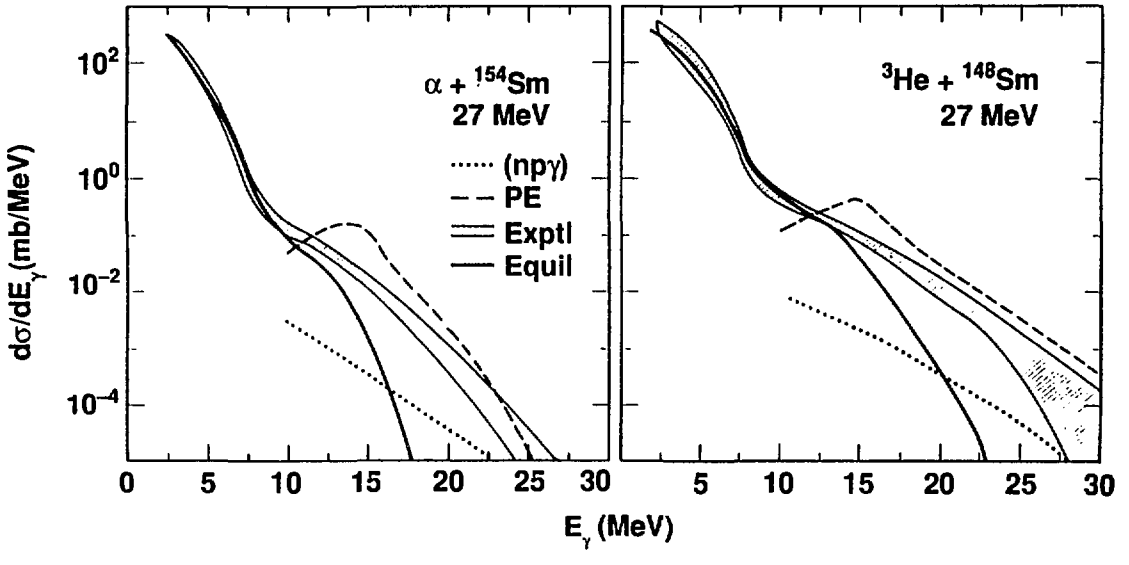
α + ^{154}Sm
27 MeV
(npγ)
PE
Exptl
Equil
^{3}He + ^{148}Sm
27 MeV
10²
10⁰
10⁻²
10⁻⁴
0
5
10
15
20
25
30
dσ/dE$_\gamma$ (mb/MeV)
E$_\gamma$ (MeV)

Fig. 2.

3. Calculation of Cross Sections and Differential Spectra for Reactions of 2-20 MeV Neutrons on Selected Reactor Materials
(M. Blann and T. Komoto)

For the natural isotopic targets ^{27}Al, Cr, Fe, and Ni, we have calculated dσ/dE, product yields, and equilibrium γ-ray spectra for incident neutrons of energies 2-12 MeV in one MeV energy steps, and 14-20 MeV in two MeV steps. To carry out these calculations, the ALICE code was modified to permit weighted-average results over isotopes of arbitrary abundance. We are in the process of comparing the calculated yields with experimental results where they exist. The calculated spectra and yields are summarized in Lawrence Livermore National Laboratory reports UCID-21309 to 21312.

4. Effects of Realistic Partial State Densities on Preequilibrium Decay
(M. Blann and G. Reffo*)

We reported earlier on the inclusion in the code ALICE of a subroutine which calculate partial state densities for preequilibrium decay using realistic single particle levels.[1] In this work, we present results using single-particle levels due to Seeger-Howard[2] and Seegar-Perisho.[3] Since the earlier work, we have modified the intranuclear transition rates for nucleon scattering based on the final density of three exciton states available.

Fig. 1 presents the results of the experimental[4] and calculated neutron spectra from the ^{90,91,92,94}Zr(p,n) reactions for 25 MeV incident protons. Calculated results are shown using the geometry-dependent hybrid model (GDH), and using the hybrid model with realistic two- and three-quasiparticle densities. For the latter, we use the single-particle sets of Seegar-Howard (S-H) and of Seegar-Perisho (S-P). The deformation parameter δ was taken to be -0.05 for all results shown.

These results give some encouragement in the use of realistic single-particle levels for preequilibrium calculations. They also leave much to be desired. Some improvement may result from adding the capability of doing a geometry-dependent calculation. More important will be a search for a better set of single-particle levels.

---

* ENEA, Bologna, Italy

[1] M. Blann et al., Lawrence Livermore National Laboratory Report UCRL-95397 (1986) unpublished.

[2] P. A. Seegar and W. M. Howard, Nucl. Phys. A238, 491 (1975).

[3] P. A. Seegar and R. C. Perisho, Los Alamos National Laboratory Report No. LA3751 (1967) unpublished.

[4] W. Scobel et al., Phys. Rev. C30, 1480 (1984).

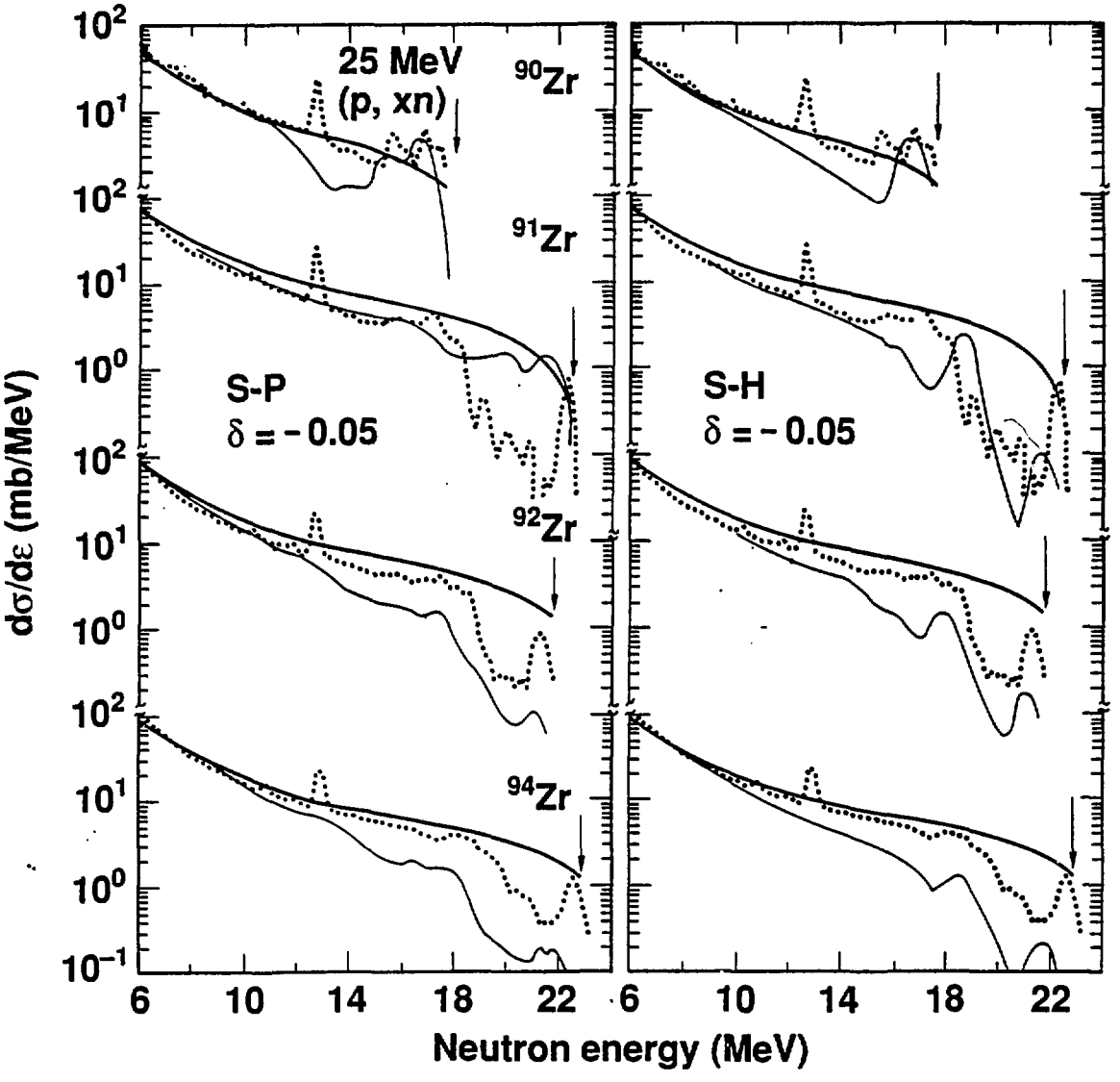

Fig. 1 Calculated and experimental neutron spectra for the (p,n) reaction on $^{90,91,92,94}Zr$. Experimental results of Ref. 4 are given by the dots. The heavy smooth solid line is the result of the GDH model. The thin solid line with structure is the result of the hybrid model using realistic single-particle levels.

5. Integral Testing of ENDF/B-V Gamma-Production Cross Sections

(R. J. Howerton and R. E. Dye)

During the past two years our pulsed-sphere program has been extended to include measuring the gamma spectra emitted from spheres of selected materials with 14-MeV neutron sources at their centers. These measurements, coupled with Monte Carlo transport calculations, have been extremely valuable for integral testing of the evaluated photon production data in the Livermore library of evaluated neutron reaction data (ENDL). In view of the value of these data for the integral testing of ENDL, the Livermore translation code that converts the ENDF/B-V data to the ENDL format has been extended to include translation of ENDF/B-V photon production data. The objective is to provide a capability to compare calculated spectra using the ENDF/B-V data with the experimental results of our pulsed-sphere program. The translation code has just been completed and testing of some of the ENDF/B-V photon production data is underway.

6. Microscopic Optical Model Calculations of Neutron Total Cross Section and Cross Section Differences

(H. S. Camarda* and F. S. Dietrich)

A microscopic optical model based on the prescription of Jeukenne, Lejeune and Mahaux has been used to calculate the neutron total cross section of ^{140}Ce and cross section differences of ^{139}La-^{140}Ce, ^{141}Pr-^{140}Ce, and ^{142}Ce-^{140}Ce over the energy range 3 to 60 MeV. Satisfactory agreement with the La-Ce and Pr-Ce difference data was obtained by using point proton (determined from electron and muon scattering data) and neutron densities to generate the appropriate potential for these nuclei. For the ^{142}Ce-^{140}Ce data, modifications beyond changes in the proton and neutron point densities were required in order to find agreement with the data.

* Pennsylvania State University

7. Fission Fragment Angular Distribution for the $^{232}Th(n,f)$ Reaction

(J. A. Becker and R. W. Bauer)

The angular distribution of fission fragments produced in the $^{232}Th(n,f)$ reaction for $0.72 \leq E_n(MeV) \leq 31.0$ in steps of 0.04 MeV have been parameterized in terms of the Legendre polynomial expansion:

$$W(\Phi) = 1 + A_2P_2(\cos\Phi) + A_4P_4(\cos\Phi) + A_6P_6(\cos\Phi).$$

The coefficients A_2, A_4, and A_6 are presented in UCID-21200.

8. Shell Model Description of the Beta Decay of the N = 21 Isotones ^{35}Si and ^{36}P

(E. K. Warburton* and J. A. Becker)

The nuclear structure of the N = 21 isotones ^{35}Si and ^{36}P and the N = 20 isotones ^{35}P and ^{36}S is considered in the spherical nuclear shell model with the SDPF interaction. Beta and gamma decay, as well as energy spectra are calculated. Results are compared to recent data on ^{36}P(β$^-$)^{36}S and ^{35}Si(β$^-$)^{35}P. Unique and nonunique first-forbidden beta decay are considered, as well as allowed (Gamow-Teller) decay. The predictions give a good description of the observed features of the four nuclei; in particular, the predicted beta decay rates are in agreement with experiment.

As an example of the quality of the results, Fig.1 presents our results for the β-decay of ^{36}P. Tables of transition matrix elements and energy eigenvalues are available.

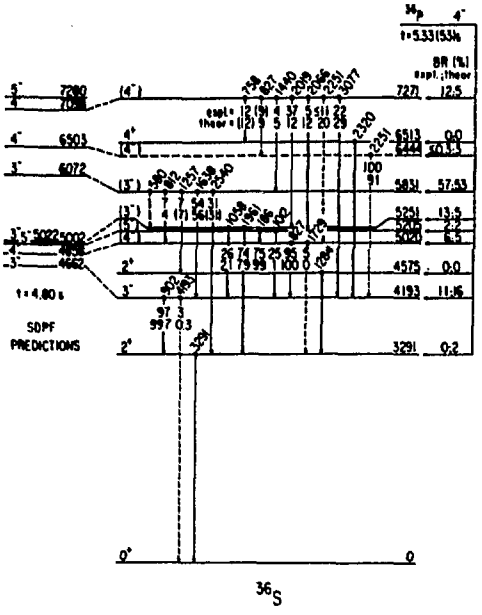

Fig. 1 The beta decay of ^{36}P. The SDPF predicted excitation energies to the left have been raised by 195 keV as in the β-decay calculation. The γ-ray energies are indicated in keV above the levels from which they originate. Gamma-ray branching ratios (in %) are given below the levels: the top numbers are experimental (Ref.1) and the bottom are the SDPF predictions. Numbers in parentheses are assumed. The experimental and theoretical β branching ratios are indicated on the right.

---

* Brookhaven National Laboratory

[1] J. P. Dufour et al., Z. Physik A324, 487 (1986).

9. Calculated Moments and Transition Rates for the 2_1^+ and 8_1^+ States of $^{86,88}Sr$
(E. K. Warburton* and J. A. Becker)

The values of B(E2, $2_1^+(8_1^+) \rightarrow 0$) and the quadrupole moment and g-factor of the 2_1^+ (8_1^+) states have been calculated for $^{86,88}Sr$, within the framework of the spherical shell model. The model space included the $2p_{1/2}$, $2p_{3/2}$ and $1g_{9/2}$ orbitals; the number of $g_{9/2}$ particles was restricted to ≤ 12. Results obtained with $\Delta q = 0.5$ and $g_\ell(\pi) = 1.10$, $g_\ell(\nu) = -0.05$, $g_s(\pi) = 3.541$, and $g_s(\nu) = -3.826$ are presented in Table 1, where they are also compared with experimental results of Kucharska.

Table 1. Moments for $^{86,88}Sr$

	^{86}Sr		^{88}Sr	
	Model	Exp.	Model	Exp.
B(E2; $2_1^+ \rightarrow 0_1^+$)[Wu]	5.03	14.55	5.78	7.04(41)
B(E2; $8_1^+ \rightarrow 0_1^+$)[Wu]	0.98	<0.86	2.76	
$Q(2_1^+)$ [efm^2]	+7.76		+23.4	
$Q(8_1^+)$ [efm^2]	+22.30		-48.9	
$g(2_1^+)$	0.363	0.265	1.23	0.96(17)
$g(8_1^+)$	-0.180	-0.243	1.36	

* Brookhaven National Laboratory

10. Microscopic Optical Model Analysis of Elastic Neutron Scattering Differential Cross Sections and Analyzing Powers
(L. F. Hansen, F. S. Dietrich, and R. L. Walter*)

The microscopic optical model potentials of JLM[1] and Yamaguchi et al.[2] have been tested against the measurements of differential cross sections and analyzing powers of neutrons elastically scattered from targets ranging from ^9Be to ^{208}Pb done by the TUNL neutron group for energies between 8-17 MeV. The comparison with the experimental data has been made by least-squares adjustment of only three normalyzing parameters, λ_V, λ_W, and λ_{SO}, for the real and imaginary parts of the central potential, and the real spin-orbit potential respectively. Figs. 1 and 2 show the quality of the fits to the elastic scattering and polarization measurements for ^{89}Y as function of energy. Both potentials give fairly good agreement for all the measurements with practically only one parameter, λ_W, since for all these calculations $\lambda_V \simeq 1$ and $\lambda_{SO} = 1.3$.

The fits compare well with those obtained with phenomenological model potentials which have as many as 20 parameters.

* Physics Department, Duke University

[1] J. P. Jeukenne, A. Lejeune, and C. Mahaux, Phys. Rev. C16, 80 (1977).

[2] Yamaguchi, et al. Prog. Theor. Phys. Japan 70, 459 (1983).

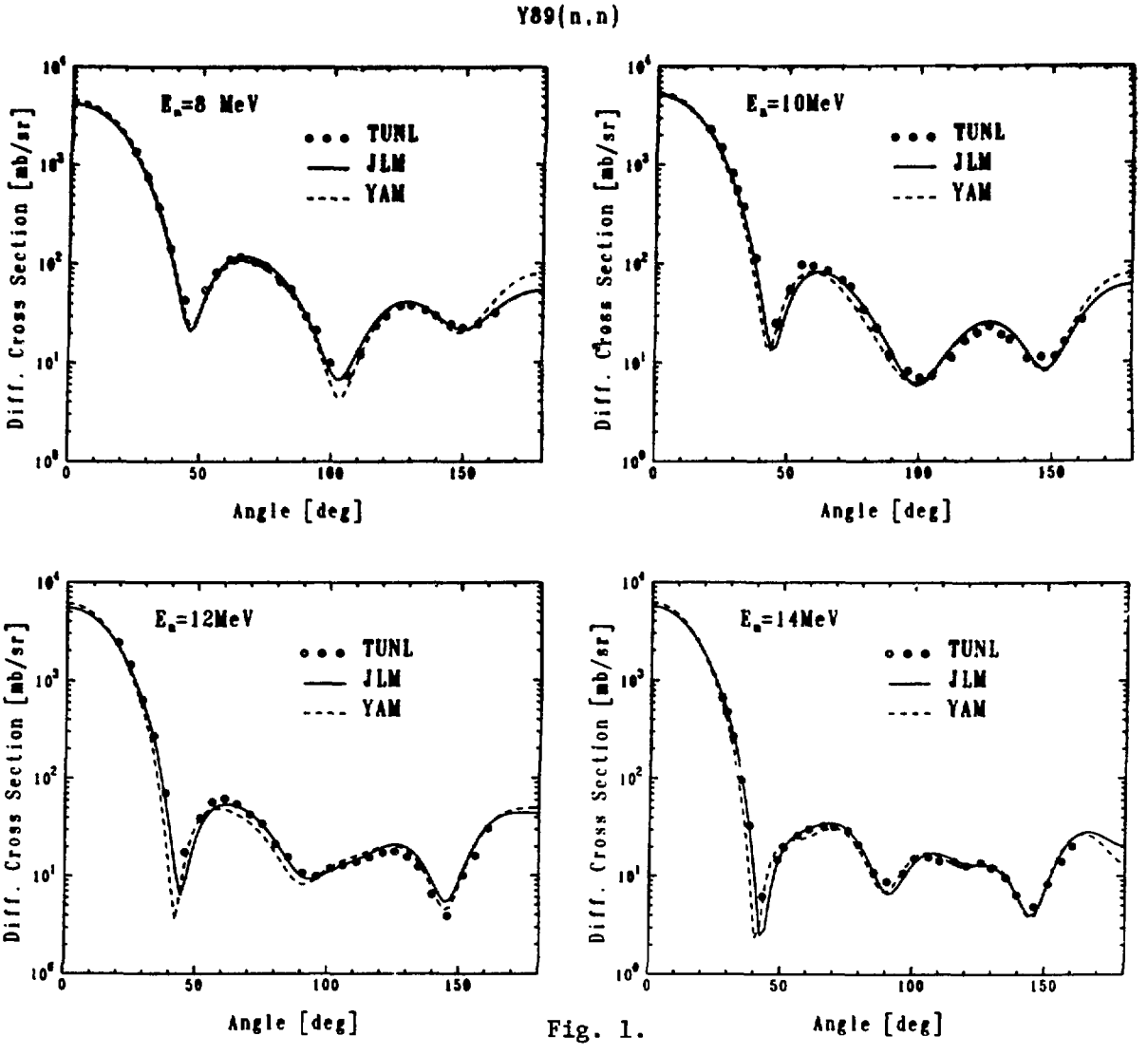

Fig. 1.

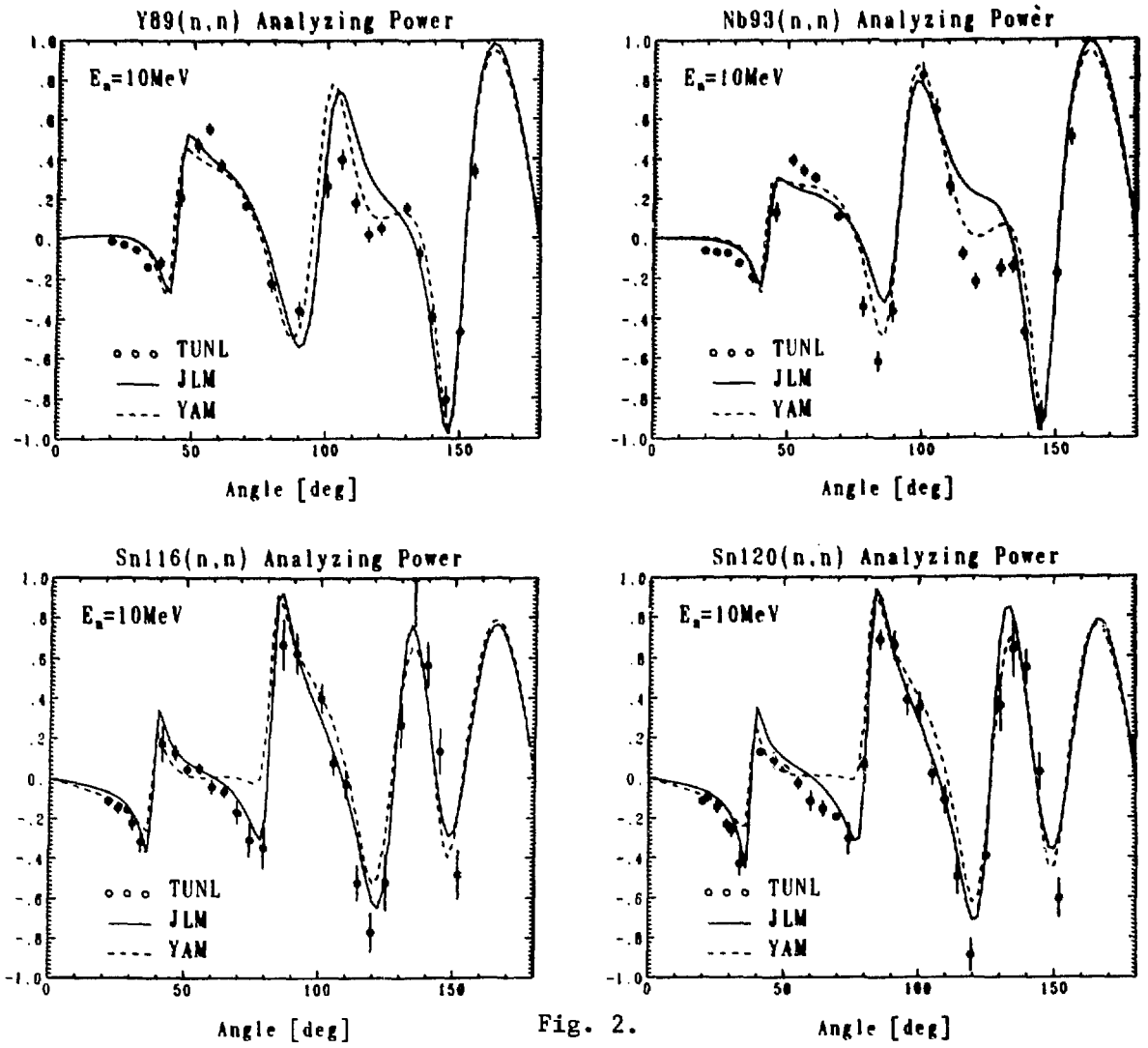

Fig. 2.

11. New Computer Network for Nuclear Modeling Calculations
(D. A. Resler, R. M. White, T. T. Komoto, and J. D. McGowan)

We have installed a network of Sun Microsystems computers for performing our nuclear modeling calculations. Our shell model calculations require large amounts of CPU time, core memory, and disk storage that are not available on a day-to-day basis on large shared systems. Our present network is dedicated to our nuclear modeling calculations and consists of two Sun 3/260's and four 3/50's. Both 3/260's are configured with 8 Mbyte real memory and floating point accelerator. One has a 1/4" tape drive and 2.4 Gbyte disk storage and the other has a 1/2" 1600 BPI tape drive and 575

Mbyte disk storage. The 3/50's each have 4 Mbyte of real memory and share the disk storage of the larger machines. The preequilibrium/evaporation code ALICE runs 19 times slower on the 3/260 with FPA when compared to a CRAY-1 supercomputer. The shell model code CRUNCHER runs only 5 times slower when compared to the CRAY. In the next month, both 3/260's will be upgraded to Sun 4/260's giving us another factor of two increase in computational speed. In addition, we will be adding another 32 Mbyte of real memory to each system allowing for calculations 5 times larger than what we can handle presently.

12. Implementation of the Ohio University Shell Model and R-Matrix Codes
(D. A. Resler and H. D. Knox*)

The Ohio University Shell Model Code CRUNCHER, R-matrix code, and auxillary codes have been implemented on our dedicated Sun network. The codes are now fully operational and production calculations have been performed. A new code SM2RM has been written to facilitate the conversion of shell model quantities to the R-matrix input. In collaboration with Ohio University, we will be implementing and generalizing the coding for calculation of multinucleon spectroscopic amplitudes. Upon completion, the entire set of programs will be capable of calculating virtually any two-body reaction cross section from a fundamental nucleon-nucleon interaction.

* Ohio University, Athens, Ohio

13. Implementation of the IDA System of Nuclear Modeling Codes
(D. A. Resler, J. D. McGowan, T. T. Komoto, M. MacGregor, and G. Reffo*)

Over the past 20 years, G. Reffo has developed IDA, a modular system of nuclear modeling codes based on preequilibrium/Hauser-Feshbach theory. We have implemented this extensive system of codes on our dedicated Sun network. We are currently debugging some of the modules and also learning how to most efficiently run various problems. We project that it will take at least a year or more to run all the types of problems of which this system is capable. However, some production calculations have already been performed and more are currently underway.

* ENEA, Bologna, Italy

14. Development of Neutron-Induced Cross-Section Libraries for Bismuth and Iridium for Use in Radiochemical Diagnostics of Nuclear Tests
(M. Gardner, D. Gardner, R. Meyer, N. Namboodiri, and D. Nethaway)

Bismuth and iridium are frequently used as detectors to measure neutron fluences in the course of radiochemical diagnostics of underground nuclear tests. In the case of ^{209}Bi, the availability of four successive (n,2n) reaction products that have convenient half-lives and relatively low neutron-capture cross sections makes bismuth an attractive radiochemical detector. We have nearly completed the calculation of 108 excitation functions for neutron-induced reactions involving 15 ground and isomeric states of bismuth isotopes in the mass range 204 to 210. To demonstrate the differences in the capture cross sections for different isomeric target states, we show in Fig. 1 the excitation functions for each of the three target states of ^{206}Bi leading to the ground state and isomer of ^{207}Bi. The two lowest cross sections arise from the large spin differences between the respective target and product species.

We are now in the process of making a "first-pass" set of calculated cross sections for iridium for use in sensitivity studies. The iridium detector - ^{191}Ir (37.3% abundant) and ^{193}Ir (62.7% abundant) - not only provides information about low- and high-energy neutron fluences in devices via the formation of the double (n,2n) product, $^{189}Ir/^{190}Ir$, and the capture product, ^{194}Ir, respectively, but also about mid-range neutron energies, via the production of the ^{193m}Ir by the (n,n') reaction. Our calculated cross-section set presently consists of 22 ground and isomeric states as targets and products, connected via a total of 174 excitation functions for (n,γ) and (n,xn) reactions.

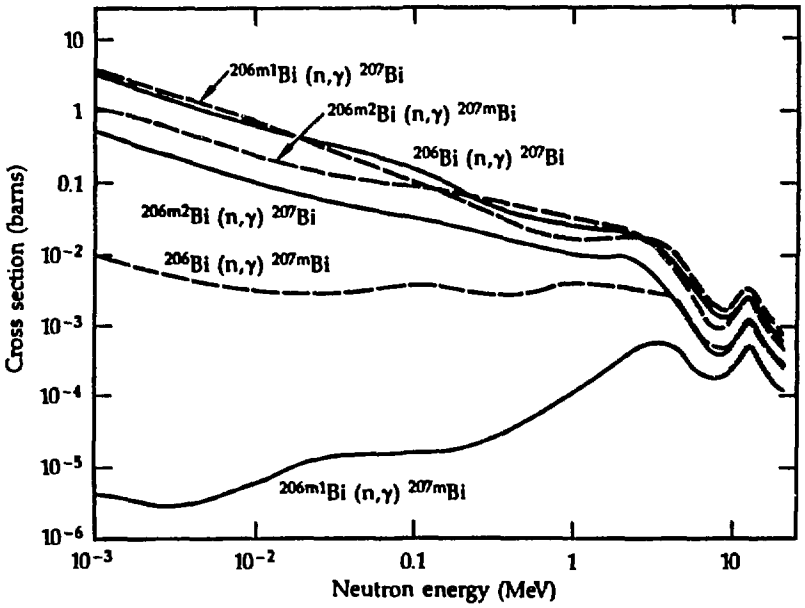

Fig. 1 Calculated (n,γ) excitation functions for the ground state and isomers of ^{206}Bi.

15. Further Studies of Actinide Dipole Strength Functions
(D. Gardner, M. Gardner, and R. Hoff)

We have continued to make calculations for a number of neutron- and photon-induced reactions on actinide nuclei. We deduced absolute dipole strength functions for ^{233}Th and ^{239}U by fitting total neutron-capture data and average resonance-capture (ARC) measurements. Two types of cross-section data available in the literature for (n,γ) reactions on ^{232}Th and ^{238}U were studied. Neutron-capture excitation functions, measured or evaluated over the incident neutron energy range of 20 keV to about 2 MeV, allowed us to determine the magnitude of the total radiation widths for ^{233}Th and ^{239}U. We used ARC studies[1,2] of 2-keV neutrons on ^{232}Th and ^{238}U to determine what the relative M1/E1 strengths should be for gamma-ray energies of 3.6 to 4.8 MeV. Large sets of modeled discrete levels were used for the daughter nuclei: ^{233}Th (119 levels) and ^{239}U (147 levels).

As we had observed in earlier studies, in order to achieve agreement between our calculated neutron-capture cross sections and those in the literature, we had to increase the total radiation-width values for ^{233}Th and ^{239}U by increasing the E1 and M1 strength functions 27% each. We then checked their relative magnitudes against the ARC data. We calculated the relative primary gamma-ray intensities to all the modeled discrete levels of the product nuclei, following 2-keV neutron capture. Because these neutrons are essentially s-wave in nature, they primarily produce $1/2^-$ states in each of the product nuclei. Transitions going to $1/2^-$ and $3/2^-$ discrete levels represent E1 transitions, while those proceeding to $1/2^+$ and $3/2^+$ levels are transitions of the M1 type.

Figure 1 shows our results for the thorium case. The bands are the calculated relative values of the reduced dipole transition intensities to the modeled ^{233}Th levels, I_γ/E_γ^5, together with a 1 standard deviation error limit. The markers represent the relative experimental values, with spin and parity assignments as given by the key. The calculations and measurements are both normalized to the average of several E1 transitions. Similar results were obtained for the ^{238}U target. The overall good agreement in the two cases confirms that the relative M1/E1 strengths that we deduced from the ^{176}Lu ARC data are also valid in the actinide region. We now feel confident of our modeling of the E1 strength function in four mass regions: mass-90, rare-earth masses around lutetium, bismuth, and the actinides. Further study is needed, however, on the energy and mass dependence of M1 strengths.

---

[1] P. Jeuch et al., Nucl. Phys. A317, 363 (1979).

[2] R. E. Chrien and J. Kopecky, Nucl. Phys. A414, 281 (1984).

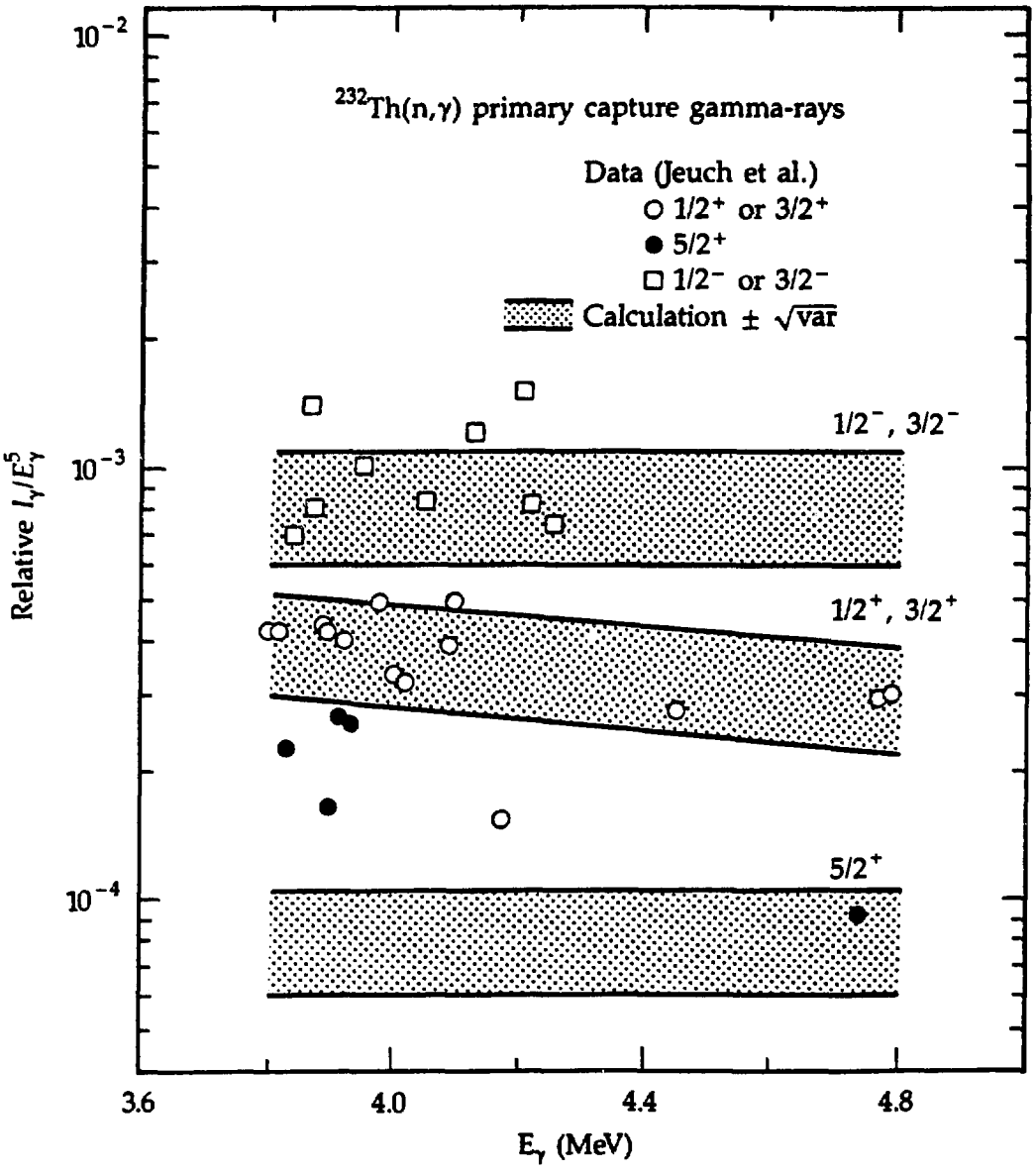

Fig. 1 Comparison of the calculated and measured[2] reduced relative transition intensities for primary gamma rays following 2-keV neutron capture by ^{232}Th.

16. Neutron-Neutron Elastic Scattering Determined from Potentials
(V. Brown and P. Anthony)

Two-nucleon cross sections are more difficult to measure when one of the nucleons is a neutron as compared to proton-proton scattering. In the absence of a complete and reliable data base, one must resort to predictions based on model calculations. At low enough energies one can use model-independent effective-range expansions, which connect cross sections with the nn scattering lengths and effective-range parameters. These expansions are limited to an energy range in which only the lowest partial waves play a role. If one is interested in the nn elastic scattering results for higher energies, it is necessary to include the effects of higher partial waves. One way to do this is to use two-nucleon potential models that have been fitted to the phase shifts. There are a number of these in the literature with a varying range of sophistication. For calculating nn scattering it is prudent to choose a potential with low-energy scattering parameters that are in good agreement with the available data. We are currently calculating differential and total cross sections for nn scattering up to energies of 60 MeV using a variety of nucleon-nucleon potentials that satisfy these criteria.

It is well known that different potentials give different on-shell results. These differences will serve as a measure of the theoretical uncertainties in our predictions. Where available, nn scattering data will be used to estimate the experimental uncertainties. Since such data are rare, another measure of the experimental uncertainties, based on isospin considerations, is a comparison of the predictions to pp and np (isospin = 1 only) empirically determined phase shifts. Since to a very good approximation isospin is conserved in the two-nucleon interaction, the channel with isospin equal to one, appropriate for identical particles, is the same, after Coulomb corrections, for nn, np, and pp scattering.

B. NUCLEAR DATA APPLICATIONS - MEASUREMENTS

1. Integral Measurements and Calculations of Neutron and Gamma Ray Emission at 14 MeV

(E. Goldberg, L. F. Hansen, T. T. Komoto, and B. A. Pohl)

The Monte Carlo calculational analysis of integral measurements of the gamma-ray and neutron emission spectra (reported last year) from a 14-MeV neutron source for materials of interest to thermonuclear reactors (see Table 1), have been completed using the codes TART and SANDYL. The photon-neutron library, ENDL, has been tested against the measurements. Calculations with ENDF/B-V are underway. By measuring simultaneously the gamma-ray and neutron emission spectra, we facilitate the search for the source of the discrepancies between the calculated and measured gamma spectra. Fig.1 illustrates some of the problems presently existing in the libraries. A detailed report of the comparisons between measurements and calculations for all the materials listed in Table 1 is underway.

Table 1

Material	Radius [cm]	ρr [g/cm^2]	mfp[a] [14 MeV]
C	10.16	17.7	1.5
O[b]	14.76	13.4	1.4
CF_2	16.50	35.2	2.0
Al	8.94	22.4	0.9
Si	10.16	23.7	0.9
Ti	8.94	40.6	1.1
Fe	4.46	31.3	1.0
Cu	4.00	32.9	1.0
Ta	3.40	51.1	1.0
W	10.36[c]	49.0	1.0
Au	6.21	120.0	1.9
^{232}Th	5.76	61.6	1.0
^{238}U	3.63	55.7	1.0

[a] Mean free path calculated using the total cross sections from the ENDL library.

[b] H_2O (13.6 g/cm^2 H_2O + 1.11 g/cm^2 pyrex).

[c] 2.2 cm-thick shell.

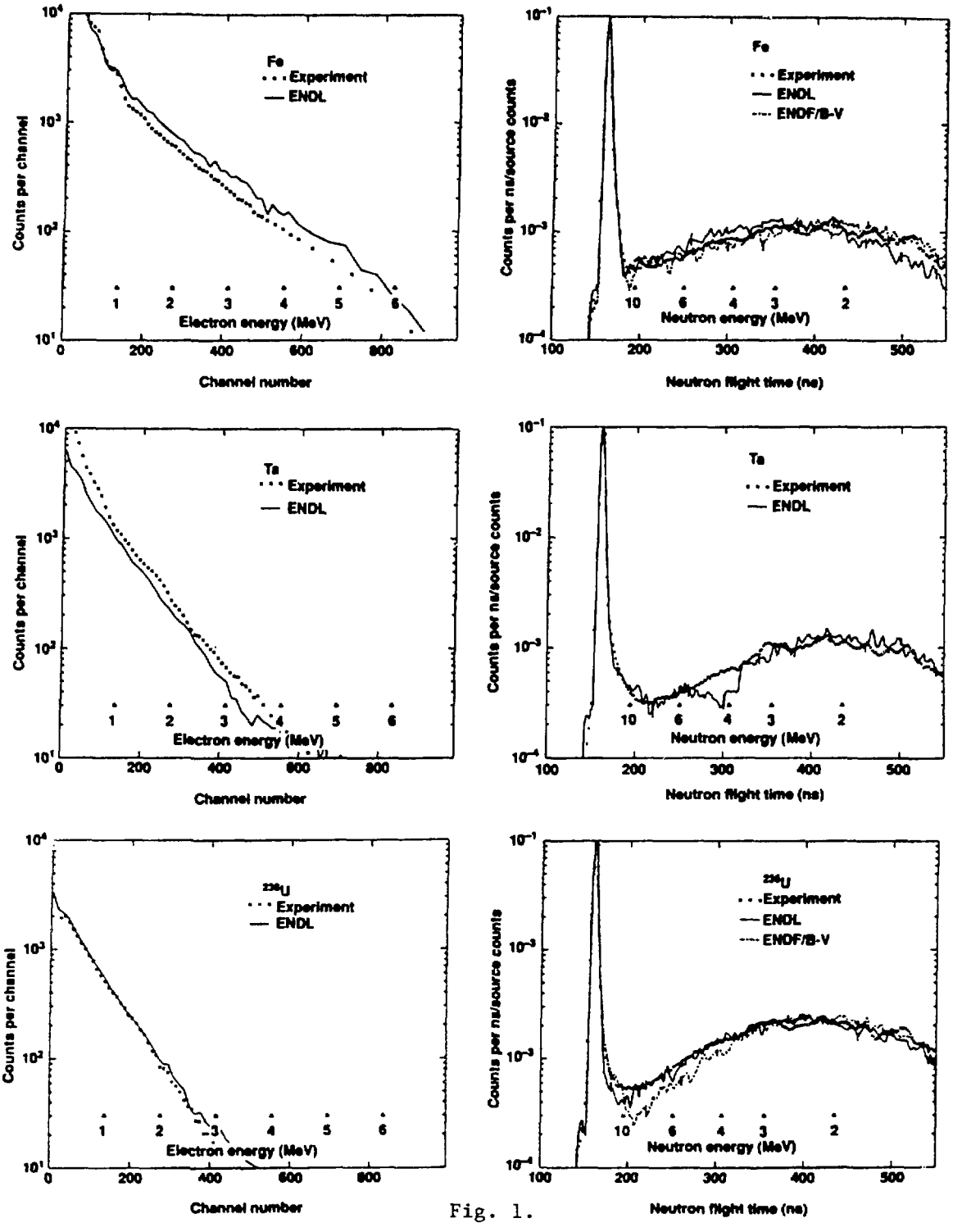
Fe
Experiment
ENDL
ENDF/B-V
Counts per channel
Electron energy (MeV)
Channel number
Counts per ns/source counts
Neutron energy (MeV)
Neutron flight time (ns)
Ta
Experiment
ENDL
Counts per channel
Electron energy (MeV)
Channel number
Counts per ns/source counts
Neutron energy (MeV)
Neutron flight time (ns)
238U
Experiment
ENDL
ENDF/B-V
Counts per channel
Electron energy (MeV)
Channel number
Counts per ns/source counts
Neutron energy (MeV)
Neutron flight time (ns)

Fig. 1.

2. Excitation Functions for ^{48}V and ^{47}Sc Produced by Tritons on Titanium

(H. West, R. Lanier, M. Mustafa, and H. O'Brien)

We measured the excitation functions of nuclides produced by the bombardment of natural Ti and separated ^{48}Ti by tritons with energies from 1.5 to 18 MeV with the tandem Van de Graaff accelerator at the Los Alamos National Laboratory. We show results obtained for $^{48}Ti(t,\alpha)^{47}Sc$ (Ref. 1) and

$$\sum_{x=1}^{3} + \sum_{x=2}^{3} \text{Ti}(t,xn)\ ^{48}V$$

(Ref. 1 and 2) in Figs. 1 and 2, respectively. In each case the effects of the finite energy range of the protons in the foils on the rising portions of the curves have been corrected and the results plotted as circles.

The data were modeled by the statistical-model code, STAPRE. For the $^{48}Ti(t,\alpha)^{48}V$ data (see Fig. 1), the STAPRE results are surprisingly low. There possibly is an appreciable contribution due to direct reactions. Our efforts at modeling the production of ^{48}V from natural titanium (see Fig. 2) were much more successful. However, the differences between the theory and experiment are enough to support the possibility that break-up fusion may be occurring in analogy to deuteron-induced reactions.[3,4]

---

[1] H. West, R. Lanier, M. Mustafa, and H. O'Brien, Lawrence Livermore National Laboratory, UCAR 10062/87 (1987).

[2] H. West, R. Lanier, M. Mustafa, and H. O'Brien, Lawrence Livermore National Laboratory, UCID-21063 (1987).

[3] H. West, R. Lanier, and M. Mustafa, Phys. Rev. C 35, 2067 (1987).

[4] M. Mustafa, T. Tamura, and H. Udagawa, Phys. Rev. C 35, 2077 (1987).

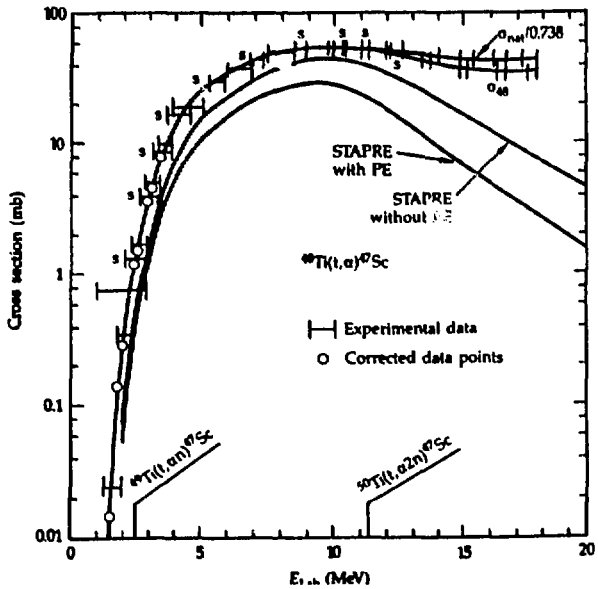

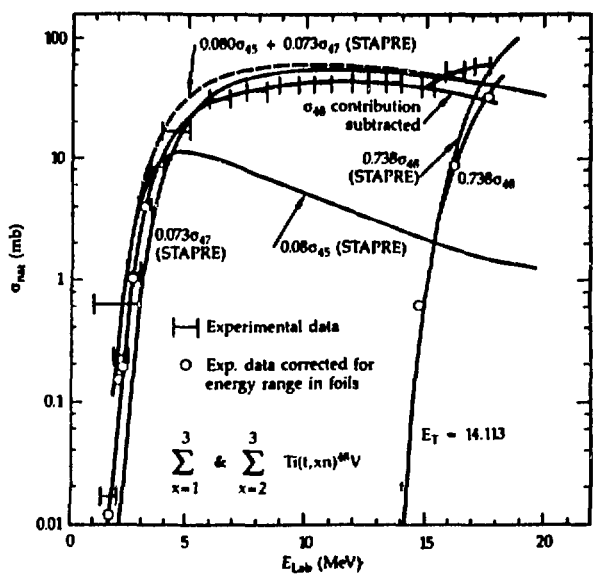

Fig. 1 Excitation function for the $^{48}Ti(t,\alpha)^{47}Sc$ reaction. Note that the data marked "s" and σ (at high energy) are for separated ^{48}Ti. The other data are for natural titanium divided by the natural abundance, 0.738, of ^{48}Ti. There is an almost negligible contribution from the $^{49}Ti(t,\alpha n)^{47}Sc$ reaction in the data.

Fig. 2 The excitation function for the production of ^{48}V from tritons on natural titanium. Note that the cross sections are presented in terms of their abundances in natural titanium; the STAPRE calculations have been adjusted to reflect this factor.

3. Proton and Deuteron Excitation Functions for the $^{87}Zr^{g} \rightarrow {}^{87}Y^{g,m} \rightarrow {}^{87}Sr^{m}$ Decay Chain

(H. West, R. Lanier, M. Mustafa, H. O'Brien, and R. Nagle)

We have studied the excitation functions of the nuclides produced by protons and deuterons on ^{89}Y. The lower-order reactions have been reported earlier. By extending the bombarding energies to 40 MeV, using the Crocker Cyclotron at the University of California at Davis, we have studied the higher-order reactions exemplified by the $^{87}Zr^{g} \rightarrow {}^{87}Y^{g,m} \rightarrow {}^{87}Sr^{m}$ decay chain.[1] In order to study the decay chain, we had to improve on the $^{87}Zr^{g}$ decay scheme before absolute decay rates could be established.

The results of our excitation function measurements are shown in Figs. 1-4. For Figs. 1-3 the data are compared with our first results from the statistical-model code STAPRE. STAPRE models the $^{89}Y(p,3n)^{87}Zr$ data in Fig. 1 quite well. However, for the $^{89}Y(d,4n)^{87}Zr$ data, the

experimental data is low. This is consistent with our observation of break-up fusion for lower order deuteron reactions.[2,3] Figure 2 shows a comparison of data and theory for the $^{89}Y(p,2np)^{87}Yg,m$ reaction. Clearly more physics than that contained in STAPRE is needed to explain the data. We attribute the skirts at low energy to the (p,nd) reaction. There is possibly a strong component due to a direct reaction. Figure 3 shows data and theory for the $^{89}Y(d,3np)^{87}Yg,m$ reaction. If the break-up fusion mechanism is used to explain the data in Fig. 1, it will occur here as well. These results would seem to be in the wrong direction, suggesting problems with our choice of level-density parameters. However, the appearance of a strong (d,2nd) channel and the effects of direct reactions must be considered at both low and high energies. Figure 4 shows the production cross section for $^{87}Sr^{m}$ by both protons and deuterons on ^{89}Y. No attempt has yet been made to model the data.

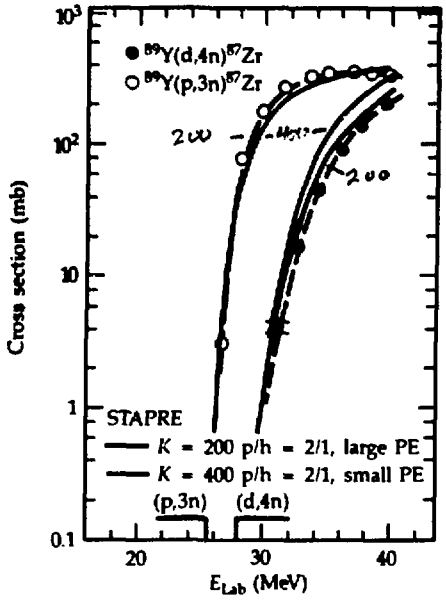

Fig. 1

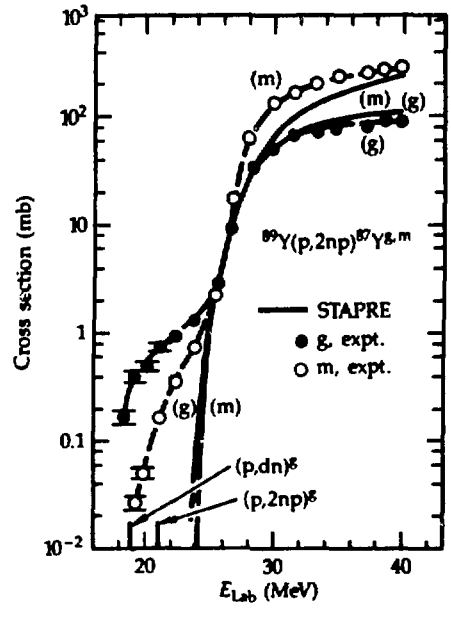

Fig. 2

[1] H. West, R. Lanier, M. Mustafa, H. O'Brien and R. Nagle, Lawrence Livermore National Laboratory Report UCAR 10062/87 (1987).

[2] H. West, R. Lanier, and M. Mustafa, Phys. Rev. C 35, 2067 (1987).

[3] M. Mustafa, T. Tamura, and H. Udagawa, Phys. Rev. C 35, 2077 (1987).

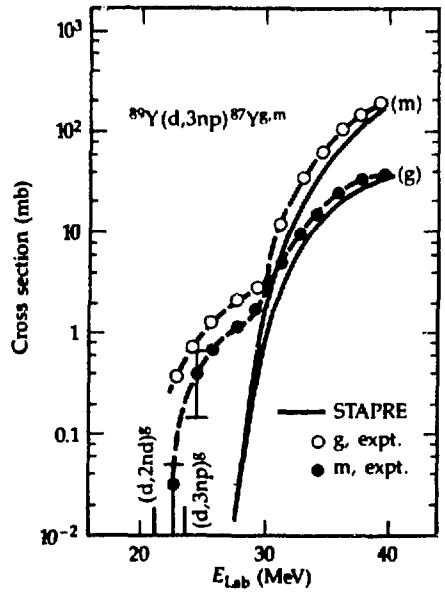

Fig. 3 The ^{89}Y(d,3np)^{87}Yg,m excitation functions. Note the skirts at low energy. As for the corresponding proton data, the skirts are attributed to direct reactions. Note that at the higher energies, STAPRE underestimates experiment in an apparent contradiction of our concepts of breakup fusion for the deuteron.

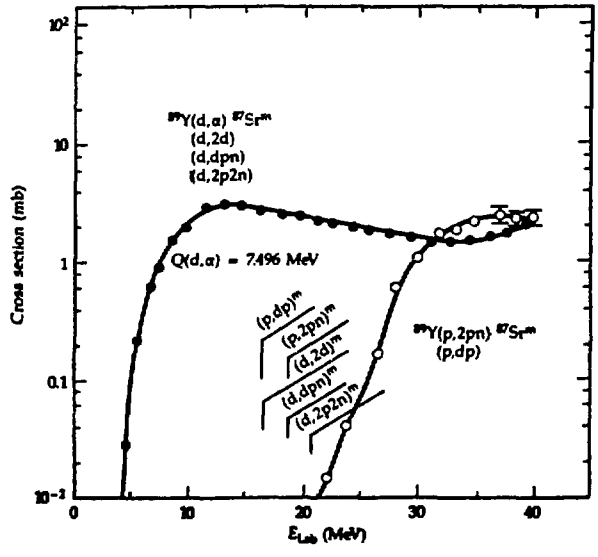

Fig. 4 The ^{89}Y(d,α + other reactions)^{87}Sr^{m} and ^{89}Y(p,2pn)^{87}Sr^{m} excitation functions. STAPRE calculations have not been carried out as yet.

4. Measurements and a Direct-Reaction Plus Hauser-Feshbach Analysis of the $^{89}Y(p,xn)^{88,89}Zr$ Data up to Ep = 40 MeV
(M. Mustafa, M. Benhamou, T. Tamura, H. West and R. Lanier)

Some of our foil-activated measurements of the excitation functions for the reactions $^{89}Y(p,xn)^{88,89}Zr$ were reported to the DOE Nuclear Data Committee in 1986. The measurements of these cross sections are now complete. Here we report the final data and an analysis of the data using a direct-reaction plus Hauser-Feshbach formalism (HFDR). Our direct-reaction approach is based on the multi-step direct reaction theory of Tamura, Udagawa, and Lenske.[1]

The results in Fig. 1 show that the measured excitation functions for both of the reactions are well reproduced by the calculation, thereby providing a quantum mechanical understanding of the low-energy activation cross sections. For completeness, we have analyzed these data with the Hauser-Feshbach plus phenomenological preequilibrium models (HFPE) and show that a good fit to the data can be achieved with these models as well, but with one free parameter. A detailed report is in preparation. Although the HFDR calculations are somewhat more complicated than the usual (HFPE) calculations, we expect the HFDR approach to be used routinely in the future modeling of excitation functions below 50 MeV. We plan to develop an optimized HFDR code based on one- and two-step direct-reaction theory.

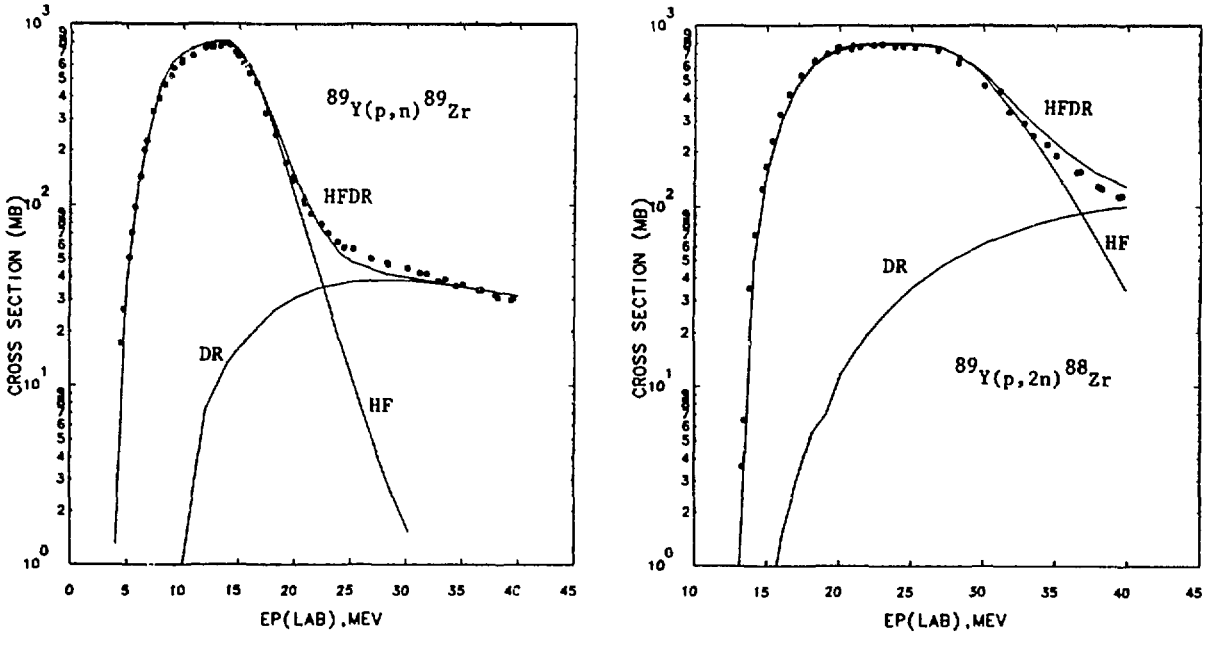

Fig. 1 Hauser-Feshbach (HF) plus direct reaction (DR) excitation functions are compared with our foil-activated data.

[1] T. Tamura, T. Udagawa, and H. Lenske, Phys. Rev. C 26, 379 (1982).

A. NUCLEAR DATA MEASUREMENTS

1. Low energy Fusion Cross Sections: Charged Particle Reactions
(Nelson Jarmie and Ronald E. Brown)

The goal of this project is to determine cross sections for interactions among the hydrogen isotopes in the bombarding-energy range 10-120 keV. Such cross sections are fundamental to the operation of future controlled-fusion reactors. Experimental work with the facility constructed for this purpose [LEFCS: Low-energy Fusion Cross Sections] is complete. Analysis and publication are continuing.

Work on the D(t,α)n reaction is complete. A new paper: *Fusion-energy reaction $^3H(d,\alpha)n$ at low energies*, Phys. Rev. C 35, 1999 (1987); erratum C 36, 1220 (1987); describes the last 8 data points at higher energies: 80-116 keV. The discovery of a "shadow pole" in the R-Matrix analysis of the data (with G. Hale) has been published: Phy. Rev. Letters **59**, 763 (1987), and has evoked considerable interest: see: *Comments* in Phys. Rev. Letters

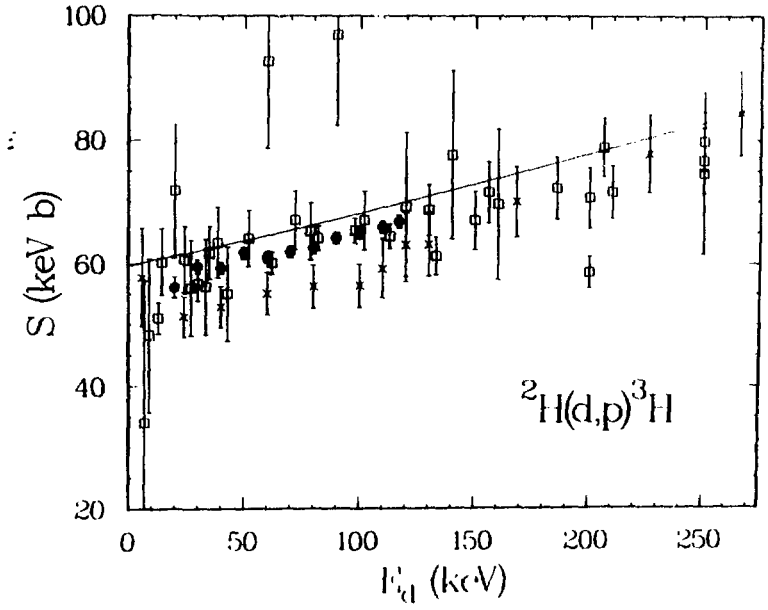

FIG. A-1. The S function for the $^2H(d,p)^3H$ reaction integrated cross section as a function of deuteron bombarding energy. Both tritons and protons were detected. Total errors are shown. The solid circles are the present Los Alamos data. The crosses are from the Münster data.[1] The squares are a representative selection of other data from other experiments. The curve is from a unified, mass-4, R-Matrix analysis[2,3] that does not include the Los Alamos or Münster data. Note the suppressed zero.

59, 2818-2819 (1987). Bound states and resonances of a compound system are often represented as S-Matrix poles in the complex-energy plane. Our analysis appears to require a pole on a continued complex sheet ("second Riemann sheet")--the so-called "shadow" pole.

The calculations by G. Hale of Los Alamos extending R-Matrix phenomenology to handle 3-body breakup are continuing. This development is of great interest to us to help analyze the three-body breakup alpha spectra of the T(t,α)nn reaction; and, in particular, to be able to estimate the shape of the neutron spectrum, which we have found impossible to measure experimentally.

The final analysis of the $^2H(d,p)^3H$ and $^2H(d,n)^3He$ data is now complete. We have measured differential cross sections for both reactions at 11 deuteron bombarding energies from 20 to 117 keV. The differential data are accurate to 2.0% over most of the energy range, with a scale error of 1.3%. Integrated cross sections are derived with total errors generally about 1.5%. In Figs. A-1 and A-2, our integrated cross section results are compared with other measurements and with an existing R-matrix analysis. The cross section is given in the form of the so-called astrophysical S

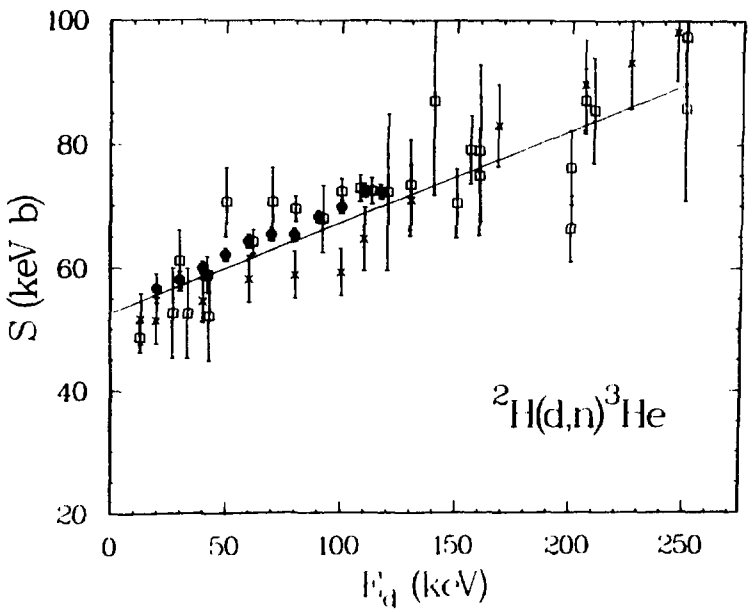

FIG. A-2. The S function for the $^2H(d,n)^3He$ reaction integrated cross section as a function of deuteron bombarding energy. The ^3He nuclei were detected. Total errors are shown. The solid circles are the present Los Alamos data. The crosses are from the Münster data.[1] The squares are a representative selection of data from other experiments. The curve is from a unified, mass-4, R-Matrix analysis[2,3] that does not include the Los Alamos or Münster data. Note the suppressed zero.

function, which factors out from the cross section the energy dependences of the de Broglie wavelength and the Coulomb penetrability. The improvement in accuracy over previous measurements is evident.

Fig. A-3 shows an example of the final differential data. The unusually large anisotropy (for this low energy) stems from the dominance of negative parity states in the ^{4}He compound state which helps the P waves compete with S waves in spite of the suppression by the angular momentum barrier. By analyzing the angular distribution, we find a larger D-wave reaction amplitude than previously reported. Formulas for the cross sections and for reactivities up to a plasma temperature of 20 keV will be given in the final paper which is now being written.

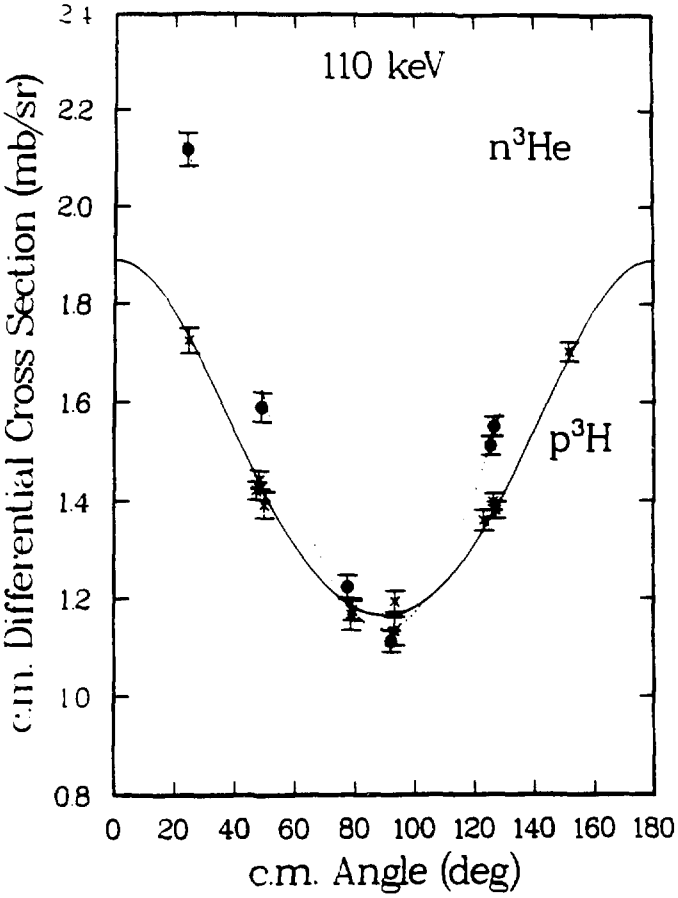

FIG. A-3. The c.m. differential cross section $\sigma(\theta)$ for both branches of the d + d reactions at a deuteron bombarding energy of 110 keV. The dashed line and solid circles are for the n + ^{3}He channel, and the solid curve and crosses are for the p + t channel. Relative errors are shown. Note the suppressed zero. The curves are from a least-squares fit of to the data of the form $(a + b \cos^2\theta + c \cos^4\theta)$.

A standard "handbook" of the best evaluated fuel-cycle cross sections and reactivities is still under consideration. Some fusion-reactor designers are still using old and sometimes grossly inaccurate data, and there exists no world standard collection of charged-particle data such as exists for neutron data.

[1]A. Krauss, H. W. Becker, H. P. Trautvetter, C. Rolfs, and K. Brand, Nucl. Phys. **A465**, 150 (1987).
[2]G. M. Hale and D. C. Dodder, in *Nuclear Cross Sections for Technology*, edited by J. L. Fowler, C. H. Johnson, and C. D. Bowman (National Bureau of Standards, Washington D.C., 1980), Special Publications 594, p. 650.
[3]G.M.Hale and D.C. Dodder, Conference on Few Body Problems in Physics, Vol.II: Contributed papers, page 433, edited by B. Zeitnitz, Elsevier Science Pub. (1984); (1983 Karlsruhe conference).

2. Low-Energy (n,charged particle) Cross Sections on Unstable Nuclei: The ^{7}Be(n,p)^{7}Li Cross Section from 25 meV to 13.5 keV
P. E. Koehler, C. D. Bowman, F. J. Steinkruger, D. C. Moody, G. M. Hale, J. W. Starner, S. A. Wender, R. C. Haight, P. W. Lisowski and W. L. Talbert)

Preliminary results of our measurement of the ^{7}Be(n,p)^{7}Li cross section from 25 meV to 13.5 keV were reported here last year. A paper describing our final results has been accepted for publication by the Physical Review C.[1]

The sample used in the measurements was made at the isotope production facility at LAMPF and consisted of 90 ng of ^{7}Be. Simultaneous measurement of the outgoing proton energy and incident neutron energy was made possible by using the white neutron source at LANSCE.

In addition to the LANSCE measurements, the absolute ^{7}Be(n,p)^{7}Li cross section at thermal energy was measured at the Omega West Reactor. For thermal neutrons the cross sections to the ground state and first excited state of ^{7}Li are 38400 ± 800 b and 420 ± 120 b respectively. This result is 20-30% lower than and has an error almost a factor of 10 smaller than previous published measurements.[2,3]

For energies above 100 eV a significant departure from a 1/v shape for the cross section is observed. Our new cross sections were analyzed together with data for other reactions using charge-symmetric, multilevel-multichannel R-matrix theory. The data are well described by a 2^{-} threshold state in combination with another nearby 2^{-} state. In particular, our examination of the properties of the S-matrix poles resulting from our R-matrix analysis has resolved reported conflicts in the literature about the width of the 2^{-} threshold state as observed in different reactions and has resulted in a more correct (and also larger) value for the T = 1 isospin mixing (24%) in this predominantly T = 0 state.

The astrophysical reaction rate was calculated from the measured cross sections. The resulting reaction rate is approximately 60-80% of the rate in use[4] before our measurements were made. This reduction in the reaction rate could result in a calculated increase in the production of ^{7}Li in the standard hot big-bang model by as much as 20%.

---

[1]P.E. Koehler et al., accepted for publication in the March 1988 issue (volume 37) of Phys. Rev. C.
[2]R.C. Hanna, Philos. Mag. 46, 381 (1955).
[3]Yu.M. Gledenov et al., JINR Rapid Communications, 17-86, 36 (1986).
[4]N.E. Bahcall and W.A. Fowler, Ap. J. 157, 659 (1969).

3. Low-Energy (n,charged particle) Cross Sections on Unstable Nuclei: The $^{22}Na(n,p)^{22}Ne$ and $^{36}Cl(n,p)^{36}S$ Cross Sections from 25 meV to Approximately 100 keV (P. E. Koehler and H. A. O'Brien)

The measurement of cross sections for (n,p) reactions on radioactive nuclei can provide information important to both basic nuclear physics and nuclear astrophysics.[1] To this end, we have recently completed measurements of the $^{22}Na(n,p)^{22}Ne$ and $^{36}Cl(n,p)^{36}S$ cross sections, relative to $^{6}Li(n,\alpha)t$, from thermal energy to about 100 keV using the white neutron source at the Los Alamos Neutron Scattering Center (LANSCE). Also, we have measured the absolute $^{22}Na(n,p)^{22}Ne$ cross section using the Omega West Reactor (OWR) at Los Alamos.

As is shown in figures 1 and 2, our results for $^{22}Na(n,p)^{22}Ne$ are in agreement with previous data[2-4], while in general, the errors on our data are much smaller than in previous measurements, and our results extend to much higher energies. Our measurements are the first for the relatively small $^{22}Na(n,p_0)^{22}Ne$ cross section at other than thermal energy. Hence, our data are the first to show that the resonance near 170 eV that is responsible for the large $^{22}Na(n,p_1)^{22}Ne$ cross section does not contribute much to the ground state cross section. We have calculated the astrophysical reaction rate for the $^{22}Na(n,p)^{22}Ne$ reaction using our measurements. This reaction may be important to understanding the nucleosynthesis of ^{22}Na and/or ^{22}Ne, and the neon-E anomaly found in some meteorites. Our measurements show that the theoretical calculations currently used[5] in nucleosynthesis studies underestimate the measured cross section, and hence the true reaction rate by as much as a factor of 10 at some temperatures. We are currently exploring the implications of this result on nucleosynthesis calculations for ^{22}Na and ^{22}Ne.

The results of our $^{36}Cl(n,p)^{36}S$ measurements are shown in figure 3. As we have not yet measured the absolute thermal cross section, we display our LANSCE data as yields rather than cross sections. As can be seen in figure 3, several resonances contribute to the $^{36}Cl(n,p)^{36}S$ cross section at these

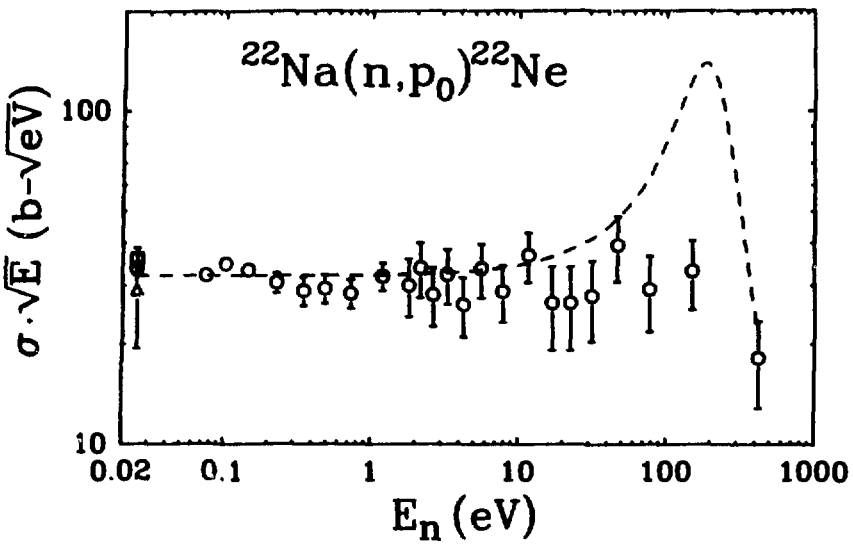

Fig 1. The $^{22}Na(n,p_0)^{22}Ne$ reduced cross section verses neutron energy. Our data are shown as circles. Also shown are the thermal energy data of refs. 2 (square) and 3 (triangle). The dashed curve shows the expected p_0 cross section if the resonance near 170 eV that is responsible for the large p_1 thermal cross section also was responsible for the p_0 thermal cross section.

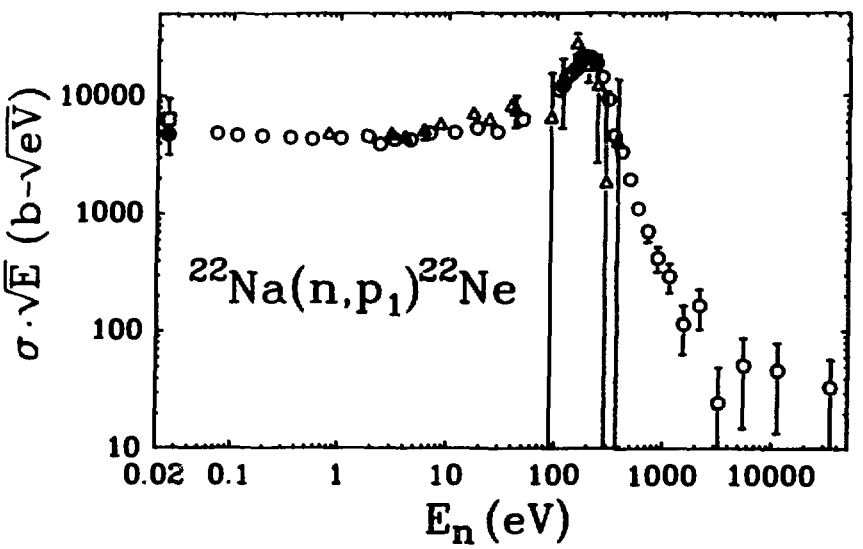

Fig 2. The $^{22}Na(n,p_1)^{22}Ne$ reduced cross section verses neutron energy. Our data are shown as circles. Also shown are the data of ref. 3 (triangles) and the thermal energy measurements of refs. 1 (square) and 2 (diamond). For clarity, only every tenth data point from our measurements is shown for energies below 100 eV.

energies. We plan to measure the absolute thermal cross section for this reaction at the OWR in the near future. Our final results may be important to calculations[6] of the nucleosynthesis of the rare isotope ^{36}S.

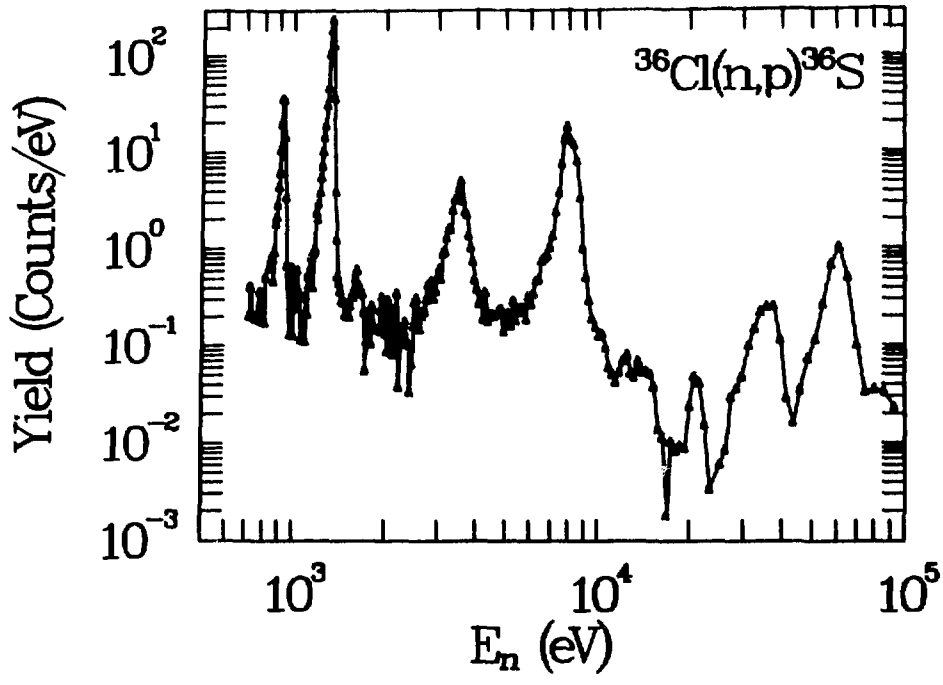

Fig 3. Preliminary yield verses neutron energy from our $^{36}Cl(n,p)^{36}S$ measurements. Because we have yet to measure the absolute thermal cross section, the yields have not been corrected for the variation with energy of the neutron flux, or normalized to absolute cross sections.

[1]P. E. Koehler, H. A. O'Brien and C. D. Bowman, to be published in the Proceedings of the Workshop on Nuclear Spectroscopy of Astrophysical Sources, Washington D.C., December 1987.
[2]R. Ehehalt, H. Morinaga and Y. Shida, Z. Naturforsch, **26a**, 590 (1971).
[3]J. Kvitek et al., Z. Phys. **A299**, 187 (1981).
[4]Yu. M. Gledenov et al., Z. Phys. A308, 57 (1982).
[5]S. E. Woosley et al., At. Data Nucl. Data Tables 22, 371 (1978).
[6]W. M. Howard et al., Ap. J. 175, 201 (1972).

4. Thermal-neutron Fission Cross Section of 26.1-min $^{235}U^{m}$ (W. L. Talbert, Jr., J. W. Starner, M. E. Bunker, R. J. Estep, S. J. Balestrini, M. Attrep, Jr., D. W. Efurd, and F. R. Roensch)

We have measured the thermal-neutron fission cross section of $^{235}U^{m}$ using a radiochemical procedure to separate samples of about 10^{11} atoms

from a 200-mg ^{239}Pu cow, followed by observation of the fission rate produced in these samples during irradiation in the Omega West Reactor.[1]

The 26.1-min isomeric state of ^{235}U has been studied extensively since its discovery and isolation in 1957 (Refs. 2,3). Despite efforts to obtain samples large enough to make a measurement of its fission cross section, no such measurements were reported until 1984 (Ref. 4), while the present work was in progress.

A radiochemical process for separating U from Pu was developed that provides a chemical yield of about 50% and a separation factor exceeding 10^{10}. The time required for separation with this procedure is about 30 min. The uranium samples obtained were placed in a low-background proportional counter fission chamber and irradiated in a 5 x 10^{11} n/cm^{2}s thermal flux (cadmium ratio for ^{197}Au of 117). Fission events were multiscaled for 180 min., and the time spectrum was analyzed to determine the 26.1-nim component resulting from fission of $^{235}U^m$.

Measurements were made on a total of eight samples, and the data resulted in a value for the isomer-to-ground-state cross-section ratio of 1.42 ± 0.04, which differs considerably from the value of 2.2 ± 0.4 reported in Ref. 4.

The thermal-neutron cross section measurement was carried out as a first step toward development of the techniques required from cross-section measurements with higher-energy neutrons at LANSCE.

---

[1]W. L. Talbert, Jr., J. W. Starner, R. J. Estep, S. J. Balestrini, M. Attrep, Jr., D. W. Efurd, and F. R. Roensch, Phys. Rev. C **36**, 1896 (1987).
[2]F. Asaro and I. Perlman, Phys. Rev. **107**, 318 (1957).
[3]J. R. Huizenga, C. L. Rao, and D. W. Engelkemeir, Phys. Rev. **107**, 319 (1957).
[4]V. I. Mostovoi and G. I. Ustroiev, Atomnaya Energiia **57**, 241 (1984).

5. (n,Charged Particle) Reactions at En ≤ 50 MeV (R. Haight)

Charged-particle emission in neutron-induced reactions can be used to infer nuclear level densities in the component nucleus and in residual nuclei. Two approaches are underway at Target-4 to study these reactions.

At the 90-meter flight path (15-degree left) (n,p) and (n,α) reactions in silicon were observed by means of a silicon surface-barrier detector placed in the beam. This was a feasibility experiment for a high resolution study of the nuclear level density in the compound nucleus, ^{29}Si. Interference between these levels gives rise to fluctuations in the individual reaction channels. An Ericson fluctuation analysis will be used to derive level densities from the data. The recent experiment showed that it is possible

to measure excitation functions of (n,p) and (n,α) reactions to discrete states with the neutron energy resolution required.

A shorter, 10-meter flight path is being constructed at 90° for the measurement of cross sections, energy spectra, and angular distributions of charged particles emitted in neutron-induced reactions. The useful neutron energy range will extend up to 50 MeV and the flux will be the highest of any existing station at Target-4. From the evaporation component of the spectra, level densities in the residual nucleus can be inferred. From the excitation function for charged-particle emission, level densities in nuclei reached by (n,2n) reactions can also be obtained. This flight path and detector station will be completed and partially instrumented this year, enough so that the neutron flux and energy spectrum can be characterized and so that initial measurements can begin.

6. Neutron-Induced Charged Particle Reactions [(J. L. Ullmann, P. W. Lisowski, R. C. Haight, N. S. P. King (Los Alamos); Jack Rapaport, R. W. Finlay (Ohio University); F. P. Brady, J. L. Romero, J. Drummond, E. Hjort, D Sorenson (Univ. California at Davis); C. Howell, and W. Tornow (Duke University)].

During the 1988 running period at LAMPF/WNR, a new facility designed to study neutron-induced charged particle reactions, in particular the (n,p) reaction, was built on the WNR Target-4 15L flight path. The 15 degree flight path provides a white flux of neutrons with usable flux up to about 700 MeV. A detector station was established at 90 meters, and a deflection magnet, wire chambers, and prototype 250 MeV calorimeter detectors were obtained. Preliminary measurements were made to establish the neutron beam flux, investigate experimental backgrounds, and characterize NaI and CsI as stopping detectors. Based on this information we are constructing a detector "wall" about 20 inches wide and 6 inches high to detect protons above about 50 MeV. We expect to embark on a full experimental program in the summer of 1988, concentrating on p-shell nuclei during the first year.

7. Neutron Induced Fission Cross Section Ratios for ^{232}Th, ^{235,238}U, ^{237}Np, and ^{239}Pu from 1 to 400 MeV: [P. W. Lisowski, J. L. Ullmann, S. J. Balestrini, A. D. Carlson, O. A. Wasson (National Bureau of Standards), N. W. Hill (Oak Ridge National Laboratory)]

Time of flight measurements of neutron induced fission cross section ratios for ^{232}Th, ^{235,238}U, ^{237}Np, and ^{239}Pu, were performed during the last LAMPF operating cycle using the WNR high intensity spallation neutron source located at Los Alamos National Laboratory. A multiple-plate gas ionization chamber located at a 20-m flight path was used to simultaneously

measure the fission rate for all samples over the energy range from 1 to 400 MeV.

Reduction of the data is in progress. For energies below 30 MeV, ratios will be obtained relative to hydrogen using an annular proton-recoil spectrometer. From 30 to 400 MeV, cross sections for ^{232}Th, ^{238}U, ^{237}Np, and ^{239}Pu, will be determined relative to ^{235}U by comparison with data obtained in a separate experiment.

Because the measurements have been made with nearly identical neutron fluxes we expect to be able to cancel many systematic uncertainties which were unavoidable in previous measurements. This will allow us to resolve discrepancies among different data sets. In addition these will be the first neutron-induced fission cross section values for most of the nuclei at energies above 30 MeV.

8. Gamma-ray Production in Ho, Eu, and Gd [(S. A. Wender, S. Hansen, J. Aubrey, P. G. Young, and D. C. Larson (ORNL)]

The analysis of neutron-induced, continuum gamma-ray production data on Ho, ^{nat}Eu, and ^{nat}Gd is essentially complete. Results have been obtained for gamma-rays with energies between 600 keV and 10 MeV in 19 neutron energy bins from 800 eV to 3 MeV. Data were taken with a 7.6 x 7.6 cm BGO detector placed at 125° with respect to the incident neutron beam. Calculations describing these results are in progress.

9. Proton Induced Gamma-ray Production [(S. Seestrom-Morris, R. O. Nelson, C. E. Moss, D. Drake, S. A. Wender, and N. W. Hill (ORNL)].

The analysis of thick target gamma-ray production data on samples of ^{nat}C, ^{nat}Al, ^{nat}Fe, and ^{nat}U is essentially complete. The yield/incident proton has been obtained for detector angles of 30° and 120° using 7.6 x 7.6 cm BGO detectors. The results of these measurements are compared to Monte-carlo production and transport calculations.

10. Neutron Induced Gamma-ray Production (R. O. Nelson, S. Seestrom-Morris, S. A. Wender)

Gamma-ray production cross section and angular distribution data have been obtained for samples of ^{12}C, ^{11}B, ^{14}N, and ^{15}N using the new target-4 white neutron source at the WNR. The gamma-ray yield was measured from approximately 2 to 25 MeV at angles of 40°, 55°, 90°, 125°, and 145° for neutron energies from 1 to 200 MeV in approximately 700 neutron bins.

Cross section and angular distribution data were obtained in a short exploratory run on ^{nat}Eu and ^{nat}Gd samples for the gamma-ray energy range

from approximately 0.5 to 15 MeV and neutron energies ranging from 0.5 to 200 MeV. These data extend the neutron energy range beyond that already covered at ORNL for these samples. A more precise experiment is planned for next year.

11. Neutron Capture on ^{40}Ca (S. A. Wender, R. O. Nelson, S. Seestrom-Morris)

Differential cross sections for neutron capture on ^{40}Ca were measured at 55°, 90°, 125°, and 145° in a preliminary run at the target-4 white neutron source of the WNR. The data cover the neutron energy range from approximately 2 MeV to 50 MeV. The goal of this study was to determine the feasibility of searching for the isovector quadrupole resonance and measuring its properties. We plan future experiments with improved statistics.

12. Status of the WNR Facility (P. W. Lisowski and S. A. Wender)

The second phase of the Weapons Neutron Research (WNR) facility white neutron source upgrade (target-4) was completed in time for operation during 1987. This upgrade consisted of increasing the shielding in the direction of forward angle neutron production to the design thickness and relocating four neutron shutters and flight paths. Multiplexed operation of target-4 and the Los Alamos Neutron Scattering Center (LANSCE) is now possible. With improvements to the beam transport system and completion of the remainder of the shield, we will be able to increase the proton beam current from the 1μA level in 1987 to as much as 10μA in 1988.

During the 1987-1988 Los Alamos Meson Physics Facility (LAMPF) operating cycle, four neutron flight paths will be available with multiple experiments planned for each. In addition, the WNR low-current target and external beam facility will be used throughout the period for up to 20% of the scheduled time for experiments requiring proton beams of energies ranging from 113 to 800 MeV.

B. NUCLEAR DATA EVALUATION

1. Unconventional Poles in Nuclear Physics (G. M. Hale)

We are finding evidence in well-studied nuclear reactions that unconventional S-matrix poles, that is, those on unphysical sheets of the Riemann energy surface far removed from the physical sheet, have important effects on the measured data. The first example we found was the "shadow" pole accompanying the famous $J^{\pi} = 3/2^{+}$ resonance in ^{5}He,[1] which was mentioned in a contribution to the previous progress report. This pole, through its associated zero lying close to the real axis of the physical sheet, causes the $^{3}H(d,n)^{4}He$ reaction cross section to approach the maximum value allowed by unitarity at a center-of-mass d-t energy of about 80 keV. The sheet on which the shadow pole appears indicates that the resonance has essentially an n-a character, in contradiction to the usual picture of the low-energy reaction mechanism.

The second example is the S-wave ($J^{\pi} = 2^{-}$) resonance near the n - ^{7}Be threshold in ^{8}Be that causes a threshold cusp in p - ^{7}Li elastic scattering and an enormous 1/v cross section (~40000 barns at thermal) in the $^{7}Be(n,p)^{7}Li$ reaction at low energies. The properties of this resonance have been a subject of much disagreement in the literature. The width appears to differ widely, depending on the reaction in which it is observed and the analysis method used to extract it, and the amount of isospin mixing is quite uncertain. The S-matrix pole corresponding to the 2^{-} resonance we obtain from a charge-symmetric R-matrix analysis of the nucleon-seven-nucleon reactions has unconventional properties. It is located at a complex energy E_0 such that $Re(E_0)$ corresponds to $E_x = 18.89$ MeV in ^{8}Be, as expected, but on an unphysical sheet of the Riemann energy surface that is directly connected to the physical sheet only at the n - ^{7}Be threshold. As a consequence, the relatively small width $\Gamma = -2Im(E_0) = 122$ keV is evident only as a narrow threshold effect in reactions open at energies below the n - ^{7}Be threshold, whereas the relatively large partial widths, $\Gamma_p = 1.41$ MeV and $\Gamma_n = 0.22$ MeV, are indicative of the broad structure seen in the $^{7}Li(p,n)$ or $^{7}Be(n,p)$ reactions at energies above threshold. The fact that $\Gamma \neq \Gamma_p + \Gamma_n$ is an aspect of the unconventionality of the resonance.

The resonance is strongly isospin mixed, being about 76% T = 0 and 24% T = 1. The isospin mixing in our model results from two R-matrix levels of pure isospin, the lower one having T = 0 and the upper one having T = 1, in the parameterization of the 2^{-} matrix. Further discussion of these results was included in a paper[2] reporting new experimental measurements of the $^{7}Be(n,p)$ cross sections at low neutron energies.

---

[1] G. M. Hale, R. E. Brown, and N. Jarmie, Phys. Rev. Lett. *59*, 763 (1987).

[2] P. E. Koehler, C. D. Bowman, F. J. Steinkruger, D. C. Moody, G. M. Hale, J. W. Starner, S. A. Wender, R. C. Haight, P. W. Lisowski, and W. L. Talbert to appear in Phys. Rev. C (March 1988).

2. Covariance Analysis of n + ^{7}Li Data for ENDF/B-VI (P. G. Young)

A new covariance analysis of n + ^{7}Li experimental data has been completed for Version VI of ENDF/B. The analysis basically updates our 1981 work[3] for ENDF/B-V.2 to include new data that have become available since that time and to incorporate cross correlations between different experiments. The bulk of the new measured data consists of some 10 new (or newly revised) tritium-production experiments involving about 70 additional data points.

In the present study, individual covariance analyses are performed for each of the major n + ^{7}Li cross section types for which experimental data exist. The results for individual reactions are then combined under the constraint that all partial reactions sum to the neutron total cross section, with full account being taken of all covariances. The newly evaluated ^{7}Li(n,nt) cross section is compared in Fig.B-1 with the previous ENDF/B-V.2 evaluation and with experimental data obtained since that evaluation. The new analysis results in only small changes in the previous evaluation of tritium production but significantly reduces the magnitudes of uncertainties due to the more extensive and accurate data base that was used.

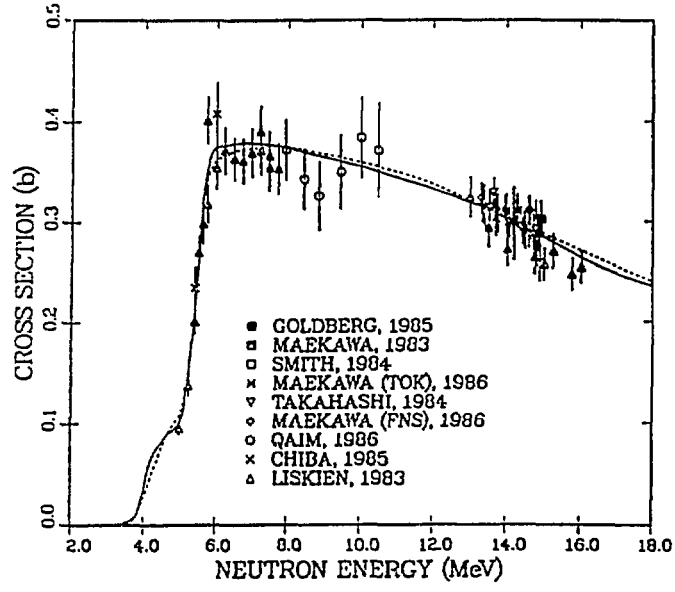

Fig. B-1 Measured and evaluated ^{7}Li(n,nt) cross sections. The solid curve results from the present analysis and the dashed curve is from ENDF/B-V, Revision 2.

[3] P. G. Young, Trans. Am. Nucl. Soc. *39*, 272 (1981).

3. Development and Application of Nuclear Models to the Calculation of 20-100 MeV Nucleon-Induced Reactions (E. D. Arthur, M. Bozoian, D. G. Madland, R. T. Perry, W. B. Wilson, and P. G. Young)

The GNASH nuclear theory code has been improved to permit reliable calculation of neutron- and proton-induced reactions to 100 MeV. Improvements to the code include incorporation of an Ignatyuk-type level density formulation, inclusion of multistage preequilibrium reaction contributions, and development of memory- and time-saving approximations to Hauser-Feshbach calculations. New models have been developed to describe gamma-ray competition relative to particle emission in detail, even for higher energy processes. The code has been expanded to include up to 400-500 reaction paths in a single calculation with options for simple automatic problem setups. A new formulation of the Kalbach angular distribution phenomenology has been implemented to permit accurate calculation of double-differential cross sections and spectra.

To date, the GNASH code system has been used to calculate data libraries or incident neutron and proton energies to 50 MeV for isotopes and natural elements of Al, Fe, Ni, Cu, and W; for neutrons to 100 MeV on ^{16}O, ^{27}Al, ^{28}Si, ^{40}Ca, and ^{56}Fe; and for protons to 100 MeV on ^{12}C and ^{27}Al. These libraries are intended primarily for particle- and gamma-ray transport applications, so they do not contain detailed information on individual reactions above $E_n \sim 20$ MeV. The neutron libraries are matched to ENDF/B-V files below 20 MeV and include total, elastic, and nonelastic cross sections, elastic angular distributions, and production cross sections and energy-angle emission spectra for neutrons, protons, deuterons, alphas, and gamma rays. Both the neutron- and proton-induced libraries utilize the new File 6 format of ENDF/B-VI to accurately describe the coupled energy-angle emission spectra.

4. Calculated Neutron Activation Cross Sections for $E_n \leq 100$ MeV for a Range of Accelerator Materials (M. Bozoian, E. D. Arthur, R. T. Perry, W. B. Wilson, and P. G. Young)

Activation problems associated with particle accelerators are commonly dominated by reactions of secondary neutrons produced in reactions of beam particles with accelerator or beam stop materials. Measured values of neutron-activation cross sections above a few MeV are sparse. Calculations with the GNASH code have been made for neutrons incident on all stable nuclides of a range of elements common to accelerator materials. These elements include B, C, N, O, Ne, Mg, Al, Si, Ar, K, Ca, Cr, Mn, Fe, Ni, Cu, Zn, Zr, Mo, Nd, and Sm. Calculations were made for a grid of incident neutron energies extending to 100 MeV. Cross sections leading to the direct production of as many as 87 activation products for each of 81 target nuclides were tabulated on this grid of neutron energies, each beginning with the threshold for the product nuclide's formation. Multigrouped values of these cross sections, assumed to vary linearly

between grid values, have been calculated and employed in a modified version of the REAC neutron activation code.

5. Calculated Alpha-Induced Thick-Target Neutron Yields and Spectra (W. B. Wilson, M. Bozoian, and R. T. Perry)

One component of the neutron source associated with the decay of actinide nuclides in many environments is due to the interaction of decay alpha particles in (α,n) reactions on low Z nuclides. Measurements of (α,n) thick-target neutron yields and associated neutron spectra have been made for only a few combinations of alpha energy and target nuclide or, more applicably, mixtures of actinide and target nuclides. Calculations of thick-target yields and spectra require alpha-energy dependent cross sections for (α,n) reactions, as well as branching fractions leading to the energetically possible levels of the product nuclides. A library of these data has been accumulated for target nuclides below Z = 15, using data available from measurements and from recent GNASH code calculations.

6. Calculation of Neutron Cross Sections of ^{64,66,68}Zn for Fusion Applications (P. G. Young and D. A. Rutherford)

A Hauser-Feshbach statistical theory analysis of n + ^{64}Zn reactions performed earlier has been extended to include neutron reactions with ^{66}Zn and ^{68}Zn.[4] The analysis utilizes a neutron optical potential obtained by fitting neutron total cross sections, neutron elastic angular distributions, and low-energy resonance data. Preequilibrium effects are calculated with an exciton model, and direct reaction effects are included through DWBA calculations using deformation parameters for (p,p') scattering. The results are available for Version VI of ENDF/B.

7. Development of Nuclear Models for Higher Energy Calculations (M. Bozoian, E. R. Siciliano, and R. D. Smith)

Two nuclear models for higher energy calculations have been developed in the regions of high- and low-energy transfer, respectively. In the former, a preequilibrium, hybrid-type model incorporating three particle-hole chaining options, a relativistic-invariant free scattering kernel for calculating both angle-integrated and angular-distributed spectra, and intranuclear transition rates based upon realistic mean free paths in nuclear matter from ^{27}Al to ^{209}Bi has been compared with data ranging from 60 MeV to 800 MeV. In the latter region of low-energy transfer, nucleon-nucleus scattering is predominantly a direct reaction involving hard collisions with one or two nucleons in the target. In this region of "quasi-elastic" scattering, many features of intermediate energy cross sections and spin observables can be understood with a simple model

[4] P. G. Young and D. A. Rutherford, "Calculation of Neutron Cross Sections of Zn for Fusion Applications," presented at IAEA Advisory Group Meeting on Nuclear Theory for Fast Neutron Data Evaluation, Beijing, Peoples Republic of China, 12-16 October 1987.

in which the reaction mechanism is treated in Glauber Theory, and the nuclear structure is described by the RPA surface response function.[5] We have extended this model to include (1) contributions from two-step processes, (2) the effect of optical and spin-dependent distortion, (3) damping of the nuclear response from 2p - 2h excitations. Future work will attempt to unite these two models to span the entire energy transfer range.

8. The Medium-Energy Nuclear Data Library (MENDLIB) Project (E. R. Siciliano)

A joint effort between T and MP Divisions at Los Alamos is underway to compile LAMPF data and to provide access to this data through an easy to use, menu-driven, dial-up computer program. Depending on user interest and funding, future expansion of this database to include data from other medium-energy facilities may be possible.

The MENDLIB data base will consist of three tables: (1) a bibliographic table containing references and contact information; (2) a measurement description table containing details of the measurement such as target, beam, reaction, and final state characteristics; and (3) the data table. Data retrieval will utilize a database management system (INGRES); retrieval for one reaction type has thus far been written. The user interface will be written in FORTRAN for the initial system. The first part of the interface, which allows the user to enter his request, has been completed.

9. Fission Product Yield Evaluations [(T. R. England and B. F. Rider (Retiree, General Electric Co.)]

Reference[6] reviews the evaluation status of 20 yield sets. Twelve fissioning nuclides at one or more incident energies are included. The basic library of measured data has been updated through late 1987, and supplemented with values based on new parameters in systematic nuclear models. The evaluation of these data consists of independent and cumulative yields, the latter type including the most recent delayed neutron branching[7] Following some minor changes, an additional 30 yield set evaluation will begin.

---

[5]H. Esbensen, G. F. Bertsch, Ann. Phys. *157* (1984) 255.

[6]B. F. Rider and T. R. England, "Evaluation of Fission Product Yields for the U.S.A. National Nuclear Data Files,"invited paper, Specialists' Meeting on Data for Decay Heat Predictions, Studsvik, Sweden, 7-10, September 1987 (LA-UR-87-2462). Proceedings NEACRP-302-'L', NEANDC-245 'U'.

[7]T. R. England, "Review of ENDF/B Fission Product and Delayed Neutron Data Plans and Status," presented at the Specialists' Meeting on Delayed Neutrons at the University of Birmingham, Birmingham, England, September 15-19, 1986.

Future evaluations should be improved by participation in a newly formed IAEA Coordinated Research Program; the participants are primarily from the United States, United Kingdom, and China.

10. Global Medium-Energy Nucleon-Nucleus Optical-Model Potential (D. G. Madland)

Initial results have been obtained[8,9,10] for the determination of a global medium-energy nucleon-nucleus phenomenological optical-model potential using a relativistic Schrödinger representation. The starting point for this work is the global phenomenological proton optical-model potential of Schwandt et al.,[11] which is based on measured elastic scattering cross sections and analyzing powers for polarized protons ranging from 80 to 180 MeV. This potential was optimally modified to reproduce experimental proton total reaction cross sections as a function of energy, while allowing only minimal deterioration in the fits to the elastic cross sections and analyzing powers. Further modifications in the absorptive potential were found necessary to extrapolate the modified potential to higher energies. The final potential was converted to a neutron-nucleus potential by use of standard Lane model assumptions and by accounting approximately for the Coulomb correction. Comparisons of measured and calculated proton reaction and neutron total cross sections were performed for ^{27}Al, ^{56}Fe and ^{208}Pb. Further studies led to the conclusion that the present potential can be considered a satisfactory first pass attempt in achieving a *global* medium-energy potential for nucleon scattering. Note, however, that the potential is discontinuous at the boundary point of 140 MeV, which divides the absorptive part into two regions of applicability:

Region I: $50 \text{ MeV} \leq E_n, E_p \leq 140 \text{ MeV}$

Region II: $140 \text{ MeV} < E_n, E_p \leq 400 \text{ MeV}$.

Future work on the potential will remedy this current deficiency. The original and modified proton potentials are given in Table B-10. They are converted to neutron potentials using the following transformation:

a. $(N-Z) \rightarrow (N-Z)/A$

b. $V_R \rightarrow V_R - 0.4Z/A^{1/3}$

[8]D. G. Madland, Bull. Am. Phys. Soc. *31*, 1230 (1986).
[9]D. G. Madland, Proc. IAEA Advisory Group Meeting on Nuclear Theory for Fast Neutron Data Evaluation, October 12-16, 1987, Beijing, Peoples Republic of China (to be published).
[10]D. G. Madland, Proc. OECD/NEANDC Specialists' Meeting on Preequilibrium Nuclear Reactions, February 10-12, 1988, Semmering, Austria (to be published).
[11]P. Schwandt et. al., Phys. Rev. C *26*, 55 (1982).

TABLE B-10. Medium-Energy Nucleon-Nucleus Optical-Model Potential

ORIGINAL POTENTIAL

$$V_R = 105.5(1 - 0.1625 \ln E_p) + 16.5\,(N-Z)/A \quad ,$$

$$r_R = 1.125 + E_p/10^3 \quad , \quad E_p \le 130 \text{ MeV}$$
$$= 1.255 \quad , \quad E_p > 130 \text{ MeV}$$

$$a_R = 0.675 + 3.1\,E_p/10^4 \quad ,$$

$$W_V = 6.6 + 2.73\,(E_p - 80)/10^2 + 3.87\,(E_p - 80)^3/10^6 \quad ,$$

$$r_I = 1.65 - 2.4\,E_p/10^3 \quad ,$$

$$a_I = 0.32 + 2.5\,E_p/10^3 \quad ,$$

$$V_{SO} = 19.0(1 - 0.166 \ln E_p) - 3.75\,(N-Z)/A \quad ,$$

$$W_{SO} = 7.5(1 - 0.248 \ln E_p) \quad ,$$

$$r_{VSO} = 0.920 + 0.0305\,A^{1/3} \quad ,$$

$$a_{VSO} = 0.768 - 0.0012\,E_p \quad , \quad E_p \le 140 \text{ MeV}$$
$$= 0.60 \quad , \quad E_p > 140 \text{ MeV}$$

$$r_{WSO} = 0.877 + 0.0360A^{1/3} \quad , \text{ and}$$

$$a_{WSO} = 0.62 \quad ,$$

MODIFIED POTENTIAL

Region I: W_V is unchanged.
r_I is unchanged, and
$a_I = 0.27 + 2.5\,E/10^3$.

Region II: $W_V = 7.314 + 0.0462E$,
$r_I = 1.17$, and
$a_I = 0.59$ for ^{27}Al
$= 0.66$ for ^{56}Fe
$= 0.79$ for ^{208}Pb

The energy E is either the proton energy E_p or the neutron energy E_n.

A. NEUTRON SCATTERING IN THE ACTINIDES

(L.E. Beghian, G.H.R. Kegel, J.J. Egan, A. Mittler, A. Aliyar, and C.A. Horton)

In earlier studies[1] we have shown that the direct-interaction process plays an important role in the excitation of members of the ground state rotational band in Th-232 and U-238. Later[2,3] we made similar studies, on the same nuclei, on levels which do not belong to the ground state rotational band; these investigations covered incident neutron energies from 800 to 2000 keV. At these energies there was no convincing evidence for the presence of a significant direct interaction component. We have now extended these measurements determing angular distributions at 2.4 and 2.8 MeV incident neutron energies for levels in Th-232 and U-238 up to 1 MeV and measuring 125° excitation functions for these levels from 2.2 to 3.2 MeV. We used an iron scatterer in addition to Th and U samples to cross check the time and energy calibrations and to obtain scattered neutron time resolution profiles appropriate for the unfolding of U and Th spectra. Fig. A-1 shows a Th(n,n') spectrum, measured at $\theta = 85^{\circ}$ at an incident neutron energy of 2.4 MeV, after background subtraction and tail suppression (see ref. 4). The measurements have all been completed, and data reduction is in progress

Exploratory measurements on a small Pu-239 scatterer have shown the need for a miniaturized neutron target assumbly which incorporates an adjustable shadow bar and which permits us to reduce the target-scatterer distance to about 5 cm.

BaF_2 scintillators and uv-sensitive photormultiplier tubes have been received and are being assembled for testing; these units will be used in fission neutron time-of-flight spectroscopy.

---

[1]L.E. Beghian, G.H.R. Kegel, B.K. Barnes, G.P. Couchell, J.J. Egan, P. Harihar, T.V. Marcella, A. Mittler, D.J. Pullen and W.A. Schier, Nucl. Sci. and Eng. 69 137 (1979).

[2]C.A. Ciarcia, G.P. Couchell, J.J. Egan, G.H.R. Kegel, S.Q. Li, A. Mittler, D.J. Pullen, W.A. Schier and J.Q. Shao, Nucl. Sci. and Eng. 91 428 (1985).

[3]J.Q. Shao, G.P. Couchell, J.J. Egan, G.H.R. Kegel, S.Q. Li, A. Mittler, D.J. Pullen, W.A. Schier and E.D. Authur, Nucl. Sci. and Eng. 92 350 (1986).

[4]G.H.R. Kegel, C. Ciarcia, G.P. Couchell and J. Shao, in Nuclear Date for Science and Technology (Proc. of the 1982 Antwerpen Conference), Pg. 897.

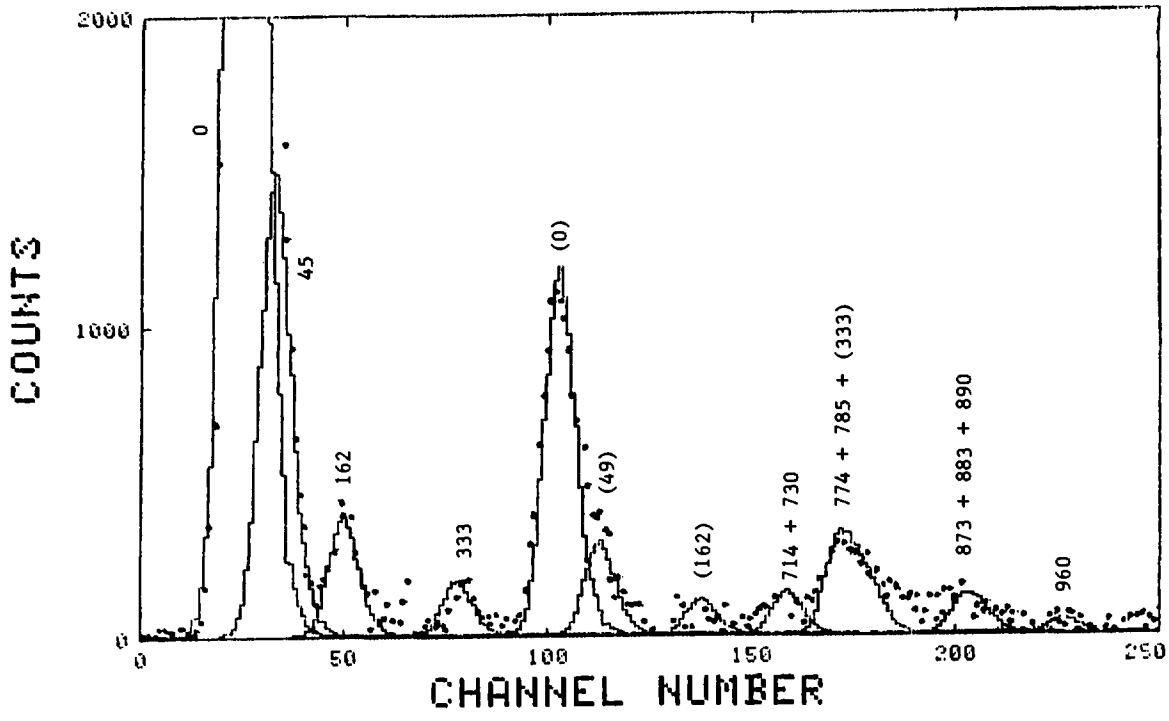

Fig. A-1 $^{232}Th(n,n')$ time-of-flight spectrum at E_n=2.4 MeV and θ = 85°. The background has been subtracted and the peak shapes are resolution profiles derived from singlet spectra obtained using an iron scatterer. Peaks are labeled with their excitation energies in keV. Energies in parentheses correspond to peaks due to scattering of the second group of neutrons from $^{7}Li(p,n)^{7}Be^{*}$.

B. ELASTIC NEUTRON SCATTERING CROSS SECTION CALCULATIONS FOR THE ACTINIDES

(E. Sheldon)

To supplement the past compilations of computed angle-integrated and differential cross sections for neutron inelastic scattering on the even-mass actinides (^{232}Th, ^{238}U, 240, 242, ^{244}Pu), as detailed in past (1983-87) Reports to the DOE Nuclear Data Committee, the principal thrust of the current work has been to evaluate elastic neutron scattering cross sections up to 2.5 MeV and beyond, with computations based upon either the standard (CN + DI) or statistical S-matrix (HRTW) approach. The latter, employing the formalism of Hofmann, Richert, Tepel and Weidenmuller (HRTW) in the program "NANCY" has within the past weeks successfully been extended to

provide differential as well as total energy-averaged cross sections, thereby permitting the analysis of measured angular distributions as well as elastic excitation functions. The transfer of "NANCY" from the CDC Cyber 170/825 computer system to the newly installed DEC VAX/VMS 8650 facility is still underway; with the exception of a few remaining minor problems, the other major computer programs (in particular, CINDY and JACQUI/NRLY for CN computations and JUPITOR/KARJUP for DI computations) have now been recompiled and are running on the VAX.

This reorganization has somewhat hampered the progress of new computations, but nevertheless sufficient data were accumulated for the presentation of elastic angular distribution results in the standard (CN + DI) formalism at 0.185 and 0.550 MeV for ^{232}Th and $^{235,\ 238}$U, as well as elastic excitation functions for these nuclides in this formalism up to 2.5 MeV incident energy in a contributed paper[1] to the New England's Section NES/APS 1987 Fall Meeting at Middlebury College, VT in October, 1987. The HRTW analyses of elastic angular distributions for ^{232}Th and ^{238}U have been prepared and submitted for presentation in a preliminary contribution[2] to the NES/APS 1988 Spring Meeting at Fairfield University next April, the HRTW elastic excitation fuctions for the entire set of aforementioned nuclides to 2.5 MeV and beyond have been prepared for comparison with the standard (CN + DI) values and the ENDF/B-V evaluations in a paper[3] to be presented at the APS 1988 Spring Meeting at Baltimore. The entire batch of elastic results will be the subject of a report[4] at the 1988 International Conference on Nuclear Data for Science and Technology in Mito, Japan in May/June and a comprehensive review featuring additional data as they become available meanwhile is scheduled to be an Invited Paper at the 20th International Summer School in Nuclear Physics at Mikolajki, Poland next September.

An ancillary activity in this connection has been the participation in a global comparative survey of statistical computer programs organized by Dr. E. Sartori under the aegis of the OECD NEA Nuclear Data Committee, in which test computations were undertaken with "CINDY", "JACQUI" and "NANCY".

---

[1] E. Sheldon and A. Mittler, Bull. Am. Phys. Soc. (in publication: February 1988).

[2] M. O'Connor and E. Sheldon, Bull. Am. Phys. Soc. (submitted for publication).

[3] E. Sheldon, J.J. Egan, G.H.R. Kegel and A. Mittler, Bull. Am. Phys. Soc. (submitted).

[4] E. Sheldon, Proc. Int. Conf. Nucl. Data for Science and Technology, Mito, Japan, May 30 - June 3, 1988 (accepted for publication).

C. DELAYED-NEUTRON MEASUREMENTS

(G.P. Couchell, D.J. Pullen, W.A. Schier, P.R. Bennett, M.H. Haghighi, E.S. Jacobs and M.F. Villani)

The main thrust of our recent research effort has been in the meaurement of composite delayed neutron (DN) spectra as a function of time following the fast neutron fission of U-238. This study was recommended at the 1986 Specialist Meeting on Delayed Neutrons in Birmingham, England, since U-238 is the highest contributor (40%) to the DN yield in prototype 1000-MWe heterogeneous fast reactors. Additional work includes the following. Benchmark equilibrium DN spectra measurements from the neutron fission of U-235, Pu-239 and U-238 are underway. Fission fragment transfer uniformity using our helium-jet system is also under study. The extension of our DN spectra measurements to high energies is presently under consideration and calculations of the sensitivity of our spectrometer system show that measurements could be extended to at least 6 MeV DN energy.

1. Fast Neutron Fission of U-238

We report good progress in our measurements of composite (aggregate) DN energy spectra following the fast fission of U-238. Beta-neutron time-of-flight measurements have been made for six nearly contiguous delay-time intervals between 0.17 s and 10.2 s. Fission fragments are transferred from the fission chamber and neutron source to the counting room using a helium-jet. A tape transport then selects the delay time interval by regulating the dwell time at the beta detectors. Neutron detectors were BC501 liquid scintillators incorporating neutron-gamma pulse shape discrimination so as to span 0.13-4.00 MeV with good background suppression. Although the production of fission fragments using the $^{7}Li(p,n)$ reaction with our 5.5 MV Van de Graaff is moderate, the very high ν_d (DN/fission ratio) relative to other fissionable isotopes has resulted in composite DN spectra that often surpass in quality our earlier U-235 and Pu-239 DN spectra (e.g. see Fig. C-1). The U-238 DN spectra appear to be considerably harder than those of U-235 and Pu-239 as demonstrated in Fig. C-2. We shall next measure the missing low energy portions of the spectra by switching to Li-6 loaded glass scintillators. With six composite DN spectra measurements completed, our constrained least-squares six-group decomposition analysis will be applied to extract DN spectra for groups 2-6 (Keepin six-group approximation).

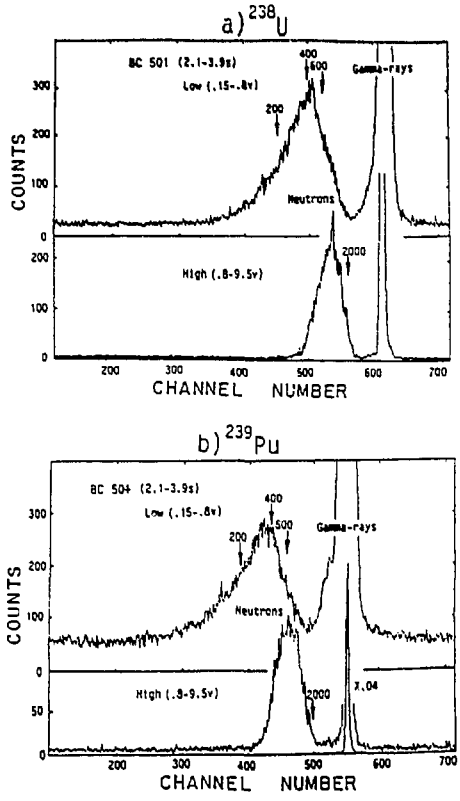

Fig. C-1. Delayed neutron time-of-flight spectrum measured in the time interval 2.1 - 3.9 s following fission of a) ^{238}U and b) ^{239}Pu.

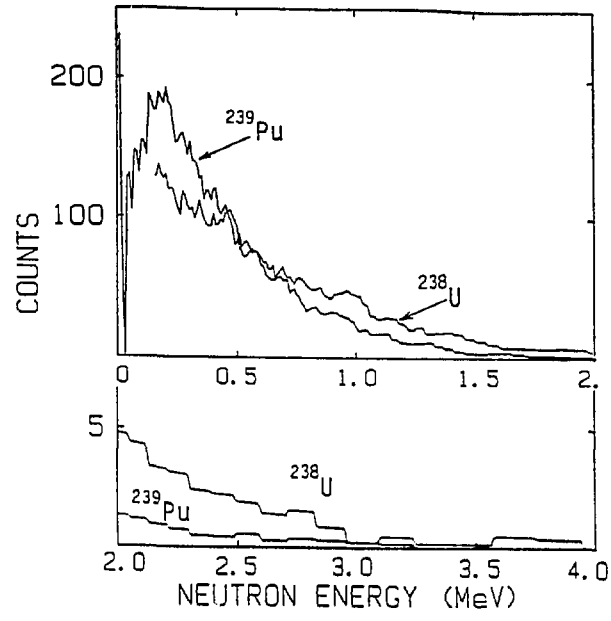

Fig. C-2. Energy spectra of delayed neutrons following fission of ^{238}U and ^{239}Pu deduced from TOF spectra of Figure C-1.

2. Delayed Neutron Equilibrium Spectra for U-235, U-238 and Pu-239

Transfer time of the fission fragments by the helium-jet method is very short (0.12 s) which suggests that DN time-of-flight measurements can be made having uniform sensitivity to nearly all delay times. By changing to a new beta detector assembly, the fission fragments are made to imbed themselves on a very thin KAPTAN tape at the beta scintillator detector. By moving the tape very slowly, a delay time interval, 0.12 - 180 s, is spanned encompassing > 95% of all delayed neutrons emitted. This very nearly provides, therefore, a direct measurement of a DN equilibrium spectrum. Such DN equilibium spectra are currently being measured for U-235, U-238 and Pu-239 with the BC501 scintillators. The low-energy regions of these DN spectra will later be measured with the Li-6 glass detectors.

3. Helium-Jet Fission Fragment Transfer Measurements

Measurements to test the uniformity of fission fragment transfer efficiency are underway. X-ray spectra associated with the transferred fission fragments and their progeny produced in the subsequent beta decay chains were measured with a thin-window high-purity germanium detector. The fission fragments from the thermal neutron fission of U-235 are imbedded in a catcher at the exit of the helium jet in one case and in a cylindrical rabbit enveloped by a U-235 foil near the neutron source in the other. The rabbit shuttles between the fission foil and the detector, dwelling at each for nearly 5 s with approximately 0.5 s lost in the transfer. This cycle repeats continually, giving a time integral that roughly matches that for the helium-jet case. The resulting spectra compared in Fig. C-3 appear nearly identical except for the weaker cesium x-ray line in the helium-jet case. Although a detailed analysis is proceeding, it would appear that the helium-jet system using forepump oil vapors for nucleation does little to distort our measured composite delayed neutron spectra.

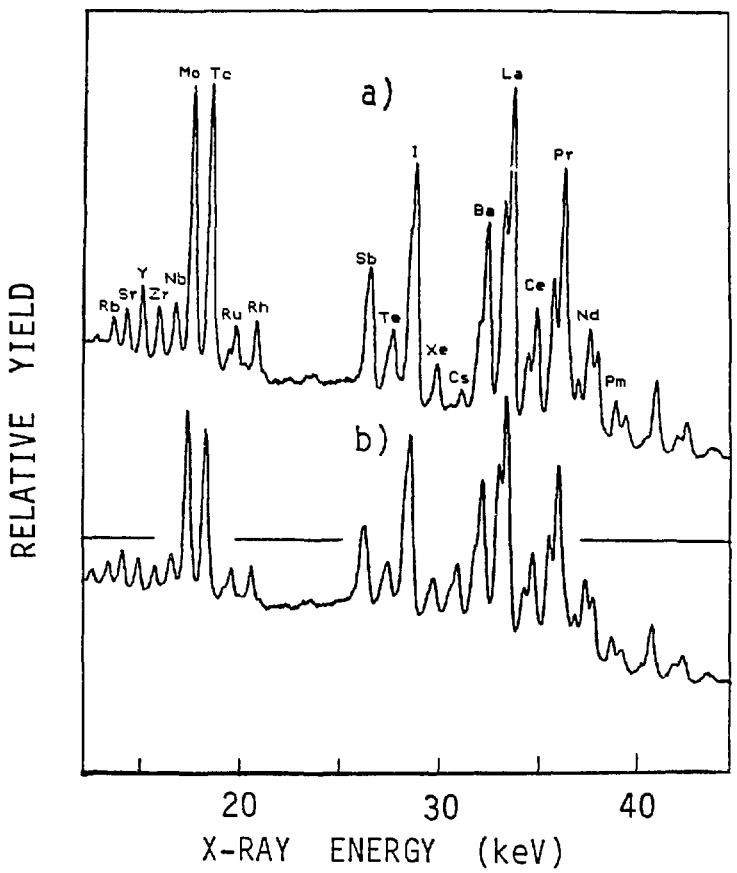

Fig. C-3. X-ray spectra associated with fission fragments transferred by a) helium-jet and b) rabbit systems. Element designations indicate positions of $K\alpha$ lines.

A. INTRODUCTION

In the 14 MeV Neutron Laboratory, we have completed the last of our current set of activation cross section measurements, and have moved into the phase of rebuilding our accelerator to produce pulses of one nanosecond width. This renovation has required extensive changes in the laboratory, including the relocation of the 150 kV accelerator to a balcony overlooking the main part of the Neutron Bay. We have procured and installed a 90° bending magnet, and are currently fabricating the major components of the beam pulsing system. We expect that the fabrication work will be completed soon, and intend to move into initial testing of the system within the next several months.

In the Photoneutron Laboratory, we have demonstrated the feasibility of a series of radiochemical separations that are an essential part of our effort to carry out measurements of the U-238 capture cross section. We have also demonstrated the accuracy of a new technique to calibrate our gamma detector efficiency using alpha particle spectrometry. We are now fabricating the uranium targets for this experiment and expect that the first irradiations will take place within the next several months.

B. ABSOLUTE MEASUREMENTS OF THE $^{65}Cu(n,2n)^{64}Cu$, $^{64}Zn(n,p)^{64}Cu$ AND $^{56}Fe(n,p)^{56}Mn$ CROSS SECTIONS AT 14.6 MeV

(K. Zasadny, G. Knoll)

Prior to moving the accelerator into the 14 MeV Neutron Bay, we completed a set of measurements on targets of copper, zinc, and iron. These measurements served as the basis of the doctoral dissertation of Kenneth Zasadny. A brief abstract of this measurement is given below.

The $^{65}Cu(n,2n)^{64}Cu$ and $^{64}Zn(n,p)^{64}Cu$ cross sections are measured relative to the $^{56}Fe(n,p)^{56}Mn$ cross section by the activation method. The $^{56}Fe(n,p)^{56}Mn$ cross section is then measured relative to an absolutely calibrated neutron flux monitor. Neutrons are produced by a 150 kV Cockcroft-Walton accelerator using the $^{3}H(d,n)^{4}He$ reaction. Measurements are conducted under low-scatter conditions at 0° with respect to the incident deuteron beam direction.

Measurement of the induced ^{64}Cu activity is conducted by positron absorption and annihilation in copper. Annihilation photons are counted in two 3in. x 3in. NaI(Tl) detectors, where the counting geometry takes advantage of the angular correlation of the emitted photons. Absolute efficiency of this counting system is determined by a ^{22}Na standard activity. The ^{22}Na absolute source activity is determined by β^{+}-γ ray coincidence counting.

Induced ^{56}Mn activity is measured by $4\pi\beta^-$ counting in a gas-flow proportional counter. Absolute efficiency of this counter is determined by $4\pi\beta$-γ coincidence counting techniques. In all measurements, the time-dependence of the neutron flux is monitored by a standard BF_3 long counter in multichannel scaling mode.

Absolute measurement of the neutron flux is conducted by a Dual-Thin Scintillator (DTS) detector developed at the National Bureau of Standards (NBS). Absolute efficiency of the DTS detector is measured by NBS by the time-correlated associated alpha particle technique. The calibration agrees with the efficiency determined by a Monte Carlo simulation of the detector response.

The neutron energy is measured by irradiation of a totally-depleted silicon surface barrier detector. The energy shift of the $^{28}Si(n,\alpha_0)$ peak from irradiation at 96° to 0° with respect to the deuteron beam direction is a direct measure of the average neutron energy.

Results of the measurements are as follows:

$^{65}Cu(n,2n)^{64}Cu$	991 ± 16 mb
$^{64}Zn(n,p)^{64}Cu$	163.2 ± 2.8 mb
$^{56}Fe(n,p)^{56}Mn$	112.7 ± 2.8 mb

C. CONVERSION TO PULSED 14 MEV NEUTRON FACILITY

(J. Yang, V. Rotberg, D. Wehe, N. Tsirliganis, G. Knoll)

The 150 kV Cockcroft-Walton accelerator has been moved to a new location on the balcony overlooking the large volume Neutron Bay. The height of the beam line was readjusted to conform to the approximate midpoint between the floor and ceiling of the laboratory. Good vacuum conditions have been re-established and the accelerator operated in its new location. Measurements have been made on the focusing properties of the deuteron beam and used in our beam optics code in the design of the remainder of the beam line components.

A 90° bending magnet has also been procured and put into place on the same balcony. The magnet not only serves to direct the beam out into the large volume laboratory but also serves to separate the atomic from the molecular beam produced in the deuterium ion source. The molecular beam, if present, adds to the heat that must be dissipated in the target and contributes to a deuterium buildup over long term use of the target, but does not contribute substantially to the neutron yield.

The layout of the pulsing and bunching system is shown in figure C-1. The beam from the accelerator is first passed through an electric quadrupole to provide focusing. It then enters into a region containing a set of deflection plates that sweep the beam across an aperture defined downstream by a set of slits. The sweeper plates operate at a frequency of 2 MHz to provide a full period of 500 nanoseconds. The pulse width is approximately 30 ns. After turning 90° through the bending magnet, the beam enters the

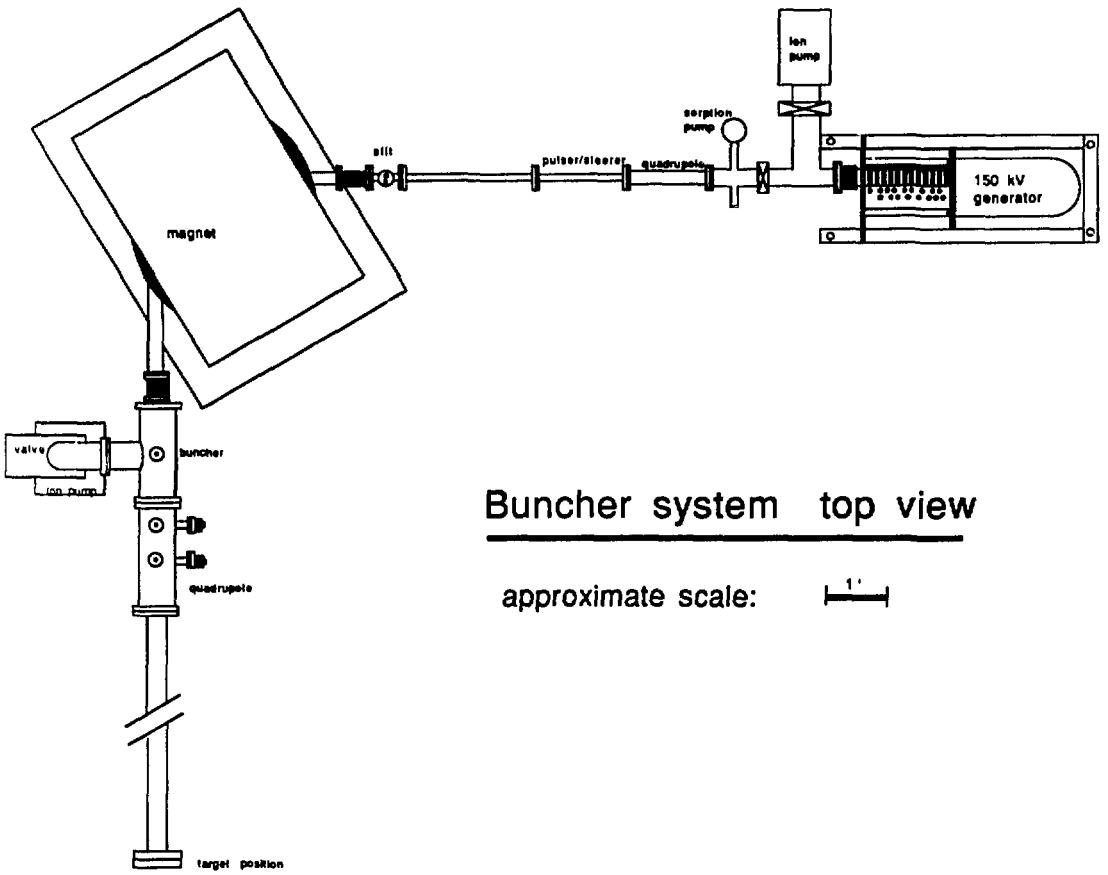

Figure C-1. Layout of Pulsing and Bunching System

klystron buncher where the leading edge of the pulse is decelerated and the trailing edge accelerated. A time focus is achieved at the target position approximately 3.5 meters from the buncher. The target position isapproximately 4 meters from both the floor and ceiling of the laboratory. A low mass grid floor is present under the beam line for convenient access.

We have employed a beam optics code for the design of all system components. The buncher is under fabrication in our own shops. An existing pair of sweeper plates will be used to provide the initial pulsing. All other components of the beam line and vacuum systems have either been obtained or are on order. We anticipate that all beam line components will be assembled within the next several months.

Electronic designs have been obtained for the RF amplifiers required to drive both the sweeper plates and the buncher. These designs were originated in the Applied Physics Division of Argonne National Laboratory and were supplied to our group by Dr. A. B. Smith. ANL has also supplied the printed circuit boards necessary for these components.

A 7.5-inch diameter liquid scintillator has been fabricated for use as the time-of-flight detector. It was designed with the help of an optical simulation code that used Monte Carlo techniques to predict the uniformity of light collection and the spread in scintillation photon arrival time at the photocathode of the PM tube. A pulse shape discrimination unit is now being fabricated for use in suppressing the gamma ray background in the detector.

D. MEASUREMENT OF THE URANIUM CAPTURE CROSS SECTION IN THE PHOTONEUTRON LABORATORY

(E. Quang, S. Melton, G. Knoll)

In the report of a year ago, procedures were outlined for the measurement of the U-238 capture cross section using our available photoneutron sources. This experiment has progressed well, and we are now anticipating that the final measurements will be carried out within the next several months.

A vital part of this measurement is the absolute determination of the Np-239 activity induced in the uranium target. Work over the past year has concentrated on finding absolute methods for measuring this activity. The general strategy is to employ a separate source of Am-243, whose daughter activity is the same Np-239 induced by neutron capture in the uranium target. Our germanium detector can then be calibrated using the Np-239 that has grown into equilibrium with the Am-243 sample. The detection efficiency of the germanium spectrometer can be determined if the activity of the Am-243 can be absolutely measured. Because its decay mode is alpha decay, we feel that this task can be carried out by absolute limited solid angle alpha counting to a precision of better than 1%.

Our recent work has therefore concentrated on developing methods for the precise determination of the alpha activity of Am-243. The technique that has been employed uses a vacuum chamber in which the defining aperture diameter and the source-aperture distance can be accurately varied. We

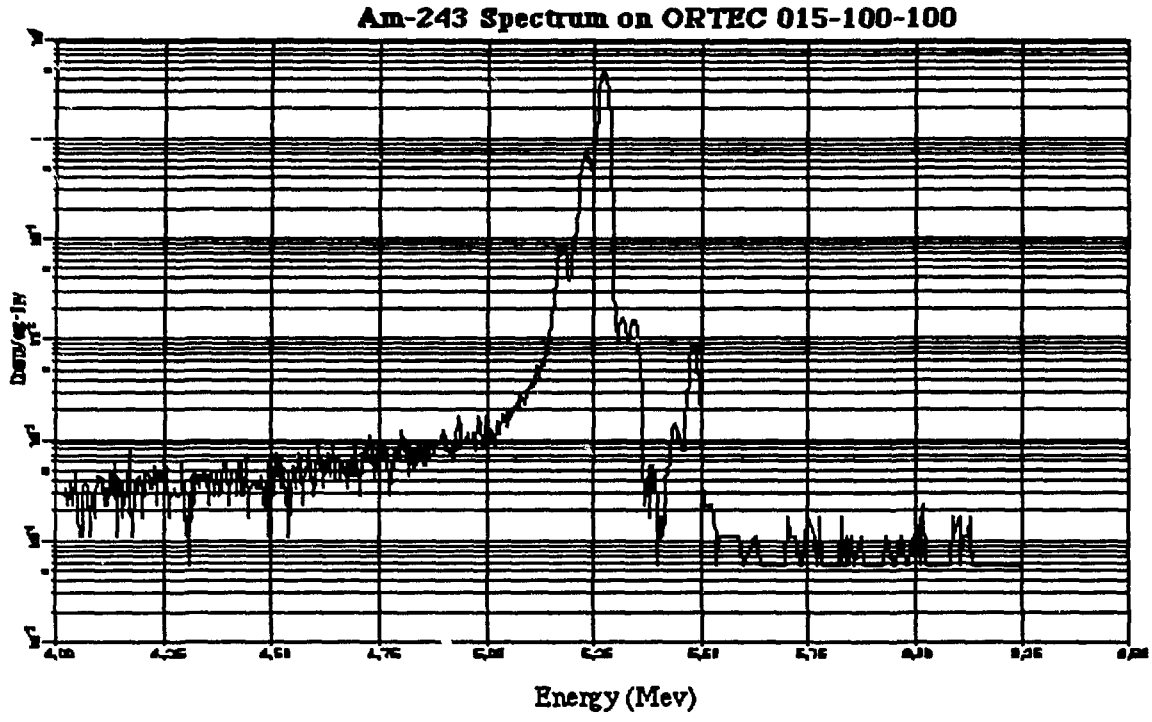

Figure D-1. Measured Am-243 Alpha Spectrum.

have carried out a series of measurements in which the apparent counting rate has been measured as a function of solid angle. The results have shown that the consistency and reproducibility over a wide range of solid angle are excellent. We have determined the activity of our source to be 0.463 microcuries, with a systematic error of less than 0.5%. With this standard source in hand, we are now able to calibrate our germanium system to a high accuracy, in preparation for our final induced activity measurements.

We have obtained depleted uranium metal targets from the Manufacturing Science Corporation of Oak Ridge. These targets are currently being fabricated into cylindrical shells for use in the experiment. The induced neptunium activity will be extracted following the irradiation using the chemical separation techniques described in the report of a year ago. This activity can be concentrated into a small volume and evaporated onto a planchet of similar size and characteristics as the reference Am-243 source. We therefore feel that the absolute activity determinations can be carried out with a precision of approximately 1-2%.

In order to obtain such precision, very clean alpha particle spectra are required. In figure D-1, an example is given of a measured Am-243 spectrum using a newly acquired low noise detector and preamplifier system. Evident in the spectrum is a contribution from 0.19% Am-241 in the Am-243 source. No other peaks are present. We have also investigated contributions to the continuum that result from Rutherford backscattering from the target backing, aperture edges, and detector face. Each of these contributions has been theoretically modelled and can account for the magnitude of continuum actually observed.

NATIONAL BUREAU OF STANDARDS

A. NUCLEAR DATA MEASUREMENTS

1. $^{235}U(n,f)$ Cross Section from Thermal to 1 keV

(R. A. Schrack, A. D. Carlson, and R. G. Johnson)

Although preliminary results, as reported last year, were in good agreement with other data up to 50 eV, there was poor agreement and obvious instability in the results obtained above 50 eV. It was observed that there was an obvious sensitivity to the power level at which the LINAC was operated. Several sets of data obtained under different operating conditions gave inconsistent results. A wide ranging diagnostic program was initiated. The possible sources of difficulty considered were timing errors, background variations, electronic instabilities, ground-loop pickup of LINAC interference, and errors in the analysis programs.

Diagnostic runs were made using the LINAC under different operating conditions. Runs were also made with the LINAC off using an Am-Be neutron source. A number of changes were made to provide for more stable operation. New pre-amps were installed to reduce instability, noise, and sensitivity to gamma-flash overload. In addition, the electronics were modified to provide for easier calibration checks and adjustments. Cable lengths were shortened to reduce capacitive loading of amplifiers.

Backgrounds were checked above and below the energy range being measured. Additional cadmium shielding in the detector area and iron in the collimator were added to reduce the ambient neutron flux. The LINAC was operated about a half cycle above the line frequency to avoid any possible problems with line pickup that would be synchronous with the data.

Marked improvements were obtained in stability. Amplifier oscillations were eliminated and sensitivity to the gamma flash was reduced so that there was no distortion of the pulse height distribution by 10 microseconds after the gamma flash (this is quite adequate since data is not recorded until 16 microseconds after the gamma flash). Thermal neutron background was reduced to below 0.4%.

Data has been reduced for four successive runs. These runs are in good agreement showing good stability for the system. The data obtained from these runs has been compared to results reported recently by other laboratories and the agreement is quite good. The experiment is now being written up for publication.

2. Measurements of the $^{235}U(n,f)$ Fission Cross Section Standard in the MeV Energy Region (A. D. Carlson, O. A. Wasson, P. W. Lisowski,* J. Ullmann,* and N. W. Hill**)

The introductory stages of this work were reported in the last status report. The measurements are being made at the 20 meter flight path end station of the LANL WNR target 4 facility with an annular proton telescope to measure the neutron flux and a multi-plate fission chamber to measure the fission reaction rate. The earlier phases of the work involved tests of the detector systems, diagnostic studies, and some preliminary results with a limited amount of accelerator time. The latest measurements, which were completed during the 1st LAMPF-WNR cycle provided significant data accumulation. These data are now being examined for subsequent data analysis. These measurements should provide accurate determinations of the $^{235}U(n,f)$ cross section in that portion of the MeV energy region where the present uncertainties are large or very little data exist.

3. Measurement of the $^{3}He(n,p)T$ Cross Section from 1 eV to 750 keV (J. W. Behrens and A. D. Carlson)

Having designed, built, and tested a $^{3}He/Xe$ gas scintillation counter which has an energy resolution of 17% (FWHM) for the $^{3}He(n,p)T$ reaction and with which we can separate out most of the ^{3}He recoil events, we decided to use the detector to measure the $^{3}He(n,p)T$ cross section. Our first measurements utilized the $^{10}B(n,\alpha)$ reaction as the reference standard. The energy range of interest was from 1 eV to 750 keV and the NBS linac was chosen to produce the neutrons. Data have been taken using our two-detector, two-parameter data taking system. The ^{10}B ionization chamber and the $^{3}He/Xe$ gas scintillation counter were both located at the 20-meter time-of-flight station. There were 1024 time channels and 512 pulse-height channels per detector. For the measurement from 1 keV to 750 keV, each time channel was 64 ns; whereas, for the 0.6 eV to 25 keV measurement, the time channels were changed to 2048 ns each. We measured neutron backgrounds with gold, sodium, and aluminum filters. These data are presently being analyzed. We plan to present preliminary results at the upcoming Nuclear Data Conference to be held in Mito, Japan in June 1988.

4. Cross-Section Measurements in the Intermediate-Energy Standard Neutron Field (G. P. Lamaze, C. M. Eisenhauer, J. A. Grundl, F. J. Schima, and V. Spiegel)

Measured and calculated results are reported for the spectrum averaged cross sections of the $^{23}Na(n,\gamma)^{24}Na$, $^{115}In(n,n')^{115m}In$, $^{197}Au(n,\gamma)^{198}Au$, $^{59}Co(n,\gamma)^{60}Co$, $^{110}Ag(n,\gamma)^{110m}Ag$, and $^{45}Sc(n,\gamma)^{46}Sc$ reactions in the Intermediate Energy Standard Neutron Field (ISNF) at the National Bureau of Standards (NBS). The ISNF is a fission-neutron driven system in spherical geometry that employs two materials with well-understood neutron

*Los Alamos National Laboratory, Los Alamos, NM
**Oak Ridge National Laboratory, Oak Ridge, TN

transport parameters (carbon and ^{10}B) to produce a strong spectral component in the energy range of interest for fast-reactor and related technologies. Located in the graphite thermal column of the NBS research reactor, the ISNF consists of eight ^{235}U fission source disks mounted symmetrically near the surface of a 30-cm diameter cavity in the graphite and a ^{10}B shell centeredwithin the cavity. The resulting neutron spectrum at the cavity center resembles a fission spectrum at energies above 3.7 MeV; between 0.18 and 3.7 MeV, the spectrum is dominated by neutrons returning from the graphite after several collisions; and at lower energies the shape is determined by the 1/v absorption in the ^{10}B shell. The median energy is about 0.58 MeV, with 98% of the neutron fluence rate occurring between 1.2 keV and 5.6 MeV. The spectrum shape for this spherically symmetrical system has been determined by discrete ordinates and Monte-Carlo calculations at Los Alamos National Laboratory, Oak Ridge National Laboratory, and NBS.

The fluence at the center of the cavity was determined by a fluence transfer reaction from a ^{252}Cf fission source of known emission rate. The transfer reaction was $^{235}U(n,f)^{140}Ba$. Samples of ^{235}U were irradiated to a known fluence in compensated beam geometry in a known californium field and the ^{140}Ba-^{140}La count rate determined with a high purity germanium detector. Similar ^{235}U samples are then irradiated in the ISNF as a fluence monitor and then counted in the identical geometry. Corrections are made for the spectrum-averaged cross-section differences in the two fields (1.236 b in californium and 1.602 b in the ISNF), time history and scattering.

Samples of interest, together with the ^{235}U monitors are placed in a holder at the center of the ISNF cavity. To correct for resonance self-shielding, samples of different thicknesses were irradiated and the reaction rate extrapolated to zero thickness. The samples are irradiated for a measured time interval and the samples are removed for gamma analysis. The activity is determined by measuring the count rate ratio to a standard reference material when available or by counting with a well-calibrated germanium detector.

5. A Study of Fission Cross-Section Systematics (J. W. Behrens)

A publication has been completed giving the results from a study of the neutron-induced fission cross-section systematics for the uranium, neptunium and plutonium isotopes. Future studies will examine the thorium and protactinium isotopes and will extend into the transplutonium mass region.

B. DETECTORS AND FACILITIES FOR NUCLEAR DATA MEASUREMENTS

1. Development of a ^{3}He/Xe Gas Scintillation Counter to Measure the ^{3}He(n,p)T Cross Section in the Intermediate Energy Range

(J. W. Behrens, O. A. Wasson, A. D. Carlson, and Ma Hongchang*)

We have designed, tested, and implemented a ^{3}He gas scintillation counter to measure the ^{3}He(n,p)T cross section from thermal to 3 MeV incident neutron energy. The detector contains improvements essential toward the elevation of this reaction cross section to the standards level. This reaction has been suggested as a standard for intermediate neutron energy flux monitoring; however, its implementation has been blocked by earlier detector's sensitivity to gas impurities and by generally poor energy resolution.

A prototype detector, constructed using high-vacuum techniques to ensure a clean system, operated for over two years without significant deterioration of ultraviolet light output; however, the energy resolution was not adequate to separate the nuclear reaction from the recoil scattering. A second detector, constructed to increase the light collected by reducing the cell size and increasing the size and number of photomultipliers used to collect the light, boasts an improved 17% FWHM energy resolution for 2 MeV neutrons and has excellent separation of the ^{3}He(n,p)T pulse-height distribution from the ^{3}He recoil pulse-height distribution. The second detector was made part of an experimental setup at the NBS Linac to measure the ^{3}He(n,p)T cross section from 1 eV to 100 keV relative to the accepted ^{10}B(n,α) reaction standard. Our detector had a fast recovery from Linac gamma flash and had a timing resolution less than 10 ns.

In addition, other measurements will extend the measurement to the 300 keV to 3 MeV energy range at our Linac and will include absolute measurements at our 3 MV Positive Ion Accelerator. When completed, our work should greatly improve the status of the ^{3}He(n,p)T reaction by showing an improved detector design together with accurate measurements of the cross section over the intermediate neutron energy range.

2. Progress in the Development of a 2.5 MeV Neutron Source Facility for Fission Cross Section Measurements

(K. C. Duvall, O. A. Wasson, and Ma Hongchang*)

A 2.5 MeV neutron source facility has been established on the beamline of a 100 kV, 0.5 mA ion accelerator. The ion accelerator provides a 100 kV deuteron beam of about 200 μA into a 3 mm beam spot at the target position. The neutron source is produced by the D(d,n)^{3}He reaction with a yield of about 10^7 s^{-1}. The time-correlated associated particle method (TCAP) is utilized for the neutron fluence determination and for neutron background elimination. An associated particle chamber has been installed in which the ^{3}He associated-particles are detected at 90 degrees behind a thin aluminum absorber and the corresponding neutrons are emitted at about 70

---

* Institute of Atomic Energy, Beijing, People's Republic of China

degrees with an energy near 2.5 MeV. Also, the protons from the competing D(d,p)T reaction are monitored at 135 degrees for normalization and diagnostic purposes. A fission chamber containing six uranium tetrafluoride deposits has been designed for use in a $^{235}U(n,f)$ cross section measurement at 2.5 MeV. The 5-cm diameter deposits range in thickness from 150-300 $\mu g/cm^2$ and have good uniformity. Preparations are underway for the initial fission cross section measurements.

3. Characterization of the Moderating Neutron Detector (J. B. Czirr,* G. Jensen,* R. G. Johnson, A. D. Carlson, and O. A. Wasson)

An innovative series of neutron detectors has been developed at MESA Services International by Dr. J. B. Czirr. In collaboration with Drs. Czirr and G. Jensen, the Neutron Research and Measurement Group are conducting measurements to help characterize this detector.

The detector consists of 2 to 9 sheets of ^6Li-enriched glass scintillator. (Each sheet is 10-cm square and 0.5-mm thick.) the ^6Li-glass scintillators are surrounded by a neutron-moderation liquid and viewed by two photomultiplier tubes. With five pieces of glass the efficiency drops from 75% to 32% over the 1-eV to 1-MeV range. The timing resolution over this same energy range is 8.1 to 4.0 μs.

At the NBS Neutron Time-of-Flight Facility (NTOFF) a shape measurement of the efficiency for neutron energies from 100 eV to 30 keV has been performed. A thin ^6Li-glass transmission detector placed at 69 m was used as a flux monitor. The moderating neutron detector was placed at the 200-m station. The data obtained in this measurement are presently being analyzed and the measured efficiency will then be compared to the predictions of a Monte Carlo code.

4. Absolute Thermal Neutron Counter Development (D. M. Gilliam and G. P. Lamaze)

A gamma-alpha coincidence method is being employed to make an accurate calibration of a totally absorbing ^{10}B capture-gamma neutron beam monitor; and subsequently, the "black" ^{10}B detector will be used to calibrate a thin ^{10}B transmission monitor. These neutron counters have potential applications, such as improvement of thermal neutron cross section standards and improved calibration of the NBS manganous bath, with possible implications for ^{252}Cf nubar data.

During the past year, preliminary measurements were made of the efficiency of one germanium detector using the coincidence technique. The initial results have been very encouraging and a paper on the technique was presented at the International Conference on Methods and Applications of Radioanalytical Chemistry. A second germanium detector has been acquired to both double the efficiency of the system and reduce effects of position uncertainty of the neutron beam. A special shielded table is being constructed to hold both

* Brigham Young University

gamma detectors and a vacuum chamber for the ^{10}B samples and the surface barrier detector. This chamber is expectd to be available in March of this year.

5. Data Acquisition System Development (R. G. Johnson)

Upgrading of the data acquisition systems for the Linac Dedicated Pulsed Neutron Facility and the 3 MV Positive Ion Accelerator is nearly complete. Code development for two-parameter data acquisition through CAMAC into a super-microcomputer is in the final testing stage. The code is written almost entirely in a high level language (PASCAL) and uses the assembler language drivers from CERN for the commercially available CAMAC-VME interface. An ethernet local area network is being purchased to connect the two data acquisition systems to a third computer which has larger disk space, a faster printer, and a 9-track tape drive.

C. NUCLEAR DATA EVALUATIONS AND COMPILATIONS

1. The ENDF/B-VI Neutron Cross Section Standards Evaluations (A. D. Carlson, W. P. Poenitz,* G. M. Hale,** and R. W. Peelle†)

The evaluation process for the ENDF/B-VI standards, as outlined in the status report for last year, has been completed. The output of the simultaneous evaluation and R-matrix analyses were combined to provide the cross sections for $^{6}Li(n,t)$, $^{10}B(n,\alpha_1)$, $^{10}B(n,\alpha_2)$, $^{10}B(n,\alpha)$, $^{197}Au(n,\gamma)$ and $^{235}U(n,f)$. Data on the $^{238}U(n,\gamma)$, $^{238}U(n,f)$, and $^{239}Pu(n,f)$ cross sections were also obtained which will be used by the evaluators of the ^{238}U and ^{239}Pu cross sections. New R-matrix evaluations for H(n,n) by Dodder and Hale and $^{3}He(n,p)$ by Hale are also now completed. These evaluations have been added to the ENDF/B-V standards file. The ENDF/B-VI standards are available on request from the National Nuclear Data Center at Brookhaven National Laboratory. Work is now underway to define the cross section uncertainties and establish the uncertainty (variance-covariance) files for these standards.

2. Photon Cross Section Database (E. B. Saloman, J. H. Hubbell, and M. J. Berger)

A systematic graphical comparison has been made between the experimental photon attenuation coefficients in the database at the NBS Photon and Charged Particle Data Center and, (a) a corresponding set of theoretical values based on Scofield's photo-effect calculations and theoretical scattering cross sections that include binding effects, and (b) a set of recommended semi-empirical values from Henke. This comparison covers the energy region from 100 eV to 100 keV and atomic numbers from 1 to 92. It has been published in Atomic Data and Nuclear Data Tables, 38, 1-197 (1988).

---

* Argonne National Laboratory, Argonne-West, Idaho Falls, ID

** Los Alamos National Laboratory, Los Alamos, NM

† Oak Ridge National Laboratory, Oak Ridge, TN

At energies above 1 keV, agreement between theory and experiment is rather good except for some special situations which prevent the accurate description of the measured samples as free atoms. These include molecular effects near absorption edges and solid-state and crystal effects (for example for silicon).

A computer-readable database has been prepared of the available experimental photon attenuation coefficients at energies from 100 eV to 10 GeV, which can be used on a personal computer for further analyses and comparisons of these data. This database includes 20,000 data points from more than 500 independent experiments.

3. A Simultaneous Evaluation of Kerma in Carbon and the Carbon Cross Sections (E. J. Axton and J. J. Coyne)

Recent measurements of kerma in carbon indicate that values of this quantity calculated on the basis of cross sections taken from the ENDF/B-V file are probably too high, particularly in the energy range from 15 to 20 MeV. Measurements of the inelastic scattering cross section to the first excited state, and of the n-n'3α cross section in this energy range which have appeared since the establishment of ENDF/B-V suggest that the former should be higher, and the latter lower.

Experimental data on the total and elastic scattering, which was not used in the ENDF/B evaluation, is now available and will also be used in two evaluations. The purpose of this exercise is to perform a least squares fit to the available data for kerma and the cross sections in order to find best values for these parameters. A final report is now in preparation and will contain tabulations of all cross sections for carbon and the newly reevaluated kerma factors for carbon which will be lower than that previously published.

4. Calculated Microdosimetric Energy Distribution Spectra and Their Use to Indicate Neutron Source Quality (H. M. Gerstenberg and J. J. Coyne)

Microdosimetric energy distribution spectra, or y spectra, have been calculated for four different distributed neutron sources using the analytical computer code developed at the National Bureau of Standards. The code is currently in use on the new NBS computer. The neutron spectra used as the input for the code were obtained from calculations of the neutron fluence expected from a ^{252}Cf source, a source with a large component of high-energy neutrons up to 16.9 MeV, and a source of neutrons from a pulsed thermal reactor with and without a lead shield. The resulting energy distribution spectra for each of the four input neutron spectra are compared and explained in terms of the proportion of low-energy neutrons to high-energy neutrons in the input neutron spectra. The variations, as well as the similarities, in the shape of the resulting energy distribution spectra show that the y spectra can be a useful tool in understanding the quality of different spectra.

A paper describing this work was given at the 8th International Congress of Radiation Research held in Edinburgh, Scotland, July 19-24, 1987. Calculations are now in progress for other energy distributed neutron spectra. Some of these spectra are for cancer therapy and have a large component of high energy neutrons while other spectra are for radiation protection and have more low energy neutrons.

5. Initial Spectra of Neutron-Induced Secondary Charged Particles (H. M. Gerstenberg, R. S. Caswell, and J. J. Coyne)

Initial spectra of secondary-charged particles (such as p,α, C, N, O) which result from neutron interactions with material such as tissue, will be tabulated in 200 keV neutron energy bin sizes from 0 to 20 MeV. Tabulations will also be made for 76 almost logarithmic bins extending from thermal energy for 2 MeV. These calculations use as input neutron cross section data in an ENDF/B data format and we are in the process of putting the Axton reevaluation in the correct format to be used in our calculations. Supplementary information is also needed on the angular distribution of neutron reactions leading to charged particles and on the final excitation of residual nuclei. The calculations for these tables will be started when the final version of all of the partial cross sections in carbon from the Axton reevaluation are available.

6. Fifty Years with Nuclear Fission, a Conference (J. W. Behrens, A. D. Carlson, B. S. Carpenter, W. A. Cassatt, E. V. Hayward, and O. A. Wasson)

The National Bureau of Standards and the American Nuclear Society will sponsor a conference entitled "Fifty Years with Nuclear Fission" to be held at the National Bureau of Standards from April 25-28, 1989. Joining as co-sponsors are the American Chemical Society and its Division of Nuclear Chemistry along with the American Physical Society and its Division of Nuclear Physics, in cooperation with the Electric Power Research Institute, the National Academy of Sciences, the National Science Foundation, Princeton University, University of California at Berkeley, the U. S. Department of Energy and the U.S. Nuclear Regulatory Commission. Professors John Wheeler and Edoardo Amaldi will serve as Honorary Co-Chairman. Glenn T. Seaborg and Emilio Segre are general Co-Chairmen.

The conference's program committee met on April 22, 1987 to select the general topics and to nominate members to the International Advisory Committee. The general topics chosen were: 1) The History of Fission, 2) Fission Theory, 3) Fission-Experiment, 4) Fission-Applied Data, 5) Applications Utilizing Fission, and 6) The Impact of Fission on Society of the Discovery of Fission. A first announcement which was mailed to approximately 5000 individuals world-wide produced approximately 300 responses. We presently estimate that the conference will be attended by 400-500 participants.

A. CROSS SECTION MEASUREMENTS

1. Capture, Total and Reactions

a. Total Cross Section and Resonance Spectroscopy for n + Kr-86,[1] (R. F. Carlton,[2] R. R. Winters,[3] C. H. Johnson, N. W. Hill, and J. A. Harvey)

The neutron total cross section for n + ^{86}Kr has been measured over the incident neutron energy range 0.015 to 25 MeV. The average total cross section is obtained for neutron energies from 1 to 25 MeV. For the energy region from 0.015 to 1 MeV, an R-matrix analysis yields resonance parameters which provide a complete representation of the neutron scattering functions for the $s_{1/2}$, $p_{1/2}$, and $p_{3/2}$ scattering channels. From this analysis level densities, neutron strength functions and external R-functions are obtained for the 1-MeV energy region just above the neutron separation energy. The back-shifted Fermi gas model provides excellent descriptions of the level densities for the $1/2^+$, $1/2^-$, and $3/2^-$ states. Some evidence for doorway states is found in the level spacings for the $1/2^-$ resonances and in the reduced neutron width distribution for the $3/2^-$ resonances.

b. Nuclear Structure of Ca-49 Above 5 MeV Excitation from n + Ca-48 and Astrophysics for 30-keV Neutrons[4] (R. F. Carlton,[2] J. A. Harvey, R. L. Macklin, C. H. Johnson, and B. Castel[5])

c. Resonance Structure of S-33 + n from Transmission Measurements[6] (G. Coddens,[7] M. Salah,[8] J. A. Harvey, N. W. Hill, and N. M. Larson)

d. 189-Os + n S-Wave Mean Level Spacings and Strength Functions[9] (R. F. Carlton,[2] R. R. Winters,[3] G. W. Tweed, J. A. Harvey, and N. W. Hill)

The total neutron cross section has been measured for ^{189}Os+n over the incident neutron energy range 6 eV to 500 keV. R-Matrix analysis of 45 s-wave resonances over the range 6-170 eV has been performed. The

---

[1]Submitted to Physical Review C.
[2]Middle Tennessee State University, Murfreesboro, Tennessee 37132.
[3]Department of Physics, Denison University, Granville, Ohio 43023.
[4]Nucl. Phys. **A465**, 274 (1987).
[5]Queen's University, Kingston, Ontario, Canada K71 3N6.
[6]Nucl. Phys. **A469**, 480 (1987).
[7]Commisariat a L'Energie Atomique, Laboratoire Leon Brillouin, France.
[8]Graduate student from Minia University, Egypt.
[9]Bull. Am. Phys. Soc. 32, 1110 (1987).

preliminary s-wave mean level spacings and strength function for the 16 resonances with J=1 are $\langle D \rangle = (10.6 \pm 1.4)$ eV and $S = (3.0 \pm 1.1) \times 10^{-4}$. For the 29 s-wave resonances with J-2 we find $\langle D \rangle = (5.7 \pm 0.6)$ eV and $S = (3.1 \pm 0.9) \times 10^{-4}$. The s-wave strength function (without regard to J) is $S = (3.1 \pm 0.7) \times 10^{-4}$). These results are of interest in determining the optical model potential (OMP) for the osmium mass region and in estimating the duration of galactic nucleosynthesis. A paper on this subject is in preparation.

e. Level Densities from Resonance Spectroscopy for n + Kr-86,[1] (R. F. Carlton,[2] R. R. Winters,[3] C. H. Johnson, N. W. Hill, and J. A. Harvey.)

High resolution transmission measurements on a high purity ^{86}Kr gas sample were performed at the ORELA facility over the neutron energy range of 0.015-25 MeV. From R-matrix analysis of these data in the resolved resonance region below 1 MeV we have determined the n + ^{86}Kr level densities for $J^{\pi} = 1/2^+$, $1/2^-$, $3/2^-$ reaction channels in the 1-MeV energy interval above neutron binding. The energy dependence of the $3/2^-$ level density, for which the uncertainties are smallest, is suitably modeled by a back-shifted Fermi gas model with two adjustable parameters. This model is then used to predict the level densities for $j^{\pi} = 1/2^+$ and $1/2^-$. Except for an unusual non-statistical behavior in the 500-600 keV region for the $1/2^-$ cumulative number of levels, the model is seen to give an excellent description of all three data sets. Parameters obtained are consistent with systematic trends in this mass region. A paper on this subject is ready for submission.

f. Resonance Neutron Capture by 20,22-Ne Stellar Environments[4] (R. R. Winters[3] and R. L. Macklin)

We have measured the neutron capture cross sections over the neutron energy range 2.5 to 200 keV of ^{20,22}Ne at the Oak Ridge Electron Linear Accelerator (ORELA) using enriched samples at high pressures. The cross sections, averaged using a Maxwell-Boltzmann distribution weighting function for a range of temperatures thought to be appropriate for the sites of s-process stellar nucleosynthesis, are small. For example, the Maxwellian-averaged ^{22}Ne(n,γ) cross section for kT = 30 keV derived from the present work is smaller than 0.27 mb. This result increases the calculated net neutron production from ^{22}Ne by reducing the importance of ^{22}Ne(n,γ) as a neutron poison in s-process calculations. The number of neutrons per ^{56}Fe seed available for s-process stellar nucleosynthesis appears sufficient to account for the observed abundances of the heavier elements.

---

[1]To be presented at the American Physical Society Annual Meeting, Baltimore, MD, April 1988.
[2]Middle Tennessee State University, Murfreesboro, Tennessee 37132.
[3]Department of Physics, Denison University, Granville, Ohio 43023.
[4]Submitted to the Astrophysical Journal.

g. Neutron Capture by 79-Br, 81-Br, and 75-As[1] (R. L. Macklin)

Neutron capture up to 700 keV was measured for arsenic and bromine and for an enriched sample of ^{81}Br. Individual resonance capture was parameterized in the first several keV and average capture cross sections derived at the higher energies. Maxwellian average cross sections found for ^{79,81}Br and ^{75}As, respectively, were (741 ± 10) mb and (455 ± 18) mb for a temperature kT=30 keV. Resonance capture integrals calculated for ^{79,81}Br, respectively, were (130 ± 5) b and (46.6 ± 1.8) b.

h. Maxwellian-Averaged Neutron Capture Cross Sections for 99-Tc and 95,96-Mo[2] (R. R. Winters[3] and R. L. Macklin)

i. Neutron Capture Cross Sections of Rhenium from 3 to 1900 keV[4] (R. L. Macklin and P. G. Young[5])

j. Neutron Capture Resonances of Gadolinium-152 and 154[6] (R. L. Macklin)

k. The 151-Sm Branching, a Probe for the Irradiation Time Scale of the S-Process[7] (H. Beer[8] and R. L. Macklin)

The excitation functions for the reactions ^{152,154,155,157}Gd (n,γ) have been measured over the neutron energy range of 5 keV to 500 keV. Maxwellian-averaged capture cross sections for thermal energies kT=5-100 keV have been calculated. At kT=30 we have found: $\sigma(^{152}\text{Gd})$ = 1003 ± 30 mb, $\sigma(^{154}\text{Gd})$ = 878 ± 27 mb, $\sigma(^{155}\text{Gd})$ = 2721 ± 90 mb, $\sigma(^{157}\text{Gd})$ = 1355 ± 39 mb. The data, in conjunction with other cross sections and solar abundances, were used to carry out an s-process analysis of the branchings in the Sm to Gd mass range. The s-process is treated in the classical as well as in the pulsed model. The solution of the classical model is contained in the pulsed model as the asymptotic solution for large pulse widths. It is shown that this solution is the only one which can reproduce the abundance pattern of the different branchings. Pulse durations are limited to values larger than about 3 yr.

---

[1]Submitted to Nuclear Science and Engineering.
[2]Astrophysical Journal 313, 808 (1987).
[3]Department of Physics, Denison University, Granville, Ohio 43023.
[4]Nucl. Sci. Eng. 97, 239 (1987).
[5]Los Alamos National Laboratory, P. O. Box 1663, Los Alamos, NM 87545.
[6]Nucl. Sci. Eng. 95, 304 (1987).
[7]Submitted to the Astrophysical Journal.
[8]Kernforschungszentrum Karlsruhe, Institut fur Kernphysik III, D-7500 Karlsruhe, Federal Republic of Germany.

l. The 189-Os(n,γ) Cross Section and Implications for the Duration of Stellar Nucleosynthesis[1] (R. R. Winters[2], R. L. Macklin, R. H. Hershberger[3])

m. 10,11-B(n,xγ) Reactions for Incident Neutron Energies Between 0.1 and 10 MeV[4] (J. K. Dickens and D. C. Larson)

Measurements have been made of gamma-ray production due to neutron interactions with samples of boron for the incident neutron energies between 0.1 and 10 MeV. For ^{11}B a 54-gm sample of naturally-occurring boron in the shape of a solid cylinder was used for the sample. For ^{10}B, samples enriched to 92% in the ^{10}B isotope were used. One sample, of about 49 gm, was used to obtain gamma-ray data following inelastic scattering; the other sample, of about 15 gm, was used to delineate the production of the 478-keV gamma ray following the $^{10}B(n,\alpha)^{7}Li$ reaction for E_n between 0.1 and about 3 MeV. This smaller sample was used to reduce the neutron multiple scattering corrections for $E_n < 1$ MeV. The Oak Ridge Electron Linear Accelerator (ORELA), a white source, was used to provide the incident neutrons. Data were obtained using a high-purity intrinsic-germanium photon detector positioned at 125° with respect to the incident neutron beam. Incident neutron energies were determined by flight time over a 22-m flight path. Because the peak shapes in the raw data are substantially broadened by Doppler motion, peak yields were determined with graphic-interactive methods. Preliminary data reduction indicates that, except for the 478-keV gamma ray, for $E_n < 1$ MeV, the photon production cross sections are all small, the largest being on the order of 100 mb.

These data will satisfy a high-priority request on the current U.S. Magnetic Fusion Energy request list. In addition, data for the 478-keV gamma ray may be included to extend this reaction as a standard to higher neutron energies.

n. Gamma-Ray Decay of Levels in 53-Cr[5] (J. K. Dickens and D. C. Larson)

Gamma-ray decay of levels in the stable isotope ^{53}Cr has been studied using $^{53}Cr(n,n'\gamma)$ reactions for incident neutron energies between threshold and 10 MeV. Of the 65 gamma rays or gamma-ray groups observed for neutron interactions with ^{53}Cr, 50 have been placed or tentatively placed among 34 levels in ^{53}Cr up to an excitation energy of 4.36 MeV. Deduced branching ratios are in reasonable agreement with previous measurements except for decay of the E_x = 1537-keV level. For the decay of the E_x = 1537-

---

[1]Astronomy and Astrophysics 171, 9 (1987).
[2]Department of Physics, Denison University, Granville, Ohio 43023.
[3]University of Kentucky, Lexington, Kentucky.
[4]To be published in Proceedings of International Conference on Nuclear Data for Science and Technology, Mito, Japan, May 30--June 3, 1988.
[5]ORNL-6418 (November 1987).

keV level we are unable to explain variations in the branching ratios of the transition gamma rays as a function of incident neutron energy within the framework of the presently known level structure of ^{53}Cr and suggest the possibility of a second energy level at E_x = 1537 keV.

2. Actinides

a. High Resolution Measurement of the U-238 Neutron Capture Yield for Incident Neutron Energies from 1 to 100 keV[1] (Roger L. Macklin)

b. High Energy Resolution Measurement of the U-238 Neutron Capture Yield from 1 to 100 keV[2] (Roger L. Macklin, R. B. Perez, G. de Saussure, and R. W. Ingle)

The purpose of this work is the precise determination of the ^{238}U neutron capture yield (i.e., the probability of neutron absorption) as a function of neutron energy with the highest available neutron energy resolution. The motivation for this undertaking arises from the central role played by the ^{238}U neutron capture process in the calculation of the neutron balance of both thermal reactors and fast breeder reactors. The present measurement was performed using the Oak Ridge Electron Linear Accelerator (ORELA) facility.

The pulsed beam of neutrons from the ORELA facility is collimated on a sample of ^{238}U. The neutron capture rate in the sample is measured, as a function of neutron time-of-flight (TOF), by detecting the gamma rays from the $^{238}U(n,\gamma)^{239}U$ reaction with a large gamma-ray detector surrounding the ^{238}U sample. At each energy, the capture yield is proportional to the observed capture rate divided by the measured intensity of the neutron beam. The constant of proportionality (the normalization constant) is obtained as the ratio of theoretical to experimentally measured areas under small ^{238}U resonances where the resonance parameters have been determined from high resolution ^{238}U transmission measurements. The cross section for the reaction $^{238}U(n,\gamma)^{239}U$ can be derived from the measured capture yield if one applies appropriate corrections for multiple scattering and resonance self-shielding.

The present work will allow the extension of the resolved resonance region in ^{238}U from its current limit of 4 keV up to 20 keV. In addition, some 200 ^{238}U neutron resonances in the energy range from 250 eV to 10 keV have been observed which had not been detected in previous measurements. These results are relevant for both reactor design and for the understanding of the structure of the (^{238}U + n) compound nucleus.

---

[1]Master of Science Thesis, University of Tennessee, Knoxville, Tennessee, December 1987.
[2]Trans. Am. Nucl. Soc. 54, 344 (1987).

c. High Energy Resolution Measurement of the U-238 Neutron Capture Yield in the Energy Region Between 1 and 100 keV[1] (Roger L. Macklin, R. B. Perez, G. de Saussure, and R. W. Ingle)

A measurement of the ^{238}U neutron capture yield was performed at the 150-meter flight path of the ORELA facility on two ^{238}U samples (0.0124 and 0.0031 atoms/barn). The capture yield data were normalized by Moxon's small resonance method.

The high-energy resolution achieved in this measurement frequently resulted in doublet and triplet splittings of what appeared to be single resonances in previous measurements. This resolution should allow extension of the resolved resonance energy region in ^{238}U from the present 4-keV limit up to 15 or 20 keV incident neutron energy.

Some 200 small resonances of the (^{238}U + n) compound nucleus have been observed which had not been detected in transmission measurements, in the energy range from 250 eV to 10 keV.

A substantial amount of fine structure has been detected above 20 keV which is very well reproduced in the capture yield measurements of the two sample thicknesses of ^{238}U. These results will allow the development of improved resonance parameter sets, particularly when combined with high resolution ^{238}U transmission measurements currently in progress at ORELA.

d. High-Resolution Neutron Transmission Measurements on U-238 from 1 to 100 keV with an NE-110 Scintillation Detector[1] (J. A. Harvey, N. W. Hill, and F. G. Perey)

The NEANDC ^{238}U Task Force has emphasized the importance of the resolution function (and its tail) in the analysis of keV transmission data of ^{238}U, and the need for new high-resolution transmission data with good statistics on several sample thicknesses of ^{238}U.

We have developed a neutron detector with a narrow resolution function which is efficient for keV energy neutrons, has low background, and is not sensitive to overlap neutrons (<200 eV) so the pulsed accelerator can be operated at a high repetition rate (800 pps). The detector consists of a 9- by 9-cm NE 110 scintillator, 1 cm thick, mounted in a 0.025-mm mylar reflecting cylinder, and epoxy-coupled on opposite edges to two 12.5-cm-diameter RCA 8854 photomultipliers (PMs). Each PM is biased below the single photoelectron level, and a coincidence is required between the outputs of the two PMs to eliminate counts due to PM noise. The detector has been studied down to a neutron energy of 50 eV. The observed signal-to-background ratio was 300 at 12 keV and 30 at 2 keV. The detector has an efficiency of 40% at

---

[1]To be published in Proceedings of International Conference on Nuclear Data for Science and Technology, Mito, Japan, May 30--June 3, 1988.

15 keV (ten times that of a 1-cm-thick ^{6}Li glass scintillation detector) and its efficiency equals that of the ^{6}Li detector at 4 keV. The timing resolution of the detector is 7 nsec for 10-keV neutrons, limited by the neutron flight time through the scintillator, and is less for higher energy neutrons.

High-resolution neutron transmission measurements have been made on three sample thicknesses of ^{238}U (99.92 and 99.99%) at room temperature from 1 to 100 keV using neutrons from the water-moderated Ta target at ORELA, this new NE 110 proton-recoil scintillation detector, and the 200-m flight path. The measurements on the thickest sample (36.2 mm) were made using 6-nsec bursts at 800 pps, and on 2.5- and 8.3-mm-thick samples using 15-nsec bursts and 415 pps. The neutron energy resolution (0.03%) is less than the Doppler broadening below 15-keV neutron energy. Analysis of these data will be done with the R-matrix code SAMMY which incorporates a detailed resolution function characterizing the source and detector.

e. High-Resolution Transmission Measurements on U-235 and Pu-239 from 1 to 10,000 eV[1] (J. A. Harvey, N. W. Hill, G. L. Tweed, and L. Leal)

High-resolution transmission measurements have been made on three sample thicknesses of both ^{235}U (99.6%, 24.3 gms) and ^{239}Pu (99.96%, 71.9 gms) at liquid nitrogen temperature using neutrons from the water-moderated Ta target at ORELA. A 1-mm-thick ^{6}Li glass scintillator, 10 cm in diameter, mounted in a 0.025-mm mylar reflecting cylinder between two RCA 8854 PM tubes was used at a 17.909-m flight path for the low-energy data, and a 12.5-mm-thick ^{6}Li scintillator, 11.1 cm in diameter, mounted in a similar cylinder between two RCA 8854 PM tubes was used at a 80.394-m flight path at higher energies. The photomultiplier bases are gated to eliminate the gamma flash. In order to minimize background, a coincidence is made between fast-timing windows from each PM and a 40-nsec smoothed sum signal from the two PMs.

Both ^{235}U and ^{239}Pu data have been corrected for the deadtime (1104 nsec) of the time digitizer and for several backgrounds which total <3% over most of the energy region studied. These backgrounds consist of a constant beam-independent background, a 17.6-μsec gamma-ray background from the capture of neutrons by the water moderator, overlap neutrons from the previous burst, and a time-dependent background arising from neutrons scattered from the ^{6}Li glass scintillator. For the ^{235}U data, corrections were made for the contribution from a 0.385% Ta impurity in two of the samples and for contributions from the ^{234}U (0.033%), ^{236}U (0.184%), and ^{238}U (0.128%) in the three samples; these percentages were determined from the analyses of low-energy resonances of these nuclides.

---

[1]To be published in Proceedings of International Conference on Nuclear Data for Science and Technology, Mito, Japan, May 30--June 3, 1988.

These transmission data (along with fission data) have been analyzed by Derrien et al. using the program SAMMY.

f. Parameters of the 1.056-eV Resonance in 240-Pu and the 2200 m/s Neutron Total Cross Sections of 235-U, 239-Pu, and 240-Pu[1] (R. R. Spencer, J. A. Harvey, N. W. Hill, and L. W. Weston)

g. Fission-Product Yields for Fast-Neutron Fission of Cm-243,244,246,248[2] (J. K. Dickens)

h. Review of New Integral Determinations of Decay Heat[3] (J. K. Dickens)

Over a decade ago, concern over possible serious consequences of a loss-of-coolant accident in a commercial light-water reactor prompted support in several countries of several experiments designed specifically to measure the decay heat of beta-ray and gamma-ray emanations from fission products for thermal reactors. In 1979, a new standard for use in computing decay heat in real reactor environs (for example, for regulatory requirements) was approved by the American Nuclear Society. Since then there have been additional experimental measurements, in particular for fission induced by fast neutrons. In addition, the need for decay-heat data has been extended well beyond the time regime of a loss-of-coolant accident. The efficacy of the 1979 ANS standard has been a subject of study with generally positive results. However, a specific problem, namely, the consequences for decay heat of fission-product neutron capture merits further experimental study.

3. Experimental Techniques

a. A NE 110 Scintillator Detector for keV-Energy Neutrons[4] (J. A. Harvey and N. W. Hill)

We have developed a neutron detector with a narrow resolution function which is efficient for keV energy neutrons, has low background, and is not sensitive to overlap neutrons (<200 eV) so the pulsed accelerator can be operated at a high repetition rate (800 pps). The detector consists of a 9- by 9-cm NE 110 scintillator, 1 cm thick, mounted in a 0.025-mm mylar reflecting cylinder, and epoxy-coupled on opposite edges to two 12.5-cm-diameter RCA 8854 photomultipliers (PMs). Each PM is biased below the single

---

[1]Nucl. Sci. Eng. **96**, 318-329 (1987).
[2]Nucl. Sci. Eng. **96**, 8 (1987).
[3]Proceedings of a Specialists' Meeting on Data for Decay Heat Predications, Studsvik, Sweden, September 7-10, 1987, NEACRP-302 'L", NEANDC-245 "U" (1987).
[4]To be presented at the American Physical Society Annual Meeting, Baltimore, MD, April 1988.

photoelectron level, and a coincidence is required between the outputs of the two PMs to eliminate counts due to PM noise. The detector has been studied down to a neutron energy of 50 eV. The observed signal-to-background ratio was 300 at 12 keV and 30 at 2 keV. The detector has an efficiency of 40% at 15 keV (ten times that of a 1-cm-thick ^{6}Li detector at 4 keV. The timing resolution of the detector is 7 nsec for 10-keV neutrons, limited by the neutron flight time through the scintillator and is less for higher energy neutrons. Results from transmission measurements on ^{238}U will be presented.

b. Responses of C_6D_6 and C_6F_6 Gamma-Ray Detectors[1] (F. G. Perey, J. O. Johnson, and T. A. Gabriel)

Recently, Van de Graaff experiments were performed at BCMN and AERE Harwell where high energy gamma rays from proton-induced reactions were detected with the C_6D_6 detectors they had used in neutron capture measurements. The observed responses of these detectors to high-energy gamma rays differ considerably from what had been previously calculated and used in capture measurements. Far more low-energy pulses were observed, sometimes by more than a factor of two, than had been calculated. A weighting function based upon the responses observed in the BCMN Van de Graaff experiments removes the long standing discrepancy for the capture in the 1.15 keV resonance of ^{56}Fe as determined from capture measurements.

We have used the electron gamma-ray transport code EGS to investigate the responses to gamma rays of the C_6D_6 detectors used at BCMN and Harwell and of the C_6F_6 detectors used at ORELA. These responses are found to be very sensitive to materials close to the sources of gamma rays or the detectors themselves. Very good agreement was obtained with the response obtained in the Harwell experiment. In the case of the BCMN experiments, the responses were found to be strongly affected by the germanium detector used in these coincidence experiments. The EGS calculations do not agree as well with the results. This is possibly due to the fact that these results should be sensitive to angular correlations in the gamma-ray cascades used, angular correlations that were not included in the calculations since they are not available. For the ORELA C_6F_6 detectors EGS calculations were compared with single gamma rays observed in capture of neutrons from ^{207}Pb.

Weighting functions based upon the EGS calculations for these detectors, in the geometry used in capture experiments, are considerably different from what had previously been used. We conclude that state-of-the-art gamma-ray electron transport codes, such as EGS, should be used in calculating response functions for these detectors in the precise geometry used in the capture experiments, including the samples since electrons created there by high energy gamma rays may be detected.

---

[1]To be published in Proceedings of the International Conference on Nuclear Data for Science and Technology, Mito, Japan, May 30-June 3, 1988.

c. Calculated Fraction of an Incident Current Pulse That Will Be Accelerated by an Electron Linear Accelerator and Comparisons with Experimental Data[1] (R. G. Alsmiller, Jr., F. S. Alsmiller, and T. A. Lewis)

In a series of previous papers, calculated results obtained using a one-dimensional ballistic model were presented to aid in the design of a prebuncher for the Oak Ridge Electron Linear Accelerator. As part of this work, a model was developed to provide limits on the fraction of an incident current pulse that would be accelerated by the existing accelerator. In this paper experimental data on this fraction are presented and the validity of the model developed previously is tested by comparing calculated and experimental data. Part of the experimental data is used to fix the physical parameters in the model and then good agreement between the calculated results and the rest of the experimental data is obtained.

B. DATA ANALYSIS

1. Theoretical

a. Unified Description of the Neutron 208-Pb Mean Field Between -20 and +165 MeV from the Dispersion Relation Constraint[2] (C. H. Johnson, D. J. Horen, and C. Mahaux[3])

The real part of the central neutron-^{208}Pb mean field is the sum of a Hartree-Fock component plus a dispersive component. In keeping with theoretical expectations, the Hartree-Fock field is assumed to have a Woods-Saxon shape whose depth decreases exponentially with increasing energy and whose radius and diffuseness are independent of energy. The dispersive component is determined from the imaginary part of the optical-model potential by making use of the dispersion relation which connects these two quantities. The imaginary part is written as the sum of a volume and a surface-peaked contribution. The dispersion relation then implies that the real dispersive contribution is also the sum of volume and surface-peaked components. The parameters of the complex mean field are determined by fitting the available differential and polarization cross sections in the energy domain (4, 40 MeV) and the total cross sections in the domain (1, 120 MeV); these data are contained in previous published or unpublished reports, but new measurements of the total cross sections are presented from 1 to 25 MeV. Good fits to these cross sections, and also to unpublished total cross sections for energies up to 165 MeV, are obtained despite the fact that the number of adjusted parameters is quite small because of our use of the constraint implied by the dispersion relation. The real part of the mean field is well approximated by a Woods-Saxon shape whose radius decreases with

---

[1]Nucl. Instrum. Meth. in Phys. Research **A256**, 409 (1987).
[2]Physical Review C 36(6), 2252 (December 1987).
[3]Institut de Physique B5, Universite de Liege, B-4000 Liege 1, Belgium.

increasing energy between 5 and 25 MeV; its depth is approximately constant from 5 to 15 MeV and then decreases with increasing energy; these findings are in keeping with recent empirical evidence. When the neutron energy decreases below 2.5 MeV, the potential radius decreases; it increases again when the neutron energy decreases below -14.5 MeV. In the domain -20 MeV < E < 0 the deduced potential accurately reproduces the experimental single-particle energies as well as the asymptotic values of the single-particle wave functions as measured from sub-Coulomb pickup reactions; it also yields excellent agreement with the spreading width of the deeply bound $1h_{11/2}$ hole state. The rms radii, absolute spectroscopic factors, and occupation numbers are calculated for the valence particle and hole states. At the Fermi energy (-6 MeV), the mean field can be identified with the Hartree-Fock potential, for which the present analysis yields a depth of 46.4 MeV, a radius of 1.24 $A^{1/3}$ fm, and a diffuseness of 0.68 fm. In the energy domain $4 \leq E \leq 10$ MeV, the already good agreement between the predicted and measured cross sections is further improved if the imaginary part of the mean field is allowed to have its strength depend upon the neutron orbital angular momentum, and its surface diffuseness is allowed to be energy dependent.

b. Evidence for Shell Dependence of the Imaginary Part of the Neutron Optical Potential[1] (R. R. Winters[2] and C. H. Johnson)

For neutron energies of 5 to 10 MeV, there is empirical evidence from the literature that the shape of the surface imaginary part of the phenomenological neutron optical model potential depends upon energy; the radius increases with decreasing energy while the diffuseness decreases. For the specific cases of neutrons on ^{89}Y and ^{208}Pb we have shown that the empirical variation in shape has the effect of reducing compound nuclear processes for the partial waves that are associated with the unoccupied bound single-particle orbits. Thus, the variation in shape can be reinterpreted as a shell dependence in the depth of the surface imaginary potential. This interpretation facilitates the incorporation of the dispersion relation into otherwise phenomenological optical model analyses of neutron scattering data. A paper on this subject has been accepted for publication in Physical Review C.

c. A Simplified Unified Hauser-Feshbach/Pre-Equilibrium Model for Calculating Double Differential Cross Sections[3] (C. Y. Fu)

A unified Hauser-Feshbach/Pre-Equilibrium model is extended and simplified. The extension involves the addition of correlations among states of different total quantum numbers (J and J') and the introduction of consistent level density formulas for the H-F and the P-E parts of the

---

[1]To be presented at the American Physical Society Annual Meeting, Baltimore, MD, April 1988.

[2]Department of Physics, Denison University, Granville, Ohio 43023.

[3]Presented at NEANDC Specialists' Meeting on Pre-Equilibrium Reactions, Semmering, Austria, February 10-12, 1988.

calculation. The simplification, aimed at reducing the computational cost, is achieved mainly by keeping only the off-diagonal terms that involve strongly correlated 2p-1h states. A correlation coefficient is introduced to fit the experimental data. The model has been incorporated into the multistep H-F model code TNG. Calculated double differential (n,xn) cross sections at 14 and 25.7 MeV for iron, niobium, and bismuth are in good agreement with experiments. In use at ORNL and JAERI, the TNG code in various stages of development has been applied with success to the evaluation of double differential (n,xn) cross sections from 1 to 20 MeV for the dominant isotopes of chromium, manganese, iron, nickel, copper, and lead.

d. Approximation of Precompound Effects in Hauser-Feshbach Codes for Calculating Double Differential (n,xn) Cross Sections[1] (C. Y. Fu)

A simplified method for approximating precompound nuclear-reaction effects in Hauser-Feshbach codes for the calculation of double-differential (n,xn) cross sections is presented. The method is developed from an existing quantum-mechanical formula of unified compound and precompound reaction theories. The compound part of the unified formula is made identical to that of Hauser and Feshbach by applying the unified level-density formulas derived previously for the two theories. The precompound part, much more complicated than the compound part, is simplified and globally parameterized for practical purposes. Calculated double-differential (n,xn) cross sections at 14 and 26 MeV for iron, niobium, and bismuth are shown to be in good agreement with the available experimental data. The method at various stages of development has been applied with success to the generation of evaluated files of double-differential (n,xn) cross sections from 5 to 20 MeV for the major isotopes of chromium, manganese, iron, nickel, and copper.

e. Calculations of Double Differential 184-W(n,xn) Cross Sections at 25.76 MeV by the TNG Code[2] (C. Y. Fu and D. M. Hetrick)

f. Calculated Neutron-Induced Cross Sections for 52-Cr from 1 to 20 MeV and Comparisons with Experimental Data[3] (D. M. Hetrick, C. Y. Fu, and D. C. Larson)

Nuclear model codes were used to compute cross sections for neutron-induced reactions on ^{52}Cr for incident energies from 1 to 20 MeV. The input parameters for the model codes were determined through analysis of experimental data in this energy region. Discussion of the models used, the input data, the resulting calculations, extensive comparisons to measured

---

[1]Submitted to Nucl. Sci. Eng.
[2]Included in NEA Data Bank Report entitled "Blind Intercomparisons for n + ^{184}W at 25.7 MeV, H. K. Vonach and P. Nagel, eds. (accepted for publication).
[3]ORNL/TM-10417 (September 1987).

data, and comparisons to the Evaluated Nuclear Data File (ENDF/B-V) for Cr (MAT 1324) are included in this report.

g. Calculated Neutron-Induced Cross Sections for 53-Cr from 1 to 20 MeV[1] (K. Shibata[2] and D. M. Hetrick)

Neutron-induced cross sections of ^{53}Cr have been calculated in the energy regions from 1 to 20 MeV. The quantities obtained are the cross sections for the reactions (n,n'γ), (n,2n), (n,np), (n,nα), (n,pγ), (n,pn), (n,$\alpha\gamma$), (n,αn), (n,d), (n,t), (n,^{3}He), and (n,γ), as well as the spectra of emitted neutrons, protons, alpha particles, and gamma rays. The precompound process was included above 5 MeV in addition to the compound process. For the inelastic scattering, the contribution of the direct interaction was calculated with DWBA.

h. Calculated Neutron-Induced Cross Sections for Ni-58,60 from 1 to 20 MeV and Comparisons with Experiments[3] (D. M. Hetrick, C. Y. Fu, and D. C. Larson)

Nuclear model codes were used to compute cross sections for neutron-induced reactions on both ^{58}Ni and ^{60}Ni for incident energies from 1 to 20 MeV. The input parameters for the model codes were determined through analysis of experimental data in this energy region. Discussion of the models used, the input data, the resulting calculations, extensive comparisons to measured data, and comparisons to the Evaluated Nuclear Data File (ENDF/B-V) for Ni (MAT 1328) are included in this report.

i. Resonance Parameter Analysis with SAMMY[4] (N. M. Larson and F. G. Perey)

Analysis of resonance neutron cross-section data requires the use of sophisticated techniques to describe correctly all aspects of the experimental situation. Not only must the cross sections be calculated properly, but also Doppler- and resolution-broadening effects must be incorporated correctly, backgrounds and normalizations must be included as needed, and methods must be designed for simultaneous analysis of different data sets. The computer code SAMMY has evolved over a period of years to meet these needs. SAMMY uses the Reich-Moore formalism for the generation of theoretical cross sections, and Bayes' method as the fitting procedure. The 1985 version of SAMMY was described at the Santa Fe Conference; what will be described here are primarily innovations subsequent to that conference.

---

[1]ORNL/TM-10381 (May 1987).
[2]Visitor on assignment from Japan Atomic Energy Research Institute, Japan.
[3]ORNL/TM-10219 (June 1987).
[4]To be published in Proceedings of the International Conference on Nuclear Data for Science and Technology, Mito, Japan, May 30--June 3, 1988.

Doppler broadening is simulated either by numerical integration using a Gaussian kernel (original method), or by rigorous solution of the partial differential equation. This new method, based on work by L. Leal and R. Hwang at Argonne National Laboratory, permits evaluation of Doppler-broadened cross sections near zero energy as well as at higher energies. Modifications have been introduced into the original method of Doppler broadening as well, in order to more accurately represent the Doppler-broadened cross sections for nearly all data sets, including those for which the data points are widely spaced in energy.

Resolution broadening effects are included either approximately with the use of Gaussian and/or exponential kernels in the integral equation (original method), or through the use of a more realistic kernel in which the effects of each experimental contribution are included explicitly. Though this new method of resolution broadening was developed to represent faithfully the experimental situation at ORELA, it is sufficiently general that it should also be applicable to data from other facilities.

SAMMY is currently available on VAX, Floating-Point-System Array Processor, and IBM computers. A detailed user's guide provides thorough documentation for researchers using the code.

j. R-Matrix Analyses of the U-235 and Pu-239 Neutron Cross Sections[1] (H. Derrien,[2] G. de Saussure, L. C. Leal, R. B. Perez, and N. M. Larson)

The resonance analysis code SAMMY was used to perform consistent resonance analyses of several ^{235}U and ^{239}Pu neutron fission and capture cross section and transmission measurements, up to 100 eV for ^{235}U and up to 1 keV for ^{239}Pu.

The program SAMMY uses the multilevel R-matrix Reich-Moore formalism and leads to a physically sound representation of the neutron cross sections in the resonance region. The Bayesian approach, which includes the direct introduction of experimental uncertainties on sample thicknesses, broadening parameters, etc., allows the successive incorporation of new data in a consistent manner. The option to search on sample thicknesses, effective sample temperature, and the parameters of the instrumental resolution function all consistent with predetermined uncertainty limits, leads to realistic parameter uncertainties and covariance matrices.

The data analyzed include recent high-resolution transmission measurements of Harvey et al., done on a flight path of 80 meters and with samples cooled to liquid nitrogen temperature, and recent high-precision

---

[1]To be published in Proceedings of the International Conference on Nuclear Data for Science and Technology, Mito, Japan, May 30--June 3, 1988.

[2]Commissariat a l'Energie Atomique, Centre d'Etudes Nucleaires de Cadarache, Boite Postale No. 1, 13115, Saint-Paul-Lez-Durance, France.

measurements of the fission cross sections by Weston and Todd and Gwin et al. Older measurements were also included in the analysis, particularly the liquid nitrogen fission cross-section measurements of Blons, and for ^{235}U the spin separated data obtained by Moore et al. from a measurement by Keyworth et al. The resonance parameters for both isotopes will be submitted for the ENDF/B-VI and JEF evaluations.

k. R-Matrix Analysis of the U-235 Neutron Sections[1] (L. C. Leal, G. de Saussure, and R. B. Perez)

The ENDF/B-V representation of the ^{235}U neutron cross sections in the resolved resonance region is unsatisfactory; below 1 eV the cross sections are given by "smooth files" (file 3) rather than by resonance parameters; above 1 eV the single-level formalism used by ENDF/B-V necessitates a structured file 3 contribution consisting of more than 1300 energy points; furthermore, information on level-spins has not been included. Indeed, the ENDF/B-V ^{235}U resonance region is based on an analysis done in 1970 for ENDF/B-III and therefore does not include the results of high quality measurements done in the past 18 years. The present paper presents the result of an R-matrix multilevel analysis of recent measurements as well as older data. The analysis also extends the resolved resonance region from its ENDF/B-V upper limit of 81 eV to 110 eV.

l. Some Notes on the Calculation of Energy-Angle Correlated Distributions with TNG and Their Representation in File 6 Formats[2] (D. C. Larson, C. Y. Fu, and D. M. Hetrick)

The model code TNG has been extensively used in evaluation work of structural materials for ENDF/B-VI performed at Oak Ridge National Laboratory. A new aspect of ENDF/B-VI is the use of File 6 formats for energy-angle correlated data. Such data are generally calculated, anchored by experimental data. In this informal note we outline how the TNG results are calculated and entered in the File 6 formats.

---

[1]To be presented at the Summer American Nuclear Society Meeting, San Diego, CA, June 12-16, 1988.

[2]Proceedings of the IAEA Specialists' Meeting on the International Nuclear Data Library for Fusion Reactor Technology, Vienna, Austria, November 16-18, 1987.

2. ENDF/B Related Work

a. Neutron Standard Reference Data[1] (R. W. Peelle and H. Conde[2])

The neutron reference standards are reviewed with emphasis on proposals for ENDF/B-VI, activation cross sections useful in verification of neutron spectra, and standards for neutron energies larger than 20 MeV.

The proposed ENDF/B-VI standard cross sections were generated by a committee of the U.S. Cross Section Evaluation Working Group consisting of A. Carlson, Chairman, G. Hale, W. Poenitz, and R. Peelle. Values are proposed for $^{12}C(n,n)$, $^{3}He(n,p)$, and $^{1}H(n,n)$, but the emphasis here is on the joint evaluation used to determine the smooth cross section values for $^{6}Li(n,\alpha)$, $^{10}B(n,\alpha_0)$, $^{10}B(n,\alpha_1)$, $^{197}Au(n,\gamma)$, and $^{235}U(n,f)$ along with the important cross sections $^{238}U(n,\gamma)$, $^{238}U(n,f)$, and $^{239}Pu(n,f)$. The goals were to correctly apply all types of absolute and ratio data while taking full advantage of the R-matrix representation for the light-element standards. The Poenitz simultaneous least-squares fitting system was applied to the body of data that are independent of those data sets used in the R-matrix fits. The 2.2-km/s results of E. J. Axton were included with the experimental pointwise data. The outputs of these studies, including their full covariance matrices, were combined in a single least-squares adjustment. The results have received review comments that the fission cross sections seem smaller than expected, that some of the input values were inconsistent with the data preferred in new parameterizations of the ^{235}U and ^{239}Pu resonance cross sections, and that output uncertainties seem too small.

Energy-dependent activation cross sections have received wide application in "neutron dosimetry" studies designed to determine or verify the neutron spectral intensity at points of interest to material activation or radiation damage. These cross sections are often measured as ratios to each other, so it is vital that the ad hoc activation standards, such as the $^{27}Al(n,\alpha)$ reaction, be consistent with the traditional cross sections standards.

Neutrons with energies higher than 20 MeV are used, so cross section standards are considered that may be useful in the extended energy range.

---

[1]To be published in Proceedings of the International Conference on Nuclear Data for Science and Technology, Mito, Japan, May 30-June 3, 1988.
[2]Uppsala University, Uppsala, Sweden.

b. Description of Evaluation of Cr-50,52,53,54 Performed for ENDF/B-VI[1] (D. C. Larson, D. M. Hetrick, and C. Y. Fu)

Isotopic evaluations for ^{50,52,53,54}Cr performed for ENDF/B-VI are briefly reviewed. The evaluations are based on analysis of experimental data and results of model calculations which reproduce the experimental data. Evaluated data are given for neutron induced reaction cross sections, angular and energy distributions, and for gamma-ray production cross sections associated with the reactions. File 6 formats are used to represent energy-angle correlated data and recoil spectra. Uncertainty files are included for the major cross sections. Detailed evaluations are given for ^{52,53}Cr, and results of calculations for reactions with large cross sections are used for evaluation of the minor isotopes.

c. Description of Evaluation of Fe-54,56,57,58 Performed for ENDF/B-VI[1] (D. C. Larson, C. Y. Fu, and D. M. Hetrick)

Isotopic evaluations for ^{54,56,57,58}Fe performed for ENDF/B-VI are briefly reviewed. The evaluations are based on analysis of experimental data and results of model calculations which reproduce the experimental data. Evaluated data are given for neutron induced reaction cross sections, angular and energy distributions, and for gamma-ray production cross sections associated with the reactions. File 6 formats are used to represent energy-angle correlated data and recoil spectra. Uncertainty files are included for the major cross sections. A detailed evaluation is given for ^{56}Fe and results of calculations for the major reactions are used for evaluations of the minor isotopes, with particular attention paid to inelastic scattering to the low-lying levels in ^{57}Fe.

d. Description of Evaluation of Ni-58,60,61,62,64 Performed for ENDF/B-VI[1] (D. C. Larson, D. M. Hetrick, and C. Y. Fu)

Isotopic evaluations for ^{58,60,61,62,64}Ni performed for ENDF/B-VI are briefly reviewed. The evaluations are based on analysis of experimental data and results of model calculations which reproduce the experimental data. Evaluated data are given for neutron induced reaction cross sections, angular and energy distributions, and for gamma-ray production cross sections associated with the reactions. File 6 formats are used to represent energy-angle correlated data and recoil spectra. Uncertainty files are included for the major cross sections. Detailed evaluations are given for ^{58,60}Ni, and results of calculations for the major reactions are used for evaluations of the minor isotopes.

---

[1]Proceedings of the IAEA Specialists' Meeting on the International Nuclear Data Library for Fusion Reactor Technology, Vienna, Austria, November 16-18, 1987.

e. Description of Evaluation for Cu-63,65 for ENDF/B-VI[1] (D. C. Larson, D. M. Hetrick, and C. Y. Fu)

Isotopic evaluations for ^{63,65}Cu performed for ENDF/B-VI are briefly reviewed. The evaluations are based on analysis of experimental data and results of model calculations which reproduce the experimental data. Evaluated data are given for neutron-induced reaction cross sections, angular and energy distributions, and for gamma-ray production cross sections associated with the reactions. File 6 formats are used to represent energy-angle correlated data and recoil spectra. Uncertainty files are included for the major cross sections. Full evaluations are given for ^{63,65}Cu.

f. Description of Evaluation of nat-Pb Performed for ENDF/B-VI[1] (D. C. Larson and C. Y. Fu)

An evaluation of data for neutron induced reactions on natural lead was performed for ENDF/B-VI and is briefly reviewed. The evaluation is based on experimental data and results of model calculations which reproduce the experimental data. Evaluated data are given for neutron induced reaction cross sections, angular and energy distributions, and for gamma-ray production cross sections associated with the reactions. File 6 formats are used to represent energy-angle correlated data. Uncertainty files are included for the major cross sections. Much of the present evaluation is taken over from ENDF/B-IV and ENDF/B-V; emphasis is placed on updates for ENDF/B-VI.

g. Evaluation of the Neutron Cross Sections for Pu-240[2] (L. W. Weston and E. D. Arthur)

The present evaluation is proposed to supersede the ENDF/B-V, Revision 2 file for ^{240}Pu by L. W. Weston et al., dated September 1978. In this work, resonance parameters, cross sections, energy distributions, and angular distributions have been modified. These changes are outlined in detail and appropriate references included.

---

[1]Proceedings of the IAEA Specialists' Meeting on the International Nuclear Data Library for Fusion Reactor Technology, Vienna, Austria, November 16-18, 1987.

[2]ORNL/TM-10386 (ENDF-343) (April 1987).

OHIO UNIVERSITY

A. MEASUREMENTS

1. Proton and Neutron Transitions Densities in ^{6,7}Li from Low Energy Neutron and Proton Scattering.*[1] (L.F. Hansen,** J. Rapaport, X. Wang, F.A. Barrios, F. Petrovich,*** A.W. Carpenter*** and J. Threapleton***)

New elastic and inelastic neutron scattering data for ^{6,7}Li taken at 24.0 MeV have been analyzed in connection with existing proton scattering data for these targets at 24.4 MeV. The new data allows us to infer that $\rho_n \approx \rho_p$ in ^{6}Li and ^{7}Li in contrast with the results $\rho_n \approx (N\backslash Z)\rho_p$ deduced from earlier proton and electron work.

2. First (n,p) Measurements with the Indiana University Cyclotron Facility.†[2] (D. Pacanic,†† K. Wang,†† C.J. Martoff,†† S.S. Hanna,†† R.C. Byrd,††† C.C. Foster,††† D.L. Friesel††† and J. Rapaport)

A new monochromatic neutron–beam facility has been set up at the Indiana University Cyclotron Facility, primarily for (n,p) reaction measurements at intermediate energies (100–200 MeV). Reported are the experimental layout of the facility and preliminary results of the first measurements: ^{6}Li(n,p)^{6}He cross sections at six angles ranging from $\Theta_{cm} = 0$–$22°$, with $E_n = 118$ MeV (laboratory). Good agreement is found between the measured $\sigma(0°)$ and the cross sections measured for the mirror reaction

---

* Work supported by U.S. Department of Energy under contract number W–7405–ENG–48 and by the National Science Foundation under Grant PHY–8507137.

** Present Address: Lawrence Livermore National Laboratory, Livermore, CA 94550.

*** Present Address: Florida State University, Tallahassee, FL 32306.

† Work supported by the National Science Foundation.

†† Present Address: Stanford University, Stanford, CA 94305.

††† Present Address: Indiana University Cyclotron Facility, Bloomington, IN 47405.

1 Submitted for publication in Phys. Rev. C.

2 Published in Can. J. Phys. 65, 687 (1987).

^{6}Li(p,n) at 120 and 144 MeV. Results of a distorted wave calculation, while slightly lower, are consistent with the preliminary experimental 0° cross section.

3. Inelastic Scattering of Neutrons to Unbound Levels of ^{13}C.* (R. Conatser, R.O. Lane, E.T. Sadowski and H.D. Knox)

In the investigation of the high–lying levels of ^{14}C, deep inelastic scattering is being studied to the first nine levels of ^{13}C unbound to neutron emission. Initial measurements at 9.26 MeV and 11.15 MeV confirmed our earlier observations[1] via 2n sequential decay of ^{14}C, that in this region the 7.457 MeV level is strongly populated, the 6.86 MeV level may be weakly populated, but evidence for other unbound levels appear from these preliminary data to be weak or not resolved from contaminants as yet.

4. Neutron Scattering Cross Sections and Partial Kerma Values for Oxygen, Nitrogen and Calcium at $18 < E_n < 60$ MeV.**[2] (M.S. Islam,*** R.W. Finlay, J.S. Petler,† J. Rapaport, R. Alarcon,†† and J. Wierzbicki)

Recent measurements of differential elastic and inelastic neutron scattering from oxygen, nitrogen and calcium at $18 < E_n < 26$ MeV are presented and analyzed in terms of the optical model. These data, together with earlier measurements of scattering and total cross sections, are used to construct model potentials that may be used to calculate various quantities of interest in neutron dosimetry in an energy region (20–60 MeV) where very little cross section data are available. The heavy–ion–recoil contribution to kerma is obtained directly from the data at each energy. The value of proton inelastic scattering data for validating potential models at high energy is discussed.

5. Neutron Scattering and Partial Kerma Factors for Carbon, Nitrogen, Oxygen and Calcium—A Final Report.**[3] (R.W. Finlay)

Recent measurements of differential elastic and inelastic neutron scattering from carbon, nitrogen, oxygen and calcium at $18 < E_n < 26$ MeV are presented and

---

* Work supported by U.S. Department of Energy.

** Work supported by PHS grant number CA–25193 awarded by the National Cancer Institute, Department of Health and Human Services.

*** Present address: Physics Department, Ohio State University, Columbus, OH 43210.

† Present address: British Petroleum Research Centre, Sunbury–on–Thames, Middlesex, UK.

†† Present address: University of Illinois, Champaign, IL 61821.

1 D.A. Resler, R.O. Lane and H.D. Knox, Phys. Rev. C35, 855 (1987).

2 Accepted for publication in Physics in Medicine and Biology.

3 Proceedings of the Sixth Symposium on Neutron Dosimetry, Munich, Oct. 1987.

analyzed in terms of the optical model. These data, together with earlier measurements of elastic scattering, total and reaction cross sections, are used to construct model potentials. These models may be used to calculate various quantities of interest in neutron transport and dosimetry. Since the energy region of interest in neutron dosimetry extends to at least 60 MeV, potentials should be useful up to that energy. However, very little neutron scattering data are available above 26 MeV, and extrapolation of the models over a wide energy range could be hazardous. Verification of the potential models for carbon and oxygen at E > 30 MeV is obtained by analyzing proton elastic scattering data in a consistent manner.

The heavy–ion–recoil contribution to kerma is obtained directly from the data from two cases: 1) elastic scattering and 2) inelastic scattering to final states that do not decay into charged particles. Since these quantities can be calculated with the model potentials, another test of the models is provided. Inelastic proton scattering is again useful in evaluating the predictions of the models.

Inelastic scattering to the 9.63 MeV state in ^{12}C is particularly interesting. This state decays into three alpha particles over 99% of the time and provides a significant contribution to total kerma. Cross sections for population of this state were measured in the present experiments. Cross sections for decay have been measured in emulsion experiments. Both types of measurement are in good agreement with the predictions of the present model.

6. Energy Levels of ^{24}Mg.* (C.E. Brient, P. Egun,** S.M. Grimes, S.K. Saraf and H. Satyanarayana***)

States in ^{24}Mg were excited through the $^{23}Na(d,n)$ reaction to study the suitability of (d,n) reactions for level counting.[1] Because many levels in ^{24}Mg are well known, the comparision of our results with literature will reveal to what extent the result of (d,n) reactions can be used in level counting. The study was conducted between 2.5 and 9.0 MeV incident energy and excited levels to 16.0 MeV in ^{24}Mg. The results using the Ohio University Beam Swinger and the neutron TOF method will be compared to literature.

7. Measurement of Spectra from the $^{59}Co(p,n)^{59}Ni$ Reaction at E_p = 6, 7 and 8 MeV.* (R.S. Pedroni, C.E. Brient, P.M. Egun,** S.M. Grimes, V. Mishra and S.K. Saraf)

Spectra for the $^{59}Co(p,n)^{59}Ni$ reaction have been measured at the bombarding energies 6, 7 and 8 MeV. The measurements utilized the Ohio University tandem and beam swinger facility. The measurements have been compared with Hauser–Feshbach calculations for both the resolved states and the continuum to allow level density information to be deduced.

* Work supported by the U.S. Department of Energy.

** Present address: Institut für Mittelenergiephysik, Zurich, Switzerland.

*** Present address: 1221 Cambia Dr., Apt. 1218, Schaumburg, IL 60193.

[1] H. Satyanarayana, M. Ahmed, C.E. Brient, P.M. Egun, S.L. Graham, S.M. Grimes and S.K. Saraf, Phys. Rev. C32, 394 (1985).

8. Study of Proton and Alpha Emission from Isotopes of Iron Bombarded with 8 MeV Neutrons.* (S.K. Saraf, C.E. Brient, P.M. Egun,** S.M. Grimes, M.S. Islam,*** R.S. Pedroni and H. Satyanarayana†)

We have measured emission cross sections for ^{54}Fe and ^{56}Fe for (n,p) and (n,α) reactions induced by 8 MeV neutrons. The measurements were performed at the Ohio University accelerator facility with a new large acceptance charged particle time–of–flight spectrometer.[1] Preliminary results will be presented to show how well the measured cross sections agree when compared with Hauser–Feshbach calculations.

9. Cross Sections and Spectra for (n,xp) and (n,xα) Reactions on ^{58}Ni and ^{60}Ni at Energies of 9.4 and 11 MeV.*[2] (S.L. Graham, M. Ahmad,†† S.M. Grimes, H. Satyanarayana† and S.K. Saraf)

Cross sections and spectra for (n,xp) and (n,xα) reactions on ^{58}Ni and ^{60}Ni at energies of 9.4 and 11 MeV and for ^{58}Ni at 8 MeV have been measured. This energy range spans the threshold for the (n,n'p) reaction. Based on comparison of Hauser–Feshbach calculations with the measured spectra, this reaction provides a large fraction of the proton spectrum at 11 MeV for ^{58}Ni. Both (n,xp) and (n,xα) processes appear to be due largely to compound nuclear processes. Comparison of the measurements obtained here and those previously published at 15 MeV with calculations allows us to infer information about the nuclear level densities. Cross sections for (n,d) reactions are sufficiently small that only upper limits can be derived from them.

---

* Supported in part by the U.S. Department of Energy.

** Present address: Institut für Mittelenergiephysik, Zurich, Switzerland.

*** Present address: Physics Dept., Ohio State University, Columbus, OH 43210.

† Present address: 1221 Cambia Dr., Apt. 1218, Schaumburg, IL 60193.

†† Present address: Memorial Sloan–Kettering Cancer Inst., New York, NY 10021.

1 M. Ahmad, S.L. Graham, S.M. Grimes, R. Longfellow, H. Satyanarayana and G. Randers–Pehrson, Nucl. Inst. Meth. 228, 349 (1985).

2 Published in Nucl. Sci. and Eng. 95, 60 (1987).

10. Microscopic Distorted–Wave Approximation Study of Low–Energy Nucleon Scattering from ^{89}Y.*[1] (S. Mellema,** J.S. Petler,*** R.W. Finlay, F.S. Dietrich,† J.A. Carr†† and F. Petrovich††)

New differential cross section data for inelastic neutron scattering to the first three excited states of ^{89}Y at E_n = 11 MeV are studied using a microscopic folding model and three energy– and density–dependent effective interactions. Results are also presented for the corresponding transitions in inelastic proton scattering at 14.7, 24.5 and 61.2 MeV. Transition densities were obtained from a combination of available inelastic electron scattering data and theoretical considerations. The calculated angular distributions provide a reasonable description of the experimental data for the predominantly quadrupole ($\Delta J = 2$), $1/2^- \rightarrow 3/2^-$ (E_x = 1.509 MeV) and $1/2^- \rightarrow 5/2^-$ (E_x = 1.745 MeV) transitions in the target. It is shown that the neutron scattering data for these two transitions are sensitive to the shape differences in the transition densities suggested by theory and electron scattering. The theoretical results for the predominantly $\Delta J = 5$, $1/2^- \rightarrow 9/2^+$ (E_x = 0.909 MeV) transition significantly underestimate the proton and neutron scattering cross sections at $E_p < 25$ MeV and E_n = 11 MeV but provide a reasonable description of the proton scattering data for this transition at E_p = 61.2 MeV.

11. Study of Neutrons Scattering from Isotopes of Zirconium.††† (Y. Wang, J. Rapaport, R. Finlay, D. Wang,†††† R.K. Das and J. Wierzbicki)

Neutron elastic and inelastic scattering cross sections have been measured from ^{91,92,94}Zr at 8.0 MeV and ^{94}Zr at 24.0 MeV over an angular range of 15 to 157 degrees

---

* This work was supported by the U.S. National Science Foundation under Grants No. PHY–8414810, PHY–8108456 and PHY–8122131, and by the U.S. Department of Energy under Contract No. W–7405–ENG–48 and Cooperative Agreement No. DE–FC05–85ER250000.

** Present address: Physics Dept., Gustavus Adolphus College, St. Peter, MN 56082.

*** Present address: British Petroleum Research Centre, Sunbury–on–Thames, Middlesex, U.K.

† Present address: Lawrence Livermore National Laboratory, Livermore, CA 94550.

†† Present address: Florida State University, Tallahassee, FL 32306.

††† Work supported by NSF Grant PHY–8507137.

†††† Present address: Physics Dept., University of Kentucky, Lexington, KY 40506.

[1] Published in Phys. Rev. C36, 577 (1987).

using the Ohio University time–of–flight facility. These data, along with previously measured 8.0 and 24.0 MeV data from ^{90}Zr, are analyzed using three different approaches to the optical model potential: Woods–Saxon parameterization, model independent analysis and microscopic calculations. The results using Woods–Saxon form factors for transitions are compared with those form factors derived from a model independent analysis.

12. Energy Dependence of Neutron Scattering from ^{209}Bi in the Energy Range of 1.5 to 60.0 MeV from the Dispersion Relation Constraint.* (R.K. Das, R. Finlay, D. Wang,** Y. Wang and J. Wierzbicki)

Elastic neutron scattering from ^{209}Bi have been measured recently at 20.0 and 24.0 MeV over an angular range of 10 to 160 degrees using the Ohio University time–of–flight facility to cover a range of differential cross sections in the energy domain 1.5 to 24.0 MeV. Total cross sections in the domain 1.0 to 60.0 MeV have recently been measured at ORNL. All of these data have been used aiming to study the real part of the n+^{209}Bi mean field which is the sum of a Hartree–Fock term plus a dispersive component determined from the imaginary part of the Optical Model Potential by making use of the dispersion relation which connects these two quantities.

13. Preliminary Measurement of the ^{235}U(n,f) Cross Section up to 750 MeV.***[1] (J. Rapaport, J. Ullmann,† R.O. Nelson,† S. Seestrom–Morris,† S.A. Wender† and R.C. Haight†)

The recently commissioned Los Alamos National Laboratory high energy white neutron source was used to measure the neutron fission cross section of ^{235}U in the energy range from 0.6 to 750 MeV. The shape of the cross section from 0.6 to 20 MeV agrees well with previously reported data. Absolute values for the ^{235}U(n,f) cross section from 20 MeV to 750 MeV were obtained by normalizing the measured shape of the cross section to data in the 10 to 20 MeV range.

---

* Work supported by NSF Grant PHY–8507137.

** Present address: Physics Dept., University of Kentucky, Lexington, KY 40506.

*** Work supported by U.S. Department of Energy.

† Present address: Los Alamos National Laboratory, Los Alamos, NM 87545.

[1] Published in Los Alamos National Laboratory Report LA–11078–MS.

B. MODEL CALCULATIONS AND ANALYSES

1. The Nuclear Shell Model Code CRUNCHER.*[1] (D.A. Resler** and S.M. Grimes)

A new nuclear shell model code, patterned after the code VLADIMIR, has been developed. This new code employs the techniques of an uncoupled basis and the Lanczos process. Improvements in the new code allow it to handle much larger problems than previous codes and to perform them more efficiently.

2. Shell Model Calculations for the Lithium and Carbon Isotopes.*[2] (D.A. Resler**)

Shell model calculations are performed for the lithium isotopes ^{5,6,7,8}Li, the carbon isotopes ^{13,14}C, and for some of the neighboring nuclei: ^{4}He, ^{8}Be and ^{13}N. Normal parity states are calculated in a full $0\hbar\omega$ space and non–normal parity states in a full $1\hbar\omega$ space. Spurious center–of–mass states are completely removed. Five different two–body interactions are obtained. In each case, both parities are calculated from the same interaction. Results of the present work are compared with previous works obtained from the literature.

3. Shell Model Calculations for ^{9}Be, ^{10}Be, ^{10}B and ^{11}B.* (H.D. Knox and D.A. Resler**)

Model calculations for ^{9}Be, ^{10}Be, ^{10}B and ^{11}B for both normal and non–normal parity states have been carried out using the shell model code CRUNCHER. The nucleon–nucleon potential used in these calculations is given by

$$V(r) = f(r)\,[V_0 + V_\sigma\,\vec{\sigma}\cdot\vec{\sigma} + V_\tau\,\vec{\tau}\cdot\vec{\tau} + V_{\sigma\tau}\,\vec{\sigma}\cdot\vec{\sigma}\;\vec{\tau}\cdot\vec{\tau}]$$

with f(r) a Yukawa form factor of range R_0,

$$f(r) = (\exp(-r/R_0))/(r/R_0)\,.$$

---

* Work supported by U.S. Department of Energy.

** Present address: Lawrence Livermore National Laboratory, Livermore, CA 94550.

1 Submitted for publication in Computers in Physics.

2 Submitted for publication in Phys. Rev. C.

The parameters V_0, V_σ, V_τ, $V_{\sigma\tau}$, R_0 and the single particle energies, $E_{1p_{3/2}}$, $E_{1p_{1/2}}$, $E_{1d_{5/2}}$, $E_{2s_{1/2}}$ and $E_{1d_{3/2}}$, were determined by fitting energies of known states in these four nuclei. Comparisons of the predicted structure for these nuclei with previous theoretical studies are presently underway. The results of the present beryllium calculations will be used in a combined shell–model R–matrix calculation[1] of cross sections of reactions leading to the ^{10}Be system. This work is part of a collaborative study of the ^{9}Be(n,2n) reaction as developed at a recent coordination meeting of the Office of Basic Energy Sciences Program to Meet High Priority Nuclear Data Needs of the Office of Fusion Energy.[2] The boron calculations are part of a comprehensive study of the ^{11}B system, including extensive measurements of n+^{10}B cross sections and combined shell–model and R–matrix analysis of those data.

4. R–Matrix Analysis of ^{11}B Above the Neutron Separation Energy.* (E.T. Sadowski, H.D. Knox and R.O. Lane)

Multiple scattering corrections to recent elastic and inelastic neutron scattering data[3] for 3 MeV $\leq E_n \leq$ 12 MeV have been completed. An eleven– channel R–matrix analysis of the higher energy–level structure of ^{11}B has begun. The eleven channels are (n,n_0), (n,n_1), (n,n_2), (n,n_3), (n,n_4), (n,n_5), (n,α_0), (n,α_1), (n,t_0), (n,p_0), (n,d_0). All available data for incident neutron energies from thermal to 14 MeV., i.e. 11.5 MeV $\leq E_x \leq$ 24 MeV, has been included in the analysis.

5. Modifications to the Shell Model Code, CRUNCHER.* (H.D. Knox)

Work is currently underway to add subroutines to the shell model code CRUNCHER to allow the computation of spectroscopic amplitudes for decay of a compound system by n, p, d, t, α or ^{5}He emission. Codes for n, d and t emission are completed at this time. These subroutines will be used to obtain R–matrix input parameters from the shell model calculation wave functions for calculations of reaction cross sections for the p–shell nuclei.

---

* Work supported by U.S. Department of Energy.

1 H.D. Knox, D.A. Resler and R.O. Lane, Nucl. Phys. A466, 245 (1987).

2 D.L. Smith and H.D. Knox, "Office of Basic Energy Science Program to Meet High Priority Nuclear Data Needs of the Office of Fusion Energy, 1986 Review", Argonne National Laboratory, Sept. 1986, Ohio University Report DOE/ER/02490–4.

3 E.T. Sadowski, H.D. Knox, D.A. Resler and R.O. Lane, Bull. Amer. Phys. Soc. 32, 1061 (1987).

6. Spectral Distribution Calculations of the Level Density of ^{20}Ne.*[1] (B. Strohmaier** and S.M. Grimes)

A recent paper compared moment method and Lanczos method calculations of the level density of ^{20}Ne. The present work extends this comparison to include a new type of Lanczos expansion. This expansion procedure shares the advantage of the traditional Lanczos method of a positive definite level density, but unlike the latter, may be used in an essentially infinite basis. Calculations utilizing dsdf and ppdsd bases have been compared with experimental values for the level density, parity ratio and spin cutoff parameters to determine the appropriateness of the input parameters and the model, while calculations in a dsd basis are compared with exact calculated results to test the accuracy of representation provided by the expansion technique.

7. Spectral Distribution Calculations of the Level Density of ^{24}Mg.*[2] (B. Strohmaier,** S.M. Grimes and H. Satyanarayana***)

Spectral distribution calculations of the level density of ^{24}Mg are compared with experimental values for the level density of this nucleus as well as with Fermi gas calculations. Particular attention is paid to the technique used for the expansion. Traditional techniques which have utilized knowledge of the third and fourth moments of the Hamiltonian have yielded a distribution function that is not positive definite. Two alternative expansion methods are examined. One is found to be unacceptable because of the fact it does not yield a unique fit, but the second appears to be quite useful. Not only is the resultant expansion positive definite, but it appears capable in principle of giving a more detailed representation of the level density than the traditional method. Results of the calculation for two different basis sizes are compared.

8. On the Quenching of Gamow–Teller Strength.†[3] (J. Rapaport)

The (p,n) reaction at intermediate energies has been used to measure differential cross sections in light nuclei to final states characterized with a $\Delta J^{\pi} = 1^{+}$ transfer (Gamow–Teller (GT) states). Experimental ft values for allowed beta–decay transitions in these nuclei are used to normalize the strength of the GT transitions in units

---

* Work supported in part by the U.S. Department of Energy.

** Present address: Institut für Radiumforschung und Kernphysik der Universitat Wien, Boltzmanngasse 3, A–1090 Vienna, AUSTRIA.

*** Present address: 1221 Cambia Dr., Apt. 1218, Schaumburg, IL 60193.

† Work supported by National Science Foundation under Grant PHY–8507137.

1 Accepted for publication in Zeitschrift für Physik.

2 Published in Phys. Rev. C36, 1604 (1987).

3 Published in Can. J. Phys. 65, 574 (1987).

of B(GT). This experimental GT strength is compared with predicted shell–model strength. For p–shell nuclei, the calculated excitation energies of the GT strength using Cohen and Kurath wave functions are in general agreement with the empirical GT distribution. Up to an excitation energy of about 20 MeV, the total experimental and calculated GT strengths are used to obtain the quenching factor, $Q_F = \Sigma B(GT)_{exp}/\Sigma B(GT)_{theor}$. It is found that Q_F decreases as the shell gets filled up. The lowest value seems to occur for single–hole nuclei. This decrease may be explained by configuration mixing not specifically included in the calculations.

9. The Fermi Energy Anomaly in the Nucleon–Nucleus Potential.*[1] (R.W. Finlay)

Careful comparisons of the parameters of the nucleon–nucleus optical potential at low energy (E < 10 MeV) with those at higher energies (E > 20 MeV) have revealed discrepancies. Commonly used "global optical models" tend to fail in one energy region or the other. Improved agreement with the data can be restored in phenomenological models in which certain geometrical parameters of the model are allowed to depend explicitly on neutron energy. The origin of this effect in the n+^{208}Pb system has been explained in terms of the dispersion correction to the real part of the standard local optical potential. In dispersion theory, the magnitude of this correction is obtained from the energy dependence of the phenomenological imaginary potential. In the present work, we re–examine the phenomenological parameters for n and p on ^{208}Pb. The dispersion theory explanation of the low energy behavior of the neutron potential is supported by the present analysis, but no similar effect is observed for protons in the range of available data (E_p > 9 MeV). The present analyses suggest that the Fermi energy anomaly for the p+^{208}Pb potential is located at energies well below the Coulomb barrier.

10. Evidence for Dispersion Relation Corrections in Inelastic Nucleon Scattering to the 3^- State in ^{208}Pb.*[2] (T.S. Cheema** and R.W. Finlay)

Inelastic scattering of 5–11 MeV neutrons to the 3^-_1 state in ^{208}Pb is reanalyzed in the distorted wave Born approximation using phenomenological potentials and form factors that explicitly reflect the "threshold anomaly" effects observed in the elastic scattering channel. A previously reported energy dependence of the deformation length δ_3 is largely removed by this analysis. We conclude that dispersion corrections to the one–channel optical potentials are important in the off–diagonal elements of the potential matrix.

---

* Work supported by National Science Foundation Grant Number PHY–8507137.

** Present address: Punjab University, Chandigarh, INDIA 160014.

1 Proc. International Conference on Neutron Physics, Kiev, Sept. 1987.

2 Published in Phys. Rev. C, Rapid Communications, Feb. 1988.

C. TECHNIQUES AND FACILITIES

1. Application of the Multiple Scattering Code MACHO to Account for Several Experimental Difficulties in Deep Inelastic Neutron Scattering Data.*[1] (D.A. Resler** and E.T. Sadowski)

A new multiple scattering code MACHO has been developed. In addition to multiple scattering corrections, accurate simulations of the neutron scattering process allow for reliable corrections to be made for scattering from the source continuum and source contaminants, for overlapping inelastic groups, and for slight differences in accelerator beam tuning, even for large samples containing an unknown amount of hydrogen impurity. This new code has been applied to recent elastic and deep inelastic neutron scattering data for $^{13}C+n$ and $^{10}B+n$.

2. Determination of the Light Response of BC–404*** Plastic Scintillator for Protons and Deuterons with Energies Between 1 and 11 MeV.*[1] (S.K. Saraf, C.E. Brient, P.M. Egun,† S.M. Grimes, V. Mishra, and R.S. Pedroni)

The response of BC–404 plastic scintillator is measured up to 11 MeV for protons and up to 8 MeV for deuterons using a time–of–flight spectrometer. It is shown that the response is non–linear in this energy range and can be described very well using a four–term polynomial in energy. Earlier response curves which were extrapolated from high energy data and from interpolation of low energy data at widely separeted energies are nearly linear in the low energy region. A comparison has been made between our new measured data and the existing curves.

---

* Work supported by the U.S. Department of Energy.

** Present address: Lawrence Livermore National Laboratory, Livermore, CA 94550.

*** BC–404 is obtained from Bicron, 12345 Kinsman Road, Newbury, OH 44045.

† Present address: Institut für Mittelenergiephysik, Zurich, Switzerland.

1 Accepted for publication in Nucl. Instr. Meth.

UNIVERSITY OF PENNSYLVANIA

The principal thrust of the work deals with the compilation of the information on the energy levels and on the structure of the nuclei with mass numbers A = 5-20. Approximately 1500 papers are published every year on these nuclei. During 1987 we completed and published evaluations on the "Energy Levels of Light Nuclei. A = 18-20" (Nuclear Physics A475 (1987) 1 → 198). We also prepared preliminary verions of the reviews on A = 5-6 (sent out as preprint 4-87 in August 1987) and A = 7-8 (sent out as preprint 6-87 in November 1987).

In 1987 review papers were also prepared on "Recent Developments in the Light Nuclei" (see Bull. Amer. Phys. Soc. 32 (1987) 1040; and see PPP 2-87) and "Of DHW and the Light Nuclei" (to be published in the Proceedings of the Conference on Interactions and Structures in Nuclei by the (U.K.) Institute of Physics; and see PPP 5-87).

F. Ajzenberg-Selove; with
G. C. Marshall

A. NUCLEAR DATA

1. "A Multiplicity Detector for Accurate Low-Energy Neutron Capture Measurements" (R.C. Block, N.J. Drindak, F. Feiner,* K.W. Seeman,* R.E. Slovacek*)†

Accurate capture cross section data are required in the thermal to epithermal energy range for application to advanced thermal reactors. A high-efficiency gamma-ray multiplicity detector was selected as having the best overall properties to achieve the required accuracy in the terms of low cross section error and good neutron energy resolution. A multiplicity detector, as first reported by Muradyan and co-workers [1], is a highly-efficient 4π gamma-ray detector optically divided into many segments, and the data are recorded as the number of segments detecting capture gamma rays (in coincidence) vs neutron time of flight. Measurement of multiplicity will enable background (low-multiplicity) to be accurately subtracted from capture (medium-multiplicity), will enable capture to be separated from fission (high-multiplicity) and will provide information on resonance spins and parities.

Sodium iodide was selected for this application because of its good gamma-ray energy resolution, reasonable cost and commercial availability. The detector consists of two 10 liter annuli of NaI placed coaxially adjacent to each other, with each annulus optically divided into 8 pie-shaped sections with a photomultiplier coupled to each section. A B-10 annular liner is placed inside the detector to prevent low-energy neutrons scattered by the capture sample from entering the NaI, and a computer-controlled sample changer cycles capture and flux-determination samples into the detector to average out LINAC power fluctuations. The detector is located at the 25m flight station of the RPI LINAC and it is shielded with 15 cm of lead. Both multiplicity 1 through 16 data and total gamma ray energy (deposited in all NaI segments) are recorded simutlaneously by an HP-100 computer as a function of neutron time of flight.

Preliminary measurements with a 5 liter two-section NaI detector have demonstrated that better than 200:1 peak-to-background ratios can be achieved in low-energy resonances and that neither prompt capture nor activation in iodine is a problem below the tens of eV region. Data from the 20 liter detector will be presented.

---

[1] G.V. Muradyan, Yu G. Shchepkin, Yu V. Adamchuk and G.V. Ustroev, Preprint IAE-2634, Kurchatov Institute, 1976.

*Knolls Atomic Power Laboratory operated by the General Electric Co., for the U.S. Department of Energy.

†(Abstract of a paper selected for presentation at the Int'l. Conf. on Nucl. Data for Sci. & Tech., May 30-June 3, 1988, Mito, Japan.)

2. "Measurement of the Neutron-Induced Fission Cross Sections of ^{242}Cm and ^{238}Pu" (B. Alam, R.C. Block, R.E. Slovacek (KAPL) and R.W. Hoff (LLL)†

The neutron-induced fission cross sections of ^{242}Cm and ^{238}Pu have been measured from 0.1 eV to 100 keV using the Rensselaer Intense Neutron Spectrometer. Fission areas and widths were determined for the resolved low-energy resonances of ^{242}Cm and ^{238}Pu. The fission resonance integrals for ^{242}Cm and ^{238}Pu were found respectively to be 12.9 ± 0.7 barn and 15.9 ± 0.6 barn. The gross structure observed in the unresolved energy region of the ^{242}Cm and ^{238}Pu fission cross sections is suggestive of intermediate structure, and is consistent with the second well lying 2 to 3 MeV above the first well. The ENDF/B-V library fission cross section of ^{238}Pu is, in general, not in good agreement with this measurement and a new evaluation is recommended. This is the first reported fission measurement of ^{242}Cm in the 0.1 eV through 100 keV energy range.

†(Abstract of a paper accepted for publication in Nucl. Sci. & Eng.)

A. NEUTRON PHYSICS

1. Helium Generation Cross Sections for Fusion Applications

(D. W. Kneff, B. M. Oliver, and R. P. Skowronski)

Neutron-induced helium generation is a major consideration in the development of materials for fusion reactor environments. Rockwell International is engaged in the measurement of helium production in fusion-energy neutron environments and in other neutron environments used for fusion reactor materials testing. Current emphasis is on the measurement of the cross sections of pure elements and separated isotopes for fast (~8-15 MeV) monoenergetic neutrons, and of helium production rates of pure elements irradiated in mixed-spectrum (comparable fast and thermal neutron flux) fission reactors. Most of this work is performed as a collaborative effort with L. R. Greenwood of Argonne National Laboratory (ANL), and is sponsored by the Department of Energy's Office of Fusion Energy.

The mixed-spectrum reactor experiments included the irradiation of several pure iron samples to fluences of 3×10^{26} to 2×10^{27} neutrons/m^2 in the High Flux Isotope Reactor (HFIR) at Oak Ridge National Laboratory. Helium concentrations generated in these samples were measured by isotope-dilution gas mass spectrometry, and the results compared with predictions made at ANL based on the neutron energy spectra and the ENDF/B-V Gas Production File. The comparisons showed that there is a contribution to the total helium production that increases nonlinearly with fluence at high neutron fluences ($>10^{26}$ neutrons/m^2). This nonlinear contribution is due to a multiple-step reaction process. It is of interest for fusion reactor materials testing as a mechanism to enhance helium production in ferritic materials in mixed-spectrum reactors.

The enhanced helium production mechanism was examined in detail in a joint Rockwell-ANL effort.[1] The enhancement is explainable by the thermal-neutron two-step process $^{54}Fe(n,\gamma)^{55}Fe(n,\alpha)^{52}Cr$, the thermal-plus-fast two-step process $^{56}Fe(n,\gamma)^{57}Fe(n,\alpha)^{54}Cr$, or a combination of both. The thermal two-step process would be the reaction mechanism of interest for producing high helium generation concentrations in mixed-spectrum reactors. A set of secular equations describing the growth and decay of the different iron isotopes was set up and the unknown cross sections for the contributing and competing reaction channels were evaluated by fitting them to the experimental data. The data included both the helium production measurements and post-irradiation iron isotope ratios measured at ANL. The results gave an ^{55}Fe(n,total absorption) cross section for thermal neutrons of 13.2 $\pm$ 2.1 barns. The $^{55}Fe(n,\alpha)$ thermal cross section was evaluated to be 18 $\pm$ 3 mb if an average fast Fe(n,α) cross section is used in the helium production

[1] Greenwood, Graczyk, and Kneff, "New Technique for Enhancing Helium Production in Ferritic Materials," Third Intl. Conf. Fusion Reactor Materials, October 1987, Karlsruhe, F. R. Germany.

calculations. If the fast (n,α) cross sections for the individual iron isotopes are instead calculated using the computer code THRESH2, the thermal ^{55}Fe(n,α) cross section is reduced to 9 $\pm$ 4 mb, and each of the two reaction processes contributes about half of the enhanced helium. Further irradiations are planned using separated iron isotopes in order to further evaluate the ^{55}Fe(n,α) reaction for fusion materials testing applications.

B. RADIOACTIVE DECAY

1. Tritium Half-life Measured by Helium-3 Growth

(B. M. Oliver, Harry Farrar IV, and M. M. Bretscher[1])

Measurements of the half life for tritium decay have been made by a variation of the ^{3}He growth technique.[2] The method involved the measurement of the ^{4}He/^{3}He isotopic ratio in 15 samples of natural lithium metal which had been irradiated in a mixed thermal-fast neutron spectrum in the core of a Triga Mark 1 research reactor. The ^{3}He in the lithium was formed by the decay of tritium generated during the irradiation by the reactions ^{6}Li(n,t)^{4}He and ^{7}Li(n,n't)^{4}He. The tritium half life was determined by the measurement of the helium isotopic ratio in the samples after different decay times following the irradiation.

The results of the isotopic ratio measurements yielded a mean tritium half life of 12.38 $\pm$ 0.03 y. This value is higher than earlier measurements but is consistent within uncertainties with a recent NBS recommendation[3] of 12.43 $\pm$ 0.05 y. Calculations for the average energy of tritium decay,[4] combined with existing measurements of the tritium decay energy emission rate, gave an independent value for the tritium half life of 12.38 $\pm$ 0.04 y. This agrees with the mass spectrometrically determined value. Based on the present results and those of NBS, it appears that the tritium half life is somewhat longer than recommended in current evaluations.[5,6]

---

[1] Argonne National Laboratory.

[2] Oliver, Farrar, and Bretscher, "Tritium Half-Life Measured by Helium-3 Growth," Int. J. Appl. Radiat. Isot. 38, 959 (1987).

[3] Unteweger, Coursey, Schima, and Mann, "Preparation and Calibration of the 1978 National Bureau of Standards Tritiated-Water Standards," Int. J. Appl. Radiat. Isot. 31, 611 (1980).

[4] Oliver, Bretscher, and Farrar, "Mass Spectrometric Determinations of the Absolute Tritium Activities of NBS Tritiated Water Standards", submitted to Int. J. Appl. Radiat. Isot. (1988).

[5] C. M. Lederer and V. S. Shirley (Eds.), Table of Isotopes, 7th Edition, John Wiley, New York, 1978.

[6] M. J. Martin, Nuclear Decay Data for Selected Radionuclides, ORNL-5114, Oak Ridge National Laboratory, Oak Ridge, Tennessee, 1976.

TRIANGLE UNIVERSITIES NUCLEAR LABORATORY

Starting with the present report this year, the review of the TUNL program will reflect the breadth of the entire program as it relates to nuclear data and nuclear models. That is, work of others beyond the neutron scattering group will be included from now on. Furthermore, the rationale behind the individual projects will be outlined in brief statements in order to provide the uninitiated reader with an indication of the significance or purpose of the work. Much of the information given here has been excerpted from the annual report TUNL XXVI which can be obtained by writing Prof. Edward G. Bilpuch, Director of TUNL, Physics Department, Duke University, Durham, NC 27706. In TUNL XXVI many illustrations are given that elaborate on the condensed version given here for the Nuclear Data Committee.

A. FUNDAMENTAL STUDIES WITH NEUTRON BEAMS

1. Brief Overview

(R. L. Walter, C. R. Howell, W. Tornow, H. G. Pfützner, M. L. Roberts, P. D. Felsher, G. Weisel, M. Al Ohali, R. S. Pedroni*, J. P. Delaroche**, I. Slaus+)

During the past year we have focused on several types of fundamental physics problems that can be explored solely or most sensitively by using the unique properties of the neutron. For instance, in this regard we emphasize that the use of neutron beams gives one the most direct measure of the isospin T=0 part of the nucleon-nucleon interaction. Also, the long range Coulomb interaction, which is difficult to take into account exactly and which can mask details of the nuclear interaction, is not a problem in experiments involving neutron beams in both the incoming and outgoing channels. In general, the developments or tests of the nuclear theories in which we are interested concern comparisons to spin-sensitive observables, and most of our experimental program involves measuring quantities for reactions initiated with polarized neutron, proton or deuteron beams.

2. Failures and Sensitivities of Few-Nucleon Calculations and the Analyzing Power for n-d Elastic Scattering

(with J. Lambert, P. Treado, Georgetown University, and Y. Koike, Hosei University)

The traditional theoretical approach to nuclear physics is based on a nonrelativistic Hamiltonian in which the nucleons interact pairwise. It is clear, however, that no two-nucleon-force model adequately describes all

---

* Present address: Dept. of Physics, Ohio University, Athens, Ohio
** Permanent address: Centre d'Etudes de Bruyeres-le-Chatel, France
+ Permanent address: Ruder Boskovic Institute, Zagreb, Yugoslavia

of the fundamental properties of nuclei and nuclear reactions. Such disagreement between calculations and data includes nucleon-deuteron scattering. The three-nucleon force (3NF) has been proposed to explain some or all of the observed discrepancies. In particular, the vector analyzing power $A_y(\theta)$ in neutron-deuteron elastic scattering may be sensitive to the 3NF. Via the coupling of the ^3P NN-states to the ^3P NΔ-states, sizeable 3NF effects are expected.

In order to investigate the sensitivity of $A_y(\theta)$ calculations for n-d elastic scattering to various angular momentum components of the NN-interaction, a separable approximation of the Paris[1] NN-potential, referred[2] to as PEST, was chosen. The calculations compared with experimental data recently obtained at TUNL at E_n=12 MeV. (See Few-Body Systems 2 (1987) 19.) Except for the region at the maximum at $\theta_{c.m.}$ = 125° of $A_y(\theta)$, the PEST calculation reproduces the data impressively well. Successive calculations that individually exclude the $^3P_0$, $^3P_1$, and $^3P_2$ interactions clearly demonstrate that the magnitude of $A_y(\theta)$ near 125° is extremely sensitive to the ^3P interactions.

However, before attributing the discrepancy between the PEST calculation near 125° and our data as being due to 3NF effects, it is important to establish that the above differences also exist when compared with calculations that employ "realistic" NN-potentials rather than a separable expansion of the potentials. Very recently, the first of such realistic calculations with the Paris and Bonn[3] potentials became available.[4] The calculations confirm the sensitivity of $A_y(\theta)$ to the ^3P NN- interactions as reported above. However, while the separable approximation of the Paris potential yields a 10% difference between calculation and data near 125°, surprisingly the new realistic and rigorous calculations differ by more than 20% from the data. It remains to be seen whether such a large discrepancy can be attributed to on-shell or especially off-shell shortcomings of the Paris and the Bonn potential, or whether 3NF effects can definitely be established.

3. Isospin Consistency of the Nucleon Interactions with ^{28}Si from 8 to 80 MeV

In light of a new report on charge-symmetry breaking in nucleon scattering from ^{28}Si, we have conducted a new, more critical analysis of available nucleon + ^{28}Si scattering data from 8 to 40 MeV. Included in the data base is our differential cross section $\sigma(\theta)$ and our analyzing power $A_y(\theta)$ obtained across the incident neutron energy range from 8 to 17 MeV.[5] In addition to a spherical optical model (SOM) analysis of the elastic

---

[1] M. Lacombe et al., Phys. Rev. C21 (1980) 861
[2] H. Zankel, W. Plessas and J. Haidenbauer, Phys. Rev. C28 (1983) 538
[3] R. Machleidt et al., Phys. Report 149, 1 (1987) 1
[4] H. Witala, W. Glöckle and T. Cornelius, preprint 1987
[5] W. Tornow et al., Phys. Rev. Lett. 49 (1982) 312

scattering data for neutrons, a coupled-channels (CC) analysis of scattering to the 0^+ ground state and the first 2^+ and 4^+ excited states was performed for both neutrons and protons. In the SOM analysis of the neutron data very good descriptions of the $\sigma(\theta)$ and total cross-section data were obtained; the description of the $A_y(\theta)$ data was reasonable at 14 and 17 MeV, but needs slightly greater amplitude in the structure at 10 MeV. These SOM parameters are important for comparisons to earlier analyses for ^{28}Si and for other nuclei, but are also important for a basic set with which to commence the time-consuming CC searches. The description for the elastic neutron scattering in the CC analysis is of the same good quality as for the SOM. The proton analysis proceeded using the same geometry parameters and spin-orbit terms as found in the neutron analysis. Two methods were tried for establishing the Coulomb correction term ΔV_C from the fits. When no constraint was placed on the search condition for V(E), the difference between the potentials yielded a Coulomb correction of only 0.33 MeV, much less than the expected correction of about 1.8 MeV. For the imaginary potential the analysis indicated a small constant absorptive Coulomb correction ΔW_D above 20 MeV and a linear energy-dependent correction below this energy.

In the second method to obtain the Coulomb correction, the proton energy was merely shifted relative to the neutron energy in order to compensate for the Coulomb barrier (according to the method of Winfield et al. in Phys. Rev. C33 (1986) 1), and the strength of the real well was fixed at that for the neutrons. This assigns the value $\Delta V_C \cong 1.8$ MeV. A search on the data led to an unexpected result that the volume integrals for the imaginary potential were nearly identical (except for a curious broad structure at 26-30 MeV for neutrons) indicating that there is no need for a ΔW_C when the real potential is adjusted to account for the Coulomb repulsion in this conventional way. However, the major question is the size of ΔV_C and whether the method of Winfield et al. is proper, because their conclusion about the magnitude of charge-symmetry breaking in nucleon scattering from ^{28}Si is intimately tied to whether ΔV_C is 0.33 or 1.8 MeV. Better neutron data in the 22 to 40 MeV region should help in constraining ΔV_C.

4. Nucleon + ^{6}Li Scattering

It has been demonstrated previously at TUNL that moderate success can be achieved in describing nucleon scattering cross-section data from ^{6}Li with a phenomenological spherical optical model (SOM). Neutron and proton $A_y(\theta)$ data were obtained at TUNL to test these optical models, but in particular to characterize the spin-orbit potential of such a model. These new data are also valuable for testing the reliability of calculations for the nucleon-plus-^{6}Li system based on the resonating group method.

The $A_y(\theta)$ measurements were made for neutron and proton scattering from ^{6}Li in the range of 5 to 17 MeV and cross section measurements for proton scattering in this energy range were made as well. When the neutron data are merely superimposed on proton data at energies which are 2 MeV higher

than the neutron energies, the neutron and proton $A_y(\theta)$ are nearly identical to one another. This energy difference is close to the Coulomb barrier of 1.6 MeV for p+ ^{6}Li. Interestingly, though, a comparison of $\sigma(\theta)$ data shows that an energy difference of zero between the incident proton and neutron data gives nearly identical cross-section shapes for the angular region beyond 30° where Rutherford scattering becomes important. We attempted to make an SOM analysis to provide a parameter set which fit both the neutron and proton data in a consistent way. However, the data below 9 MeV could not be described with meaningful geometry parameters and suggested that (broad) resonance effects have a strong influence. For the higher-energy data the geometry parameters were fixed, and the search converged on a suitable solution in which all the differences between proton and neutron scattering could be incorporated into the surface absorption term W_D. That is, a suitable description could be obtained with the Coulomb correction term ΔV_c for the real part of the potential set to zero.

5. Paris and Bonn Nucleon-Nucleon Potentials and A(θ) for n-p Scattering

While the triton binding energy has been underestimated by all nucleon-nucleon potentials in the past (that is, ~7 MeV compared to the experimental value of ~8.5 MeV), binding energy calculations using the "new Bonn"[3] potential are in good agreement with the experimental value. This spectacular result and other observations at Nijmegen[6] logically make the "new Bonn" potential the favored NN-potential -- a role that the Paris potential[7] held over the last 10 years. In order to check on the isospin T=0 components of the Bonn potential, a comparison to n-p observables, especially to the n-p analyzing power $A_y(\theta)$, is very important.

However, before this comparison can be made properly it was necessary to correct our previously published n-p $A_y(\theta)$ measurements[8] at E_n=16.9 MeV for an instrumental effect that had not been taken into account. The concern was an effect due to the large and rapidly changing analyzing power in n-^{12}C scattering in the organic neutron detectors; the process in which polarized neutrons scatter first from ^{12}C and then from ^{1}H can create an instrumental asymmetry that does not cancel. After extensive Monte Carlo calculations, we were able to show that the effect is indeed small, but at certain angles, which correspond to scattered neutron energies where the n-^{12}C $A_y(\theta)$ changes rapidly with energy, the effect is important compared to the experimental uncertainty of ±0.002.

Comparison to the revised data shows that the new Bonn potential[6] describes the $A_y(\theta)$ data best at forward angles, but the Paris potential[7] gives the best overall representation. The prediction using the results of Arndt's n-p phase shift analysis[9] from 0.0 to 1 GeV misses the data at large

---

[6] J. R. Bergervoet et al., Nucl. Phys. A463 (1987) 300
[7] M. Lacombe et al., Phys. Rev. C21 (1980) 861
[8] W. Tornow et al., Nucl. Phys. A340 (1980) 34
[9] R. A. Arndt, private communication

scattering angles. We conclude that the new Bonn potential is inconsistent with the data. (Submitted to Phys. Rev. C.) This finding is now under consideration by the developers of the Bonn potential.

6. Impact of the Dispersion Relation on the Analyzing Power for Neutron Elastic Scattering from ^{40}Ca

In our recent coupled-channel (CC) analysis[10] of proton and neutron scattering measurements on ^{40}Ca, a sizeable imaginary spin-orbit potential W_{so} was required to improve the desciption of the analyzing power $A_y(\theta)$ data. Although the uncertainty assigned to the W_{so} values given in Ref. 10 are large, there is a definite tendency for W_{so} to be positive at low energies (e.g., W_{so} = +0.9 MeV at 10 MeV), to cross through zero near 50 MeV, and to be negative at higher energies (W_{so} = -0.6 MeV around 70 MeV). Positive W_{so} values below 20 MeV have also been found at TUNL in optical model (OM) analyses of $A_y(\theta)$ data in $(\vec{n},n)$ scattering studies for several nuclei ranging from ^{9}Be to ^{208}Pb. These positive values are in contradiction to theoretical expectations; according to Refs. 11 and 12, W_{so} should take on small and negative values at incident nucleon energies below 50 MeV.

New calculations for nucleon + ^{40}Ca have been made in which the dispersion relation (DR) between the real and imaginary parts of the OM potential has been taken into account. As shown by Mahaux and Ngô[13], the DR yields a surface correction to the real part of the central (volume) potential. Since the spin-orbit interaction is also a surface interaction, this correction may have important significance in attempts to describe polarization observables. Good fits were achieved with the DR term included into a coupled-channel analysis with W_{so}=0) The surface DR term is directly responsible for this result. That is, no imaginary spin-orbit potential is required to fit our n+^{40}Ca data: the presence of ΔV_D apparently compensates for the need of a sizeable W_{so} component in the OM potential. However, it remains to be seen whether or not this finding is of a more general nature. A report on this work has been submitted to Phys. Lett.

7. Precision Test of the Neutron-Nucleus Interaction at Low Energies for ^{208}Pb (with D. Horen, Oak Ridge National Laboratory)

In the past, data for nucleon scattering from ^{208}Pb has provided one of the most important test cases for developing nuclear models. However, below 10 MeV, proton scattering from ^{208}Pb is dominated by Coulomb scattering, and detailed information about the nuclear interaction is

---

[10] G. M. Honoré et al., Phys. Rev. C33 (1986) 1129
[11] F. A. Brieva and J. R. Rook, Nucl. Phys. A307 (1978) 493
[12] B. C. Clark et al., in *The Interaction between Medium Energy Nucleons in Nuclei*, AIP Conf. Proc. No. 97, ed. by H. O. Meyer (New York, 1982), p.260
[13] C. Mahaux and H. Ngô, Nucl. Phys. A378 (1982) 205

lacking. Therefore, neutron scattering from ^{208}Pb plays a special role at low energies. With the recent emphasis on the dispersion relation in the calculation of the shape and energy dependence of the optical model potential, high-quality nucleon-nucleus scattering data for energies below 10 MeV have become essential to our understanding.

For this purpose the analyzing power for ^{208}Pb(n,n) has been measured at 6, 7, 8, 9 and 10 MeV. These data are the most complete and precise $A_y(\theta)$ data for any neutron scattering study for A > 2 in this energy range. In addition to the $A_y(\theta)$ data we have obtained $\sigma(\theta)$ data at 8 MeV to complement previous $\sigma(\theta)$ data from Ohio University reported in Nucl. Phys. A443 (1985) 249 for 5, 6, 7, 9 and 11 MeV, and from TUNL for 10, 14 and 17 MeV. Up to this reporting date the TUNL $A_y(\theta)$ data have been corrected for all known instrumental and multiple scattering effects except for the so-called Mott-Schwinger scattering. We are presently running lengthy Monte Carlo calculations to include this effect.

We will combine our $A_y(\theta)$ data with the available $\sigma(\theta)$ data to create a fairly complete data base in the 4 to 26 MeV range in order to investigate the energy dependences of the strengths and geometries of the optical potential terms, and to examine the inclusion of the dispersion terms in optical potentials.

8. Vector Analyzing Power Measurements of n-p Quasifree Scattering and the n-p Final-State Interaction for the ^{2}H($\vec{n}$,pn)n Breakup Reaction
(with P. Treado and G. Lambert, Georgetown University)

Although much is known about the two- and three-nucleon systems, many basic questions still remain unanswered. For example, the nature of the three-nucleon force (3NF) is very uncertain. Most of the evidence for 3NF effects comes from bound state observables. The most popular illustration of 3NF effects is the inability of realistic two-body interactions based in meson-exchange to properly predict the ^{3}H and ^{3}He binding energies. However, considering only bound-state observables limits our understanding of 3NF effects. Scattering experiments can provide a much broader assortment of kinematic, spin, and geometrical arrangements of the three nucleons than available in the bound state.

Therefore, at TUNL we have measured the vector analyzing power $A_y(\theta)$ for the n-p final-state interaction (FSI) and n-p quasi-free scattering (QFS) in the ^{2}H($\vec{n}$,pn)n breakup reaction at 12 MeV at several two-body center-of-mass angles. The breakup experiments were conducted in a kinematically incomplete scattering arrangement.

We have compared the data to calculations of collaborators at Bochum (see H. Witala, W. Glöckle and T. Cornelius, in European Few Nucleon Conf., Paris 1987 for our first results) and find reasonable agreement between the data and three-body calculation. These calculations suggest that 3NF effects are minute in these kinematic and spin arrangements of the three nucleons. Further interpretations of the data are underway.

9. Microscopic Model Predictions for Nucleon-Nucleus Analyzing Powers below 17 MeV (with L. Hansen and F. Dietrich, Lawrence Livermore National Laboratory)

We have undertaken a collaboration with the LLNL group to conduct a more thorough study of the models of Brieva and Rook in Nucl. Phys. A291 (1977) and Jeukenne, Lejeune and Mahaux (JLM) in Phys. Rev. C10 (1974) 1391 and C16 (1977) 80 to describe neutron scattering for a wide range of nuclei, focusing primarily on the TUNL data sets for $\sigma(\theta)$ and, for the first time, a broad set of $A_y(\theta)$ data. At present we are concentrating on the 8 to 17 MeV region. We will likely extend the range to energies above 17 MeV and also include some (p,p) data for $\sigma(\theta)$ and $A_y(\theta)$ above 15 MeV. Our aim in this work is to determine the adequacy of the existing models and to obtain better insight into the applicability of some of the assumptions and approximations involved. Reasonable agreement has been observed for ^{89}Y(n,n), ^{93}Nb and ^{120}Sn with the JLM model when the scale factor for the spin-orbit potential is taken to be $\lambda_{so} = 1.3$. Our preliminary results were presented at the Nuclear Physics Division meeting in New Jersey. We are planning to investigate ^{9}Be, ^{11}B, ^{54}Fe and ^{208}Pb in a similar manner.

10. Feasibility Tests for Measuring Polarized Deuteron Scattering from Neutrons: Quasifree Scattering Processes in the $\vec{d}$ + d Breakup Reaction (with J. Lambert, P. Treado, Georgetown University, and Y. Koike, George Washington University and Hosei University, Tokyo)

The rate of theoretical advances in solving the four-body problem using realistic microscopic approaches with no free parameters is quite impressive. Recently, Mdlalose et al. in Nucl. Phys. A457 (1986) 273 have investigated the d+d→d+p+n breakup reaction using a parameter-free microscopic calculation. Their calculations successfully described the shape of the cross section for d-p quasi-free scattering (QFS) at incident deuteron energies less than 25 MeV, but failed to reproduce higher energy data. However, the magnitude of their calculated cross sections had to be normalized by roughly a factor of two to obtain agreement with the low energy data. Nevertheless, these results are encouraging, especially for understanding d+d breakup processes. The QFS processes in this four-nucleon system are convenient observables for theoretical interpretations, since they are not significantly contaminated by final-state interactions (FSI). That is, the neutron-proton (n-p) FSI in the $^1S_0$ state is isospin forbidden in the d+d→d+p+n reaction, since it occurs in a T=1 isospin state. Furthermore, the $^3S_1$ n-p FSI contributes merely in the form of a weak uniform background.

In order to expand our capability for studying the d + d system, we have investigated techniques for measuring polarization observables in the $\vec{d}$ + d reactions at low bombarding energies, concentrating on the three-body breakup processes. We have measured the vector analyzing power A_y and the tensor analyzing powers A_{yy} and A_{zz} for d-n and d-p QFS in a kinematically complete experimental arrangement at an incident deuteron energy of 12 MeV. Experimentally, the choice of 12 MeV proved to be a nice compromise between

background considerations in the neutron detectors and having sufficient energy in the outgoing charged particles to exit the containment foil of the gas target.

11. Kerma Factors for n+^{12}C near 18 MeV

A paper on this project has been accepted for publication in J. Phys. G: Nucl. Phys. The abstract is given below:

> "The analyzing power $A_y(\theta)$ for $^{12}C(n,n)^{12}C$ elastic scattering and for inelastic scattering to the first excited state ($J^\pi = 2^+$, Q = -4.44 MeV) of ^{12}C was measured at 18.2 MeV. A pulsed polarized neutron beam was produced via the $^2H(\vec{d},\vec{n})^3He$ polarization transfer reaction. The A_y data, together with published cross sections, were analyzed in the framework of the spherical optical model and in the coupled-channels formalism. A phase-shift analysis at 18.2 MeV gives supporting evidence for a broad $5/2^+$ resonance. The ^{12}C recoil kerma factors and values for the n+^{12}C reaction cross section were deduced and compared to previous estimates and predictions."

12. System Improvements for Neutron Experimental Systems

In the past year several modifications were made to improve the quality of the data obtained with the neutron time-of-flight (TOF) spectrometer. A new RF system, which operates at 5 MHz, is being installed in the tandem injection area. This system will drive the main chopper, the bunchers and the injection sweeper. In addition, a variable length buncher was constructed. It permits rapid switching from proton to deuteron beams without letting the beam pipe up to atmosphere. This new buncher will remain permanently in the beam pipe, as transmission is good for all DC (polarized and unpolarized) and pulsed beams.

B. POLARIZED TARGET STUDIES

1. Overview (C. R. Gould, D. G. Haase, J. Koster, M. Nagadi, K. Nash, N. R. Roberson, M. B. Schneider, L. W. Seagondollar, J. P. Soderstrum, W. S. Wilburn, X. Zhu)

The TUNL cryogenically polarized target facility consists of a ^{3}He-^{4}He dilution refrigerator and a superconducting magnet, together capable of maintaining samples at between 10 and 20 mK in magnetic fields up to 7 Tesla. At these temperatures and magnetic fields brute-force nuclear orientation occurs. Polarizations from 20 to 60% are attainable in about twenty nonzero-spin nuclei. Most are metals, ranging in mass from ^{6}Li to ^{209}Bi, but the nuclei ^{1}H and ^{3}He are also polarizable via this method. The research effort is directed towards two main areas: 1) determination of the effective nucleon-nucleus spin-spin force and 2)

searches for violations of the symmetries of parity conservation and time reversal invariance. Spin-spin cross section measurements in ^{27}Al and ^{93}Nb with the present polarized ion source are essentially completed. The small cross sections in ^{93}Nb are indicative of a strong 1/A dependence. Further studies in heavier nuclei will require the higher intensity beams available from the polarized ion source presently under construction. Lighter nuclei such as ^{3}He and the lithium isotopes appear to be more promising candidates for study. Polarized few nucleon systems such as ^{3}He are particularly interesting since their wave functions can be accurately predicted. A proposal for the construction of a brute force polarized solid ^{3}He target has recently been submitted.

A preliminary search for parity non-conserving effects in longitudinal analyzing power measurements on ^{165}Ho and ^{nat}Ag yielded a null result at the few times 10^{-4} level. A factor of ten improvement will be possible with the new polarized source. But the result appears to suggest that the enhancement of parity violating effects seen in individual compound nucleus resonances at epithermal neutron energies is not present coherently when one averages over many compound nucleus levels in higher energy neutron scattering.

Studies of time reversal violations are being considered at a number of laboratories, and the TUNL-LANL workshop heard a number of presentations on the theoretical and experimental aspects of this work. The TUNL effort is directed towards experiments with polarized and aligned holmium targets. A new beam line is under construction to go with the rotating holmium crystal target being developed at TUNL. Tests of time reversal invariance with polarized MeV neutrons are feasible at the 10^{-3} to 10^{-4} level and will yield upper limits in systems not previously studied experimentally.

2. Spin-Spin Potentials in ^{27}Al + n and the Nuclear Ramsauer Effect

This work was published in Phys. Rev. Lett. 57 (1986) 2371. The abstract follows:

> "Spin-spin effects in neutron-nucleus interactions have been studied with a polarized ^{27}Al target and polarized neutrons of energies 5 to 17 MeV. Due to nuclear Ramsauer interference, real and imaginary spin-spin terms in the optical potential give rise to energy dependences of spin-spin effects which are out of phase. We find a central real potential V_{ss}= 750±440 keV, consistent with folding model calculations, and a central volume imaginary potential W_{ss} = -780±320 keV, related to compound nuclear absorption effects."

3. Spin-Spin Potentials in $^{93}\vec{Nb} + \vec{n}$

As mentioned in TUNL XXV, we have essentially completed a study of spin-spin effects with transverse polarized ^{27}Al and 5 to 17 MeV transverse

polarized neutrons. To investigate the A-dependence of the spin-spin potentials, we have performed a similar study with polarized ^{93}Nb and 5 to 11 MeV polarized neutrons. The experiments were performed with the TUNL Cryogenic Polarized Target Facility described in TUNL XXV and previous annual reports. The following modifications have been made in the past year: 1) The coldfinger was a bundle of copper wires soldered together at the end. It has been replaced with a solid copper coldfinger. With this new coldfinger, we have been able to cool the target to 9.5-11 mK, yielding target polarizations of 49-56%. 2) The two 13 cm diameter by 5 cm long NE213 liquid scintillator detectors were replaced by a single 13 cm diameter by 13 cm long NE213 liquid scintillator detector. 3) Instead of storing energy spectra in the computer, the data were fed into scalers. Measurements of the transverse (spins oriented transverse to the neutron momentum) spin-spin cross section were taken at E_n = 5.8, 7.5, 9.0, and 10.5 MeV, while the longitudinal s_{ss} was measured at 7.5 MeV. The results are summarized in Fig. B3-1.

The results for the spin-spin cross section are compared in Fig. B3-1 to spherical optical model calculations. Assuming V_{ss} and W_{ss} are energy-independent, the best fit to the data was obtained with the condition V_{ss} = -14 keV and W_{ss} = 73 keV. The uncertainties are about ± 56 keV for both strengths.

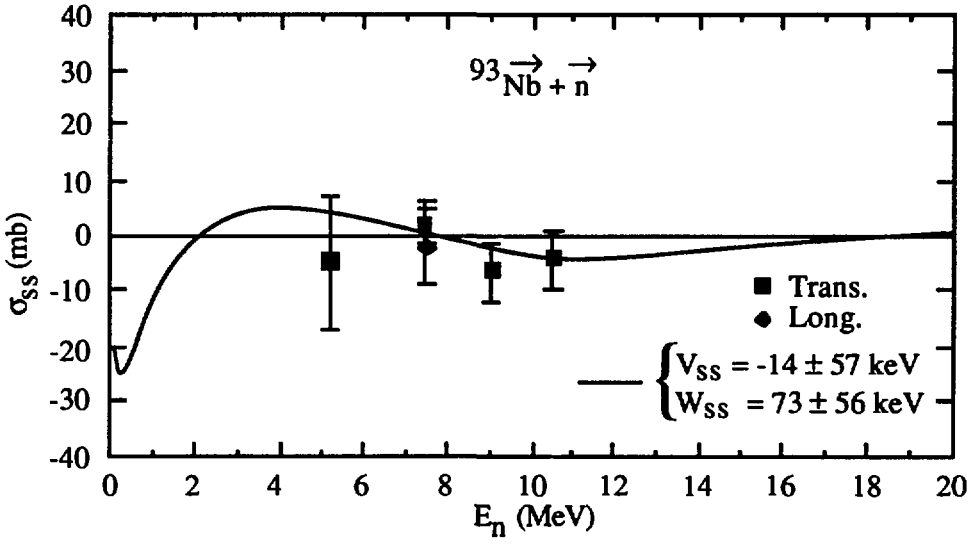

Fig. B3-1. Spin-spin cross section for ^{93}Nb measured in the present experiment, and the best fit prediction assuming energy independent real and volume imaginary central spin-spin potentials of V_{ss} = -14 keV and W_{ss} = 73 keV.

C. RADIATIVE CAPTURE REACTIONS (H. R. Weller, D. R. Tilley, G. Feldman, J. Langenbrunner, J. C. Riley, M. Whitton, Z. Williams, L. Kramer, M. Balbes, Z. D. Huang, E. Hayward (NBS), W. R. Dodge (NBS), S. Kuhn (LBL))

The major efforts of the group during the past year have been directed towards extending our tensor polarized deuteron capture measurements on few-nucleon systems to both lower and higher energies. The $^{2}H(d,\gamma)^{4}He$ reaction continues to be a major interest of our group. We have made measurements at energies as low as 400 keV and as high as 50 MeV. For the low energy measurements the beam was stopped in the target so that we are integrating over incident energies from 0.0 to 400 keV. Our emphasis here is to learn more about the reaction at energies of interest for astrophysics and fusion problems. Measurements of $A_{yy}(\theta)$, $A_{y}(\theta)$ and $\sigma(\theta)$ are being used to improve our understanding of the low energy capture process and, in particular, the role of the D-state of the alpha-particle. We also measured $A_{y}(\theta)$ and $A_{yy}(\theta)$ at incident deuteron energies of 30 and 50 MeV using the 88" cyclotron of the Lawrence Berkeley Laboratory. Data were obtained by detecting the recoiling ^{4}He particles in coincidence with the γ-rays. The A_{y} results indicate that the non-E2 radiation observed at lower energies is virtually absent at these energies. On the other hand the A_{yy} data show tensor analyzing powers which are almost twice as large as those seen in the 10 to 15 MeV region. We are looking forward to comparing these results with theoretical calculations, especially since we expect these higher energy data to be sensitive to the short range behavior of the theoretical D-state wavefunction.

We are presently involved in an analysis of the low-energy $^{2}H(d,\gamma)^{4}He$ data in order to determine which multipoles are contributing. Searches for simultaneous fits to $\sigma(\theta)$, $A_{y}(\theta)$ and $A_{yy}(\theta)$ are being made. Theoretical work, done in collaboration with Prof. D Lehman, has deepened our understanding of the origin of E1 radiation in this reaction. We have considered both spin-flip E1 and E1 due to charge polarization of the deuteron(s).

We also made new measurements on the $^{3}H(d,\gamma)^{5}He$ reaction using a tensor polarized beam. Data were obtained in the region of the fusion resonance by using a 400-keV beam and stopping it in a tritiated titanium target. Preliminary results indicate a tensor analyzing power which is somewhat smaller than that predicted for pure S-wave capture to the $3/2^{+}$ resonance. We hope to extract the amount of $1/2^{+}$ strength present in this energy region.

We are planning to complete our 30 to 50 MeV study of the $^{2}H(d,\gamma)^{4}He$ reaction by measuring $\sigma(\theta)$ and $A_{xx}(\theta)$. We are planning to begin measurements on the $^{3}He(\vec{d},\gamma)^{5}Li$ reaction at low energies in the near future. Work has also begun on designing an arrangement to make measurements of the $^{4}He(\vec{d},\gamma)^{6}Li$ reaction.

D. PHOTON PRODUCTION CROSS SECTION MEASUREMENTS FOR Ta AND Be

(C. R. Gould, G. E. Mitchell, P. Ramakrishnan, G. F. Auchampaugh (LANL), R. C. Little (LANL), S. A. Wender (LANL))

Neutron-induced photon production cross sections and the spectra of the secondary gamma rays are needed in a variety of applications. Recently intense beams of neutrons have become available at the white neutron source (WNR) at the Los Alamos Meson Physics Facility. This source has excellent characteristics for γ-ray production cross section studies. A program of measurements is now in progress using an array of five bismuth germanate (BGO) detectors. The good detection efficiency of BGO at high γ-ray energy, combined with the ability to measure complete angular distributions, provides a unique capability for performing neutron-induced g-ray production cross section measurements. When the new facility is fully operational these measurements can be extended up to E_n = 400 MeV.

Our first continuum gamma-ray production measurements were for ^{181}Ta and E_n up to 100 MeV. Beryllium was measured to simulate the neutron-induced photon background. A paper on the method of analysis "Neutron-Induced Photon Production Cross Sections" has been accepted for publication in Nucl. Sci. Eng. The abstract follows:

> "A procedure for the determination of neutron-induced photon production cross sections is described, including corrections for the neutron-induced photon background and the unfolding of the γ-ray spectra. As an example, data have been obtained for tantalum and beryllium with five bismuth germanate detectors and the high energy white neutron source at LAMPF. Calculations and measurements indicate that a beryllium sample may be used to simulate neutron-induced photon background. Results for the Ta(n,xγ) reaction for neutron energies below E_n = 20 MeV are compared with previous measurements at ORELA."

The data on ^{181}Ta are preliminary, obtained mainly to develop the analysis procedure and to provide limited statistical accuracy at higher neutron and γ-ray energies. Even these preliminary results are interesting, since they provide the first such data for high neutron energies. A paper entitled "Photon Production Cross Section for ^{181}Ta" has been accepted for publication in Nucl. Sci. Eng. The abstract follows:

> "The $^{181}Ta(n,x\gamma)$ reaction has been measured for neutron energies E_n = 2 - 100 MeV and for γ-ray energies E_γ = 2 - 25 MeV using an array of BGO detectors and the pulsed neutron source at LAMPF. The integrated photon production cross section reaches a maximum at about 7.5 MeV. Above 20 MeV, the cross section increases slowly with energy. The angular distributions of the photon production cross sections for different neutron energies are isotropic. At all measured energies the γ-ray spectra have the simple evaporation form."

TRIANGLE UNIVERSITIES NUCLEAR LABORATORY

Starting with the present report this year, the review of the TUNL program will reflect the breadth of the entire program as it relates to nuclear data and nuclear models. That is, work of others beyond the neutron scattering group will be included from now on. Furthermore, the rationale behind the individual projects will be outlined in brief statements in order to provide the uninitiated reader with an indication of the significance or purpose of the work. Much of the information given here has been excerpted from the annual report TUNL XXVI which can be obtained by writing Prof. Edward G. Bilpuch, Director of TUNL, Physics Department, Duke University, Durham, NC 27706. In TUNL XXVI many illustrations are given that elaborate on the condensed version given here for the Nuclear Data Committee.

A. FUNDAMENTAL STUDIES WITH NEUTRON BEAMS

1. Brief Overview (R. L. Walter, C. R. Howell, W. Tornow, H. G. Pfützner, M. L. Roberts, P. D. Felsher, G. Weisel, M. Al Ohali, R. S. Pedroni*, J. P. Delaroche**, I. Slaus+)

During the past year we have focused on several types of fundamental physics problems that can be explored solely or most sensitively by using the unique properties of the neutron. For instance, in this regard we emphasize that the use of neutron beams gives one the most direct measure of the isospin T=0 part of the nucleon-nucleon interaction. Also, the long range Coulomb interaction, which is difficult to take into account exactly and which can mask details of the nuclear interaction, is not a problem in experiments involving neutron beams in both the incoming and outgoing channels. In general, the developments or tests of the nuclear theories in which we are interested concern comparisons to spin-sensitive observables, and most of our experimental program involves measuring quantities for reactions initiated with polarized neutron, proton or deuteron beams.

2. Failures and Sensitivities of Few-Nucleon Calculations and the Analyzing Power for n-d Elastic Scattering (with J. Lambert, P. Treado, Georgetown University, and Y. Koike, Hosei University)

The traditional theoretical approach to nuclear physics is based on a nonrelativistic Hamiltonian in which the nucleons interact pairwise. It is clear, however, that no two-nucleon-force model adequately describes all of the fundamental properties of nuclei and nuclear reactions. Such disagreement between calculations and data includes nucleon-deuteron scattering. The three-nucleon force (3NF) has been proposed to explain some or all of the observed discrepancies. In particular, the vector analyzing power $A_y(\theta)$ in neutron-deuteron elastic scattering may be sensitive to the 3NF. Via the coupling of the ^3P NN-states to the ^3P NΔ-states, sizeable 3NF effects are expected.

---

* Present address: Dept. of Physics, Ohio University, Athens, Ohio
** Permanent address: Centre d'Etudes de Bruyeres-le-Chatel, France
\+ Permanent address: Ruder Boskovic Institute, Zagreb, Yugoslavia

In order to investigate the sensitivity of $A_y(\theta)$ calculations for n-d elastic scattering to various angular momentum components of the NN-interaction, a separable approximation of the Paris[1] NN-potential, referred[2] to as PEST, was chosen. The calculations compared with experimental data recently obtained at TUNL at E_n=12 MeV. (See Few-Body Systems 2 (1987) 19.) Except for the region at the maximum at $\theta_{c.m.}$ = 125° of $A_y(\theta)$, the PEST calculation reproduces the data impressively well. Successive calculations that individually exclude the $^3P_0$, $^3P_1$, and $^3P_2$ interactions clearly demonstrate that the magnitude of $A_y(\theta)$ near 125° is extremely sensitive to the ^3P interactions.

However, before attributing the discrepancy between the PEST calculation near 125° and our data as being due to 3NF effects, it is important to establish that the above differences also exist when compared with calculations that employ "realistic" NN-potentials rather than a separable expansion of the potentials. Very recently, the first of such realistic calculations with the Paris and Bonn[3] potentials became available.[4] The calculations confirm the sensitivity of $A_y(\theta)$ to the ^3P NN- interactions as reported above. However, while the separable approximation of the Paris potential yields a 10% difference between calculation and data near 125°, surprisingly the new realistic and rigorous calculations differ by more than 20% from the data. It remains to be seen whether such a large discrepancy can be attributed to on-shell or especially off-shell shortcomings of the Paris and the Bonn potential, or whether 3NF effects can definitely be established.

3. Isospin Consistency of the Nucleon Interactions with ^{28}Si from 8 to 80 MeV

In light of a new report on charge-symmetry breaking in nucleon scattering from ^{28}Si, we have conducted a new, more critical analysis of available nucleon + ^{28}Si scattering data from 8 to 40 MeV. Included in the data base is our differential cross section $\sigma(\theta)$ and our analyzing power $A_y(\theta)$ obtained across the incident neutron energy range from 8 to 17 MeV. In addition to a spherical optical model (SOM) analysis of the elastic scattering data for neutrons, a coupled-channels (CC) analysis of scattering to the 0^+ ground state and the first 2^+ and 4^+ excited states was performed for both neutrons and protons. In the SOM analysis of the neutron data very good descriptions of the $\sigma(\theta)$ and total cross-section data were obtained; the description of the $A_y(\theta)$ data was reasonable at 14 and 17 MeV, but needs slightly greater amplitude in the structure at 10 MeV. These SOM parameters are important for comparisons to earlier analyses for ^{28}Si and for other nuclei, but are also important for a basic set with which to commence the time-consuming CC searches. The description for the elastic neutron scattering in the CC analysis is of the same good quality as for the SOM. The proton analysis proceeded using the same geometry parameters and spin-orbit terms as found in the neutron analysis. Two methods were tried for establishing the Coulomb correction term ΔV_C from the fits. When no constraint was placed on the search condition for V(E), the difference between the potentials yielded a Coulomb correction of only 0.33 MeV, much less than the expected correction of about 1.8 MeV. For the imaginary potential the analysis indicated a small constant absorptive Coulomb correction ΔW_D above 20 MeV and a linear energy-dependent correction below this energy.

---

[1] M. Lacombe et al., Phys. Rev. C21 (1980) 861
[2] H. Zankel, W. Plessas and J. Haidenbauer, Phys. Rev. C28 (1983) 538
[3] R. Machleidt et al., Phys. Report 149, 1 (1987) 1
[4] H. Witala, W. Glöckle and T. Cornelius, preprint 1987
[5] W. Tornow et al., Phys. Rev. Lett. 49 (1982) 312

In the second method to obtain the Coulomb correction, the proton energy was merely shifted relative to the neutron energy in order to compensate for the Coulomb barrier (according to the method of Winfield et al. in Phys. Rev. C33 (1986) 1), and the strength of the real well was fixed at that for the neutrons. This assigns the value $\Delta V_c \equiv 1.8$ MeV. A search on the data led to an unexpected result that the volume integrals for the imaginary potential were nearly identical (except for a curious broad structure at 26-30 MeV for neutrons) indicating that there is no need for a ΔW_c when the real potential is adjusted to account for the Coulomb repulsion in this conventional way. However, the major question is the size of ΔV_c and whether the method of Winfield et al. is proper, because their conclusion about the magnitude of charge-symmetry breaking in nucleon scattering from ^{28}Si is intimately tied to whether ΔV_c is 0.33 or 1.8 MeV. Better neutron data in the 22 to 40 MeV region should help in constraining ΔV_c.

4. Nucleon + ^{6}Li Scattering

It has been demonstrated previously at TUNL that moderate success can be achieved in describing nucleon scattering cross-section data from ^{6}Li with a phenomenological spherical optical model (SOM). Neutron and proton $A_y(\theta)$ data were obtained at TUNL to test these optical models, but in particular to characterize the spin-orbit potential of such a model. These new data are also valuable for testing the reliability of calculations for the nucleon-plus-^{6}Li system based on the resonating group method.

The $A_y(\theta)$ measurements were made for neutron and proton scattering from ^{6}Li in the range of 5 to 17 MeV and cross section measurements for proton scattering in this energy range were made as well. When the neutron data are merely superimposed on proton data at energies which are 2 MeV higher than the neutron energies, the neutron and proton $A_y(\theta)$ are nearly identical to one another. This energy difference is close to the Coulomb barrier of 1.6 MeV for p+ ^{6}Li. Interestingly, though, a comparison of $\sigma(\theta)$ data shows that an energy difference of zero between the incident proton and neutron data gives nearly identical cross-section shapes for the angular region beyond 30° where Rutherford scattering becomes important. We attempted to make an SOM analysis to provide a parameter set which fit both the neutron and proton data in a consistent way. However, the data below 9 MeV could not be described with meaningful geometry parameters and suggested that (broad) resonance effects have a strong influence. For the higher-energy data the geometry parameters were fixed, and the search converged on a suitable solution in which all the differences between proton and neutron scattering could be incorporated into the surface absorption term W_D. That is, a suitable description could be obtained with the Coulomb correction term ΔV_c for the real part of the potential set to zero.

5. Paris and Bonn Nucleon-Nucleon Potentials and $A(\theta)$ for n-p Scattering

While the triton binding energy has been underestimated by all nucleon-nucleon potentials in the past (that is, ~7 MeV compared to the experimental value of ~8.5 MeV), binding energy calculations using the "new Bonn"[3] potential are in good agreement with the experimental value. This spectacular result and other observations at Nijmegen[6] logically make the "new Bonn" potential the favored NN-potential -- a role that the Paris potential[7] held over the last 10 years. In order to check on the isospin T=0 components of the Bonn potential, a comparison to n-p observables, especially to the n-p analyzing power $A_y(\theta)$, is very important.

---

[6] J. R. Bergervoet et al., Nucl. Phys. A463 (1987) 300
[7] M. Lacombe et al., Phys. Rev. C21 (1980) 861

However, before this comparison can be made properly it was necessary to correct our previously published n-p $A_y(\theta)$ measurements[8] at E_n=16.9 MeV for an instrumental effect that had not been taken into account. The concern was an effect due to the large and rapidly changing analyzing power in n-^{12}C scattering in the organic neutron detectors; the process in which polarized neutrons scatter first from ^{12}C and then from ^{1}H can create an instrumental asymmetry that does not cancel. After extensive Monte Carlo calculations, we were able to show that the effect is indeed small, but at certain angles, which correspond to scattered neutron energies where the n-^{12}C $A_y(\theta)$ changes rapidly with energy, the effect is important compared to the experimental uncertainty of ±0.002.

Comparison to the revised data shows that the new Bonn potential[6] describes the $A_y(\theta)$ data best at forward angles, but the Paris potential[7] gives the best overall representation. The prediction using the results of Arndt's n-p phase shift analysis[9] from 0.0 to 1 GeV misses the data at large scattering angles. We conclude that the new Bonn potential is inconsistent with the data. (Submitted to Phys. Rev. C.) This finding is now under consideration by the developers of the Bonn potential.

6. Impact of the Dispersion Relation on the Analyzing Power for Neutron Elastic Scattering from ^{40}Ca

In our recent coupled-channel (CC) analysis[10] of proton and neutron scattering measurements on ^{40}Ca, a sizeable imaginary spin-orbit potential W_{so} was required to improve the desciption of the analyzing power $A_y(\theta)$ data. Although the uncertainty assigned to the W_{so} values given in Ref. 10 are large, there is a definite tendency for W_{so} to be positive at low energies (e.g., W_{so} = +0.9 MeV at 10 MeV), to cross through zero near 50 MeV, and to be negative at higher energies (W_{so} = -0.6 MeV around 70 MeV). Positive W_{so} values below 20 MeV have also been found at TUNL in optical model (OM) analyses of $A_y(\theta)$ data in ($\vec{n}$,n) scattering studies for several nuclei ranging from ^{9}Be to ^{208}Pb. These positive values are in contradiction to theoretical expectations; according to Refs. 11 and 12, W_{so} should take on small and negative values at incident nucleon energies below 50 MeV.

New calculations for nucleon + ^{40}Ca have been made in which the dispersion relation (DR) between the real and imaginary parts of the OM potential has been taken into account. As shown by Mahaux and Ngô[13], the DR yields a surface correction to the real part of the central (volume) potential. Since the spin-orbit interaction is also a surface interaction, this correction may have important significance in attempts to describe polarization observables. Good fits were achieved with the DR term included into a coupled-channel analysis with W_{so}=0) The surface DR term is directly responsible for this result. That is, no imaginary spin-orbit potential is required to fit our n+^{40}Ca data; the presence of ΔV_D apparently compensates for the need of a

---

[8] W. Tornow et al., Nucl. Phys. A340 (1980) 34
[9] R. A. Arndt, private communication
[10] G. M. Honoré et al., Phys. Rev. C33 (1986) 1129
[11] F. A. Brieva and J. R. Rook, Nucl. Phys. A307 (1978) 493
[12] B. C. Clark et al., in *The Interaction between Medium Energy Nucleons in Nuclei*, AIP Conf. Proc. No. 97, ed. by H. O. Meyer (New York, 1982), p.260
[13] C. Mahaux and H. Ngô, Nucl. Phys. A378 (1982) 205

sizeable W_{so} component in the OM potential. However, it remains to be seen whether or not this finding is of a more general nature. A report on this work has been submitted to Phys. Lett.

7. Precision Test of the Neutron-Nucleus Interaction at Low Energies for ^{208}Pb (with D. Horen, Oak Ridge National Laboratory)

In the past, data for nucleon scattering from ^{208}Pb has provided one of the most important test cases for developing nuclear models. However, below 10 MeV, proton scattering from ^{208}Pb is dominated by Coulomb scattering, and detailed information about the nuclear interaction is lacking. Therefore, neutron scattering from ^{208}Pb plays a special role at low energies. With the recent emphasis on the dispersion relation in the calculation of the shape and energy dependence of the optical model potential, high-quality nucleon-nucleus scattering data for energies below 10 MeV have become essential to our understanding.

For this purpose the analyzing power for ^{208}Pb(n,n) has been measured at 6, 7, 8, 9 and 10 MeV. These data are the most complete and precise $A_y(\theta)$ data for any neutron scattering study for $A > 2$ in this energy range. In addition to the $A_y(\theta)$ data we have obtained $\sigma(\theta)$ data at 8 MeV to complement previous $\sigma(\theta)$ data from Ohio University reported in Nucl. Phys. A443 (1985) 249 for 5, 6, 7, 9 and 11 MeV, and from TUNL for 10, 14 and 17 MeV. Up to this reporting date the TUNL $A_y(\theta)$ data have been corrected for all known instrumental and multiple scattering effects except for the so-called Mott-Schwinger scattering. We are presently running lengthy Monte Carlo calculations to include this effect.

We will combine our $A_y(\theta)$ data with the available $\sigma(\theta)$ data to create a fairly complete data base in the 4 to 26 MeV range in order to investigate the energy dependences of the strengths and geometries of the optical potential terms, and to examine the inclusion of the dispersion terms in optical potentials.

8. Vector Analyzing Power Measurements of n-p Quasifree Scattering and the n-p Final-State Interaction for the ^{2}H($\vec{n}$,pn)n Breakup Reaction (with P. Treado and G. Lambert, Georgetown University)

Although much is known about the two- and three-nucleon systems, many basic questions still remain unanswered. For example, the nature of the three-nucleon force (3NF) is very uncertain. Most of the evidence for 3NF effects comes from bound state observables. The most popular illustration of 3NF effects is the inability of realistic two-body interactions based in meson-exchange to properly predict the ^{3}H and ^{3}He binding energies. However, considering only bound-state observables limits our understanding of 3NF effects. Scattering experiments can provide a much broader assortment of kinematic, spin, and geometrical arrangements of the three nucleons than available in the bound state.

Therefore, at TUNL we have measured the vector analyzing power $A_y(\theta)$ for the n-p final-state interaction (FSI) and n-p quasi-free scattering (QFS) in the ^{2}H($\vec{n}$,pn)n breakup reaction at 12 MeV at several two-body center-of-mass angles. The breakup experiments were conducted in a kinematically incomplete scattering arrangement.

We have compared the data to calculations of collaborators at Bochum (see H. Witala, W. Glöckle and T. Cornelius, in European Few Nucleon Conf., Paris 1987 for our first results) and find reasonable agreement between the data and three-body calculation. These calculations suggest that 3NF effects are minute in these kinematic and spin arrangements of the three

nucleons. Further interpretations of the data are underway.

9. Microscopic Model Predictions for Nucleon-Nucleus Analyzing Powers below 17 MeV (with L. Hansen and F. Dietrich, Lawrence Livermore National Laboratory)

We have undertaken a collaboration with the LLNL group to conduct a more thorough study of the models of Brieva and Rook in Nucl. Phys. A291 (1977) and Jeukenne, Lejeune and Mahaux (JLM) in Phys. Rev. C10 (1974) 1391 and C16 (1977) 80 to describe neutron scattering for a wide range of nuclei, focusing primarily on the TUNL data sets for $\sigma(\theta)$ and, for the first time, a broad set of $A_y(\theta)$ data. At present we are concentrating on the 8 to 17 MeV region. We will likely extend the range to energies above 17 MeV and also include some (p,p) data for $\sigma(\theta)$ and $A_y(\theta)$ above 15 MeV. Our aim in this work is to determine the adequacy of the existing models and to obtain better insight into the applicability of some of the assumptions and approximations involved. Reasonable agreement has been observed for ^{89}Y(n,n), ^{93}Nb and ^{120}Sn with the JLM model when the scale factor for the spin-orbit potential is taken to be $\lambda_{so} = 1.3$. Our preliminary results were presented at the Nuclear Physics Division meeting in New Jersey. We are planning to investigate ^{9}Be, ^{11}B, ^{54}Fe and ^{208}Pb in a similar manner.

10. Feasibility Tests for Measuring Polarized Deuteron Scattering from Neutrons: Quasifree Scattering Processes in the $\vec{d}$ + d Breakup Reaction (with J. Lambert, P. Treado, Georgetown University, and Y. Koike, George Washington University and Hosei University, Tokyo)

The rate of theoretical advances in solving the four-body problem using realistic microscopic approaches with no free parameters is quite impressive. Recently, Mdlalose et al. in Nucl. Phys. A457 (1986) 273 have investigated the d+d→d+p+n breakup reaction using a parameter-free microscopic calculation. Their calculations successfully described the shape of the cross section for d-p quasi-free scattering (QFS) at incident deuteron energies less than 25 MeV, but failed to reproduce higher energy data. However, the magnitude of their calculated cross sections had to be normalized by roughly a factor of two to obtain agreement with the low energy data. Nevertheless, these results are encouraging, especially for understanding d+d breakup processes. The QFS processes in this four-nucleon system are convenient observables for theoretical interpretations, since they are not significantly contaminated by final-state interactions (FSI). That is, the neutron-proton (n-p) FSI in the $^{1}S_0$ state is isospin forbidden in the d+d→d+p+n reaction, since it occurs in a T=1 isospin state. Furthermore, the $^{3}S_1$ n-p FSI contributes merely in the form of a weak uniform background.

In order to expand our capability for studying the $\vec{d}$ + d system, we have investigated techniques for measuring polarization observables in the $\vec{d}$ + d reactions at low bombarding energies, concentrating on the three-body breakup processes. We have measured the vector analyzing power A_y and the tensor analyzing powers A_{yy} and A_{zz} for d-n and d-p QFS in a kinematically complete experimental arrangement at an incident deuteron energy of 12 MeV. Experimentally, the choice of 12 MeV proved to be a nice compromise between background considerations in the neutron detectors and having sufficient energy in the outgoing charged particles to exit the containment foil of the gas target.

11. Kerma Factors for n+^{12}C near 18 MeV

A paper on this project has been accepted for publication in J. Phys. G: Nucl. Phys. The abstract is given below:

"The analyzing power $A_y(\theta)$ for $^{12}C(n,n)^{12}C$ elastic scattering and for inelastic scattering to the first excited state ($J^\pi = 2^+$, Q = -4.44 MeV) of ^{12}C was measured at 18.2 MeV. A pulsed polarized neutron beam was produced via the $^2H(\vec{d},\vec{n})^3He$ polarization transfer reaction. The A_y data, together with published cross sections, were analyzed in the framework of the spherical optical model and in the coupled-channels formalism. A phase-shift analysis at 18.2 MeV gives supporting evidence for a broad $5/2^+$ resonance. The ^{12}C recoil kerma factors and values for the $n+^{12}C$ reaction cross section were deduced and compared to previous estimates and predictions."

12. System Improvements for Neutron Experimental Systems

In the past year several modifications were made to improve the quality of the data obtained with the neutron time-of-flight (TOF) spectrometer. A new RF system, which operates at 5 MHz, is being installed in the tandem injection area. This system will drive the main chopper, the bunchers and the injection sweeper. In addition, a variable length buncher was constructed. It permits rapid switching from proton to deuteron beams without letting the beam pipe up to atmosphere. This new buncher will remain permanently in the beam pipe, as transmission is good for all DC (polarized and unpolarized) and pulsed beams.

B. POLARIZED TARGET STUDIES

1. Overview (C. R. Gould, D. G. Haase, J. Koster, M. Nagadi, K. Nash, N. R. Roberson, M. B. Schneider, L. W. Seagondollar, J. P. Soderstrum, W. S. Wilburn, X. Zhu)

The TUNL cryogenically polarized target facility consists of a ^3He-^4He dilution refrigerator and a superconducting magnet, together capable of maintaining samples at between 10 and 20 mK in magnetic fields up to 7 Tesla. At these temperatures and magnetic fields brute-force nuclear orientation occurs. Polarizations from 20 to 60% are attainable in about twenty nonzero-spin nuclei. Most are metals, ranging in mass from ^6Li to ^{209}Bi, but the nuclei ^1H and ^3He are also polarizable via this method. The research effort is directed towards two main areas: 1) determination of the effective nucleon-nucleus spin-spin force and 2) searches for violations of the symmetries of parity conservation and time reversal invariance. Spin-spin cross section measurements in ^{27}Al and ^{93}Nb with the present polarized ion source are essentially completed. The small cross sections in ^{93}Nb are indicative of a strong 1/A dependence. Further studies in heavier nuclei will require the higher intensity beams available from the polarized ion source presently under construction. Lighter nuclei such as ^3He and the lithium isotopes appear to be more promising candidates for study. Polarized few nucleon systems such as ^3He are particularly interesting since their wave functions can be accurately predicted. A proposal for the construction of a brute force polarized solid ^3He target has recently been submitted.

A preliminary search for parity non-conserving effects in longitudinal analyzing power measurements on ^{165}Ho and ^{nat}Ag yielded a null result at the few times 10^{-4} level. A factor of ten improvement will be possible with the new polarized source. But the result appears to suggest that the enhancement of parity violating effects seen in individual compound nucleus resonances at epithermal neutron energies is not present coherently when one averages over

many compound nucleus levels in higher energy neutron scattering.

Studies of time reversal violations are being considered at a number of laboratories, and the TUNL-LANL workshop heard a number of presentations on the theoretical and experimental aspects of this work. The TUNL effort is directed towards experiments with polarized and aligned holmium targets. A new beam line is under construction to go with the rotating holmium crystal target being developed at TUNL. Tests of time reversal invariance with polarized MeV neutrons are feasible at the 10^{-3} to 10^{-4} level and will yield upper limits in systems not previously studied experimentally.

2. Spin-Spin Potentials in ^{27}Al + n and the Nuclear Ramsauer Effect

This work was published in Phys. Rev. Lett. 57 (1986) 2371. The abstract follows:

> "Spin-spin effects in neutron-nucleus interactions have been studied with a polarized ^{27}Al target and polarized neutrons of energies 5 to 17 MeV. Due to nuclear Ramsauer interference, real and imaginary spin-spin terms in the optical potential give rise to energy dependences of spin-spin effects which are out of phase. We find a central real potential V_{ss}= 750±440 keV, consistent with folding model calculations, and a central volume imaginary potential W_{ss} = -780±320 keV, related to compound nuclear absorption effects."

3. Spin-Spin Potentials in $^{93}\overrightarrow{\text{Nb}} + \vec{n}$

As mentioned in TUNL XXV, we have essentially completed a study of spin-spin effects with transverse polarized ^{27}Al and 5 to 17 MeV transverse polarized neutrons. To investigate the A-dependence of the spin-spin potentials, we have performed a similar study with polarized ^{93}Nb and 5 to 11 MeV polarized neutrons. The experiments were performed with the TUNL Cryogenic Polarized Target Facility described in TUNL XXV and previous annual reports. The following modifications have been made in the past year: 1) The coldfinger was a bundle of copper wires soldered together at the end. It has been replaced with a solid copper coldfinger. With this new coldfinger, we have been able to cool the target to 9.5-11 mK, yielding target polarizations of 49-56%. 2) The two 13 cm diameter by 5 cm long NE213 liquid scintillator detectors were replaced by a single 13 cm diameter by 13 cm long NE213 liquid scintillator detector. 3) Instead of storing energy spectra in the computer, the data were fed into scalers. Measurements of the transverse (spins oriented transverse to the neutron momentum) spin-spin cross section were taken at E_n = 5.8, 7.5, 9.0, and 10.5 MeV, while the longitudinal σ_{ss} was measured at 7.5 MeV. The results are summarized in Fig. B3-1.

The results for the spin-spin cross section are compared in Fig. B3-1 to spherical optical model calculations. Assuming V_{ss} and W_{ss} are energy-independent, the best fit to the data was obtained with the condition V_{ss} = -14 keV and W_{ss} = 73 keV. The uncertainties are about ± 56 keV for both strengths.

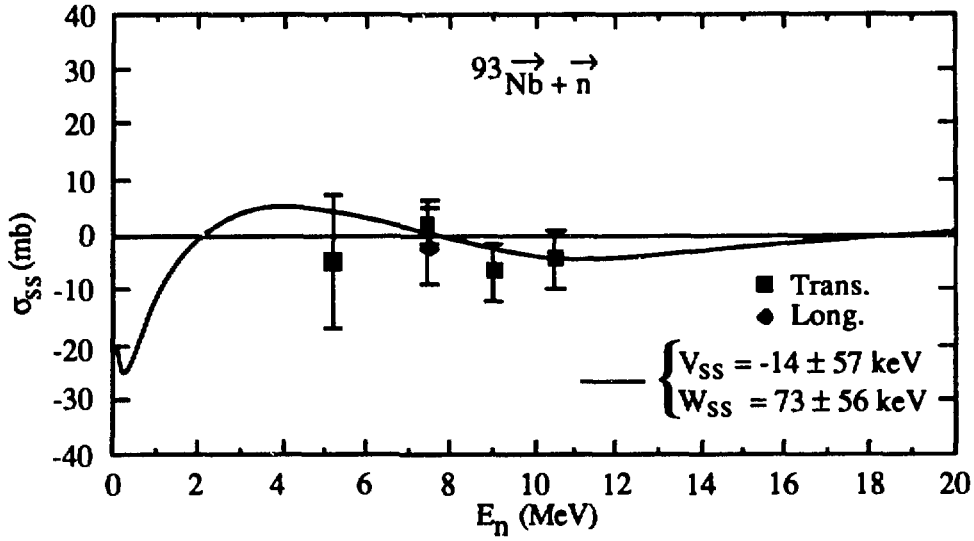

Fig. B3-1. Spin-spin cross section for ^{93}Nb measured in the present experiment, and the best fit prediction assuming energy independent real and volume imaginary central spin-spin potentials of $V_{ss} = -14$ keV and $W_{ss} = 73$ keV.

C. RADIATIVE CAPTURE REACTIONS (H. R. Weller, D. R. Tilley, G. Feldman, J. Langenbrunner, J. C. Riley, M. Whitton, Z. Williams, L. Kramer, M. Balbes, Z. D. Huang, E. Hayward (NBS), W. R. Dodge (NBS), S. Kuhn (LBL))

The major efforts of the group during the past year have been directed towards extending our tensor polarized deuteron capture measurements on few-nucleon systems to both lower and higher energies. The $^2H(d,\gamma)^4He$ reaction continues to be a major interest of our group. We have made measurements at energies as low as 400 keV and as high as 50 MeV. For the low energy measurements the beam was stopped in the target so that we are integrating over incident energies from 0.0 to 400 keV. Our emphasis here is to learn more about the reaction at energies of interest for astrophysics and fusion problems. Measurements of $A_{yy}(\theta)$, $A_y(\theta)$ and $\sigma(\theta)$ are being used to improve our understanding of the low energy capture process and, in particular, the role of the D-state of the alpha-particle. We also measured $A_y(\theta)$ and $A_{yy}(\theta)$ at incident deuteron energies of 30 and 50 MeV using the 88" cyclotron of the Lawrence Berkeley Laboratory. Data were obtained by detecting the recoiling ^4He particles in coincidence with the γ-rays. The A_y results indicate that the non-E2 radiation observed at lower energies is virtually absent at these energies. On the other hand the A_{yy} data show tensor analyzing powers which are almost twice as large as those seen in the 10 to 15 MeV region. We are looking forward to comparing these results with theoretical calculations, especially since we expect these higher energy data to be sensitive to the short range behavior of the theoretical D-state wavefunction.

We are presently involved in an analysis of the low-energy $^2H(d,\gamma)^4He$ data in order to determine which multipoles are contributing. Searches for simultaneous fits to $\sigma(\theta)$, $A_y(\theta)$ and $A_{yy}(\theta)$ are being made. Theoretical work, done in collaboration with Prof. D. Lehman, has deepened our understanding of the origin of E1 radiation in this reaction. We have considered

both spin-flip E1 and E1 due to charge polarization of the deuteron(s).

We also made new measurements on the $^{3}H(d,\gamma)^{5}He$ reaction using a tensor polarized beam. Data were obtained in the region of the fusion resonance by using a 400-keV beam and stopping it in a tritiated titanium target. Preliminary results indicate a tensor analyzing power which is somewhat smaller than that predicted for pure S-wave capture to the $3/2^{+}$ resonance. We hope to extract the amount of $1/2^{+}$ strength present in this energy region.

We are planning to complete our 30 to 50 MeV study of the $^{2}H(d,\gamma)^{4}He$ reaction by measuring $\sigma(\theta)$ and $A_{xx}(\theta)$. We are planning to begin measurements on the $^{3}He(\vec{d},\gamma)^{5}Li$ reaction at low energies in the near future. Work has also begun on designing an arrangement to make measurements of the $^{4}He(\vec{d},\gamma)^{6}Li$ reaction.

D. PHOTON PRODUCTION CROSS SECTION MEASUREMENTS FOR Ta AND Be

(C. R. Gould, G. E. Mitchell, P. Ramakrishnan, G. F. Auchampaugh (LANL), R. C. Little (LANL), S. A. Wender (LANL))

Neutron-induced photon production cross sections and the spectra of the secondary gamma rays are needed in a variety of applications. Recently intense beams of neutrons have become available at the white neutron source (WNR) at the Los Alamos Meson Physics Facility. This source has excellent characteristics for γ-ray production cross section studies. A program of measurements is now in progress using an array of five bismuth germanate (BGO) detectors. The good detection efficiency of BGO at high γ-ray energy, combined with the ability to measure complete angular distributions, provides a unique capability for performing neutron-induced γ-ray production cross section measurements. When the new facility is fully operational these measurements can be extended up to $E_n = 400$ MeV.

Our first continuum gamma-ray production measurements were for ^{181}Ta and E_n up to 100 MeV. Beryllium was measured to simulate the neutron-induced photon background. A paper on the method of analysis "Neutron-Induced Photon Production Cross Sections" has been accepted for publication in Nucl. Sci. Eng. The abstract follows:

> "A procedure for the determination of neutron-induced photon production cross sections is described, including corrections for the neutron-induced photon background and the unfolding of the γ-ray spectra. As an example, data have been obtained for tantalum and beryllium with five bismuth germanate detectors and the high energy white neutron source at LAMPF. Calculations and measurements indicate that a beryllium sample may be used to simulate neutron-induced photon background. Results for the Ta(n,xγ) reaction for neutron energies below $E_n = 20$ MeV are compared with previous measurements at ORELA."

The data on ^{181}Ta are preliminary, obtained mainly to develop the analysis procedure and to provide limited statistical accuracy at higher neutron and γ-ray energies. Even these preliminary results are interesting, since they provide the first such data for high neutron energies. A paper entitled "Photon Production Cross Section for ^{181}Ta" has been accepted for publication in Nucl. Sci. Eng. The abstract follows:

"The $^{181}Ta(n,x\gamma)$ reaction has been measured for neutron energies $E_n = 2 - 100$ MeV and for γ-ray energies $E_\gamma = 2 - 25$ MeV using an array of BGO detectors and the pulsed neutron source at LAMPF. The integrated photon production cross section reaches a maximum at about 7.5 MeV. Above 20 MeV, the cross section increases slowly with energy. The angular distributions of the photon production cross sections for different neutron energies are isotropic. At all measured energies the γ-ray spectra have the simple evaporation form."